

Copyright

by

Lonnissa Hong Nguyen

2010

The Dissertation Committee for Lonnissa Hong Nguyen Certifies that this is the approved version of the following dissertation:

Engineering Zonally Organized Articular Cartilage

Committee:

Krishnendu Roy, Supervisor

Christine Schmidt

Laura Suggs

Adriana Da Silveira

Shaochen Chen

Engineering Zonally Organized Articular Cartilage

by

Lonnissa Hong Nguyen, B.S.; M.S.

Dissertation

Presented to the Faculty of the Graduate School of

The University of Texas at Austin

in Partial Fulfillment

of the Requirements

for the Degree of

Doctor of Philosophy

The University of Texas at Austin

August 2010

Dedication

I would like to dedicate this dissertation to my fiancé, Adrien Ponticorvo, my immediate family, and my close friends for their unconditional love, support and constant encouragement during my Ph.D. career at the University of Texas.

Acknowledgements

First and foremost, I would like to thank Dr. Krishnendu Roy, my Ph.D. adviser, for giving me the opportunity to conduct research in his lab over the past five years. You always believed in me even when I did not believe in myself. Thank you for your support, guidance, and constant encouragement throughout my doctoral studies. I really appreciate your patience during my progress and growth as a researcher.

I would like to give my sincerest gratitude to Dr. Mia Markey, my faculty mentor, for all your time and heartfelt advice. Our lunch meetings are always enjoyable as well as insightful. You are the reason that I came to UT and you are the reason that I am successful in completing my degree. I cannot thank you enough for all that you have done for me.

I would like to thank my committee members, Dr. Christine Schmidt, Dr. Laura Suggs, Dr. Adriana Da Salveira, and Dr. Shaochen Chen, for their advice and invaluable input on the direction of my PhD project.

I would also like to thank everyone at the ICMB Core Facility for their help with instruments: specifically Dr. Kluas Linse for helping me with the peptide synthesis and acrylation; Dr. Angela Bardo and Dr. Dwight Romanovicz for their help with confocal and SEM microscopy.

I would also like to thank all my colleagues in my lab for their advice and help with my presentations. Special thanks to Dr. Gazell Mapili-Call for teaching me everything I needed to know, for being my role model, and finally for being a great friend. Thank you, to Eileen Dawson, who put in so much extra time effort to proof-read all of my papers. Thank you to my undergraduates, Nicole Guckert, Abhijith

Kudva, and Neha Saxena, for all their hard work and dedication. Especially to Abhi, for being good such company and making the long work hours enjoyable. To all my wonderful friends at UT, thank you for making my time at UT a memorable and enjoyable one. Special thanks to Arnold Estrada, Kavi Randhawa, Adan Hernandez, Justina Tam, and Katy Moncivais. Without you guys I would never have survived the past five years.

My special thanks also go to my parents, Lana and Cuong, and my immediate family. To my brother Tom and my sisters Lynn and Karen, whose never-ending encouragement have always reminded, me that family is the most important in life. I love you all very much. I could not have become the person that I am today without all of you. I would also like to give many thanks to my long lasting friends Lorraine Haigh, Ha Tran, and Chanty Cheang, for their unconditional love and support. I would like to give a very special thanks to my close friend, Jon Lemmens, for being such an amazing friend. You were always there for me through all my toughest moments. I am so grateful for the many hours you spent reading all my papers even when science is not your background. Most of all, I would like to thank my fiancé, Adrien, for becoming my best friend and for making me a better person. Your unconditional love, support, and patience have helped me through every difficult milestone throughout graduate school. I love you and cannot wait to marry you.

Engineering Zonally Organized Articular Cartilage

Publication No. _____

Lonnessa Hong Nguyen, Ph.D.

The University of Texas at Austin, 2010

Supervisor: Krishnendu Roy

Cartilage regeneration is one of the most widely studied areas in tissue-engineering. Despite significant progress, most efforts to date have only focused on generating homogenous tissues whose bulk properties are similar to articular cartilage. However, anatomically and functionally, articular cartilage consists of four spatially distinct regions: the superficial, transitional, deep, and calcified zones. Each zone is characterized by unique extra-cellular matrix (ECM) compositions, mechanical properties, and cellular organization. The ECM is primarily composed of type II collagen and glycosaminoglycans (GAGs), whose relative concentrations vary between zones and therefore lead to distinctive mechanical properties.

One of the major unsolved challenges in engineering cartilage has been the inability to regenerate tissue that mimics the zonal architecture of articular cartilage. Recent studies have attempted to imitate this spatial organization using zone-specific chondrocytes isolated from donor animal cartilage. Directed differentiation of a single stem population into zonally organized native-like articular cartilage has not yet been reported.

This dissertation reports that hydrogels, incorporating both synthetic and natural polymers as well as cell-induced degradability, are suitable for generating zone-specific chondrogenic phenotypes from a single MSC population. Specifically, cues provided from the unique combinations of chondroitin sulfate (CS), hyaluronic acid (HA), and MMP-sensitive peptide (MMP-pep) within a PEG-based hydrogel, direct the chondrogenic differentiation of MSCs. The findings of this dissertation demonstrate the capability of creating native-like and mechanically relevant articular cartilage consisting of zone specific layers. This ability provides a new direction in cartilage tissue engineering and could be invaluable for cartilage repair if incorporated with current minimally invasive surgical techniques.

Table of Contents

List of Tables	xv
List of Figures	xvi
List of Equations	xviii
CHAPTER ONE	1
Introduction: Specific Aims, Overview and Significance	1
1.1 INTRODUCTION	1
1.2 SPECIFIC AIMS	5
1.2.1 Specific Aim 1: To develop and fully characterize degradable PEG-based hydrogel scaffolds for differentiating MSCs into chondrocytes	5
1.2.2 Specific Aim 2: To examine the potential of biomaterial composition in directing mesenchymal stem cells (MSCs) to differentiate into specific chondrogenic phenotypes	6
1.2.2 Specific Aim 3: To fabricate a multi-layered scaffold with the biomaterial compositions	6
1.3 OVERVIEW	7
1.4 SIGNIFICANCE OF THE PROPOSED RESEARCH STUDY	7
1.5 REFERENCES	9
CHAPTER TWO	14
Background	14
2.1 ARTICULAR CARTILAGE ANATOMY	14
2.2 ARTICULAR CARTILAGE FUNCTION.....	17
2.2.1 The Role of Chondrocytes	18
2.2.2 Biomechanical Properties	18
2.3 ARTICULAR CARTILATE DEGENERATION	20

2.3.1	Trauma	20
2.3.2	Disease	21
2.3.3	Age-Related Degeneration.....	22
2.4	<i>IN VIVO</i> CARTILAGE REPAIR & <i>IN VITRO</i> CHONDROCYTE CULTURE	23
2.4.1	<i>In Vivo</i> Response for Articular Cartilage Repair	23
2.4.2	<i>In Vitro</i> Chondrocyte Culture for Various Repair Strategies.....	24
2.5	CURRENT ARTICULAR CARTILAGE REPAIR STRATEGIES ..	25
2.5.1	Lavage and Debridement	26
2.5.2	Marrow Stimulation	26
2.5.3	Osteochondral Transplants.....	27
2.5.4	Autologous Chondrocyte Implantation	28
2.5.5	Tissue Engineering Articular Cartilage	30
2.6	STEM CELLS FOR CARTILAGE TISSUE ENGINEERING	32
2.6.1	Embryonic Stem Cells	33
2.6.2	Adult Stem Cells	34
2.7	CHONDROGENIC MEDIA AND GROWTH FACTORS	41
2.7.1	Chondrogenic Media.....	42
2.7.2	Transforming Growth Factors- β	42
2.8	BIOMATERIALS FOR CARTILAGE TISSUE ENGINEERING.....	44
2.8.1	Hydrogel Scaffolds for Tissue Regeneration	44
2.8.2	Enzymatically Degradable Scaffolds in Tissue Engineering	46
2.8.3	Natural Polymers in Cartilage Tissue Engineering.....	47
2.9	FIGURES	51
2.10	REFERENCES	59

CHAPTER THREE **78**

ECM Mimicking Hydrogel Scaffolds for Cartilage Tissue Engineering.....	78
3.1 INTRODUCTION	78

3.2	MATERIALS AND METHODS.....	81
3.2.1	MMP-Sensitive Peptide Synthesis & Modification.....	81
3.2.2	Bioactivity of Modified MMP-Sensitive Peptide	82
3.2.3	Biopolymer Modification.....	83
3.2.3	Hydrogel Fabrication	84
3.2.4	Hydrogel Characterization	85
3.2.5	Statistical Analysis.....	87
3.3	RESULTS	87
3.3.1	Material Synthesis & Modification.....	87
3.3.2	Hydrogel Characterization	88
3.4	DISCUSSION.....	90
3.5	FIGURES	93
3.6	REFERENCES	108

CHAPTER FOUR **112**

	Directed Differentiation of MSCs into Specific Chondrogenic Phenotypes	112
4.1	INTRODUCTION	112
4.2	MATERIALS AND METHODS.....	114
4.2.1	Cell Encapsulation and In Vitro Culture.....	114
4.2.2	RNA Isolation and RT-PCR	114
4.2.3	Endpoint RT-PCR	117
4.2.4	Histology and Immunohistochemistry	117
4.2.5	Biochemical Characterization	118
4.2.6	Mechanical Compression of Cell Laden Hydrogels	119
4.2.7	Statistical Analysis.....	120
4.3	RESULTS	120
4.3.1	Chondrogenic Differentiation of MSCs.....	120
4.3.2	Histological Analysis of Imaged Hydrogels	122
4.3.3	Protein Analysis for Total GAG Production.....	122

4.3.4 Mechanical Strength of Hydrogel Constructs	123
4.4 DISCUSSION	124
4.5 FIGURES	129
4.6 REFERENCES	137

CHAPTER FIVE **143**

Simultaneous Differentiation of MSCs into Zonally Organized Articular Cartilage within a Multi-layered Hydrogel	143
5.1 INTRODUCTION	143
5.2 MATERIALS AND METHODS	144
5.2.1 Multi-Layered Hydrogel Fabrication	145
5.2.2 Single Layer Hydrogel Fabrication and Cell Culture	145
5.2.3 Cell Viability	146
5.2.4 RNA Isolation and RT-PCR	146
5.2.5 Histology and Immunohistochemistry	147
5.2.6 Biochemical Characterization	148
5.2.7 Compression Studies of the MLHC	149
5.2.8 Statistical Analysis	149
5.3 RESULTS	149
5.3.1 Viability of Encapsulated MSCs	149
5.3.2 Chondrogenic Differentiation of MSCs	150
5.3.3 Histological Analysis of Imaged Hydrogels	151
5.3.4 Protein Analysis for Total GAG Production	152
5.3.5 Compressive Strength of the Individual Layers	153
5.3 DISCUSSION	154
5.4 FIGURES	158
5.5 REFERENCES	170

CHAPTER SIX	172
Overall Summary, Conclusions and Future Direction	172
6.1 OVERALL SUMMARY	172
6.2 CONCLUSIONS	172
6.2.1 Chapter Three Research Findings	173
6.2.2 Chapter Four Research Findings.....	173
6.2.3 Chapter Five Research Findings	174
6.3 FUTURE DIRECTIONS	175
6.3.1 Pre-Clinical Studies: Animal Models	175
6.3.2 Clinical Application	181
6.4 FIGURES	185
6.5 REFERENCES	186

APPENDIX A	192
MSC Differentiation within Bi-Layer Hydrogels	192
A.1 INTRODUCTION	192
A.2 MATERIALS AND METHODS.....	192
A.2.1 Bi-layered Hydrogel Fabrication	193
A.2.2 Cell Viability	193
A.2.3 RNA Isolation and RT-PCR	194
A.2.4 Histology and Immunohistochemistry	195
A.2.5 Biochemical Characterization	196
A.2.6 Compression Studies of Bi-layered Hydrogels.....	196
A.2.7 Statistical Analysis.....	197
A.3 RESULTS	197
A.3.1 Viability of Encapsulated MSCs.....	197
A.3.2 Chondrogenic Differentiation of MSCs.....	197
A.3.3 Histological Analysis of Imaged Hydrogels	198
A.3.4 Protein Analysis for Total GAG Production.....	198

A.3.5 Compressive Strength of the Individual Layers.....	199
A.4 DISCUSSION.....	199
A.5 FIGURES.....	201
A.6 REFERENCES.....	207
APPENDIX B	208
Supplementary Mechanical Studies for Future Work.....	208
B.1 INTRODUCTION.....	208
B.2 MATERIALS AND METHODS.....	208
B.2.1 Compression Studies of Bi-Layered Hydrogels.....	208
B.2.2 Hydrogel Culture.....	209
B.2.3 Statistical Analysis.....	209
B.3 RESULTS.....	209
B.3.1 Compressive Strength of CS and HA Hydrogels.....	209
B.4 DISCUSSION.....	210
B.5 FIGURES.....	212
APPENDIX C	215
List of Abbreviations.....	215
Bibliography.....	218
Vita.....	245

List of Tables

Table 3.1: Hydrogel Biomaterial Composition and Concentration	98
Table 3.2: Compressive Moduli of Blank Hydrogel Constructs.....	106
Table 4.1: Sequences and Primers used in Real-Time PCR Assays	124
Table 4.2: Compressive Moduli of Cell Laden Hydrogel Constructs	135
Table 5.1: Biomaterial Composition of Each Layer	158
Table 5.2: Compressive Moduli for Blank MLHC	167
Table 5.3: Compressive Moduli for Cell-Laden MLHC	168
Table 5.4: Compressive Moduli of the SLC	169
Table A.1: Biomaterial Composition of each Layer	199
Table A.2: Compressive Moduli of Bi-Layer Hydrogels	206
Table B.1: Compressive Moduli of High % (w/v) Blank CS Hydrogels.....	210
Table B.2: Compressive Moduli of Low % (w/v) Blank CS Hydrogels	213
Table B.3: Compressive Moduli of Cell-Laden CS and HA Hydrogels.....	214

List of Figures

Figure 2.1 Schematic of the Extracellular Matrix (ECM) of Articular Cartilage	51
Figure 2.2 Schematic of the Proteoglycan Structure	52
Figure 2.3 Schematic of Articular Cartilage Organization	53
Figure 2.4 Illustration and Endoscopic Images of Normal and Damage Cartilage	54
Figure 2.5 Illustration and Endoscopic Images of Current Cartilage Repair Strategies ..	55
Figure 2.6 Illustration of the Autologous Chondrocyte Implantation.....	56
Figure 2.7 Various Differentiation Pathways of Mesenchymal Stem Cells	57
Figure 2.8 Schematic of the of MSC Chondrogenic Differentiation	58
Figure 3.1 MMP-pep Chemical Formula, Structure, and Molecular Weight	93
Figure 3.2 Schematic Drawing of the MMP-Sensitive Peptide Acrylation.....	94
Figure 3.3 Chromatograph of the MMP-pep Degradation.....	95
Figure 3.4 Schematic Drawing of Chondroitin Sulfate Acrylation	96
Figure 3.5 Schematic Drawing of Hyaluronic Acid Acrylation	97
Figure 3.6 MALDI-TOF Spectra & NMR of the Crude MMP-pep	99
Figure 3.7 MALDI-TOF Spectra & NMR of the Modified MMP-pep	100
Figure 3.8 Unmodified CS NMR.....	101
Figure 3.9 Modified CS NMR	102
Figure 3.10 Unmodified HA NMR.....	103
Figure 3.11 Modified HA NMR	104
Figure 3.12 Swelling Ratio & EWC	105
Figure 3.13 Hydrogel Degradation Profiles.....	107
Figure 4.1 Collagen II and X Gene Expression	130
Figure 4.2 Collage I Gene Expression	131

Figure 4.3 End-point Agarose Gels	132
Figure 4.4 Immunohistochemical Staining	133
Figure 4.5 GAG Concentrations	134
Figure 4.6 Correlation of Hydrogel Compositions to the Zones of Articular Cartilage	136
Figure 5.1 MLHC Fabrication	159
Figure 5.2 MLHC Live/Dead Staining	160
Figure 5.3 MLHC & SLC Collagen II Gene Expression	161
Figure 5.4 MLHC & SLC Collagen X Gene Expression.....	162
Figure 5.5 MLHC & SLC Collagen I Gene Expression	163
Figure 5.6 MLHC Immunohistochemical Staining	164
Figure 5.7 MLHC GAG Concentrations.....	165
Figure 5.8 MLHC Moduli Graph.....	166
Figure 6.1 Partial & Full Thickness Articular Cartilage Defect Illustration.....	185
Figure A.1 Bi-Layer Live/Dead Staining.....	202
Figure A.2 Bi-Layer Collagen II, X, and I Gene Expression	203
Figure A.3 Bi-Layer Immunohistochemical Staining.....	204
Figure A.4 Bi-Layer GAG Concentrations.....	205

List of Equations

Equation 3.1: Swelling Ratio	85
Equation 3.2: Equilibrium Water Content	86
Equation 3.3: Hydrogel Weight Remaining.....	87

CHAPTER ONE

Introduction: Specific Aims, Overview and Significance

1.1 INTRODUCTION

Tissue engineering research for cartilage regeneration has emerged as a promising approach to address the needs caused by articular cartilage damage. Regeneration of cartilage is one of the most critical challenges in arthritis, joint disorders, and trauma. Numerous studies have demonstrated the feasibility of producing cartilage-like tissue from chondrocytes, bone marrow stromal cells (BMSCs), or adipose-derived stem cells (ADSCs) [1-3]. Despite significant progress through decades of research in cartilage tissue engineering, some major gaps remain in our ability to regenerate cartilage, especially articular cartilage.

One of the primary unsolved challenges in cartilage regeneration is the inability to create tissue substitutes that mimic the highly organized zonal architecture of articular cartilage, consisting of the superficial, transitional, and deep zones, as well as the calcified zone at the osteochondral junction. The classical cartilage tissue engineering approaches do not try to mimic the structural organization or the zonal properties of articular cartilage, which is why these approaches have failed to achieve widespread clinical effectiveness. Recently, Hutmacher and colleagues reviewed the need to create cartilage tissue that mimics the articular cartilage's zonal architecture and identified the inability to mimic the complex structure of articular cartilage as a major limitation in the field of cartilage tissue engineering [4]. Very few studies have attempted to address the challenge of reproducing the zonal architecture of articular cartilage. Elisseff and colleagues reported isolation of chondrocytes from various zones of bovine articular cartilage, culturing the chondrocytes *in vitro* in poly(ethylene glycol) (PEG)-based

hydrogels and attempted to create bi-layer hydrogels constructs to produce cartilage-like tissue comprised of two different zones [5]. Ng et al. created similar zonal structures by encapsulating zonal chondrocytes in agarose gels [6]. Additionally, Woodfield et al. was able to demonstrate that pre-designed 3D porous scaffolds can influence cellular distribution and zonal extracellular matrix (ECM) production of bovine chondrocytes [7]. All of the previous work mentioned thus far has been done using chondrocytes isolated from each zone of articular cartilage. No studies have reported generating zone specific chondrocytes and zonally organized cartilage-like tissue starting from MSCs. Directing a single stem cell population into different zonal phenotypes within a single 3D structure presents a major challenge and a new paradigm in cartilage research. The ability to direct different zonal phenotypic expressions would provide a better alternative for cartilage replacement techniques and eliminate the need for donor tissue.

Biomaterial-based scaffolds, especially hydrogels, have been shown to provide an inductive environment for the chondrogenic differentiation of progenitor cells [8, 9]. Hydrogels are three-dimensional networks of hydrophilic polymers that swell when exposed to water. The hydrogel scaffold serves as a temporary replacement matrix for the damaged tissue until the encapsulated cells have established their own ECM. Hydrogel scaffolds can be made of either natural or synthetic materials for cartilage tissue engineering. Natural materials have the desirable biological properties but are limited by their mechanical strength [10, 11]. Synthetic polymers are beneficial because they can be tailored with the desired controllable physical and chemical characteristics [12]. Many investigators have incorporated natural cartilage ECM components, such as chondroitin sulfate (CS) and hyaluronic acid (HA), into their scaffold designs to aid in mimicking the physiological environment of native cartilage. Varghese et al. fabricated a “biogel” derived from CS with encapsulated chondrocytes that remained viable,

demonstrating the potential of these biogels for cartilage tissue engineering [13]. Additionally, Hwang et al. found that CS-based hydrogels exhibited the strongest chondrogenic response in terms of gene expression and matrix accumulation when compared to collagen or HA hydrogels [14]. Leach et al. showed that HA hydrogels have good biocompatibility and minimal inflammatory response, demonstrating the potential of HA hydrogels for wound-healing applications [15]. Nettles et al. showed that methacrylated HA crosslinked into a hydrogel promoted the retention of the chondrogenic phenotype and cartilage matrix synthesis for encapsulated chondrocytes in vitro [16].

Natural polymers lack mechanical stability which can result in difficult handling and poor tissue integration. To address these limitations, researchers have taken advantage of synthetic materials that allow for the ability to fine tune physical properties to match native tissue. There are many synthetic polymers that that can be potentially used for hydrogel synthesis. For instance, poly(propylene fumarate) and polyanhydrides can be used to fabricate injectable polymers while polyurethanes are used in the formulation of degradable polymers in order to take advantage of polyurethanes' mechanical properties [17]. However, among the extensive array of synthetic polymers that are available for tissue engineering applications, PEG is by far the most widely used [8, 9, 18-23]. PEG is hydrophilic and biocompatible with properties that limit immunogenicity and antigenicity, and characteristics which elicit minimal protein and cell adhesion [8, 24]. These properties make PEG an attractive polymer for scaffold development in cell-based tissue engineering applications [18, 19, 25-30]. PEG is not naturally degradable but can be made degradable by adding degradable linkages. Sawhney et al. demonstrated that PEG can be made hydrolytically degradable by integrating polylactide (PLA) and polyglycolic acid (PGA) units with PEG monomers

[31]. However, hydrolytic degradation of PLA/PGA hydrogels occurs spontaneously and creates an acidic environment. Since hydrogel scaffolds shelter encapsulated cells, hydrolytic degradation may not be conducive for tissue formation, especially if it results in an acidic environment. Thus, degradability via cell-secreted enzymes is a better alternative because cell directed degradation can help promote tissue remodeling without creating an acidic environment. Matrix metalloproteinases (MMPs) are proteolytic enzymes that are secreted by cells during cartilage ECM remodeling. Several investigators have taken advantage of the key concept of cell directed degradation to create hydrogel scaffolds that are enzymatically degradable by incorporating MMP sensitive peptides (MMP-pep) into their scaffold design [32-34]. Hubbell et al. developed PEG hydrogels that are sensitive to proteolytic degradation by crosslinking MMP-cleavable peptide sequences into the hydrogel network [34]. Another advantage of designing a material with proteolytic sensitivity is that migrating cells can systematically degrade the synthetic polymer and eventually anchor onto the exposed ECM.

In all the previous studies mentioned above, only one component—either CS, HA, or an MMP-sensitive peptide—was incorporated into a single hydrogel network [13, 15, 35]. Each of these components has its advantages as well as limitations, their advantages may be exploited and their limitations can be eliminated if they were combined together into a single hydrogel network. No prior work explores the effects of combining these components together within a polymer network. In contrast, the research conducted in this dissertation explored the combination of both natural and synthetic biomaterials to develop a novel hydrogel-based system with both the biological components and the ability to tailor the physical properties of the engineered tissue.

The primary hypothesis of this dissertation is that the biomaterials play an important role in the chondrogenic differentiation of MSCs, especially in determining the phenotype of the resulting cartilage-like tissue. Specifically, different combinations of synthetic (e.g. PEG) and natural biopolymers (e.g. ECM components) as well as cell-induced matrix degradability, would provide unique cues for the directed differentiation of MSCs into zone-specific articular chondrocytes. The goal of this research project is to (a) identify unique hydrogel compositions that can generate the superficial, transitional, deep or calcified zones of articular cartilage from MSCs and (b) create multi-layered scaffold structures that incorporate these biomaterial compositions such that a single stem cell population gives rise to zonally organized articular cartilage.

1.2 SPECIFIC AIMS

In order to address the challenge of creating zonally organized articular cartilage tissue substitutes, the three specific aims for this research project are as follows:

1.2.1 Specific Aim 1: To develop and fully characterize degradable PEG-based hydrogel scaffolds for differentiating MSCs into chondrocytes by (a) crosslinking a Matrix Metalloprotease (MMP)-sensitive peptide within PEG scaffolds and (b) integrating different natural matrix materials.

The hypothesis of this aim is that the integration of a degradable peptide into the polymer network will allow degradation of the scaffold by cell-specific secreted enzymes that can be tailored to match the rate of tissue formation. The incorporation of natural ECM components such as chondroitin sulfate (CS) and hyaluronic acid (HA) within the scaffold will mimic the natural physiological environment in which MSCs can differentiate into cartilage tissue. The purpose of this aim was to evaluate the effects

of incorporating MMP-sensitive peptide (MMP-pep), chondroitin sulfate (CS), and hyaluronic acid, (HA), or their combination into a PEG-based hydrogel on the scaffold physical properties.

1.2.2 Specific Aim 2: To examine the potential of biomaterial composition in directing mesenchymal stem cells (MSCs) to differentiate into specific chondrogenic phenotypes by utilizing scaffolds consisting of various combinations of a Matrix Metalloprotease (MMP)-sensitive peptide and different ECM biopolymers (HA, CS) within PEG-based hydrogels.

The hypothesis of this aim is that biomaterial composition provides the appropriate environmental cues that aid in the chondrogenic differentiation of MSCs into specific chondrogenic phenotypes. The effect of various matrix combinations on chondrogenic differentiation of MSCs was evaluated in order to identify the unique biomaterial compositions that can direct zonal cartilage formation.

1.2.2 Specific Aim 3: To fabricate a multi-layered scaffold with the biomaterial compositions determined in Aim 2 and examine the scaffold's ability to induce the simultaneous differentiation of MSCs into structurally organized articular cartilage.

This aim combined the results of the first two aims to create a multi-layered composite scaffold (representing each zone) that would be able to differentiate MSCs into articular cartilage with zonal architecture and mechanical properties. Using the material composition determined in Aim 2, a multi-layered hydrogel construct was created. The hydrogel's ability to simultaneously differentiate MSCs into zonally

organized articular cartilage was evaluated by measuring gene expression, matrix accumulation, and mechanical strength of each layer.

1.3 OVERVIEW

Chapter Two provides the background information for this research project. Chapter Two also highlights the most recent advances in cartilage tissue engineering and how biomaterials affect stem cell growth and behavior. Chapter Three discusses the synthesis and modification of each biomaterial component as well as the hydrogel fabrication and characterization. Chapter Four explains how the biomaterials characterized in Chapter Three were used to develop single layer hydrogels for the chondrogenic differentiation of MSCs. In Chapter Five, the findings of Chapter Four are incorporated to create a multi-layered hydrogel construct for differentiating MSCs into zonally organized chondrocytes. In both Chapters Four and Five, analyses of extracellular matrix production through immunohistochemistry and gene expression of collagens show successful differentiation of this progenitor cell population into chondrocytes. Finally, Chapter Six outlines the conclusions of each chapter, the current animal models available for future work, and possible clinical applications of the findings this research project.

1.4 SIGNIFICANCE OF THE PROPOSED RESEARCH STUDY

The preliminary goal for cartilage tissue engineering thus far has been to create a homogeneous tissue type by encapsulating chondrogenic cells uniformly within a polymer matrix to mimic the overall properties of articular cartilage. However, it is well known that articular cartilage consists of four distinctive zones, all of which differ in morphology and biosynthetic activity [5]. A major challenge in tissue engineering is the

ability to create tissue constructs that mimic the physiological structure and function of native tissue. This dissertation discusses a novel approach that utilizes a multi-layered hydrogel to induce the simultaneous differentiation of MSCs into zone-specific chondrocytes. The findings of this dissertation demonstrate the feasibility of tissue engineering structurally organized and functional articular cartilage. The ability to create native-like and mechanically relevant articular cartilage provides an innovative direction in the field of tissue engineering, towards the development of more functional cartilage tissue substitutes.

1.5 REFERENCES

1. Bryant, S.J. and K.S. Anseth, *Hydrogel properties influence ECM production by chondrocytes photoencapsulated in poly(ethylene glycol) hydrogels*. J Biomed Mater Res, 2002. **59**(1): p. 63-72.
2. Barry, F., et al., *Chondrogenic differentiation of mesenchymal stem cells from bone marrow: differentiation-dependent gene expression of matrix components*. Exp Cell Res, 2001. **268**(2): p. 189-200.
3. Awad, H.A., et al., *Chondrogenic differentiation of adipose-derived adult stem cells in agarose, alginate, and gelatin scaffolds*. Biomaterials, 2004. **25**(16): p. 3211-22.
4. Klein, T.J., et al., *Tissue Engineering of Articular Cartilage with Biomimetic Zones*. Tissue Eng Part B Rev, 2009.
5. Sharma, B., et al., *Designing zonal organization into tissue-engineered cartilage*. Tissue Eng, 2007. **13**(2): p. 405-14.
6. Ng, K.W., G.A. Ateshian, and C.T. Hung, *Zonal chondrocytes seeded in a layered agarose hydrogel create engineered cartilage with depth-dependent cellular and mechanical inhomogeneity*. Tissue Eng Part A, 2009. **15**(9): p. 2315-24.
7. Woodfield, T.B., et al., *Polymer scaffolds fabricated with pore-size gradients as a model for studying the zonal organization within tissue-engineered cartilage constructs*. Tissue Eng, 2005. **11**(9-10): p. 1297-311.
8. Alcantar, N.A., E.S. Aydil, and J.N. Israelachvili, *Polyethylene glycol-coated biocompatible surfaces*. J Biomed Mater Res, 2000. **51**(3): p. 343-51.

9. Bryant, S.J., et al., *Encapsulating chondrocytes in degrading PEG hydrogels with high modulus: engineering gel structural changes to facilitate cartilaginous tissue production*. *Biotechnol Bioeng*, 2004. **86**(7): p. 747-55.
10. Kim, B.S. and D.J. Mooney, *Development of biocompatible synthetic extracellular matrices for tissue engineering*. *Trends Biotechnol*, 1998. **16**(5): p. 224-30.
11. Nasser, B.A., K. Ogawa, and J.P. Vacanti, *Tissue engineering: an evolving 21st-century science to provide biologic replacement for reconstruction and transplantation*. *Surgery*, 2001. **130**(5): p. 781-4.
12. Elisseff, J., et al., *The role of biomaterials in stem cell differentiation: applications in the musculoskeletal system*. *Stem Cells Dev*, 2006. **15**(3): p. 295-303.
13. Li, Q., et al., *Photocrosslinkable polysaccharides based on chondroitin sulfate*. *J Biomed Mater Res A*, 2004. **68**(1): p. 28-33.
14. Hwang, N.S., et al., *Response of zonal chondrocytes to extracellular matrix-hydrogels*. *FEBS Lett*, 2007. **581**(22): p. 4172-8.
15. Leach, B.J., Bivens, K. A. Patrick, C. W., Jr., Schmidt, C. E., *Photocrosslinked hyaluronic acid hydrogels: natural, biodegradable tissue engineering scaffolds*. *Biotechnol Bioeng*, 2003. **82**(5): p. 578-89.
16. Nettles, D.L., et al., *Photocrosslinkable hyaluronan as a scaffold for articular cartilage repair*. *Ann Biomed Eng*, 2004. **32**(3): p. 391-7.
17. Gunatillake, P.A. and R. Adhikari, *Biodegradable synthetic polymers for tissue engineering*. *Eur Cell Mater*, 2003. **5**: p. 1-16; discussion 16.

18. Burdick, J.A. and K.S. Anseth, *Photoencapsulation of osteoblasts in injectable RGD-modified PEG hydrogels for bone tissue engineering*. *Biomaterials*, 2002. **23**(22): p. 4315-23.
19. Cruise, G.M., et al., *A sensitivity study of the key parameters in the interfacial photopolymerization of poly(ethylene glycol) diacrylate upon porcine islets*. *Biotechnol Bioeng*, 1998. **57**(6): p. 655-65.
20. Leach, J.B. and C.E. Schmidt, *Characterization of protein release from photocrosslinkable hyaluronic acid-polyethylene glycol hydrogel tissue engineering scaffolds*. *Biomaterials*, 2005. **26**(2): p. 125-35.
21. Lee, H.J., et al., *Collagen mimetic peptide-conjugated photopolymerizable PEG hydrogel*. *Biomaterials*, 2006. **27**(30): p. 5268-76.
22. Mapili, G., et al., *Laser-layered microfabrication of spatially patterned functionalized tissue-engineering scaffolds*. *J Biomed Mater Res B Appl Biomater*, 2005. **75**(2): p. 414-24.
23. Sawhney, A.S., C.P. Pathak, and J.A. Hubbell, *Interfacial photopolymerization of poly(ethylene glycol)-based hydrogels upon alginate-poly(L-lysine) microcapsules for enhanced biocompatibility*. *Biomaterials*, 1993. **14**(13): p. 1008-16.
24. Langer, R., *Biomaterials in drug delivery and tissue engineering: one laboratory's experience*. *Acc Chem Res*, 2000. **33**(2): p. 94-101.
25. Martens, P.J., S.J. Bryant, and K.S. Anseth, *Tailoring the degradation of hydrogels formed from multivinyl poly(ethylene glycol) and poly(vinyl alcohol) macromers for cartilage tissue engineering*. *Biomacromolecules*, 2003. **4**(2): p. 283-92.

26. Peppas, N.A., et al., *Physicochemical foundations and structural design of hydrogels in medicine and biology*. Annu Rev Biomed Eng, 2000. **2**: p. 9-29.
27. Bryant, S.J. and K.S. Anseth, *Controlling the spatial distribution of ECM components in degradable PEG hydrogels for tissue engineering cartilage*. J Biomed Mater Res A, 2003. **64**(1): p. 70-9.
28. Burdick, J.A., et al., *Delivery of osteoinductive growth factors from degradable PEG hydrogels influences osteoblast differentiation and mineralization*. J Control Release, 2002. **83**(1): p. 53-63.
29. Elisseff, J., et al., *Controlled-release of IGF-I and TGF-beta1 in a photopolymerizing hydrogel for cartilage tissue engineering*. J Orthop Res, 2001. **19**(6): p. 1098-104.
30. Williams, C.G., et al., *In vitro chondrogenesis of bone marrow-derived mesenchymal stem cells in a photopolymerizing hydrogel*. Tissue Eng, 2003. **9**(4): p. 679-88.
31. Sawhney, A.S., et al., *Optimization of photopolymerized bioerodible hydrogel properties for adhesion prevention*. J Biomed Mater Res, 1994. **28**(7): p. 831-8.
32. Kim, S., et al., *Synthetic MMP-13 degradable ECMs based on poly(N-isopropylacrylamide-co-acrylic acid) semi-interpenetrating polymer networks. I. Degradation and cell migration*. J Biomed Mater Res A, 2005. **75**(1): p. 73-88.
33. Kim, S. and K.E. Healy, *Synthesis and characterization of injectable poly(N-isopropylacrylamide-co-acrylic acid) hydrogels with proteolytically degradable cross-links*. Biomacromolecules, 2003. **4**(5): p. 1214-23.
34. Seliktar, D., et al., *MMP-2 sensitive, VEGF-bearing bioactive hydrogels for promotion of vascular healing*. J Biomed Mater Res A, 2004. **68**(4): p. 704-16.

35. He, X. and E. Jabbari, *Material properties and cytocompatibility of injectable MMP degradable poly(lactide ethylene oxide fumarate) hydrogel as a carrier for marrow stromal cells*. *Biomacromolecules*, 2007. **8**(3): p. 780-92.

CHAPTER TWO

Background

The main goal of cartilage tissue engineering is to create functional tissue replacements to treat cartilage injuries or osteoarthritis. To address this goal, many researchers have sought to combine cells, biomaterial scaffolds, and bioactive signals [1, 2] for the purpose of repairing articular cartilage defects. The research conducted in this dissertation has the same aspirations to create an articular cartilage substitute that can effectively restore joint function. Before diving into the research aspect, it is important to have a fundamental understanding of the articular cartilage anatomy, cartilage's functions and *in vivo* repair mechanisms, as well as currently available techniques for cartilage repair. Furthermore, this chapter provides a literature review of cartilage tissue engineering, the available cell sources, the important mitogenic factors, and biomaterials used for chondrogenic differentiation.

2.1 ARTICULAR CARTILAGE ANATOMY

Articular cartilage, also known as hyaline cartilage, is a smooth and firm mass that is extremely elastic and covers the ends of the bones in order to help the joints glide smoothly during movement [3]. The thickness of human articular cartilage ranges from 2 to 4 mm, but reaches up to 5 mm within the knee joint [4]. Although articular cartilage is an aneural, avascular, and alymphatic tissue, its structure is still quite complex. Since cartilage is an avascular tissue, the cell density is extremely low with chondrocytes only making up about 1 - 5% of the tissue volume. The collagen fibers and proteoglycans make up the other 20% of cartilage's wet weight [4, 5]. Chondrocytes are highly specialized cartilage cells that synthesize all of the extracellular matrix (ECM)

components and , secrete the components growth factors into the ECM, and regulate the matrix metabolism [5].

The principle component of articular cartilage ECM, the structure illustrated in **Figure 2.1** [6], is type II collagen which makes up 90-95% of the total collagen content in cartilage and is responsible for cartilage's tensile strength. Collagens V, VI, IX, X, and XI make up the other 5-10% of the collagen content. All collagen types are made up of three polypeptide chains or α -chains, arranged in a left-handed triple helix and are twisted together into a right-handed super coil. The primary amino acids of the polypeptide chains are glycine and proline, with hydroxyproline and hydroxylysine both providing structure stability through hydrogen bonds and covalent crosslinks respectively [7, 8].

Proteoglycans (PGs) are protein polysaccharide molecules that maintain the fluid and electrolyte balance of the cartilage tissue. The two subunits of proteoglycans, known as glycosaminoglycans (GAGs), are bound to a protein core by sugar bonds to form aggrecan molecules [5, 9, 10]. GAGs are unbranched chains of repeating disaccharide units, with three different types found in articular cartilage including chondroitin(4- or 6-) sulfate (CS), keratin sulfate, (KS), and dermatan sulfate (DS) [7, 8]. The negatively charged sulfate and carboxylate groups on these macromolecules regulate the flow of water, which is important for resisting mechanical stress as well as for nutrient diffusion through the synovial fluid [4, 5]. For additional structural support these proteoglycan aggrecan molecules form even larger aggregates by binding to hyaluronan via a link protein. Hyaluronan or hyaluronic acid (HA) is a non-sulfated GAG that does not bind to a protein core. Instead, HA acts as a binding site for the proteoglycans consisting of the sulfated GAGs such as chondroitin sulfate (CS) and

keratin sulfate (KS) [7, 8]. **Figure 2.2** illustrates the structural organization of the proteoglycan aggregates [8].

In addition to chondrocytes, collagen fibers, and proteoglycans, articular cartilage primarily consists of water, which accounts for 65-80% of cartilage's wet weight. Water is an important component of the articular cartilage anatomy because water aids in the transport of nutrients to chondrocytes and interacts with proteoglycans to provide articular cartilage with tremendous compressive strength [7, 8].

Articular cartilage is composed of four distinctive zones that include the superficial, the transitional, the deep, and the calcified cartilage zone as illustrated in **Figure 2.3** [6]. Each zone is characterized by a different collagen II orientation as well as different amounts of proteoglycans. The changes in proteoglycan concentration correlate to the changes in mechanical properties of each cartilage zone [11]. The superficial zone is the topmost layer, lying parallel to the joint surface and is covered by a thin film of synovial fluid, called proteoglycan 4 (PRG4) or lubricin. Lubricin provides the smooth gliding surface for articular cartilage [12]. The superficial layer also contains thin collagen fibrils and elongated chondrocytes, both arranged parallel to the articular surface. The proteoglycan content is the lowest while the cellular density is the highest in the superficial zone when compared to the other three articular cartilage zones [5, 6, 13]. The transitional, or middle zone, contains randomly oriented collagen fibers that have larger diameters than the collagen fibers of the superficial zone. The cell density and collagen II content decreases while the proteoglycan concentration increases, as compared to the superficial zone. Additionally, the chondrocytes have a more rounded appearance within the transitional zone. The deep zone contains the highest concentration of proteoglycans with the lowest water content [5, 6, 13]. The collagen fibers in the deep zone have the largest diameter, out of the four articular

cartilage zones, and are arranged perpendicular to the joint surface. In the deep zone, chondrocytes density is lowest, their morphology becomes more spherical and they are arranged in vertical columns. Finally, the calcified cartilage zone separates the hyaline cartilage from the subchondral bone [11]. This mineralized zone has a very low metabolic activity due to its extremely low cell density. The cells in the calcified cartilage zone synthesize collagen X, which functions in providing structural support as well as acting as a shock absorber along with the subchondral bone [14].

In addition to the four zones of articular cartilage, the cartilage ECM is further organized into three distinctive regions which are comprised of the pericellular, territorial, and inter-territorial matrix. The pericellular matrix contains proteoglycans, non-collagenous proteins such as decorin, and non-fibrillar type VI collagen that directly surrounds the cell membrane and is approximately 2 μm thick [5, 6, 13]. Surrounding the pericellular region is the territorial matrix, which can encase the pericellular matrix of a single chondrocyte or a cluster of chondrocytes. Within the deep zone of articular cartilage, the territorial matrix envelopes the columned chondrocytes. The territorial matrix contains criss-crossed collagen fibrils which protect the chondrocytes from mechanical compression [5]. Finally, the inter-territorial makes up the rest of the surrounding matrix beyond the territorial region. The collagen fibrils within the inter-territorial region have the largest diameter and are oriented according to their zone location [5].

2.2 ARTICULAR CARTILAGE FUNCTION

Articular cartilage's main function is to resist compression by acting as a low-friction and, wear resistant surface for shock absorption and high load-bearing [7, 8]. Resisting compression may seem like a simple task, but in reality compression

resistance involves an intricate system of cellular communication via proper chemical and environmental cues for the chondrocytes to properly synthesize and maintain the integrity of the ECM. The complex composition and structural organization of articular cartilage produced by chondrocytes is what gives cartilage the ability to withstand physiological compressive, tensile, and shear forces.

2.2.1 The Role of Chondrocytes

Chondrocytes are the key players in producing, maintaining, and remodeling the ECM, which determines the complex biochemical properties of the cartilage tissue [15]. The specific organization of collagen and varying concentrations of the cells within each zone of articular cartilage, determine the tensile and compressive properties of each zone. The crosslinking of the parallel collagen fibrils in the superficial zone is primarily responsible for the tensile strength, while the interaction between the negatively charged GAGs of the proteoglycans and the water trapped within the collagen meshwork is what provides compressive strength [7, 8]. Chondrocytes maintain the structural integrity of articular cartilage through the synthesis, assembly, and degradation of all the critical structural components of the ECM, which include collagen, proteoglycans, and a variety of enzymes [7, 8, 15]. During remodeling, the turn-over of biomacromolecules occurs when chondrocytes respond to changes in the matrix composition and replace the degraded matrix components with the correct types and amounts of the biomacromolecules [7, 8].

2.2.2 Biomechanical Properties

Articular cartilage is able to store, transmit, and dissipate mechanical energy that results from normal activity such as walking, running, and jumping. Cartilage's ability

to store energy is what prevents permanent damage, such as cartilage tear, from occurring during normal load deformations [7, 8]. During compression the GAG chains are pushed together but are also simultaneously repelled from each other due to their negative charges. This repulsion causes the chains to extend, allowing water to flow into the collagen fibril meshwork. However, the small pore size of the collagen fibril meshwork greatly reduces flow rate, which causes frictional resistance to fluid flow and build up of water pressure. This frictional resistance along with the water pressure within the ECM is what gives articular cartilage its ability to withstand high mechanical loads [7, 8].

Articular cartilage is biphasic, meaning it has two phases, one solid and one fluid. The macromolecular framework of collagens, proteoglycans, and noncollagenous proteins make up articular cartilage's solid phase while the fluid phase refers to the water within the cartilage tissue [7, 8]. When mechanical stress is applied to the solid matrix, the matrix's porous and permeable design enables water within the tissue to flow through the matrix. The water pressure of the interstitial fluid supports the majority (>95%) of the load and helps limit the stress level that is experienced by the solid matrix [7, 8].

Articular cartilage is also viscoelastic, meaning the strain rate dictates cartilage's stress-strain behavior. For instance, articular cartilage experiences increased deformation over time when constant compression is applied. The viscoelasticity of articular cartilage is due to flow-independent and flow-dependent mechanisms. The intermolecular friction of articular cartilage's proteoglycan matrix is the flow-independent aspect, while the flow-dependent aspect depends on the interstitial fluid flow and its frictional drag [7, 8]. High frictional drag occurs in substances with low permeability. The frictional drag

that results from the interstitial fluid flow is what gives healthy articular cartilage its viscoelastic property.

In healthy cartilage, the collagen fibril framework restrains the expansion of proteoglycans during fluid flow and limits the water content. Damaged or diseased cartilage results in the disruption of the collagen framework, leading to greater permeability and subsequently increasing the water content in the cartilage while lowering the frictional drag. As a result, the cartilage is unable to provide the stress-shielding effect to protect the ECM [7, 8]. Mechanical failure occurs due to decreased cartilage stiffness making the framework less capable of supporting its mechanical load [16].

2.3 ARTICULAR CARTILAGE DEGENERATION

Articular cartilage degeneration is a problem that will eventually affect the majority of the population over the age of 30. Approximately 43 million Americans are affected by arthritis or related conditions with the cost of treating cartilage defects reaching nearly \$65 billion dollars annually [17]. In the US alone, \$28 billion dollars [18, 19] is spent per year on orthopedic repair with over 900,000 people requiring surgery to treat articular cartilage injuries [20]. Articular cartilage damage can be caused by trauma, disease, or normal wear and tear caused by increased age.

2.3.1 Trauma

Physical trauma can either be a single impact injury from a sports accident or from repetitive micro-trauma events. The abrupt physical force from a sports accident or the accumulated micro-traumatic forces can cause rips and tears damaging the cartilage. Articular cartilage injuries caused by blunt force trauma are extremely difficult to repair

because these types of injuries usually involve the disruption of the collagen architecture and subsequently increase cell deaths at the defect edge [21]. It was previously thought that cellular death was only due to necrosis. However, Redman et al. discovered that necrosis occurred initially at the defect edge and was followed by a propagating wave of apoptosis that extended deeper into the tissue [21]. Therefore, any attempt to repair the defect is essentially just integrating replacement tissue with dead cartilage [21].

2.3.2 Disease

Disease of the joints is known as arthritis and there are over 100 different types of arthritis. This section will only focus on the two major forms which are osteoarthritis and rheumatoid arthritis. Osteoarthritis, also known as degenerative joint disease, is the most common form of arthritis and results from trauma to the joint, infection of the joint, or aging of the joint [22]. Osteoarthritis can affect any synovial joint, but most commonly affects knees, hips, and small hand joints [23]. Osteoarthritis is a metabolic and dynamic process that occurs in all joint tissues within the body including cartilage, bone, synovium, ligaments, and muscle tissue. During pathological changes, there is a loss of local articular cartilage as well as remodeling of the adjacent bone [23], the combination of which is viewed as a repair process of synovial joints. Generally, the repair process is slow but efficient and is able to compensate for small injuries. However, in cases of extreme trauma the repair capabilities cannot compensate for the injury and result in continued tissue damage which eventually leads to symptomatic osteoarthritis [23]. Degradation of joints from osteoarthritis results in mechanical abnormalities. The damaged articular cartilage can cause pain, stiffness, catching of the joint, all of which eventually lead to exposure of the underlying bone [3, 24]. When the underlying bone surfaces are less protected by cartilage, bone damage occurs and results

in decreased movement, localized muscle atrophy, and sometimes joint effusion, which is the buildup of intra-articular fluid [25]. There are a variety of factors that can contribute to joint degeneration, including hereditary, developmental, metabolic, and mechanical reasons [26].

Another form of arthritis is rheumatoid arthritis (RA). RA is the most common inflammatory arthritis and is responsible for 250,000 hospitalizations and 9 million physician visits each year [27]. Approximately 25 men and 54 women per 100,000 people are afflicted with rheumatoid arthritis, totaling to about 1% of the world's population. RA is a systemic inflammatory autoimmune disorder that causes hyperplasia of synovial cells, excess synovial fluid, and the development of pannus (loose cartilage) in the synovium. RA is a chronic condition that attacks the synovial joints and often results in the degeneration of articular cartilage. Subsequently RA leads to painful and debilitating joint movements, resulting in loss of functionality and mobility.

2.3.3 Age-Related Degeneration

It is well known that articular cartilage in adults has a limited ability for self-repair due to the lack of blood supply [28]. Wear and tear of the cartilage over time causes both the chondrocytes and the proteoglycan aggregates of the ECM to change in size. The chondrocytes become larger with age while the proteoglycan aggregates decrease in size, due to the shortening of the hyaluronic acid chains or the protein core [7, 8]. The GAG concentration changes as well, with chondroitin sulfate decreasing while keratin sulfate increases. Additionally, there is a shift in the ratio of chondroitin sulfate, chondroitin-4-sulfate decreases while the chondroitin-6-sulfate increases. Overall, age-related degeneration of articular cartilage causes increased protein content and decreased water content, which results in increased cartilage stiffness and decreased

solubility and elasticity [7, 8]. **Figure 2.4** is an illustration and an endoscopic image of normal cartilage compared to damaged cartilage [29].

2.4 IN VIVO CARTILAGE REPAIR & IN VITRO CHONDROCYTE CULTURE

Human articular cartilage has a very limited intrinsic capacity for repair. Its ability for self healing is dependent on the type of damage caused to the matrix as well as the number of functional chondrocytes remaining. This limitation has lead researchers to isolate chondrocytes and culture them *in vitro* for use in alternative repair strategies.

2.4.1 In Vivo Response for Articular Cartilage Repair

Articular cartilage contains only one cell type, chondrocytes, whose primary role is to maintain the ECM [8]. Due to the low cellular density of articular cartilage, the metabolic activity as a cell population is relative low with an extremely slow cell turnover rate, thus limiting cartilage's capacity for intrinsic repair [28]. Therefore, minor cartilage injuries can cause progressive damage which eventually leads to joint degeneration. Damage to the cartilage tissue can initiate a cell-mediated repair response, which is dependent on the chondrocytes' ability to sense changes in the matrix composition and synthesize new molecules to replace and repair the defect [28]. The chondrocytes' ability for matrix repair is limited. Cartilage repair can only occur if the matrix loss does not exceed the rate of matrix production, the fibrillar collagen meshwork is not damaged, and there are enough chondrocytes remaining which are capable of responding to the matrix damage [28]. During superficial repair, the chondrocytes proliferate and increase synthesis of ECM molecules on the borders adjacent to the defect area. This phenomenon rapidly terminates, leading to the

incomplete filling of the defected tissue and thereby limiting the window for tissue repair. Deep tissue defects which extend to the subchondral bone result in bleeding into the defect area and the formation of hematomas (blood clots). Since the underlying bone is exposed, bone marrow stem cells, growth factors, and differentiating factors, migrate to the injury site and initiate an inflammatory response to augment the healing process. The replacement tissue contains many chondrocyte-like cells encompassed in a matrix consisting of collagen II, proteoglycans, some collagen I, and non-collagenous proteins, which are all indicative of fibrocartilage formation [28]. Fibrocartilage has impaired mechanical stability due to the decreased stiffness and increased permeability [28]. The mechanical instability usually results in further structural damage of the joint because the macromolecular framework will experience increased mechanical stress [28].

2.4.2 *In Vitro* Chondrocyte Culture for Various Repair Strategies

The unfavorable results of *in vivo* articular cartilage repair have led to the investigation of isolating chondrocytes and culturing them *in vitro* for re-implantation. Chondrocytes are derived from mesenchymal stem cells, which differentiate until the cells reach their terminal state of hypertrophy and begin endochondral ossification [30]. At this terminal state chondrocytes rarely proliferate. However, when depleted of their ECM, chondrocytes can modulate their phenotype which enables the chondrocytes to exhibit characteristics that are normally associated with other differentiated cell types, such as resume DNA synthesis and cell proliferation capabilities [31]. The chondrocytes' ability to alter their phenotypic expression demonstrates their plasticity. De-differentiation is when chondrocytes lose their chondrogenic phenotypic expression and re-differentiation is when they regain their chondrogenic phenotype [31]. Although phenotypic expression is lost during de-differentiation, the phenotypic expression can be

re-established (re-differentiation) with critical culture conditions. Otherwise the chondrocytes cells in culture may have unstable phenotypic expression and switch from synthesizing collagen II to synthesizing type I collagen [31]. Isolated chondrocytes usually appear fibroblastic in monolayer cultures, but culturing in pellet form has been shown to allow chondrocytes to produce ECM [20, 32]. Articular chondrocytes are very sensitive to their extracellular environment and initiate appropriate responses to changes in their surroundings. Depending on the environmental signals, chondrocytes can respond by altering the products they synthesize and release. During *in vitro* culture, phenotypic de-differentiation can occur, which makes the chondrocytes appear like fibroblasts with abnormal characteristics. De-differentiated chondrocytes synthesize collagen I instead of type II collagen and engage in irregular synthesis of GAGs [31]. When these abnormal characteristics occur *in vivo*, it is an indication of a pathological condition of the articular cartilage such as osteoarthritis [31]. The ability to tailor the culture conditions and environmental signals to maintain the desired chondrogenic phenotype would be advantageous for *in vitro* cartilage repair. Various *in vitro* methods for culturing chondrocytes with the desired phenotype are discussed in Section 2.5.5

2.5 CURRENT ARTICULAR CARTILAGE REPAIR STRATEGIES

Each year more than 385,000 articular cartilage procedures are performed in the United States [33]. Out of approximately 30,000 arthroscopies, there was a 63% incident of knee cartilage lesions with only 4% representing patients who were under 40 years of age. This statistic clearly indicates that cartilage lesions are an age-related condition [33]. Due to the overwhelming number of articular cartilage repair procedures performed yearly, there are a number of cartilage repair techniques that are currently available including lavage, debridement, marrow stimulation, and transplantation of the

affected tissue. Due to the limitations of each of these techniques, there is still a need to develop novel strategies that can improve the effectiveness of cartilage repair.

2.5.1 Lavage and Debridement

Lavage is the oldest and simplest method for treating cartilage defects. This procedure involves rinsing the defected area of the joint with physiological solutions to decrease inflammation and remove loose cartilage bodies as well as fibrin debris [34]. Treatments of cartilage defects with lavage have shown improvement in 80% of patients and can benefit the patient up to 3.5 years [35]. However, lavage treatment cannot be a definitive solution because the treatment does not repair the joint damage and only provides temporary pain management. Debridement is a similar procedure, which involves smoothing the cartilage edges and removing loose cartilage pieces with a mechanical shaver [5]. This procedure is done to relieve the pain that is caused by loose cartilage irritating the joint. Similar to lavage, debridement is primarily used for small lesions and is only a temporary solution. Since debridement also does not repair the damaged cartilage, over time more loose cartilage can accumulate [36]. Even though this procedure is minimally invasive the patient will still be on crutches for 4-8 weeks [34]. **Figure 2.5A** shows an illustration and endoscopic images of cartilage debridement during and after the procedure [36]. The endoscopic image of the debrided cartilage clearly shows that the cartilage is still damaged.

2.5.2 Marrow Stimulation

Marrow stimulation, also known as microfracture surgery, involves the attempt to recruit pluripotent marrow-based stem cells into the cartilage defect area for the regeneration of neo-cartilage [33]. This technique is performed by drilling small holes to

penetrate the subchondral bone and disrupt the blood vessels. The disruption of the blood vessels allows for blood to flow into the defect area and initiate the natural healing response [5]. Mesenchymal stem cells (MSCs) migrate into the defect area and form a fibrin clot. The MSCs differentiate into chondrocyte-like cells that are capable of producing ECM [34]. The MSCs are only chondrocyte-like because they are not true chondrocytes and their differentiation results in the formation of scar cartilage or fibrocartilage [33]. Microsurgery is easy to perform and can yield positive results in patients. As mentioned at the end of Section 2.4.1, fibrocartilage lacks mechanical strength and is not as durable as native articular cartilage. **Figure 2.5B** shows endoscopic images of a cartilage defect during and after microfracture surgery [36]. The endoscopic image of the cartilage after microfracture surgery shows incomplete filling of the cartilage defect due to the rapid termination of the healing response, as discussed in Section 2.4.1

2.5.3 Osteochondral Transplants

Osteochondral transplantation is a technique which requires donated tissue that is either autogenic (the patient's own tissue), allogenic (cadaver tissue), or xenogenic (animal tissue). Xenogenic tissues are rarely used because of the high risk of disease transmission and tissue rejection. Allogenic tissue from cadavers is a feasible tissue choice and can be successful in treating large cartilage defects [37]. However, it has been shown that fresh tissue has a better success rate than frozen tissue in terms of cell death and mechanical stability [38]. Tissue rejection is still a potential problem when using allogenic tissues [39] and transplants require the patient to take immunosuppressant drugs. Autogenic plugs usually contain both cartilage and bone obtained from a non-load bearing area of the patient, as shown in **Figure 2.5C** [36].

Osteochondral autograft transfer system (OATS) has been widely used and is good for treatment of large defects or for defects where both bone and cartilage are missing [40]. Autologous transplant for treatment of extremely large defects that require multiple plugs is called mosaicplasty. Mosaicplasty involves the removal of multiple plugs which are placed into a damaged area resulting in a mosaic appearance [41]. Autologous transplants can be done on an open joint or by arthroscopy [42] and have been shown to decrease pain and improve joint function [43]. However, the drawback to autologous osteochondral transplants is that the donor site defects are as large as the areas that require repair which can result in donor site morbidity [34]. Additionally, since the donor tissue is obtained from a non-load bearing area, it has been shown that the mechanical stress experienced by the plugs can result in chondrocyte death leading to the degeneration and failure of the graft [40].

2.5.4 Autologous Chondrocyte Implantation

Autologous Chondrocyte Implantation (ACI) is a technique used to restore the damaged cartilage with cells from the patient's own knee and was first described by Brittberg in 1994 [44]. The operation is performed in two stages as illustrated in **Figure 2.6**. The first step is to harvest a small amount of healthy cartilage from a non-load bearing area of the knee joint. The cartilage cells are enzymatically removed from its matrix and then cultured in the laboratory for 3-4 weeks [40]. A second operation known as an arthrotomy is performed to place the cartilage cells back into the knee. During the second surgery a periosteal patch is obtained from the top of the shin bone (medial tibia). Debridement of the cartilage defect is performed before the periosteal patch is surgically sewn on. After the patch is sewn over the defect, cartilage cells are then injected underneath the periosteal patch into the defect area and the periosteal patch is

sealed with fibrin glue [40]. This procedure has been shown to reduce pain and restore joint function [44]. The advantage of an ACI procedure is that it does not create large donor defects. Obtaining autologous chondrocytes from a small biopsy generates only a small chondral defect [34]. The second stage operation of ACI is a larger procedure and requires 3-4 days of hospital stay. A strict rehabilitation program will commence in the hospital and continue for 12 weeks after the procedure [45].

Periosteal grafts have posed problems due to graft hypertrophy and issues with morbidity at the harvest sites. To address issues with periosteal grafts, a 2nd generation ACI has been developed, which utilizes a resorbable collagen membrane [46]. Furthermore, a 3rd generation ACI has been developed by Genzyme. This 3rd generation ACI uses various bioabsorbable scaffolds in a process called matrix-induced autologous chondrocyte implantation (MACI) [47]. The preparation for the MACI procedure is the same as for the first two generations of ACI. The difference between the first two generations of ACI and the 3rd generation ACI is that the cell suspensions produced are not injected into the defect site but rather seeded on a special 3D matrix scaffold where the cells adhere to the fibers and start the production of the extracellular cartilage matrix components. As the cells grow, the material of the matrix decomposes and is replaced by the extracellular matrix. The chondrocyte seeded scaffold is glued into the defect with fibrin glue. MACI has been shown to be as effective as the traditional ACI [47]. The advantages of MACI over the traditional ACI include reduced operation time [45] and reduced tourniquet time [48]. MACI also eliminates the need for a periosteal flap while using minimally invasive methods such as mini-arthrotomy or arthroscopy [49] during the surgery. Similar to microfracture surgery, the major disadvantage of the MACI procedure is that it induces fibrocartilage formation [50]. For this reason, some surgeons still prefer osteochondral transplants over MACI.

2.5.5 Tissue Engineering Articular Cartilage

All the therapies described above have their drawbacks offer for treating articular cartilage defects. Lavage and debridement are temporary fixes and do not provide cartilage repair. Marrow stimulation initiates the natural healing response but the replacement tissue is in the form of fibrocartilage, which is mechanically inferior to articular cartilage. Similarly, ACI and MACI have also been shown to produce fibrocartilage. Osteochondral transplants with tissue derived from patients create large defects at the harvest site while harvesting tissue from cadavers requires immunosuppressant drugs. Additionally, animal tissue cannot realistically be used for human applications due to the high risk of disease transmission. Tissue engineering presents an alternative method to repair cartilage lesions and prevent further progressive cartilage degeneration. *In vitro* production of articular cartilage grafts grown through tissue engineering offers the advantage of having definitive control over the process of chondrocyte isolation, proliferation, differentiation, and matrix production [34].

Chondrocyte isolation is necessary when engineering articular cartilage replacements. Obtaining chondrocytes for tissue engineering applications follows the same processes used when acquiring chondrocytes for ACI. To harvest the chondrocytes, surgeons obtain a small biopsy of cartilage tissue during arthroscopy of the injured joint. The biopsy is enzymatically digested to release the chondrocytes from their ECM and then the chondrocytes are suspended in culture [34]. The chondrocytes are cultured in 2D with media supplemented with growth factors which enable the cells to rapidly proliferate, doubling in number within two days [51]. Once the proliferation of chondrocytes reaches the number of cells necessary for tissue engineering applications, the cells are placed in a 3D culture system.

As discussed in Section 2.4.2, when chondrocytes are cultured *in vitro* they have the tendency to de-differentiate. The chondrocytes lose their chondrogenic phenotypic expression (decreased collagen II expression and increased collagen I expression) while taking on a more fibroblastic morphology if the cell culture environment is not carefully controlled [52-54]. Culturing chondrocytes in a biomaterial-free 3D pellet [55] and micromass [56]. have been well established. 3D pellets are formed by centrifuging a cell suspension in conical tubes. A micromass is formed by adding droplets of cell-media mix into a 24-well plate so that the cells can coalesce and form one spherical mass [57]. Both the pellet and micromass configuration can reinitiate and maintain chondrogenic differentiation of chondrocytes isolated from cartilage that are expanded in monolayer [56]. Tare et al. isolated articular chondrocytes from femoral heads of human patients and found that human articular chondrocyte cultured in pellets genetically expressed Sox-9, aggrecan, and type II collagen, as well as produced a matrix rich in collagen II and proteoglycans [20]. Additionally, there was no alkaline phosphatase activity (marker for mineralization) detected which demonstrates that the cells within the pellet are pre-hypertrophic. Pellet culture results from this study as well as from many other studies confirm that pellet cultures of isolated chondrocytes are suitable for cartilage regeneration [32, 56, 58-61]. The advantage of 3D pellet culture over the monolayer culture is in the ability to generate chondrocytes that exhibit similar morphology, gene, and protein expression, to that of *in vivo* chondrocytes [20]. Zhang et al. compared the micromass with the pellet culture system and demonstrated that the micromass system was superior over the pellet culture system for chondrogenic differentiation of human mesenchymal stem cells (hMSCs) [57]. The micromass system in their study had greater deposition of proteoglycans and collagen II than the pellet culture system. However, the disadvantages of both the micromass and pellet systems

are that these systems require an extremely high number of cells, which increases the culture time, to produce small and mechanically unstable cartilage [62]. These limiting factors have lead researchers to develop additional 3D culture methods to study, accelerate, and better control tissue regeneration. For long term success of the next generation of functional tissue replacements, additional exogenous influences such as cell-to-cell interaction may be required.

Hydrogel scaffolds and bioreactors have been developed to study and accelerate maturation and integration of chondrocytes [63]. Hydrogel scaffolds are discussed in more detail in Section 2.8. Spinner flask bioreactors provide convective mixing while perfusion bioreactors provide convective flow [63]. Bioreactors can improve size, cellularity, and molecular composition when used to culture engineered tissues [64-66]. Pei et al. showed that rotating bioreactors provides a mechanically active environment that improved *in vitro* chondrogenesis resulting in cartilaginous constructs that are larger and with better structural, functional, and molecular properties [64]. Additionally, Vunjak-Novakovic et al. utilized spinner flasks to dynamically seed bovine chondrocytes on to polyglycolic acid (PGA) scaffolds and found that the chondrocytes maintained their spherical cell shape. Their findings indicate that cell seeding in spinner flasks provides a permissive environment for chondrogenic differentiation [65]. In addition to being able to accelerate tissue growth and differentiation, bioreactors can also be utilized to test the physiological responses of the engineered constructs to environmental conditions that the constructs will be exposed to after implantation [63].

2.6 STEM CELLS FOR CARTILAGE TISSUE ENGINEERING

Section 2.5 discussed tissue engineering strategies involving isolated chondrocytes. As mentioned previously, chondrocyte isolation is a complicated and time

consuming process that requires an initial surgical procedure. To eliminate the need for chondrocyte isolation many researchers have turned to stem cells as a viable alternative cell source for cartilage tissue engineering. Stem cells are characterized by their capacity for self renewal through mitotic cell division and their ability to differentiate into a diverse assortment of specialized cell types [67]. Stem cells can be broken down into two main categories, embryonic and adult stem cells, which are distinguished by the cells' differentiation potential. Both embryonic and adult stem cells have shown great potential for cartilage tissue engineering.

2.6.1 Embryonic Stem Cells

The fertilized egg is considered the ultimate stem cell because of the cell's ability to transform into a plethora of undifferentiated cell lineages. This ability is called totipotent, meaning that this single cell can differentiate into any and all the tissue types of the body. Embryonic stem (ES) cells are the daughter cells derived from the fertilized egg. ES cells retain the same self renewing ability and they are pluripotent, meaning they can differentiate into any of the three germ layers. ES cells' self replication and pluripotent properties have made these cells of great interest for tissue engineering applications, especially in cartilage regeneration [56, 68-87]. Generally, the differentiation of ES cells parallel early embryonic development by forming embryoid bodies (EBs) [86]. It has been established that growth factors provide the necessary biological signals to induce EBs to differentiate towards the chondrogenic lineage [73, 78, 79]. Hwang et al. demonstrated that TGF- β 1 induced the chondrogenesis of EBs encapsulated in poly(ethylene glycol) (PEG) hydrogels with high aggrecan expression [74]. In the same study, Hwang et al. compared the chondrogenic capabilities of ES cells in a monolayer culture versus ES cells encapsulated in PEG hydrogels [74]. Hwang and

colleagues found that ES cells cultured in PEG hydrogels upregulated the expression of aggrecan and Sox-9, which is a transcription factor for cartilage, over the monolayer culture. They believe that the enhanced differentiation of ES cells within the 3D hydrogel construct is due to closer cell-to-cell interaction, entrapment of secreted ECM, and the maintenance of the ES cells' spherical cellular morphology. Additionally, numerous works have shown that ES cells encapsulated within 3D scaffold systems can potentially be used for tissue regeneration [82-84]. Although ES cells can serve as an unlimited cell source for tissue engineering applications, ES cell use is limited by the fact that it is extremely difficult to control the cells' differentiation and obtain a homogenous cell population [74]. Therefore, researchers have turned to autologous adult stem cells because they are non-immunogenic given that they are autogenic cells with the added benefit in that their differentiation can be better controlled.

2.6.2 Adult Stem Cells

Adult stem cells that are commonly used for cartilage tissue engineering include mesenchymal stem cells (MSC), adipose stem cells (ASC), adipose-derived stem cells (ADSC), and to a lesser extent synovial-derived stem cells (SDSC). MSCs are the most widely used adult stem cells for cartilage tissue engineering. MSCs are derived from the bone marrow and are multipotent, which means that they are progenitor cells that have the potential to give rise to multiple but not all cell lineages. MSCs are known to have the capability to differentiate into multiple cell lineages including osteocytes, chondrocytes, and adipocytes as illustrated in **Figure 2.7** [88]. In addition to MSCs being multipotent, they also have the ability to maintain cell differentiation potential in culture, they are simple to isolate, and they have been shown to grow rapidly *in vitro*, which allows for large expansions to obtain large cell numbers. MSCs also have a

number of unique properties such as potent immunosuppressant and anti-inflammatory effects. MSCs are able to influence the local tissue environment and effectively stimulate regeneration *in situ* by secreting important soluble factors [89]. These characteristics make MSCs a promising candidate for a number of therapeutic uses including tissue engineering applications [89]. Due to their array of unique properties, MSCs have been widely used for cartilage tissue engineering through a variety of techniques including pellet culture, encapsulation in scaffolds of different material composition, and dynamic culture in bioreactors [57, 90-93]. MSCs can be induced to differentiate into the chondrogenic pathway *in vitro* using serum-free media containing transforming growth factor- β (TGF- β) within a 3D structure. Biosynthesis of GAGs and genetic expression of cartilage-specific markers such as Sox-9 (chondrogenic transcription factor), aggrecan, collagen II, and collagen X have been used to determine the differentiation of MSCs into the chondrogenic pathway [94].

The differentiation pathway of MSCs into mature chondrocytes was investigated by Barry et al [30]. Results from this study indicate that the chondrogenic differentiation of adult bone marrow MSCs involves a change in cell morphology, formation of an integrated ECM, and upregulation of GAG synthesis. Barry and colleagues also determined that collagens I, II, and X are synthesized sequentially during differentiation by the same cells. The differentiated MSCs exhibit early expression of collagen I, followed by collagen II, and terminating with collagen X. Barry et al. concluded from this study that there are three separate stages that occur during cell differentiation. Stage I occurs during the first 6 days of differentiation, the cells upregulate a number of genes including fibromodulin, cartilage oligomeric matrix protein (COMP), aggrecan, versican, and decorin, as well as initiate GAG synthesis. Stage II occurs 7 days after differentiation, during which the expression of collagen II, chondroadherin, and biglycan

were observed. During stage III, the accumulation of GAG proceeds over the next 14 days and eventually leads to the formation of mature chondrocytes [30]. **Figure 2.8** shows a timeline of defined events in the chondrogenic differentiation of MSCs during pellet culture. Barry et al.'s work allowed researchers to obtain a better understanding of the MSC differentiation pathway into the chondrogenic phenotype, which in turn lead to improved strategies for directed MSC differentiation.

Pellet culture was the initial standard method for chondrogenic differentiation of MSCs but it may not be the best method for cell differentiation. As mentioned previously, Zhang et al. showed superior chondrogenesis within micromass systems over the pellet culture system, likely due to the poor nutrient diffusion resulting in MSC apoptosis within the central region of the pellet system [57].

As research has progressed and a greater understanding is gained of MSC differentiation, new and improved MSC differentiation methods have been developed. Meinel et al. encapsulated human MSCs within various protein scaffolds such as collagen, crosslinked collagen, silk, and silk modified with RGD (Arg-Gly-Asp, an adhesion peptide) [92]. Meinel et al. demonstrated that silk scaffolds performed the best in the chondrogenic differentiation of human MSCs, exhibiting the highest type II collagen expression as well as GAG production [92]. Meinel and colleagues attributed the increased chondrogenic induction to the highly porous and slow degradation nature of silk scaffolds as well as the silk scaffolds' structural stability. Additionally, Marolt et al. took MSC laden silk scaffolds and cultured them in rotating bioreactors [91] to study the MSCs' and silk scaffolds' combinatorial effect. They found that although the constructs cultured in chondrogenic medium had an increase in GAG content, the overall chondrogenic differentiation of MSCs was slow and incomplete, suggesting that the combined utilization of scaffolds and bioreactors for chondrogenesis may not be

optimal [91]. Li et al. also studied the multi-lineage differentiation capabilities of human MSCs seeded onto nanofibrous poly(ϵ -caprolactone) (PCL) scaffolds [90]. For chondrogenesis of human MSCs, Li et al. found that after 21 days of culture, the cells expressed both AGN and Col II mRNA. Additionally, the cells functionally produced aggrecan and collagen type II. Furthermore, Li and colleagues also observed morphologically round chondrocytes embedded in a sulfated proteoglycan-rich ECM with collagen type X mRNA downregulated, suggesting a stable and non-hypertrophic phenotype for the chondrocytes within the engineered construct. Finally, Varghese et al. demonstrated that incorporating chondroitin sulfate (CS) into a PEG-based hydrogel, helped mimic the native cartilage environment and thus enhances the chondrogenic differentiation of MSCs [93].

The multitude of studies done on differentiating MSCs into the chondrogenic phenotype, has established MSCs as a good cell source for cartilage repair strategies. On the other hand, the procedure to acquire bone marrow for MSC harvesting is invasive and sometimes painful for patients. Extracting bone marrow requires general or local anesthesia and can result in a low yielding cell count. The low cell count is a significant limiting factor because cell harvesting is time consuming and an expensive *ex vivo* expansion process that can also run the risk of contamination. A better alternative would be a cell source that is easily attainable and capable of yielding large enough cell counts to prevent the need for culture expansion.

In the recent years adipose stem cells (ASC) or adipose-derived adult stem cells (ADSC) have become popular among researchers for cartilage tissue engineering because these cells are easily obtainable. Adipose tissue contains a heterogeneous stromal cell population. Within this heterogeneous population there are stem cells that have the potential to differentiate into adipogenic, osteogenic, chondrogenic, and

myogenic cells when cultured *in vitro* in the presence of lineage-specific growth factors [95]. The liposuction procedure used to obtain these cells results in minimal patient discomfort and is capable of yielding enough cells to be expanded in culture [95], making ASCs and ADSCs an ideal source of adult autologous stem cells. Guilak et al. found that human ADSCs are a multipotent adult stem type and not a mixture of unipotent (differentiate into only one cell type) progenitor cells, due to ADSCs' multi-lineage differentiation capacity [96].

A number of researchers have exploited this multipotent characteristic of ADSCs to investigate ADSCs' potential application in cartilage tissue regeneration [96-98]. Guliak et al. explored the chondrogenic differentiation potential of fibroblast-like populations called processed lipoaspirate (PLA) obtained from processed liposuctioned human adipose tissue [96]. The PLA cells were cultured in a 3D micromass pellet with chondrogenic media containing dexamethasone and TGF- β 1. The PLA cells formed dense nodules exhibiting sulfated proteoglycans and collagen type II, characteristics that were not observed in undifferentiated PLA cells [96]. Estes et al. cultured ADSCs in monolayer and found that the cell culture environment as well as the growth factors such as epidermal growth factor (EGF), basic fibroblast growth factor (bFGF), and TGF- β 1, significantly influenced ADSCs' ability to proliferate and maintain their multipotent characteristics [97]. Additionally, Estes and colleagues' findings suggest that increasing passage number of ADSCs in monolayer culture may increase the adipose-derived adult cells' chondrogenic potential [97].

Mahmudifar et al. performed a comparative analysis study on the chondrogenic potential of ADSCs encapsulated in polyglycolic acid (PGA) compared to ADSCs in pellet culture [98] and found that there were higher GAG and collagen II expressions among ADSCs that were encapsulated in PGA scaffolds. The enhanced chondrogenic

induction of ADSCs within scaffold biomaterials from this study alludes to the importance of cell-matrix interactions for chondrogenic differentiation. Furthermore, additional studies done by Guilak et al. confirmed that biomaterials provide guidance for the development and commitment of stem cells towards specific tissue formation [99].

As with other stem cell sources, the use of ADSCs also has a number of drawbacks. Liposuction is a relatively simple procedure with minimal patient discomfort but if performed without the utmost care, damage to the underlying muscle or disruption of the blood vessel supply can occur, which can be harmful to the patient [95]. Damage to the muscle during liposuction can lead to the contamination of the myogenic precursor and satellite cells into the PLA population which subsequently can lead to unwanted myogenic differentiation. Pericytes have the ability to differentiate into a fibroblast, smooth muscle cell, or macrophage. Damage to the blood vessel during liposuction could release the pericytes, which then mix with the PLA population and subsequently cause simultaneous differentiation into multiple unwanted lineages.

Both MSCs and ADSCs have been widely used in the cartilage tissue engineering field. Multiple investigators have questioned which cell source is better for chondrogenic differentiation, thus numerous comparative studies have been done to determine which adults stem cells have superior chondrogenic potential for tissue engineering. Jakobsen et al. performed a comparative study between MSCs, ADSCs, and chondrocytes. In the study, MSCs and ADSCs were seeded onto hyaluronic acid (HA) scaffolds. Jackobsen and colleagues found that MSCs induced a much higher mRNA expression of type II collagen than both ADSCs and chondrocytes when cultured in chondrogenic media [100]. Additionally, Winter et al. demonstrated that the chondrogenic potential of MSCs and ADSCs were indistinguishable in monolayer culture with similar cell morphology. However, when switched to a high-density 3D cell

culture system, MSCs had improved chondrogenesis over ADSCs [101]. Furthermore, Diekman et al. confirmed that MSCs have overall greater chondrogenic response than ADSCs when cultured in alginate beads or cartilage-derived matrices exhibiting higher upregulation of type II collagen and more extensive matrix synthesis [102]. Finally, Puetzer et al. did a comparative literature review and found that MSCs repeatedly undergo chondrogenesis more thoroughly than ADSCs under the same culture conditions [101-107].

Although this dissertation focuses on the differentiation of MSCs, it is still important to acknowledge that there are other cell sources available for future work. For instance, stem cells derived from the synovial lining are termed as synovial-derived stem cells (SDSC). SDSCs serve as a good cell source for cartilage tissue regeneration because the cells share similar properties to chondrocytes. For example, SDSCs produce similar chondrogenic proteins such as cartilage oligomeric matrix protein (COMP) [108-110], link proteins [111], and sulfated GAGs [112]. Pacifici et al. determined that both articular cartilage cells and synovial cells originate from the same precursor population [113], therefore establishing their close functional relationship. Additionally, both Allard et al. and Xue et al. showed that pathological conditions can induce synovial cells to express strong chondrogenic characteristics [114, 115] such as the production of collagenase during arthritis [31].

Due to the heterogeneous nature of the synovium, Pei et al. developed a method called “negative isolation,” in which Pei and colleagues removed macrophages and purified synovial fibroblasts (SFBs) [116]. The purified SFBs have high chondrogenic potential when cultured with TGF- β 1 [117]. Pei et al. performed a comparative study to compare the chondrogenic potential of the “negative isolated” cells with conventional passage SDSCs. They found that conventionally passed SDSCs exhibited weak and

sparse distribution of GAG, type II collagen and strong expression of type I collagen when compared to the SDSCs that were purified by negative isolation [116]. The presences of macrophages were observed in the conventional passage SDSCs. The macrophages can contribute to the inhibition of SDSC-based chondrogenesis and subsequently exhibited weak and sparse distribution of GAG and collagen II with high expression of collagen I and macrophage antigen [116].

In a separate study, Fan et al. encapsulated rabbit SDSCs into two different hydrogel scaffolds. One hydrogel scaffold was a non-degradable photo-crosslinked poly(ethylene glycol) diacrylate (PEGDA) and the other scaffold was a degradable phosphoester-poly(ethylene glycol) (PhosPEG). Fan and colleagues demonstrated that SDSCs have high viability in both hydrogel scaffolds with positive chondrogenesis of SDSCs when cultured with TGF- β 1 or TGF- β 3; however the PEGDA system had the better chondrogenic outcome [118]. Although SDSCs are not as widely used as MSCs and ADSCs, these studies demonstrate that SDSCs have great potential for chondrogenic differentiation and can be a useful cell source for tissue engineering applications such as cartilage regeneration.

2.7 CHONDROGENIC MEDIA AND GROWTH FACTORS

MSCs have the ability to differentiate into multiple lineages, therefore, the proper media formulations is crucial in directing MSC differentiation into the chondrogenic pathway. Mitogenic signals, such as grow factors are essential signaling components in MSC differentiation. Members of the transforming growth factor- β (TGF- β) family have been well established as a key element for the chondrogenic differentiation of MSCs.

2.7.1 Chondrogenic Media

Chemical induction of MSC chondrogenesis has been widely used and for the most part was a process required for successful chondrogenic differentiation [30, 59, 71, 106, 119, 120]. The standard formulation of chondrogenic media is Dulbecco's modified Eagle's medium (DMEM) with high (4500mg/L) or low (1000mg/L) glucose supplement. The addition of ITS+ premix, ascorbate, and pyruvate is also quite common. ITS stands for insulin, transferrin, and selenium, with the "+" indicating that the premix also contains bovine serum albumin and linoleic acid. Although serum can still be used in the chondrogenic differentiation of MSCs, most researchers lean towards serum-free culture due to the fact that serum in media can induce de-differentiation [68, 70, 121]. The addition of various growth factors has been shown to greatly increase the chondrogenic potential of MSCs, especially when using members of the transforming growth factor- β (TGF- β) family. However, there is a dose dependent response as shown by Yoo and colleagues [59]. Yoo et al. found that lower concentrations (0.01-0.1 ng/mL) of TGF- β 1 had no significant effect on MSC differentiation while high concentrations (10 ng/mL) caused MSCs to differentiate into chondrocytes [59]. Additionally, Yoo et al. also determined that dexamethasone when combined with TGF- β 1, influences MSC chondrogenesis by increasing ECM formation [59]. Based on these studies, the chondrogenic media formulation in this dissertation is serum free, containing 1% penicillin/streptomycin, 10nM dexamethasone, 50 μ g/mL ascorbic acid-2-phosphate, 40 μ g/mL L-proline, 5 mL ITS+1, and 10 ng/mL TGF- β 1.

2.7.2 Transforming Growth Factors- β

Members of the transforming growth factor- β (TGF- β) family have been extensively studied and widely established as inductive agents for the chondrogenic

differentiation of MSCs [71, 80, 81, 85, 122-125]. TGF- β was first discovered in 1981 and named for its ability to elicit phenotypic transformations in rodent fibroblasts [126, 127]. TGF- β 1, TGF- β 2, and TGF- β 3 are all TGF- β isoforms that function through the same receptor signaling systems and. All of which have distinct spatial and temporal expressions of both mRNA and proteins in development, regeneration, and pathological responses [128]. All three isoforms are multifunctional peptides and while heterodimers of TGF- β 1 and TGF- β 2 have been known to occur [129], there have been no reports of heterodimers involving TGF- β 3. Although these three isoforms are similar, TGF- β 1, TGF- β 2, and TGF- β still show subtle differences between each other. For instance, their N-terminal regions only show 27% sequence identity to each other. TGF- β 1 only has about 72% identity to TGF- β 2 while mature TGF- β 3 shows about 80% identity to both TGF- β 1 and TGF- β 2 [130]. The contribution and expression of TGF- β 2 in MSCs during chondrogenesis has not been fully determined [128], thus this section will focus on the discussion of TGF- β 1 and TGF- β 3.

Goessler et al. found that TGF- β 1 was constantly expressed during chondrogenic differentiation of MSCs [128]. Goessler and colleagues also determined that TGF- β 1 acted in unison with other TGF- β s but that they are not involved in the de-differentiation of chondrocytes. Goessler et al. also found that although TGF- β 3 was constantly expressed during chondrogenic differentiation of MSCs, Goessler and colleagues believed that TGF- β 3 assists with the de-differentiation process in some way [128]. Barry et al. reported that the combination of dexamethasone and TGF- β 1 showed less chondrogenic induction of human MSC pellets than when hMSCs are exposed to dexamethasone combined with TGF- β 3 [30]. Lower GAG accumulation, less collagen II staining, and smaller pellet size were observed in TGF- β 1 induction than in TGF- β 3 induction. [30]. Although, Barry and colleagues showed that TGF- β 3 had a more

inductive effect on the chondrogenic differentiation of human MSCs, studies conducted by Chimal-Monroy et al. showed a reverse effect on mouse MSCs [69, 131]. Chimal-Monroy et al. demonstrated that mouse MSCs were more responsive to TGF- β 1, exhibiting higher ECM accumulation and enhanced expression of sulfated proteoglycans, type II collagen, and cartilage link protein. However, with TGF- β 3 there was a diminished effect [69, 131]. Since the research discussed in this dissertation was conducted using mouse MSCs, it was determined that TGF- β 1 would be a better choice based on the findings of Chimal-Monroy et al. Additionally, TGF- β 1 is not involved in the de-differentiation process while TGF- β 3 has been found to assist this process.

2.8 BIOMATERIALS FOR CARTILAGE TISSUE ENGINEERING

As described in Section 2.6.2, a number of investigators, including Mahmudifar and Guilak, have shown that scaffold biomaterials enhance chondrogenic differentiation of stem cells. Mahmudifar and Guilak believe that biomaterials provide guidance for the development and commitment of stem cells towards specific tissue formation [98, 99]. Therefore, this section focuses on the influence of biomaterial composition on stem cell differentiation into the chondrogenic lineage.

2.8.1 Hydrogel Scaffolds for Tissue Regeneration

Hydrogels represent an important class of biomaterials because they exhibit excellent biocompatibility, have the ability to imbibe a large amount of water, and minimize inflammatory responses which can result in thrombosis and tissue damage [132, 133]. Hydrogel scaffolds can be made of synthetic, natural materials, or a combination of both. Natural materials provide easy cell transplantation but are limited by their mechanical strength and their uncontrollable degradation rates [134-136].

Natural biopolymers will be discussed in more detail in Section 2.8.3. Synthetic polymers are beneficial because their properties can be fine-tuned to produce scaffolds with desired and controllable physical and chemical characteristics [137].

In designing a polymer scaffold, there are a number of criteria that must be satisfied before the scaffold can successfully serve its purpose. The scaffold material has to be biocompatible and biodegradable with a controlled degradation rate that is compatible with the development of nascent tissue. Scaffold properties, such as mechanical strength, must match the properties of the surrounding tissue so that tissue function can be restored immediately. Additionally, the microenvironment has to promote diffusion of nutrients or metabolic wastes, support cell viability, and provide ease of cell seeding [134]. Therefore, the usage of biodegradable synthetic polymers offers a number of advantages for developing scaffolds. For instance, biodegradable polymers provide mechanical support during tissue growth and then gradually degrade at a desired rate. In addition to being able to control degradation kinetics, other desired properties such as mechanical strength, geometric shapes, pore sizes, and morphologic features, can be manipulated to be conducive for tissue growth. Furthermore, polymers can also be designed with chemical functional groups within their polymer network or the functional groups can be attached to the polymer backbone. These attached chemical functional groups can induce and enhance a number of cellular functions such as cell signaling and adhesion to promote tissue growth.

An important synthetic polymer, and the one used in the work of this dissertation, is poly(ethylene glycol) (PEG). PEG is hydrophilic and biocompatible with properties that limit immunogenicity and antigenicity, with minimal protein and cell adhesion [138, 139]. These properties make PEG an attractive polymer for scaffold development in cell-based tissue engineering applications [140, 141]. For example,

photo-curable hydrogels that are PEG-based are widely used to encapsulate cells into scaffolds because of the hydrogels' inert and non-immunogenic nature [94, 139, 142-145]. However, scaffolds with incorporated PEG chains can be modified with bioactive peptides to do the reverse, i.e. induce cellular behavior such as adhesion to proteins [146-148]. PEG is not naturally degradable but similarly to PEG chains' stealth characteristics, PEG chains' degradation properties can be altered to make them degradable by adding degradable linkages. Sawhney et al. showed that by integrating hydrolytically degradable PLA and PGA units with PEG monomers, they could create degradable constructs [149]. This process is done by first end-capping the PEG macromers with acrylate groups and then photopolymerizing the PEG to cross-link the PLA and PGA onto the PEG chains. [149]. Tighter cross-links can be created by using lower molecular weight PEG monomers, making this system a tunable one for the desired degradation rate.

2.8.2 Enzymatically Degradable Scaffolds in Tissue Engineering

One method of regenerating tissue is by combining isolated cells with appropriate bioactive agents in a biomaterial scaffold, which supports the production of the tissue matrix. It is widely recognized that scaffold architecture can greatly influence the behavior of cells on tissue-engineering constructs. The structural environment, cell-biomaterial interaction, and biological signals incorporated in the scaffold are all essential elements that play an important role in tissue development [150]. Biodegradability and biocompatibility of the polymer are also important elements in promoting cellular function *in vivo*, as the degradation kinetics of the scaffold influences cell morphology, spreading and migrating encapsulated cells [151].

Matrix metalloproteinases (MMPs) are proteolytic enzymes that are secreted by cells in order to degrade certain components of the extracellular matrix (ECM) during ECM remodeling. Both the Healy and Hubbell research groups have taken advantage of this key concept by incorporating MMP sensitive peptides into their scaffold designs to make the scaffolds degradable [152-154]. It has been shown that osteoblasts secrete MMP-13, which functions in degrading type II collagen during bone remodeling [152]. The expression of MMP-13 during bone remodeling and its specificity for collagens is what makes MMP-13 sensitive crosslinkers ideal candidates for integration into hydrogel designs that foster bone regeneration. Healy et al. have specifically used MMP-13 degradable peptide crosslinkers to develop thermoresponsive p(NIPAAm-co-AAc) semi-interpenetrating polymer networks (sIPNs) [152]. Healy and colleagues showed that the degradation of the peptide occurred in an enzyme dose-dependent manner. Additionally, Healy et al. showed that the enzymatic degradation products did not significantly affect cell viability. Hubbell et al. developed PEG hydrogels that contain MMP-2 cleavable crosslinks in their polymer backbone making the hydrogel sensitive to proteolytic degradation via cell-derived MMP-2 [154]. The advantage of designing a material with proteolytic sensitivity is that migrating cells could systematically degrade the synthetic polymer and eventually anchor onto the exposed ECM.

2.8.3 Natural Polymers in Cartilage Tissue Engineering

There are a vast number of naturally derived polymers that have been used for tissue engineering purposes. Some of these natural polymers include ECM proteins such as collagen, glycosaminoglycan, and chitosan [155]. Sebra et al. demonstrated that collagen type I can be grafted onto polymer substrates to promote cellular adhesion through the use of cell-adhesive peptide moieties within the structure of collagen type I

[156]. Nettles et al. demonstrated that chitosan scaffolds can support chondrocyte attachment and cartilaginous matrix biosynthesis. Nettles and colleagues showed that chondrocytes grown on chitosan scaffolds can synthesize an extracellular matrix containing proteoglycans and type II collagen [157].

As discussed in Section 2.1, proteoglycans are one of the major macromolecules found in articular cartilage. These molecules consist of a core protein and covalently attached glycosaminoglycan (GAG) chains. The GAGs are long, unbranched heteropolysaccharides, consisting of repeated disaccharide units. The cartilage-specific GAGs include chondroitin 4-sulfate, chondroitin 6-sulfate, keratan sulfate, and dermatan sulfate [158].

A brief recap here, chondroitin sulfate (CS) is a sulfated GAG composed of a chain of alternating sugars consisting of N-acetylgalactosamine and glucuronic acid. Chondroitin sulfate is a major component of the ECM of cartilage and functions in maintaining the structural integrity, by retaining water and nutrients, and allowing movement of other molecules through cartilage [158]. The ability of molecules to diffuse through cartilage is essential due to the fact that there is no blood supply to the cartilage. The attachment of CS to proteins forming proteoglycans is what gives cartilage its elasticity and is also believed to play a role in cartilage formation and repair. The tightly packed and highly charged sulfate groups of chondroitin sulfate generate electrostatic repulsion which provides the compression resistance of cartilage [93, 159].

CS is a great candidate to use as scaffolding material because it is a natural component of the cartilage ECM and is naturally degraded by chondroitinase, which are produced by chondrocytes. Since CS is such an important component of the cartilage ECM, many researchers have used them to investigate MSC chondrogenesis [93, 160-163]. Varghese et al. were able to show that encapsulated chondrocytes within CS

biogels remain viable, therefore demonstrating the potential of these biogels for cartilage tissue engineering [93]. Additionally, Varghese et al. combined PEG, a synthetic polymer, with CS to form a synthetic-biological composite hydrogel scaffold for differentiating mesenchymal stem cells (MSCs) [93]. Here. In this study, Varghese and colleague were able to demonstrate that the incorporation of CS as a scaffold component enhances chondrogenic differentiation of MSCs [93]. In addition, van Susante et al. attached CS on type I collagen scaffolds and studied its effect on the cell proliferation and matrix production of encapsulated chondrocytes. Van Susante et al. showed that CS can be used as a biochemical component of a cell-delivery scaffold in tissue engineering articular cartilage [163]. Pek et al. evaluated the properties of collagen-CS scaffolds based on different methods of crosslinking; non-crosslinks, physical crosslinks, chemical crosslinks, and the combination of both physical and chemical crosslinks [161]. Pek et al. demonstrated that the swelling ratio, compressive modulus, and enzymatic degradation are all affected by the different crosslinking methods. Pek and colleagues found that the chemically crosslinked collagen-CS scaffolds resulted in matrices with higher inverse swelling ratio, higher compressive modulus, and slower degradation rates than the non-crosslinked or physically crosslinked matrices. This study showed that CS allows the scaffold to have tunable properties via chemical crosslinking, further proving CS' potential for use as a scaffold material for tissue engineering [161].

Again briefly, hyaluronan, also known as hyaluronic acid or hyaluronate (HA), is a non-sulfated GAG that is an important component of articular cartilage. HA is an important cartilage GAG because it is one of the major components in synovial fluid and contributes significantly to cell proliferation and cell migration as well as wound healing and tissue hydrodynamics. HA can form large highly negatively-charged aggregates when bound to aggrecan. The aggregates imbibe water and are responsible for the

resilience of cartilage [157]. Many unique properties of HA, including its biocompatibility, viscoelasticity, and lack of immunogenicity, have made it an appealing material for tissue engineering. Additionally, purified HA has been employed as a structural biomaterial because of its high molecular weight and gel forming ability [158]. Leach et al. demonstrated that the physical properties of their GMHA (glycidyl methacrylate-HA) hydrogels, such as swelling ratio, crosslink density, mesh size, and complex modulus, can be fine-tuned by simply varying the levels of methacrylation during their GMHA synthesis process [164]. Yoo and colleagues showed that chondrocytes that were seeded with HA modified poly(lactic-*co*-glycolic acid) (PLGA) scaffolds had increased cellular attachment, GAG, and total collagen production over unmodified PLGA scaffolds [165]. Nettles et al. demonstrated that their HA-MA (photo-crosslinkable hyaluronan) formulation promoted the retention of the chondrogenic phenotype and cartilage matrix synthesis for encapsulated chondrocytes in vitro [166]. HA may be a potential candidate for a cell-carrier material in chondrocyte transplantation therapy as shown by Robinson et al. [167]. Additionally, Butnariu-Ephrat et al. demonstrated that bone-marrow-derived mesenchymal cells, delivered in HA hydrogels, have the potential for cartilage resurfacing in animal models [168]. These studies and others have determined that HA-based hydrogels have great potential in tissue engineering.

2.9 FIGURES

Figure 2.1 Schematic of the Extracellular Matrix (ECM) of Articular Cartilage showing chondroitin sulfate (CS), hyaluronic acid (HA) and Type II collagen as components of the ECM [6].

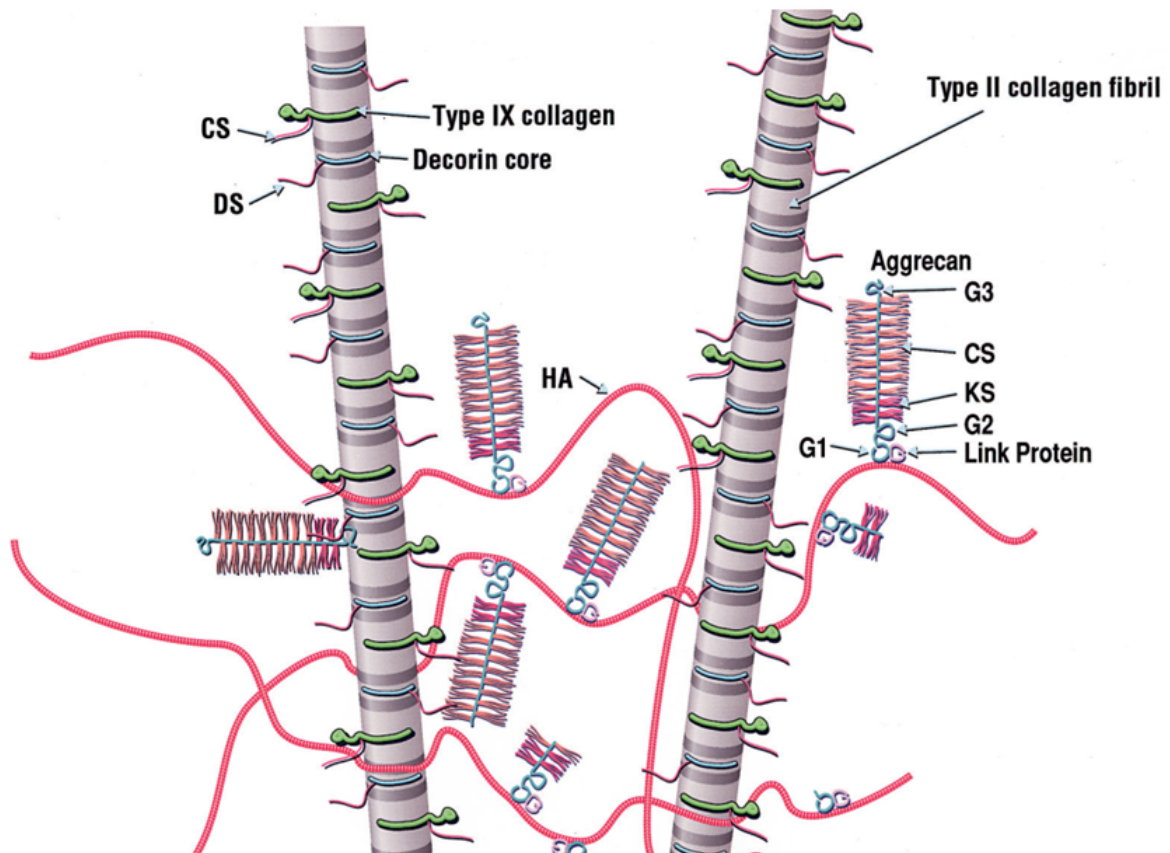


Figure 2.2 Schematic of the Proteoglycan Structure (A) Details of proteoglycan monomer structure showing chains of chondroitin sulfate (CS) and keratan sulfate (KS) as well as the attachment of the monomer to the hyaluronic acid chain via a link protein. (B) Molecular conformation of a typical proteoglycan aggregate showing size of the molecule [7].

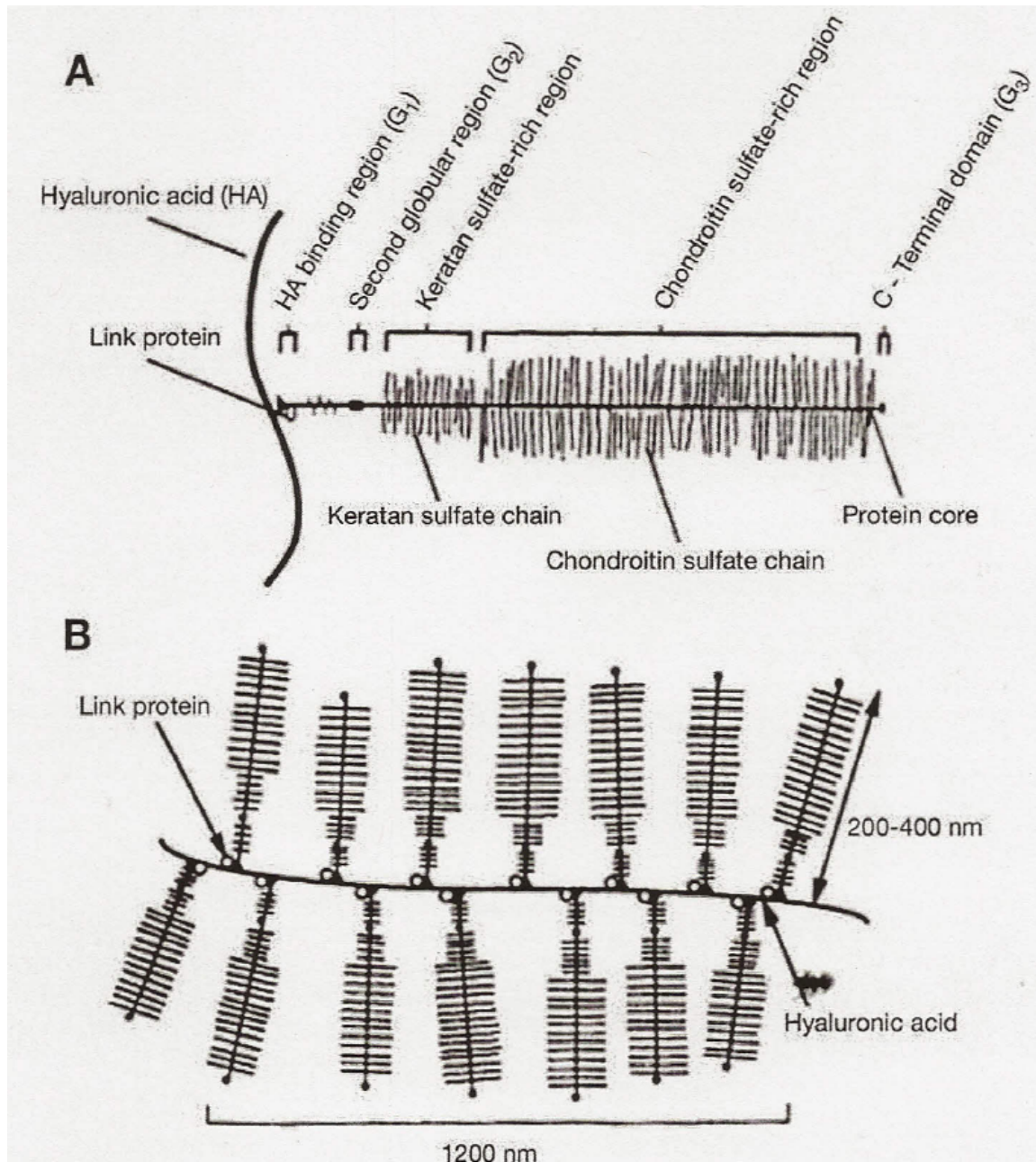


Figure 2.3 Schematic of Articular Cartilage Organization showing the four distinctive zones: the superficial, transitional, deep, and calcified zone (adopted from Poole 2001[6]).

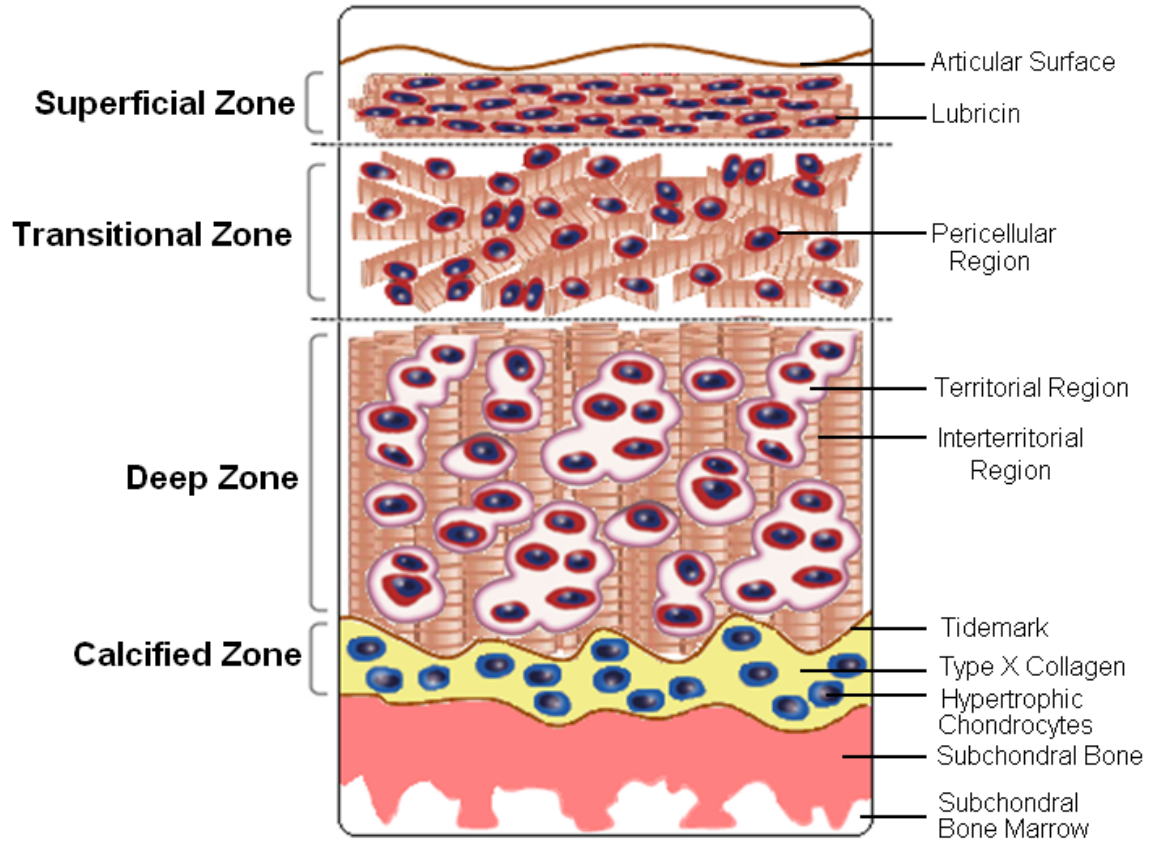


Figure 2.4 Illustration and Endoscopic Images of Normal and Damage Cartilage [29].

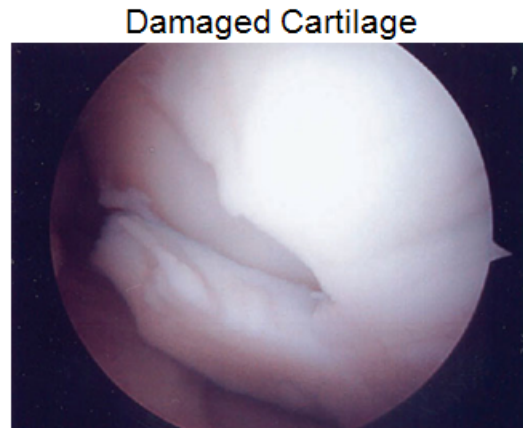
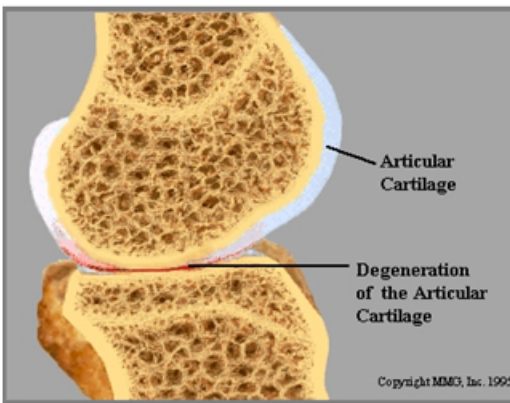
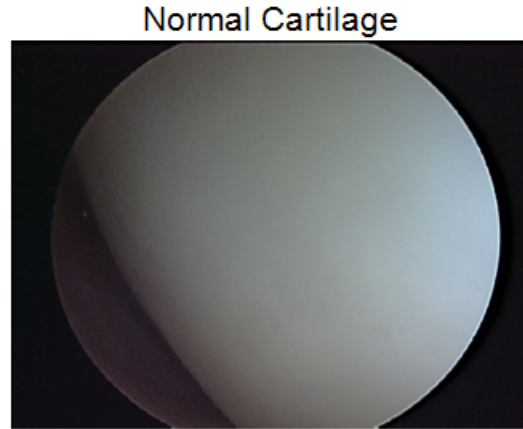
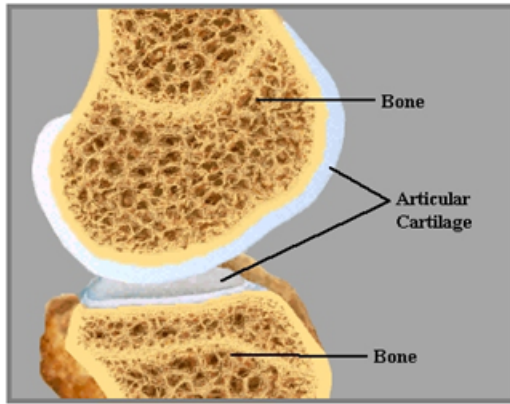


Figure 2.5 Illustration and Endoscopic Images of Current Cartilage Repair Strategies (A) Debridement (B) Microfracture Surgery (C) Osteochondral Transplants [36].

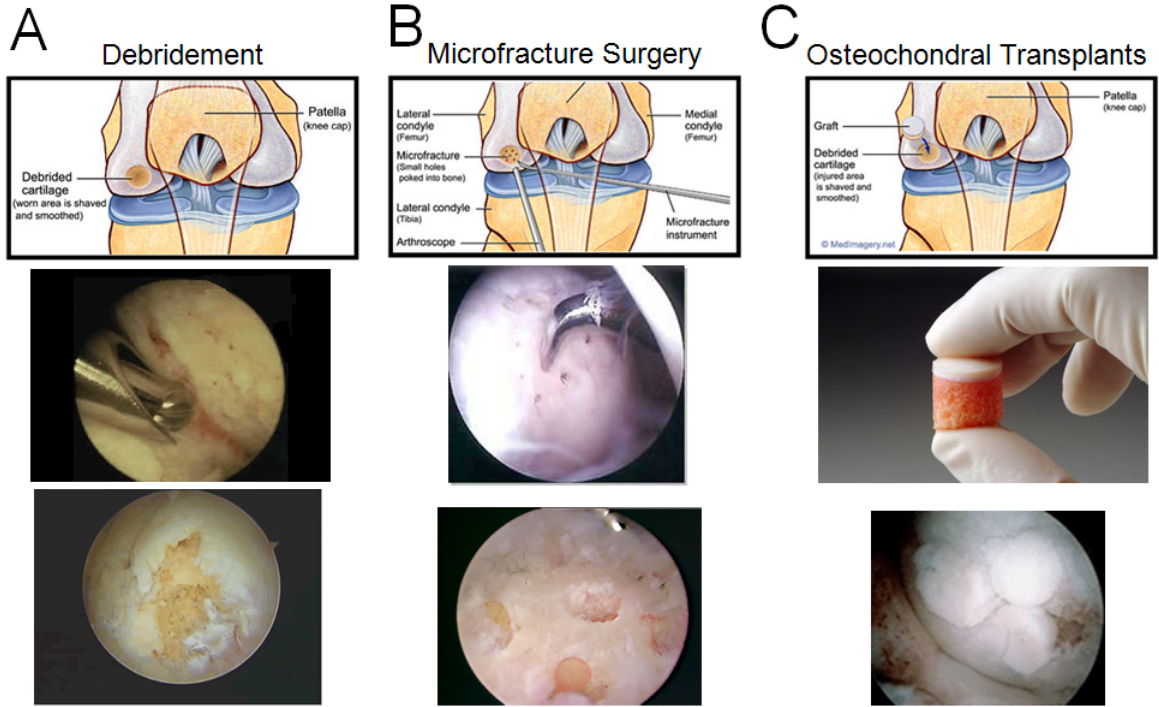


Figure 2.6 Illustration of the Autologous Chondrocyte Implantation (ACI) surgical technique for repair of chondral defect in the knee joint [5]. Surgical images of a chondral defect and a defect treated with ACI.

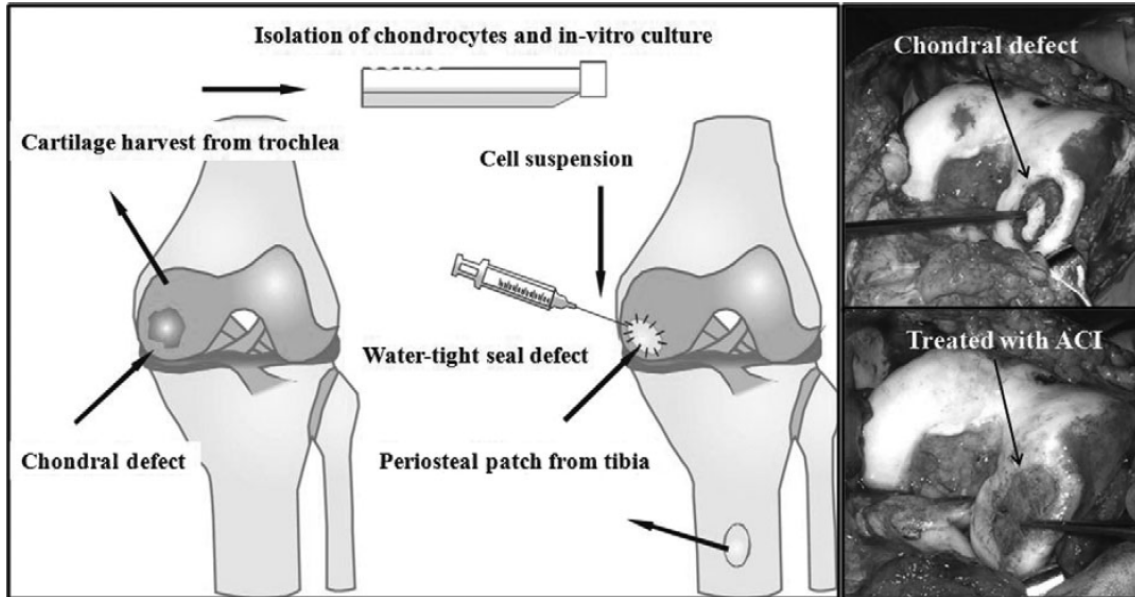


Figure 2.7 Various Differentiation Pathways of Mesenchymal Stem Cells (MSCs) [88].

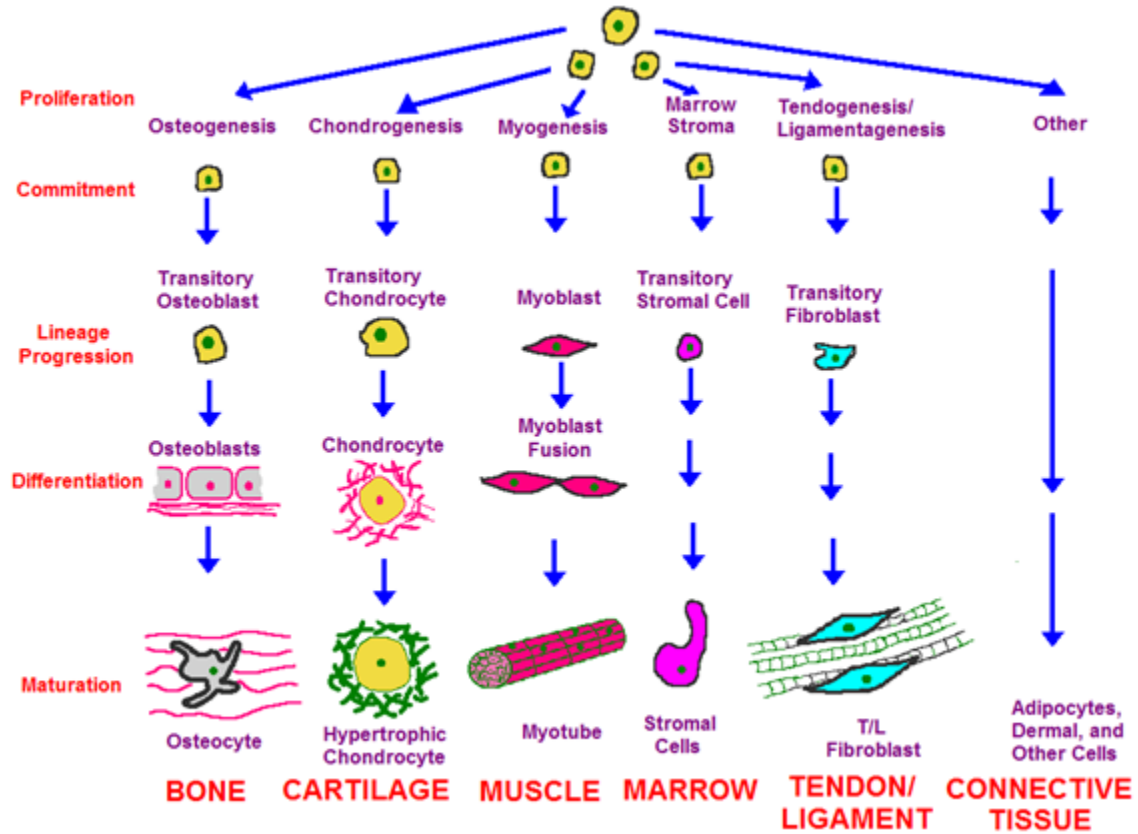
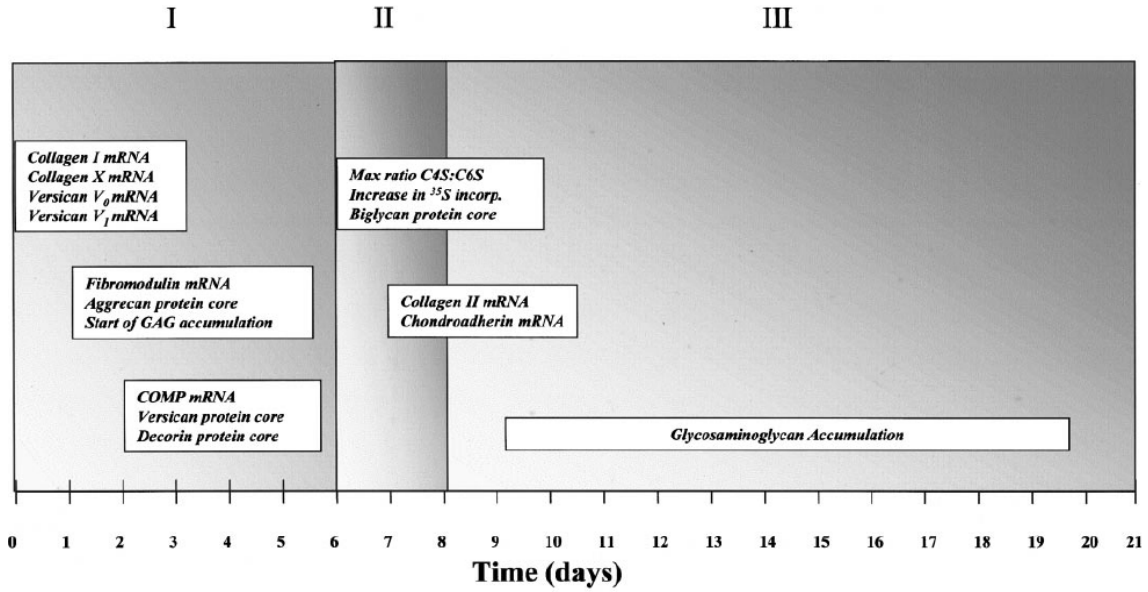


Figure 2.8 Schematic of the of MSC Chondrogenic Differentiation which illustrates the sequential expression of matrix components [30].



2.10 REFERENCES

1. Guilak, F., D.L. Butler, and S.A. Goldstein, *Functional tissue engineering: the role of biomechanics in articular cartilage repair*. Clin Orthop Relat Res, 2001(391 Suppl): p. S295-305.
2. Song, L., D. Baksh, and R.S. Tuan, *Mesenchymal stem cell-based cartilage tissue engineering: cells, scaffold and biology*. Cytotherapy, 2004. **6**(6): p. 596-601.
3. Higgs, G.B. and A.L. Boland. *Cartilage Regeneration and Repair, Where Are We?* 2007 [cited 2007 June 27, 2007]; Available from: http://www.orthojournalhms.org/volume1/html/cartilage_repair.html.
4. Erggele, C., et al., *Principles of Cartilage Repair*, ed. G. Volkert. 2008, Sturtz GmbH, Wurzburg Germany: Steinkopff Verlag. 121.
5. Bhosale, A.M. and J.B. Richardson, *Articular cartilage: structure, injuries and review of management*. Br Med Bull, 2008. **87**: p. 77-95.
6. Poole, A.R., et al., *Composition and structure of articular cartilage: a template for tissue repair*. Clin Orthop Relat Res, 2001(391 Suppl): p. S26-33.
7. Williams, R.J., L. Peterson, and B. Cole, *Cartilage Repair Strategies*. 2007, New Jersey: Humana Press Inc. 374.
8. Flik, K.R., et al., *Articular Cartilage*, in *Cartilage Repair Strategies*. 2007, Humana Press Inc.: New Jersey. p. 374.
9. Klein, T.J., et al., *Tissue Engineering of Articular Cartilage with Biomimetic Zones*. Tissue Eng Part B Rev, 2009.

10. Patel, R.V. and J.J. Mao, *Microstructural and elastic properties of the extracellular matrices of the superficial zone of neonatal articular cartilage by atomic force microscopy*. Front Biosci, 2003. **8**: p. a18-25.
11. Schinagl, R.M., et al., *Depth-dependent confined compression modulus of full-thickness bovine articular cartilage*. J Orthop Res, 1997. **15**(4): p. 499-506.
12. Bhosale, A., H. J., et al., *Articular cartilage: structure, injuries and review of managementA curriculum for the ideal orthopaedic residency*. Academic Orthopaedic Society. Br Med BullClin Orthop Relat Res: p. 77-95270-81.
13. Einhorn, T.A., R.J. O'Keefe, and J.A. Buckwalter, *Orthopaedic Basic Science Foundations of Clinical Practice*. 3 ed. 2007: American Academy of Orthopaedic Surgeons.
14. Bhosale, A.M., E.B., et al., *Articular cartilage: structure, injuries and review of managementCartilage Structure in Humans and Experimental Animals* Br Med BullArticular Cartilage Structure and Osteoarthritis, 20081992. **87**: p. 77-95183-199.
15. Grodzinsky, A.J., et al., *Cartilage tissue remodeling in response to mechanical forces*. Annu Rev Biomed Eng, 2000. **2**: p. 691-713.
16. Mow, V.C., M.H. Holmes, and W.M. Lai, *Fluid transport and mechanical properties of articular cartilage: a review*. J Biomech, 1984. **17**(5): p. 377-94.
17. Lu, L., R.G. Valenzuela, and M.J. Yaszemski, *Articular Cartilage Tissue Engineering*. e-biomed: The Journal of Regenerative Medicine. , 2000. **1**(7): p. 99-114.
18. Felson, D.T., et al., *Osteoarthritis: new insights. Part 1: the disease and its risk factors*. Ann Intern Med, 2000. **133**(8): p. 635-46.

19. Felson, D.T., et al., *Osteoarthritis: new insights. Part 2: treatment approaches*. Ann Intern Med, 2000. **133**(9): p. 726-37.
20. Tare, R.S., et al., *Tissue engineering strategies for cartilage generation--micromass and three dimensional cultures using human chondrocytes and a continuous cell line*. Biochem Biophys Res Commun, 2005. **333**(2): p. 609-21.
21. Redman, S.N., et al., *The cellular responses of articular cartilage to sharp and blunt trauma*. Osteoarthritis Cartilage, 2004. **12**(2): p. 106-16.
22. Smedslund, G., et al., *Effectiveness and safety of dietary interventions for rheumatoid arthritis: a systematic review of randomized controlled trials*. J Am Diet Assoc. **110**(5): p. 727-35.
23. *Osteoarthritis: national clinical guideline for care and management in adults*, T.N.C.C.f.C. Conditions, Editor. 2008, Royal College of Physicians: London. p. 3-10.
24. Novick, N. *Cartilage Regeneration - An Overview*. 2007 6/4/2003 [cited 2007 June 27, 2007].
25. Mathison, D.J. and S.J. Teach, *Approach to knee effusions*. Pediatr Emerg Care, 2009. **25**(11): p. 773-86; quiz 787-8.
26. Poolsup, N., et al., *Glucosamine long-term treatment and the progression of knee osteoarthritis: systematic review of randomized controlled trials*. Ann Pharmacother, 2005. **39**(6): p. 1080-7.
27. Majithia, V. and S.A. Geraci, *Rheumatoid arthritis: diagnosis and management*. Am J Med, 2007. **120**(11): p. 936-9.
28. Meyer, U. and H.P. Wiesmann, *Bone and Cartilage Engineering*, ed. G. Schroder. 2006, Berlin Heidelberg: Springer Verlag. 264.

29. Marcus, N.A. *Virginia Carilage Institute*. 2010 [cited 2010 July 3, 2010]; Available from: www.normanmarcusmd.com.
30. Barry, F., et al., *Chondrogenic differentiation of mesenchymal stem cells from bone marrow: differentiation-dependent gene expression of matrix components*. *Exp Cell Res*, 2001. **268**(2): p. 189-200.
31. Hall, B.K., *Bones and Cartilage Developmental and Evolutionary Skeletal Biology*. 2005, San Diego: Elsevier Academic Press. 760.
32. Johnstone, B., et al., *In vitro chondrogenesis of bone marrow-derived mesenchymal progenitor cells*. *Exp Cell Res*, 1998. **238**(1): p. 265-72.
33. Soloman, D.J., R.J. Williams, and R.F. Warren, *Marrow Stimulation and Microfracture for the Repair of Articular Cartilage Lesions*, in *Cartilage Repair Strategies*. 2007, Humana Press Inc.: New Jersey. p. 374.
34. Petersen, J.P., et al., *Present and Future Therapies of Articular Cartilage Defects*. *European Journal of Trauma*, 2003: p. 10.
35. Jackson, R.W. and C. Dieterichs, *The results of arthroscopic lavage and debridement of osteoarthritic knees based on the severity of degeneration: a 4- to 6-year symptomatic follow-up*. *Arthroscopy*, 2003. **19**(1): p. 13-20.
36. Abboudi, J., et al. *Cartilage Injuries and Restoration*. 2010 January 6, 2010 [cited 2010 June 23]; Available from: www.orthspec.com/cartilage_sports_injuries.htm.
37. Czitrom, A.A., et al., *Bone and cartilage allotransplantation. A review of 14 years of research and clinical studies*. *Clin Orthop Relat Res*, 1986(208): p. 141-5.
38. Tomford, W.W., D.S. Springfield, and H.J. Mankin, *Fresh and frozen articular cartilage allografts*. *Orthopedics*, 1992. **15**(10): p. 1183-8.

39. Langer, F., et al., *The immunogenicity of allograft knee joint transplants*. Clin Orthop Relat Res, 1978(132): p. 155-62.
40. Redman, S.N., S.F. Oldfield, and C.W. Archer, *Current strategies for articular cartilage repair*. Eur Cell Mater, 2005. **9**: p. 23-32; discussion 23-32.
41. Haklar, U., et al., [*Mosaicplasty technique in the treatment of osteochondral lesions of the knee*]. Acta Orthop Traumatol Turc, 2008. **42**(5): p. 344-9.
42. Hangody, L., et al., *Arthroscopic autogenous osteochondral mosaicplasty for the treatment of femoral condylar articular defects. A preliminary report*. Knee Surg Sports Traumatol Arthrosc, 1997. **5**(4): p. 262-7.
43. Hangody, L., et al., *Autologous osteochondral mosaicplasty. Surgical technique*. J Bone Joint Surg Am, 2004. **86-A Suppl 1**: p. 65-72.
44. Brittberg, M., et al., *Treatment of deep cartilage defects in the knee with autologous chondrocyte transplantation*. N Engl J Med, 1994. **331**(14): p. 889-95.
45. Bartlett, W., et al., *Autologous chondrocyte implantation versus matrix-induced autologous chondrocyte implantation for osteochondral defects of the knee: a prospective, randomised study*. J Bone Joint Surg Br, 2005. **87**(5): p. 640-5.
46. Gooding, C.R., et al., *A prospective, randomised study comparing two techniques of autologous chondrocyte implantation for osteochondral defects in the knee: Periosteum covered versus type I/III collagen covered*. Knee, 2006. **13**(3): p. 203-10.
47. Basad, E., et al., *Matrix-induced autologous chondrocyte implantation versus microfracture in the treatment of cartilage defects of the knee: a 2-year randomised study*. Knee Surg Sports Traumatol Arthrosc, 2010. **18**(4): p. 519-27.

48. Marlovits, S., et al., *Early postoperative adherence of matrix-induced autologous chondrocyte implantation for the treatment of full-thickness cartilage defects of the femoral condyle*. *Knee Surg Sports Traumatol Arthrosc*, 2005. **13**(6): p. 451-7.
49. Bartlett, W., et al., *Autologous chondrocyte implantation at the knee using a bilayer collagen membrane with bone graft. A preliminary report*. *J Bone Joint Surg Br*, 2005. **87**(3): p. 330-2.
50. Horas, U., et al., [*Osteochondral transplantation versus autogenous chondrocyte transplantation. A prospective comparative clinical study*]. *Chirurg*, 2000. **71**(9): p. 1090-7.
51. Adamietz, P. *Synergy of transforming growth factor β -1 and insulin-like growth factor in stimulating formation of neocartilage by pig articular chondrocyte pellet culture*. in *2nd Fribourg International Symposium on Cartilage Repair*. 1997. Fribourg, Switzerland.
52. Stewart, M.C., et al., *Phenotypic stability of articular chondrocytes in vitro: the effects of culture models, bone morphogenetic protein 2, and serum supplementation*. *J Bone Miner Res*, 2000. **15**(1): p. 166-74.
53. Thirion, S. and F. Berenbaum, *Culture and phenotyping of chondrocytes in primary culture*. *Methods Mol Med*, 2004. **100**: p. 1-14.
54. Thomas, B., et al., *Differentiation regulates interleukin-1 β -induced cyclooxygenase-2 in human articular chondrocytes: role of p38 mitogen-activated protein kinase*. *Biochem J*, 2002. **362**(Pt 2): p. 367-73.
55. Bradham, D.M. and W.E. Horton, Jr., *In vivo cartilage formation from growth factor modulated articular chondrocytes*. *Clin Orthop Relat Res*, 1998(352): p. 239-49.

56. Mello, M.A. and R.S. Tuan, *High density micromass cultures of embryonic limb bud mesenchymal cells: an in vitro model of endochondral skeletal development*. *In Vitro Cell Dev Biol Anim*, 1999. **35**(5): p. 262-9.
57. Zhang, L., et al., *Chondrogenic differentiation of human mesenchymal stem cells: a comparison between micromass and pellet culture systems*. *Biotechnol Lett*, 2010.
58. Lash, J.W., H. Holtzer, and M.W. Whitehouse, *In vitro studies on chondrogenesis; the uptake of radioactive sulfate during cartilage induction*. *Dev Biol*, 1960. **2**: p. 76-89.
59. Yoo, J.U., et al., *The chondrogenic potential of human bone-marrow-derived mesenchymal progenitor cells*. *J Bone Joint Surg Am*, 1998. **80**(12): p. 1745-57.
60. Oyajobi, B.O., et al., *Expression of type X collagen and matrix calcification in three-dimensional cultures of immortalized temperature-sensitive chondrocytes derived from adult human articular cartilage*. *J Bone Miner Res*, 1998. **13**(3): p. 432-42.
61. Tallheden, T., et al., *Gene expression during redifferentiation of human articular chondrocytes*. *Osteoarthritis Cartilage*, 2004. **12**(7): p. 525-35.
62. Bernstein, P., et al., *Pellet culture elicits superior chondrogenic redifferentiation than alginate-based systems*. *Biotechnol Prog*, 2009. **25**(4): p. 1146-52.
63. Freed, L.E., et al., *Advanced tools for tissue engineering: scaffolds, bioreactors, and signaling*. *Tissue Eng*, 2006. **12**(12): p. 3285-305.
64. Pei, M., et al., *Bioreactors mediate the effectiveness of tissue engineering scaffolds*. *FASEB J*, 2002. **16**(12): p. 1691-4.
65. Vunjak-Novakovic, G., et al., *Dynamic cell seeding of polymer scaffolds for cartilage tissue engineering*. *Biotechnol Prog*, 1998. **14**(2): p. 193-202.

66. Vunjak-Novakovic, G., et al., *Bioreactor studies of native and tissue engineered cartilage*. *Biorheology*, 2002. **39**(1-2): p. 259-68.
67. Caplan, A.I., *Mesenchymal stem cells*. *J Orthop Res*, 1991. **9**(5): p. 641-50.
68. Biddulph, D.M., A.A. Capelhart, and T.C. Beasley, *Comparative effects of cytosine arabinoside and a prostaglandin E2 antagonist, AH6809, on chondrogenesis in serum-free cultures of chick limb mesenchyme*. *Exp Cell Res*, 1991. **196**(1): p. 131-3.
69. Chimal-Monroy, J. and L. Diaz de Leon, *Differential effects of transforming growth factors beta 1, beta 2, beta 3 and beta 5 on chondrogenesis in mouse limb bud mesenchymal cells*. *Int J Dev Biol*, 1997. **41**(1): p. 91-102.
70. Fitzsimmons, J.S., et al., *Serum-free media for periosteal chondrogenesis in vitro*. *J Orthop Res*, 2004. **22**(4): p. 716-25.
71. Frenz, D.A., et al., *Induction of chondrogenesis: requirement for synergistic interaction of basic fibroblast growth factor and transforming growth factor-beta*. *Development*, 1994. **120**(2): p. 415-24.
72. Gerecht, S., et al., *Hyaluronic acid hydrogel for controlled self-renewal and differentiation of human embryonic stem cells*. *Proc Natl Acad Sci U S A*, 2007. **104**(27): p. 11298-303.
73. Hegert, C., et al., *Differentiation plasticity of chondrocytes derived from mouse embryonic stem cells*. *J Cell Sci*, 2002. **115**(Pt 23): p. 4617-28.
74. Hwang, N.S., et al., *Effects of three-dimensional culture and growth factors on the chondrogenic differentiation of murine embryonic stem cells*. *Stem Cells*, 2006. **24**(2): p. 284-91.

75. Hwang, N.S., S. Varghese, and J. Elisseeff, *Derivation of chondrogenically-committed cells from human embryonic cells for cartilage tissue regeneration*. PLoS ONE, 2008. **3**(6): p. e2498.
76. Hwang, N.S., et al., *Enhanced chondrogenic differentiation of murine embryonic stem cells in hydrogels with glucosamine*. Biomaterials, 2006. **27**(36): p. 6015-23.
77. Hwang, N.S., et al., *Chondrogenic differentiation of human embryonic stem cell-derived cells in arginine-glycine-aspartate-modified hydrogels*. Tissue Eng, 2006. **12**(9): p. 2695-706.
78. Kramer, J., et al., *Embryonic stem cell-derived chondrogenic differentiation in vitro: activation by BMP-2 and BMP-4*. Mech Dev, 2000. **92**(2): p. 193-205.
79. Kramer, J., et al., *Mouse ES cell lines show a variable degree of chondrogenic differentiation in vitro*. Cell Biol Int, 2005. **29**(2): p. 139-46.
80. Kulyk, W.M., et al., *Promotion of embryonic chick limb cartilage differentiation by transforming growth factor-beta*. Dev Biol, 1989. **135**(2): p. 424-30.
81. Leonard, C.M., et al., *Role of transforming growth factor-beta in chondrogenic pattern formation in the embryonic limb: stimulation of mesenchymal condensation and fibronectin gene expression by exogenous TGF-beta and evidence for endogenous TGF-beta-like activity*. Dev Biol, 1991. **145**(1): p. 99-109.
82. Levenberg, S., et al., *Neurotrophin-induced differentiation of human embryonic stem cells on three-dimensional polymeric scaffolds*. Tissue Eng, 2005. **11**(3-4): p. 506-12.

83. Levenberg, S., et al., *Differentiation of human embryonic stem cells on three-dimensional polymer scaffolds*. Proc Natl Acad Sci U S A, 2003. **100**(22): p. 12741-6.
84. Liu, H. and K. Roy, *Biomimetic three-dimensional cultures significantly increase hematopoietic differentiation efficacy of embryonic stem cells*. Tissue Eng, 2005. **11**(1-2): p. 319-30.
85. Pelton, R.W., et al., *In situ hybridization analysis of TGF beta 3 RNA expression during mouse development: comparative studies with TGF beta 1 and beta 2*. Development, 1990. **110**(2): p. 609-20.
86. Toumadje, A., et al., *Pluripotent differentiation in vitro of murine ES-D3 embryonic stem cells*. In Vitro Cell Dev Biol Anim, 2003. **39**(10): p. 449-53.
87. Varghese, S., et al., *Chondrogenic differentiation of human embryonic germ cell derived cells in hydrogels*. Conf Proc IEEE Eng Med Biol Soc, 2006. **1**: p. 2643-6.
88. Dennis, J. and A.I. Caplan, *Bone Marrow Mesenchymal Stem Cells*, in *Stem Cells Handbook*, S. Sell, Editor. 2004, Humana Press: Totowa. p. 107-117.
89. Chen, F.H. and R.S. Tuan, *Mesenchymal stem cells in arthritic diseases*. Arthritis Res Ther, 2008. **10**(5): p. 223.
90. Li, W.J., et al., *Multilineage differentiation of human mesenchymal stem cells in a three-dimensional nanofibrous scaffold*. Biomaterials, 2005. **26**(25): p. 5158-66.
91. Marolt, D., et al., *Bone and cartilage tissue constructs grown using human bone marrow stromal cells, silk scaffolds and rotating bioreactors*. Biomaterials, 2006. **27**(36): p. 6138-49.

92. Meinel, L., et al., *Engineering cartilage-like tissue using human mesenchymal stem cells and silk protein scaffolds*. Biotechnol Bioeng, 2004. **88**(3): p. 379-91.
93. Varghese, S., et al., *Chondroitin sulfate based niches for chondrogenic differentiation of mesenchymal stem cells*. Matrix Biol, 2008. **27**(1): p. 12-21.
94. Williams, C.G., et al., *In vitro chondrogenesis of bone marrow-derived mesenchymal stem cells in a photopolymerizing hydrogel*. Tissue Eng, 2003. **9**(4): p. 679-88.
95. Zuk, P.A., et al., *Multilineage cells from human adipose tissue: implications for cell-based therapies*. Tissue Eng, 2001. **7**(2): p. 211-28.
96. Guilak, F., et al., *Clonal analysis of the differentiation potential of human adipose-derived adult stem cells*. J Cell Physiol, 2006. **206**(1): p. 229-37.
97. Estes, B.T., et al., *Extended passaging, but not aldehyde dehydrogenase activity, increases the chondrogenic potential of human adipose-derived adult stem cells*. J Cell Physiol, 2006. **209**(3): p. 987-95.
98. Mahmoudifar, N. and P.M. Doran, *Chondrogenic differentiation of human adipose-derived stem cells in polyglycolic acid mesh scaffolds under dynamic culture conditions*. Biomaterials, 2010. **31**(14): p. 3858-67.
99. Guilak, F., et al., *Control of stem cell fate by physical interactions with the extracellular matrix*. Cell Stem Cell, 2009. **5**(1): p. 17-26.
100. Jakobsen, R.B., et al., *Chondrogenesis in a hyaluronic acid scaffold: comparison between chondrocytes and MSC from bone marrow and adipose tissue*. Knee Surg Sports Traumatol Arthrosc, 2009.
101. Winter, A., et al., *Cartilage-like gene expression in differentiated human stem cell spheroids: a comparison of bone marrow-derived and adipose tissue-derived stromal cells*. Arthritis Rheum, 2003. **48**(2): p. 418-29.

102. Diekman, B.O., et al., *Chondrogenesis of adult stem cells from adipose tissue and bone marrow: induction by growth factors and cartilage-derived matrix*. Tissue Eng Part A, 2010. **16**(2): p. 523-33.
103. Afizah, H., et al., *A comparison between the chondrogenic potential of human bone marrow stem cells (BMSCs) and adipose-derived stem cells (ADSCs) taken from the same donors*. Tissue Eng, 2007. **13**(4): p. 659-66.
104. Huang, J.I., et al., *Chondrogenic potential of progenitor cells derived from human bone marrow and adipose tissue: a patient-matched comparison*. J Orthop Res, 2005. **23**(6): p. 1383-9.
105. Im, G.I., Y.W. Shin, and K.B. Lee, *Do adipose tissue-derived mesenchymal stem cells have the same osteogenic and chondrogenic potential as bone marrow-derived cells?* Osteoarthritis Cartilage, 2005. **13**(10): p. 845-53.
106. Kim, H.J. and G.I. Im, *Chondrogenic differentiation of adipose tissue-derived mesenchymal stem cells: greater doses of growth factor are necessary*. J Orthop Res, 2009. **27**(5): p. 612-9.
107. Puetzer, J.L., J.N. Petite, and E.G. Lobo, *Comparative Review of Growth Factors for Induction of Three-Dimensional In Vitro Chondrogenesis in Human Mesenchymal Stem Cells Isolated from Bone Marrow and Adipose Tissue*. Tissue Eng Part B Rev.
108. Di Cesare, P.E., et al., *Expression of cartilage oligomeric matrix protein by human synovium*. FEBS Lett, 1997. **412**(1): p. 249-52.
109. Dodge, G.R., et al., *Production of cartilage oligomeric matrix protein (COMP) by cultured human dermal and synovial fibroblasts*. Osteoarthritis Cartilage, 1998. **6**(6): p. 435-40.

110. Recklies, A.D., L. Baillargeon, and C. White, *Regulation of cartilage oligomeric matrix protein synthesis in human synovial cells and articular chondrocytes*. Arthritis Rheum, 1998. **41**(6): p. 997-1006.
111. Fife, R.S., B. Caterson, and S.L. Myers, *Identification of link proteins in canine synovial cell cultures and canine articular cartilage*. J Cell Biol, 1985. **100**(4): p. 1050-5.
112. Hamerman, D., et al., *Glycosaminoglycans produced by human synovial cell cultures*. Coll Relat Res, 1982. **2**(4): p. 313-29.
113. Pacifici, M., et al., *Development of articular cartilage: what do we know about it and how may it occur?* Connect Tissue Res, 2000. **41**(3): p. 175-84.
114. Allard, S.A., R.N. Maini, and K.D. Muirden, *Cells and matrix expressing cartilage components in fibroblastic tissue in rheumatoid pannus*. Scand J Rheumatol Suppl, 1988. **76**: p. 125-9.
115. Xue, C., et al., *Characterisation of fibroblast-like cells in pannus lesions of patients with rheumatoid arthritis sharing properties of fibroblasts and chondrocytes*. Ann Rheum Dis, 1997. **56**(4): p. 262-7.
116. Pei, M., et al., *Engineering of functional cartilage tissue using stem cells from synovial lining: a preliminary study*. Clin Orthop Relat Res, 2008. **466**(8): p. 1880-9.
117. Pei, M., F. He, and G. Vunjak-Novakovic, *Synovium-derived stem cell-based chondrogenesis*. Differentiation, 2008. **76**(10): p. 1044-56.
118. Fan, J., et al., *Chondrogenesis of Synovium-Derived Mesenchymal Stem Cells in Photopolymerizing Hydrogel Scaffolds*. J Biomater Sci Polym Ed, 2010.
119. Mackay, A.M., et al., *Chondrogenic differentiation of cultured human mesenchymal stem cells from marrow*. Tissue Eng, 1998. **4**(4): p. 415-28.

120. Mehlhorn, A.T., et al., *Differential expression pattern of extracellular matrix molecules during chondrogenesis of mesenchymal stem cells from bone marrow and adipose tissue*. Tissue Eng, 2006. **12**(10): p. 2853-62.
121. Capehart, A.A. and D.M. Biddulph, *Effects of a putative prostaglandin E2 antagonist, AH6809, on chondrogenesis in serum-free cultures of chick limb mesenchyme*. J Cell Physiol, 1991. **147**(3): p. 403-11.
122. Cancedda, R., F. Descalzi Cancedda, and P. Castagnola, *Chondrocyte differentiation*. Int Rev Cytol, 1995. **159**: p. 265-358.
123. Hayamizu, T.F., et al., *Effects of localized application of transforming growth factor beta 1 on developing chick limbs*. Dev Biol, 1991. **145**(1): p. 164-73.
124. Heine, U., et al., *Role of transforming growth factor-beta in the development of the mouse embryo*. J Cell Biol, 1987. **105**(6 Pt 2): p. 2861-76.
125. Inoue, H., et al., *Stimulation of cartilage-matrix proteoglycan synthesis by morphologically transformed chondrocytes grown in the presence of fibroblast growth factor and transforming growth factor-beta*. J Cell Physiol, 1989. **138**(2): p. 329-37.
126. Moses, H.L., et al., *Transforming growth factor production by chemically transformed cells*. Cancer Res, 1981. **41**(7): p. 2842-8.
127. Roberts, A.B., et al., *New class of transforming growth factors potentiated by epidermal growth factor: isolation from non-neoplastic tissues*. Proc Natl Acad Sci U S A, 1981. **78**(9): p. 5339-43.
128. Goessler, U.R., et al., *In-vitro analysis of the expression of TGFbeta - superfamily-members during chondrogenic differentiation of mesenchymal stem cells and chondrocytes during dedifferentiation in cell culture*. Cell Mol Biol Lett, 2005. **10**(2): p. 345-62.

129. Cheifetz, S., et al., *The transforming growth factor-beta system, a complex pattern of cross-reactive ligands and receptors*. Cell, 1987. **48**(3): p. 409-15.
130. Derynck, R., et al., *A new type of transforming growth factor-beta, TGF-beta 3*. EMBO J, 1988. **7**(12): p. 3737-43.
131. Chimal-Monroy, J., M.T. Bravo-Ruiz, and L. Diaz de Leon, *Regulation of chondrocyte differentiation by transforming growth factors beta 1, beta 2, beta 3, and beta 5*. Ann N Y Acad Sci, 1996. **785**: p. 241-4.
132. Graham, N.B., *Hydrogels: their future, Part II*. Med Device Technol, 1998. **9**(3): p. 22-5.
133. Graham, N.B., *Hydrogels: their future, Part I*. Med Device Technol, 1998. **9**(1): p. 18-22.
134. Bryant, S.J., et al., *Encapsulating chondrocytes in degrading PEG hydrogels with high modulus: engineering gel structural changes to facilitate cartilaginous tissue production*. Biotechnol Bioeng, 2004. **86**(7): p. 747-55.
135. Kim, B.S. and D.J. Mooney, *Development of biocompatible synthetic extracellular matrices for tissue engineering*. Trends Biotechnol, 1998. **16**(5): p. 224-30.
136. Muggli, D.S., A.K. Burkoth, and K.S. Anseth, *Crosslinked polyanhydrides for use in orthopedic applications: degradation behavior and mechanics*. J Biomed Mater Res, 1999. **46**(2): p. 271-8.
137. Elisseeff, J.H., et al., *Biological response of chondrocytes to hydrogels*. Ann N Y Acad Sci, 2002. **961**: p. 118-22.
138. Alcantar, N.A., E.S. Aydil, and J.N. Israelachvili, *Polyethylene glycol-coated biocompatible surfaces*. J Biomed Mater Res, 2000. **51**(3): p. 343-51.

139. Elisseeff, J., et al., *Controlled-release of IGF-I and TGF-beta1 in a photopolymerizing hydrogel for cartilage tissue engineering*. J Orthop Res, 2001. **19**(6): p. 1098-104.
140. Martens, P.J., S.J. Bryant, and K.S. Anseth, *Tailoring the degradation of hydrogels formed from multivinyl poly(ethylene glycol) and poly(vinyl alcohol) macromers for cartilage tissue engineering*. Biomacromolecules, 2003. **4**(2): p. 283-92.
141. Peppas, N.A., et al., *Physicochemical foundations and structural design of hydrogels in medicine and biology*. Annu Rev Biomed Eng, 2000. **2**: p. 9-29.
142. Bryant, S.J. and K.S. Anseth, *Controlling the spatial distribution of ECM components in degradable PEG hydrogels for tissue engineering cartilage*. J Biomed Mater Res A, 2003. **64**(1): p. 70-9.
143. Burdick, J.A. and K.S. Anseth, *Photoencapsulation of osteoblasts in injectable RGD-modified PEG hydrogels for bone tissue engineering*. Biomaterials, 2002. **23**(22): p. 4315-23.
144. Burdick, J.A., et al., *Delivery of osteoinductive growth factors from degradable PEG hydrogels influences osteoblast differentiation and mineralization*. J Control Release, 2002. **83**(1): p. 53-63.
145. Cruise, G.M., et al., *A sensitivity study of the key parameters in the interfacial photopolymerization of poly(ethylene glycol) diacrylate upon porcine islets*. Biotechnol Bioeng, 1998. **57**(6): p. 655-65.
146. Elisseeff, J., et al., *Transdermal photopolymerization for minimally invasive implantation*. Proc Natl Acad Sci U S A, 1999. **96**(6): p. 3104-7.

147. Elisseeff, J., et al., *Transdermal photopolymerization of poly(ethylene oxide)-based injectable hydrogels for tissue-engineered cartilage*. *Plast Reconstr Surg*, 1999. **104**(4): p. 1014-22.
148. Elisseeff, J., et al., *Photoencapsulation of chondrocytes in poly(ethylene oxide)-based semi-interpenetrating networks*. *J Biomed Mater Res*, 2000. **51**(2): p. 164-71.
149. Sawhney, A.S., et al., *Optimization of photopolymerized bioerodible hydrogel properties for adhesion prevention*. *J Biomed Mater Res*, 1994. **28**(7): p. 831-8.
150. Chapekar, M.S., *Tissue engineering: challenges and opportunities*. *J Biomed Mater Res*, 2000. **53**(6): p. 617-20.
151. Nuttelman, C.R., M.C. Tripodi, and K.S. Anseth, *In vitro osteogenic differentiation of human mesenchymal stem cells photoencapsulated in PEG hydrogels*. *J Biomed Mater Res A*, 2004. **68**(4): p. 773-82.
152. Kim, S., et al., *Synthetic MMP-13 degradable ECMs based on poly(N-isopropylacrylamide-co-acrylic acid) semi-interpenetrating polymer networks. I. Degradation and cell migration*. *J Biomed Mater Res A*, 2005. **75**(1): p. 73-88.
153. Kim, S. and K.E. Healy, *Synthesis and characterization of injectable poly(N-isopropylacrylamide-co-acrylic acid) hydrogels with proteolytically degradable cross-links*. *Biomacromolecules*, 2003. **4**(5): p. 1214-23.
154. Seliktar, D., et al., *MMP-2 sensitive, VEGF-bearing bioactive hydrogels for promotion of vascular healing*. *J Biomed Mater Res A*, 2004. **68**(4): p. 704-16.
155. Chen, G., Ushida, Takashi, Tateishi, Tetsuya, *Scaffold Design for Tissue Engineering*. *Macromolecular Bioscience*, 2002. **2**: p. 67-77.
156. Sebra, R.P., et al., *Controlled polymerization chemistry to graft architectures that influence cell-material interactions*. *Acta Biomater*, 2007. **3**(2): p. 151-61.

157. Nettles, D.L., Elder, Steven H. and Gibert, Jerome A., *Potential Use of Chitosan as a Cell Scaffold Material for Cartilage Tissue Engineering*. TISSUE ENGINEERING, 2002. **8**(6): p. 1009-1016.
158. Suh, J.K. and H.W. Matthew, *Application of chitosan-based polysaccharide biomaterials in cartilage tissue engineering: a review*. Biomaterials, 2000. **21**(24): p. 2589-98.
159. Kerin, A.J., M.R. Wisnom, and M.A. Adams, *The compressive strength of articular cartilage*. Proc Inst Mech Eng [H], 1998. **212**(4): p. 273-80.
160. Li, Q., et al., *Photocrosslinkable polysaccharides based on chondroitin sulfate*. J Biomed Mater Res A, 2004. **68**(1): p. 28-33.
161. Pek, Y.S., et al., *Degradation of a collagen-chondroitin-6-sulfate matrix by collagenase and by chondroitinase*. Biomaterials, 2004. **25**(3): p. 473-82.
162. Rapp, A., et al., *Evaluation of chondroitin sulfate bioactivity in hippocampal neurones and the astrocyte cell line U373: influence of position of sulfate groups and charge density*. Basic Clin Pharmacol Toxicol, 2005. **96**(1): p. 37-43.
163. van Susante, J.L.C., et al., *Linkage of chondroitin-sulfate to type I collagen scaffolds stimulates the bioactivity of seeded chondrocytes in vitro*. Biomaterials, 2001. **22**(17): p. 2359-69.
164. Leach, B.J., Bivens, K. A. Patrick, C. W., Jr., Schmidt, C. E., *Photocrosslinked hyaluronic acid hydrogels: natural, biodegradable tissue engineering scaffolds*. Biotechnol Bioeng, 2003. **82**(5): p. 578-89.
165. Yoo, H.S., et al., *Hyaluronic acid modified biodegradable scaffolds for cartilage tissue engineering*. Biomaterials, 2005. **26**(14): p. 1925-33.
166. Nettles, D.L., et al., *Photocrosslinkable hyaluronan as a scaffold for articular cartilage repair*. Ann Biomed Eng, 2004. **32**(3): p. 391-7.

167. Robinson, D., N. Halperin, and Z. Nevo, *Regenerating hyaline cartilage in articular defects of old chickens using implants of embryonal chick chondrocytes embedded in a new natural delivery substance*. *Calcif Tissue Int*, 1990. **46**(4): p. 246-53.
168. Butnariu-Ephrat, M., et al., *Resurfacing of goat articular cartilage by chondrocytes derived from bone marrow*. *Clin Orthop Relat Res*, 1996(330): p. 234-43.
169. Sharma, B., et al., *Designing zonal organization into tissue-engineered cartilage*. *Tissue Eng*, 2007. **13**(2): p. 405-14.

CHAPTER THREE

ECM Mimicking Hydrogel Scaffolds for Cartilage Tissue Engineering

3.1 INTRODUCTION

The essence of tissue engineering is in the usage of synthetic or natural materials to engineer biomaterials to replace damaged or defective tissues in humans. The polymer scaffold is an important component of tissue engineering. Scaffolds made from natural or synthetic materials can be implanted temporarily into the body. Scaffolds can either degrade and absorbed into the body or be removed. Removal of scaffolds can be invasive, time consuming, and costly to the patients, thus for patient compliance purposes, degradable scaffolds are more attractive in tissue engineering applications. Degradable scaffolds can function as matrices or templates that allow cells to grow and subsequently form new tissues while the scaffolds gradually degrade [1].

In cartilage tissue engineering, degradability and cell-induced remodeling of the hydrogel microenvironment are key elements for successful tissue generation, as the degradation kinetics of the scaffold influences cell morphology, spreading, and migration [2]. Poly(ethylene glycol) (PEG) is a synthetic polymer that is widely used for scaffold development in cell-based cartilage tissue engineering applications because it is biocompatible and can be easily functionalized [3-12]. Although PEG is not naturally degradable, many investigators including Anseth and coworkers have shown that PEG hydrogels can be made hydrolytically degradable by crosslinking poly(lactic acid) (PLA) monomers into the hydrogel network, creating an acidic environment as a result [13].

Alternatively, synthetic peptide sequences that are degradable by cell-specific collagenase have been used to make PEG enzymatically degradable. Enzymatic

degradation allows for cell specific degradation as well as eliminates the creation of an acidic environment. Matrix metalloproteinases (MMPs) are proteolytic enzymes that are secreted by cells in order to degrade and remodel the extracellular matrix (ECM). Several investigators have taken advantage of this key concept by incorporating MMP - sensitive peptides (MMP-pep) into their scaffold design to make them degradable when exposed to the MMP enzymes [14-16]. Kim et al. demonstrated that osteoblasts secrete MMP-13, which functions in degrading type II collagen during remodeling [14]. Healy and colleagues developed thermoresponsive p(NIPAAm-coAAc) semi-interpenetrating polymer networks (sIPNs) with MMP-13 as degradable crosslinkers and showed that the degradation occurred in a dose-dependent manner. Additionally, this study they also showed that the enzymatic degradation products did not significantly affect cell viability. Hubbell et al. developed PEG hydrogels that are sensitive to proteolytic degradation by incorporating cell-derived MMP-2 peptide sequences onto the polymer backbone [16].

Unlike synthetic polymers, natural hydrogels have inherent biological sites for cell-mediated degradation. Thus, natural ECM proteins such as collagen and GAGs have been widely used for tissue engineering of cartilage [17]. For instance, chondroitin sulfate (CS) and hyaluronic acid (HA) are natural components of cartilage's extracellular matrix (ECM), and thus their incorporation into scaffolds helps mimic the physiological environment of native cartilage. Li et al. created CS-based hydrogels to enhance bioactivity of the scaffold and found that encapsulated chondrocytes remained viable within the hydrogels [18]. Pek et al. showed that CS incorporation into scaffolds allowed for tunable properties via chemical cross-linking [19]. Additionally, Hwang et al. examined the biological response of chondrocytes within PEG-based incorporating either type I collagen, HA, or CS. Hwang and colleagues found that CS-based

hydrogels exhibited the strongest response with high chondrogenic gene expression and matrix accumulation [20]. Another important component of articular cartilage is HA, which is a non-sulfated GAG constituent of synovial fluid. HA contributes significantly to cell proliferation and migration as well as wound healing and tissue hydrodynamics [21], characteristics which have made HA an appealing material for tissue engineering. Since HA has a high molecular weight and can easily form hydrogels, it has been employed by many investigators as a structural biomaterial [20, 22-26]. Butnariu-Ephrat et al. demonstrated that BMSCs encapsulated within HA hydrogels, have the potential for cartilage resurfacing in animal models [27]. Yoo et al. found that HA modified poly(lactide-co-glycolic acid) (PLGA) scaffolds increased cellular attachment, glycosaminoglycan (GAG), and total collagen production of seeded chondrocytes over unmodified PLGA scaffolds [26]. Nettles et al. showed that chondrocytes retained their chondrogenic phenotype and cartilage matrix synthesis when encapsulated within crosslinked methacrylated HA hydrogels [28]. Although these studies and others have determined that both CS and HA-based hydrogels individually have great potential in cartilage tissue engineering, there is still a lack of knowledge of the combined effects of CS, HA, and MMP-pep for cartilage regeneration.

In this chapter novel hydrogels containing a combination of CS, HA, and MMP-pep within a PEG-based hydrogel, were fabricated to investigate how each component affects the hydrogels' physical properties. The combination of both natural and synthetic biomaterials has not been previously explored. Thus this chapter evaluates whether or not their combination produces a synergistic effect on the differentiation of MSCs. The findings of this chapter indicate that hydrogels' physical properties can be tailored by altering their biomaterial composition. Chapter Four evaluates whether or not their combination produces a synergistic effect on the chondrogenic differentiation of MSCs.

3.2 MATERIALS AND METHODS

3.2.1 MMP-Sensitive Peptide Synthesis & Modification

The MMP-sensitive peptide (MMP-pep) (QPQGLAK: Gln-Pro-Gln-Gly-Leu-Ala-Lys) peptide shown in **Figure 3.1** was synthesized using an automatic peptide synthesizer (Protein Technologies, Inc. Symphony Quartet) and optimized protocols for the Fmoc/tBu solid-phase synthesis method. The Fmoc/tBu method utilizes orthogonal protecting groups, a base-labile N-Fmoc (9-fluorenylmethyl chloroformate) group to protect the α -amine and an acid-labile side-chain protecting group. An acid-labile rink resin was used for the synthesis of the C-terminal amidated peptide. After the peptide was synthesized, the resin was washed with N-Methylpyrrolidone (NMP), dichloromethane (Cl_2CH_2), and methanol (MeOH) three times each and dried on the synthesizer. The peptide was cleaved off the resin for 3 hours with a cleaving cocktail { CF_3COOH /triisopropylsilane/water (98:1:1, vol/vol/vol). The cleavage solution was concentrated using a stream of nitrogen and the peptide was precipitated with ether, followed by three ether washes and a lyophilization step overnight. After lyophilization the peptide was analyzed using a MALDI-TOF to ensure that the molecular weight matched the peptide sequence.

The MMP-pep was modified as illustrated in **Figure 3.2** by adding acrylate groups to the amine group of the N-terminal and to the amine group on the lysine. This acrylation method was done in aqueous solution and the pH was closely monitored to ensure the reaction continued at the proper pH. The success of the reaction was monitored by mass spectrometry to determine the optimal reaction time. Briefly, 10 mg of unprotected MMP-pep was dissolved in 1 mL of H_2O and 10 μL of DIPEA (N,N-Diisopropylethylamine) was added to the peptide solution. The pH was checked to

verify that the pH level was at 12 or 13. Once the pH was approximately at 12, then 2 μL of acryloyl chloride was added, the solution was vortexed and the reaction was allowed to occur for 1 minute. After 1 minute the pH was checked; if the pH level was too acidic then an aliquot of 10 μL DIPIA was added until the pH reached about 12 or 13. Again, once pH reached about 12, an additional aliquot of 2 μL of acryloyl chloride was added, vortexed and the reaction was allowed to continue for 1 more minute. These steps were repeated 12 more times, totaling 14 one-minute reactions. At the end of the last reaction time, 10 μL of DIPIA was added to raise the pH once again and to minimize side reactions. For analysis of the final product, 4 μL of the reaction solution was diluted with 196 μL of 50% methanol to determine the mass of the synthesized peptide on a MALDI-TOF. The reaction solution was purified using HPLC. The peptide was collected and lyophilized overnight. Nuclear Magnetic Resonance Spectroscopy (NMR) was performed on dried peptide to validate the ratio of peptide to acrylate groups.

3.2.2 Bioactivity of Modified MMP-Sensitive Peptide

The bioactivity of the modified MMP-pep was evaluated using an analytical HPLC. A 5 picomole/ μL concentration of the peptide was made by dissolving 2 mg of the dried modified peptide in 2 mL of dH_2O . An aliquot of 1.7 μL of the dissolved peptide was then added to 398.29 μL of TES (tris-EDTA) buffer as the control. Another aliquot of 1.7 μL was also added to 398.29 μL of TES containing collagenase (Collagenase Type 3, Worthington, Lakewood, NJ) to test for peptide cleavage. Both the control (peptide in TES buffer) and the peptide in TES buffer containing collagenase were allowed to sit at room temperature for 1 hour before being analyzed using a Beckman System Gold HPLC with a diode array detector. A reversed phase column was

used at room temperature (column: 0.8 mm x 250 mm, Jupiter 10 u C18 300 angstrom). Flow rate used was 120 μ L per minute. Two types of buffer were used, buffer A contained 0.1% TFA in Liquid Chromatography Mass Spectrometry (LC/MS) grade water, buffer B was 0.08% TFA in acetonitrile. The gradient was 0-2 minutes held at 0% B, 2-70 minutes linear gradient of 0-65% B, from 70-78 minutes 65-100% B, 78-82 minutes 100%, 82-84 minutes 100-0% B, and from 84 to 100 minutes at 0% B. Absorbance was monitored at 214 nm. **Figure 3.3** shows the chromatogram of the control peptide in TES buffer (red) and of the peptide in TES buffer containing collagenase (blue). The tall single peak in red clearly shows that the peptide did not degrade and the two shorter peaks in blue demonstrate that the peptide was cleaved into two fragments in the buffer containing the collagenase. The cleavage fragments of the MMP-pep indicated that the modified peptide is bioactive and degradable by collagenase.

3.2.3 Biopolymer Modification

Chondroitin Sulfate A (CS) was methacrylated using methods adopted from Li et al. [18] with slight modifications as shown in **Figure 3.4**. Briefly, 1 g of CS was dissolved in 10mL of PBS. 1 mL of glycidyl methacrylate was added to the CS solution and the reaction was stirred at room temperature for 15 days. After 15 days the CS was precipitated in acetone (1 part CS: 20 parts acetone). The precipitant was filtered with filter paper. The precipitant was re-dissolved in 100 mL of dH₂O then extracted with chloroform at equal volume (100 mL chloroform and 100 mL CS). CS was collected with a separation funnel then concentrated back to about 10mL with a rotavap. The concentrated CS solution was precipitated again in acetone (1:20). The precipitant was centrifuged and the acetone was removed and the precipitant was collected and dried

under vacuum for 48 hours. The CS was re-dissolved in water and lyophilized. NMR was performed on the dried sample to check the degree of acrylation.

Hyaluronic acid (HA) was methacrylated following a protocol adopted from Leach et al. [23] as shown in **Figure 3.5**. Briefly, 0.5 g of HA was dissolved in 25 mL of deionized water and 25 mL of acetone and mixed overnight. 3.6 mL of triethylamine was added to the solution and mixed thoroughly for 2 hours. 3.6 mL glycidyl methacrylate (GM) was then added and the reaction was allowed to occur at room temperature in a sealed flask for 24 hours. The GMHA solution was next precipitated in acetone (one part GMHA solution to 20 parts acetone). The GMHA solution was slowly added to the acetone while stirring with a glass rod. The GMHA precipitated as a cottony white solid and was collected on the glass stirrer. The precipitate was transferred to a dish and rinsed with acetone. The precipitate was then dissolved in 50 mL dH₂O overnight. The GMHA was re-precipitated in acetone, rinsed with acetone and dissolved in 50mL dH₂O overnight. The GMHA solution was then lyophilized for 48-72 hours. NMR was used to check the degree of acrylation.

3.2.3 Hydrogel Fabrication

A total of 10 groups of hydrogel scaffolds were fabricated using poly(ethylene glycol) dimethacrylate (PEGDA), MMP-pep, and the modified CS and HA biopolymers. The hydrogels were fabricated by dissolving the materials of each group in phosphate buffered saline (PBS, pH 7.4) containing 0.05 wt% photoinitiator, Irgacure 2959 (2-hydroxy-1-[4-(2-hydroxyethoxy) phenyl]-2-methyl-1propanone, Ciba Geigy Corp., McIntosh, AL) and polymerized using a long-wave ultraviolet lamp (Model B100AP, Blak-Ray) at the intensity of ~10 mW/cm² for 10 minutes. The 10 groups of hydrogels are listed in **Table 3.1**. Bryant et al. found that the crosslinking density of PEG

hydrogels influences the compressive modulus and the morphology of chondrocytes [29]. Leach et al. [22] created PEG-based hydrogels with 1-2% HA, Varghese et al. [30] incorporated equal volumes of 20% (w/v) PEG and 20% CS in their study and He et al. [31] fabricated poly(lactide ethylene oxide fumarate) (PLEOF) hydrogels with equimolar concentrations of the MMP-pep. Base on these studies, 20% (w/v) hydrogels were fabricated for the desired compressive strength and HA was incorporated at 1%, CS was incorporated at equal volume and MMP-pep was incorporated at equimolar ratio with PEG.

3.2.4 Hydrogel Characterization

The swelling ratio, compressive modulus, and enzymatic degradation of these hydrogels were examined. The swelling properties were determined by swelling the hydrogels after polymerization in PBS for 72 hours after equilibrium had been reached. The hydrogels were then lyophilized over night to obtain their dry weight. The changes in hydrogel weight between drying (W_{dry}) and swelling ($W_{swollen}$) were used to determine the volumetric swelling ratio and equilibrium water content which were calculated using the following formulas:

Equation 3.1: Swelling Ratio

$$Swollen \text{ Ratio, } Q = \left(\frac{W_{swollen} - W_{dry}}{W_{dry}} \right)$$

Equation 3.2: Equilibrium Water Content

$$\text{Equilibrium Water Content} = \left(\frac{W_{\text{swollen}} - W_{\text{dry}}}{W_{\text{swollen}}} \right)$$

The compressive modulus of the various swollen hydrogels were determined at room temperature on an In-spec 2200 Instron mechanical tester with a 125 N loading cell using a parallel plate apparatus and a loading of 20% of the initial thickness per second (0.1 mm/sec). The polymer solution was polymerized in a square mold (~ 2 mm high, ~ 7 mm wide, and ~ 7 mm long) for mechanical testing and was compressed to the maximum thickness of 2 mm. The compressive moduli of blank hydrogels were determined by analyzing the linear region of the stress versus the strain curve of the samples.

The degradation profiles of each hydrogel composition were determined. Briefly, the hydrogels were polymerized, swollen in PBS overnight, and then degraded in 1.5 mL of collagenase (25 $\mu\text{g}/\text{mL}$, Worthington), hyaluronidase (500 U/mL, Sigma) or chondroitinase (0.15 U/mL, Sigma) which was replaced every 72 hours throughout the study. The hydrogel samples were incubated at 37 °C on an orbital shaker and at various times during the course of the experiment the hydrogels were removed from the degradation solution and their swollen weights were weight was measured (n=3 per composition). The percent mass loss of the hydrogels was recorded over time based on the initial swollen weight (W_{initial}) and their weight at time t (W_{time}). The weight remaining percent was calculated using the following formula:

Equation 3.3: Hydrogel Weight Remaining

$$\text{weight remaining \%} = \left(1 - \frac{W_{\text{initial}} - W_{\text{time}}}{W_{\text{initial}}}\right) \times 100$$

3.2.5 Statistical Analysis

All quantitative data were expressed as mean \pm standard error and were verified by analysis of variance using student T-Test with equal variance. P values of less than 0.05 were considered statistically significant.

3.3 RESULTS

3.3.1 Material Synthesis & Modification

A molecular weight comparison of the synthesized peptide with the theoretical molecular weight of the peptide sequence was performed using MALDI-TOF on lyophilized peptides. **Figure 3.6A** represents the MALDI-TOF spectra of the unmodified peptide. Observed peaks at 739 [MH⁺], 761 [MH+Na⁺], and 779 [MH+Na+H₂O⁺] m/z (mass-to-ratio charge) indicate that the peptide with the correct sequence was synthesized. **Figure 3.6B** shows a proton NMR of the peptide before modification. **Figure 3.7A** represents the MALDI-TOF spectra of the modified peptide with observed peaks at 870 [Diacrylate MMP-pep+Na] m/z and 885 [Diacrylate MMP-pep+Na+H₂O⁺] m/z. The increase in molecular weight of 110 was due to the addition of the acrylate groups. **Figure 3.7B** shows a proton NMR of the modified peptide verifying that the MMP-pep was correctly modified. To analyze the degree of acrylation, the ratio of the integrals at 5.6 – 5.7 ppm and 6.0 – 6.2 ppm to the integral at 0.75 ppm

was obtained. The results indicate successful modification with two acrylate groups per peptide sequence.

The degrees of CS and HA acrylation were confirmed using NMR. **Figure 3.8A** shows the NMR of unmodified CS with an inset of the chemical structure and **Figure 3.8B** is an expanded NMR shows that there are no methacrylate protons near the anomeric proton peak at 5.14 ppm. **Figure 3.9A** shows the proton NMR spectra of the acrylated CS verifying modification and **Figure 3.9B** is the expanded NMR of the methacrylate portion showing the integrals of each individual peaks. The ratio was calculated by dividing the integral of one of the bound methacrylate proton peak at 5.5 ppm by the anomeric proton peak at 5.1 ppm, which yielded one acrylate group for every two units of CS. **Figure 3.10A** shows the NMR of unmodified HA with an inset of the chemical structure and **Figure 3.10B** is an expanded NMR that shows the HA methyl proton peak at 1.84 ppm. **Figure 3.11A** shows the proton NMR spectra of the acrylated HA with an inset of the chemical structure and **Figure 3.11B** is the expanded NMR of the methyl protons. The degree of HA acrylation was calculated by comparing the peaks at 1.92 ppm, which represents the methyl protons of HA, and 1.84 ppm which represents the methyl protons of the glycidyl methacrylate (GM) that has bounded to HA during acrylation. Calculation of the ratio of these two integrals yielded one acrylate group for every eight units of HA.

3.3.2 Hydrogel Characterization

The volumetric swelling ratios in **Figure 3.12A** demonstrate the ability of the hydrogels to absorb water. The hydrogel groups containing MMP-pep exhibited a lower swelling ratio than their corresponding matrices without MMP.-pep. However, the swelling ratio for the PEG hydrogel group was not significantly different from the PEG

hydrogels containing MMP-pep. Since the MMP-sensitive peptide sequence is short, the reduction in swelling ratio could be attributed to the decrease in mesh size during crosslinking. These results also suggest that CS aided in the absorption and retention of water which increased the equilibrium water content of the hydrogels containing CS. The equilibrium water content as shown in **Figure 3.12B** was similar for all hydrogel matrices containing CS with ratios of ~ 0.9 , whereas the hydrogel matrices without CS had lower ratios ranging from 0.76 to 0.86. The equilibrium water content of the hydrogel groups follows the same trend as their swelling ratios. The swelling ratio and equilibrium water content of the 20% w/v PEG hydrogels within this study are comparable to the values reported earlier by Bryant et al [29, 32]. The significant increase in the swelling ratio and equilibrium water content when CS is added to the PEG hydrogels is consistent with the results obtained by Li et al. who also found that pure CS hydrogels swelled and absorbed more water than PEG hydrogels [18].

The compressive moduli of the various swollen hydrogels represent their ability to withstand compression and are shown in **Table 3.2**. For the blank hydrogels, PEG, PEG:HA, and PEG:MMP,-pep had the highest compressive moduli, with no significant difference from each other. The addition of CS, MMP,-pep and the combined addition of HA and MMP-pep to the PEG hydrogels significantly ($p < 0.05$) decreased the compressive modulus. Interestingly, adding HA and MMP-pep alone to the PEG hydrogels did not significantly change the compressive modulus. The pure HA hydrogels had a significantly lower compressive modulus, compared to all other hydrogel groups. The compressive modulus of the pure CS hydrogels were only significantly lower than that of PEG, PEG:MMP-pep, PEG:HA, and PEG:HA:MMP-pep hydrogels. These results indicate that the addition of MMP-pep or CS to the hydrogel construct lowered the compressive modulus of the hydrogel matrices while adding HA

to the matrices raised the compressive modulus. In previous studies conducted by Bryant et al, the compressive modulus for a 20% (w/v) poly(ethylene glycol) dimethacrylate (PEGDA, mw: 3400) were found to be about 360 kPa, which is comparable to the 20% (w/v) PEGDA (mw: 3400) hydrogels in this study (293.21 ± 39.18 kPa) [29, 32]. **Figure 3.13A** shows the degradation profiles for the hydrogel matrices and the images of the hydrogels at day 10 (**Figure 3.13B**) and 21 (**Figure 3.13C**). As expected, the PEG hydrogels did not degrade in any of the enzyme solutions while the pure CS and HA hydrogels degraded very rapidly. Incorporating CS, HA, and MMP-pep into the PEG hydrogels made them degradable. Incorporating CS into the hydrogels demonstrated the fastest degradation kinetics while incorporating HA resulted in the slowest degradation rates.

3.4 DISCUSSION

Since the overall goal of this dissertation is to differentiate MSCs into chondrocytes, the hydrogel properties determined in this chapter need to mimic the native environment of articular cartilage, which is crucial for cell survival. The essential properties of articular cartilage include cell-mediated degradability, water absorption, and compressive strength [34]. As discussed in Chapter Two, the major component of articular cartilage ECM is type II collagen, which is degraded by matrix metalloproteinases (MMP) during ECM remodeling [33]. Native articular cartilage is made up of about 65-80% water; therefore, the hydrogels' ability to absorb water is crucial in attempting to mimic native articular cartilage environment [33]. As determined by Schinagl et al. the modulus of full-thickness cartilage is $380 \text{ kPa} \pm 120 \text{ kPa}$ [35].

Therefore, this chapter discussed the synthesis and modification of an MMP-sensitive peptide (MMP-pep). The main purpose for incorporating the MMP-pep into the hydrogel network was to enable cell-mediated degradation to occur. The results indicated that not only was peptide synthesis possible but that its modification did not interfere with the peptide's bioactivity. The degradation profile shown in **Figure 3.13A** demonstrates that the incorporation of the MMP-pep into the PEG hydrogel network made the hydrogels degradable by collagenase.

To mimic the native articular cartilage water content and compressive strength, CS and HA were modified for their incorporation into the PEG hydrogel. The findings of this chapter determined that the incorporation of CS aided in water absorption while the incorporation of HA increased the compressive strength. The results of water content within all the hydrogel compositions illustrated in **Figure 3.12B** demonstrated that all hydrogel compositions containing CS had higher water content than all the opposing compositions that did not contain CS. This clearly indicates that the incorporation of CS into the hydrogel network increased the hydrogel's ability to absorb water.

Since articular cartilage's main function is to resist compression [34], it is very critical for the hydrogel's compressive modulus to match the compressive strength of native cartilage. The compressive moduli of all the hydrogel compositions are listed in **Table 3.2**. The results indicate that the addition of MMP-pep into the hydrogel network decreased the modulus of the hydrogel constructs, whereas the incorporation of HA greatly increased the modulus. Furthermore, the PEG:HA hydrogel composition had the highest modulus of $330.6 \text{ kPa} \pm 19.13 \text{ kPa}$, which was most similar to native cartilage.

In summary, the results of this chapter demonstrated that the hydrogels' properties can be tailored by altering their material composition. For instance, incorporating an MMP-pep makes the hydrogels enzymatically degradable by cell-

secreted collagenase, whereas CS incorporation aids in the hydrogels' ability to absorb water. Finally, due to HA's high molecular weight, its incorporation into the hydrogel network significantly increased the hydrogels' compressive strength. Based on the findings of this chapter, it was determined that hydrogel properties can be fine-tuned to match all the essential properties of articular cartilage. The ability to closely mimic native articular cartilage ECM will enhance the capability of hydrogel scaffolds to direct the differentiation of MSCs into chondrocytes. In Chapter Four, hydrogels were fabricated using the specific biomaterial formulations characterized in this chapter and examined for their ability to induce chondrogenic differentiation of MSCs.

3.5 FIGURES

Figure 3.1 MMP-pep Chemical Formula, Structure, and Molecular Weight

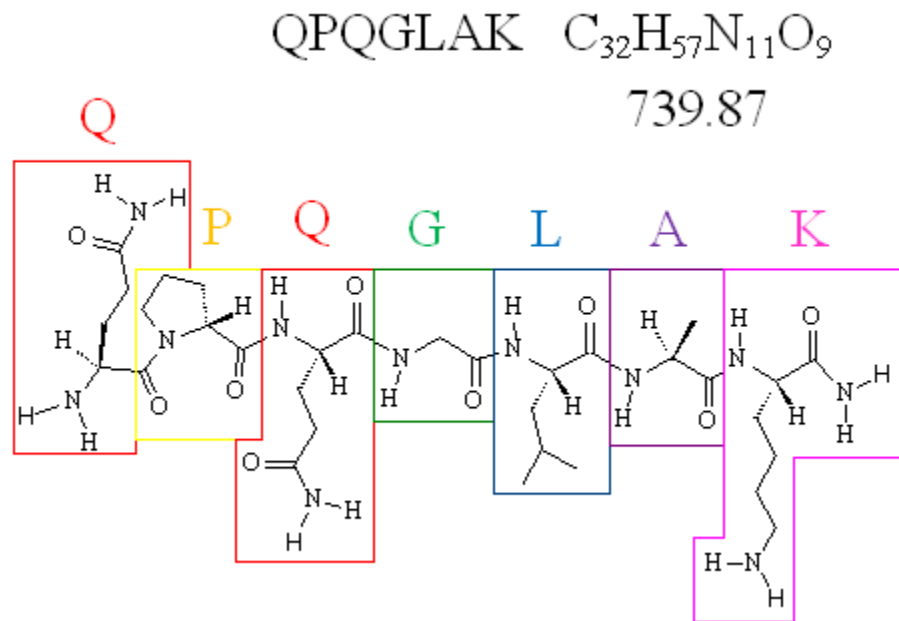


Figure 3.2 Schematic Drawing of the MMP-Sensitive Peptide Acrylation illustrating the attachment of acrylate groups onto the N-terminal amine and the primary amine that is tethered on the lysine.

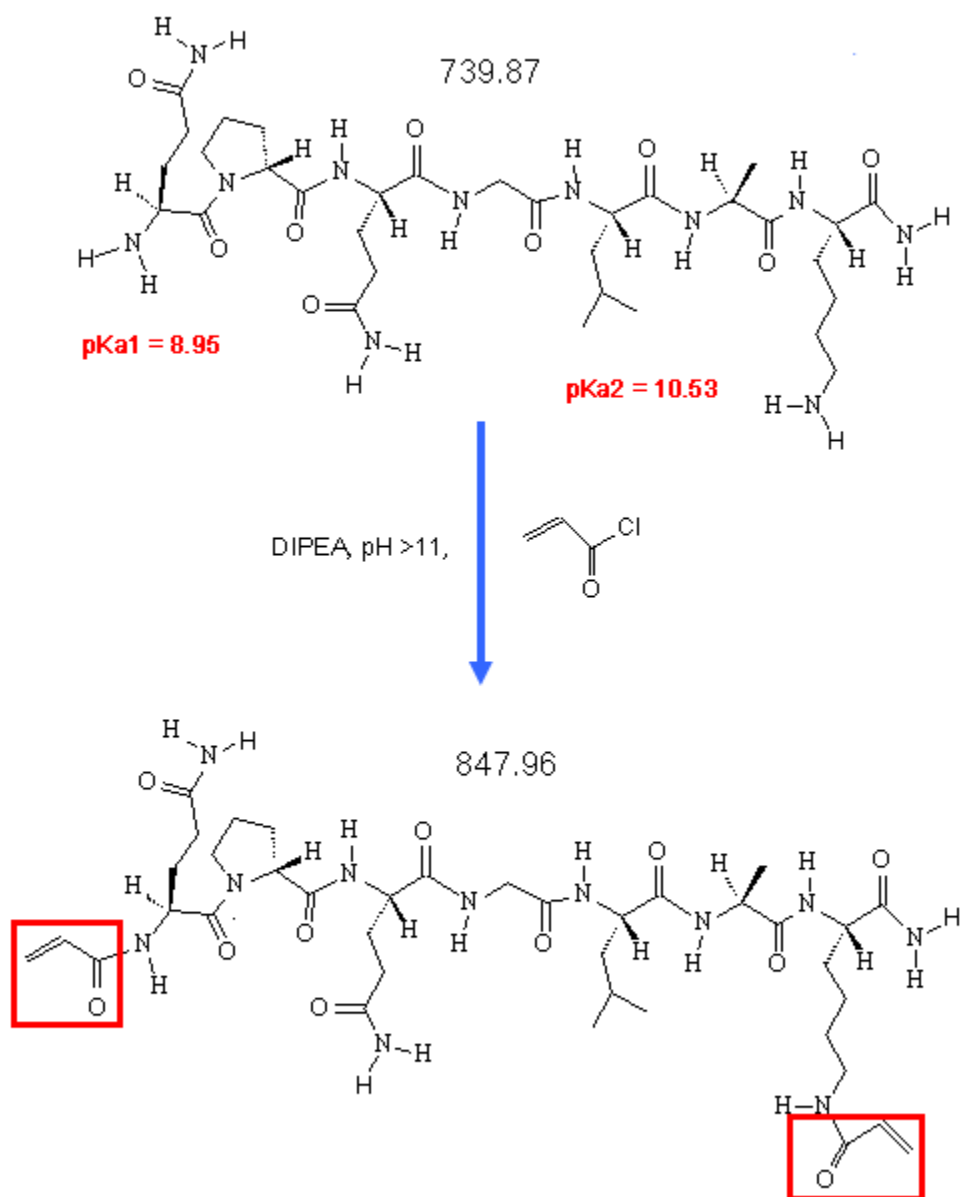
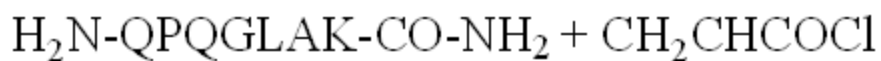


Figure 3.3 Chromatograph of the MMP-pep Degradation in collagenase. The red peak represents the intact MMP-pep in TES buffer and the blue peaks represent the degraded MMP-pep in TES buffer containing collagenase. This demonstrates that the modified MMP-pep is bioactive and degradable by collagenase.

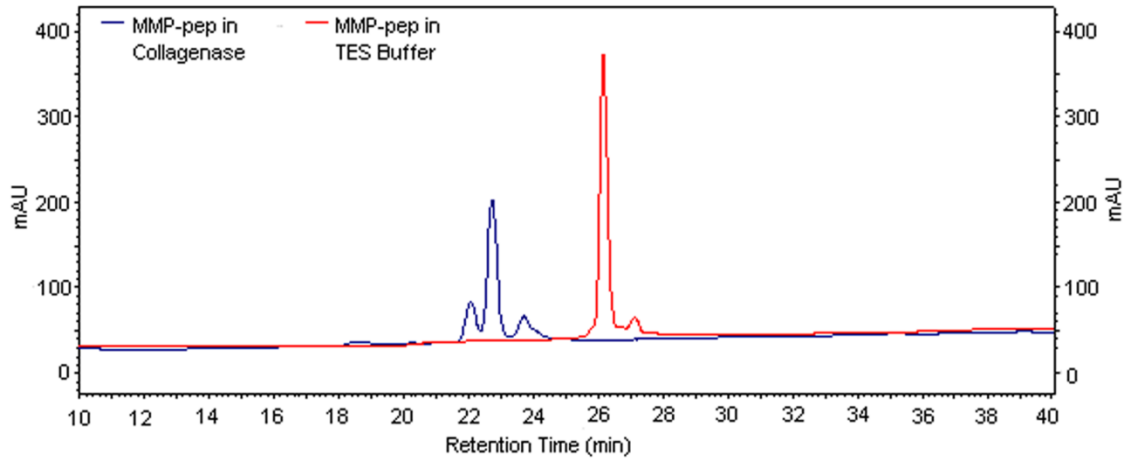


Figure 3.4 Schematic Drawing of Chondroitin Sulfate Acrylation adapted from Elisseff et al. (2003) showing the ethylene oxide ring opening up and attaching to the hydroxyl group on the backbone the CS chain [18].

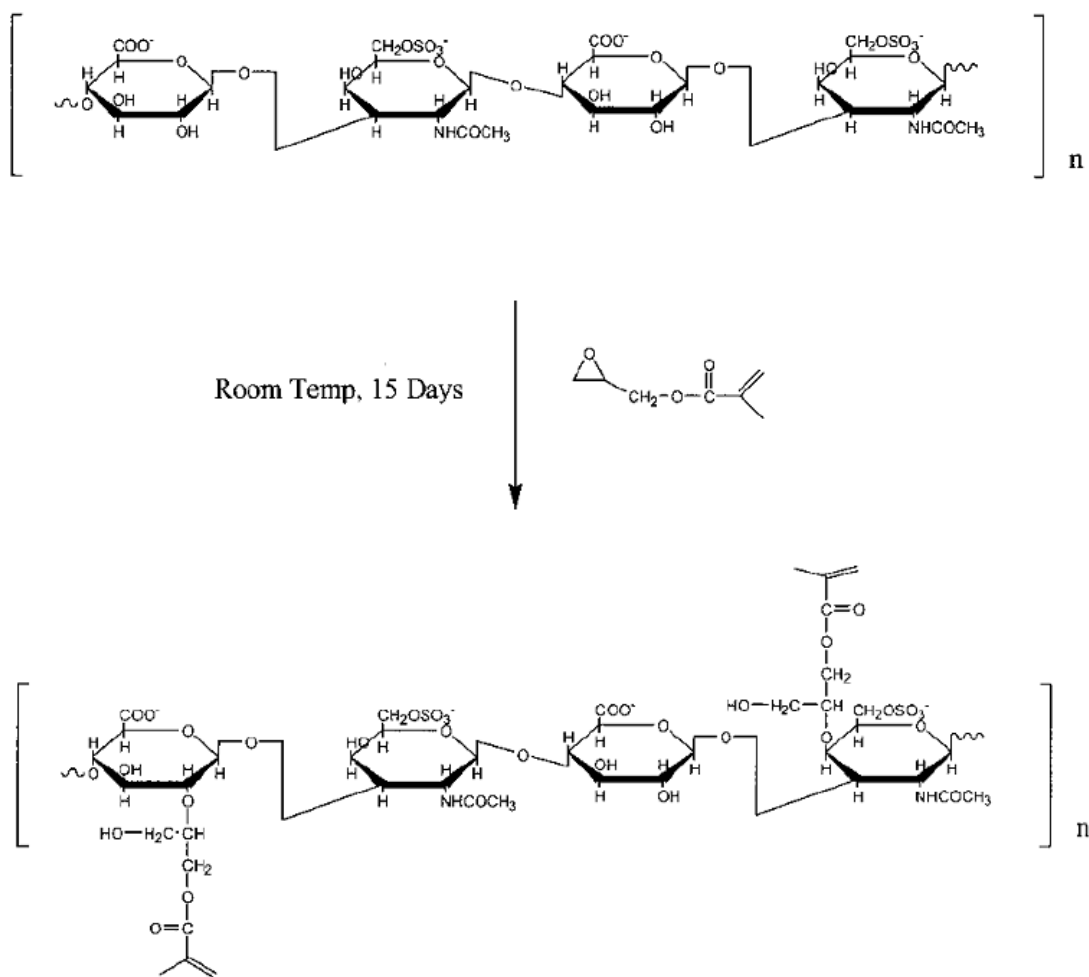


Figure 3.5 Schematic Drawing of Hyaluronic Acid Acrylation adapted from Schmidt et al. (2005) showing the ethylene oxide ring opening up and attaching to the hydroxyl group on the backbone of the HA chain [23].

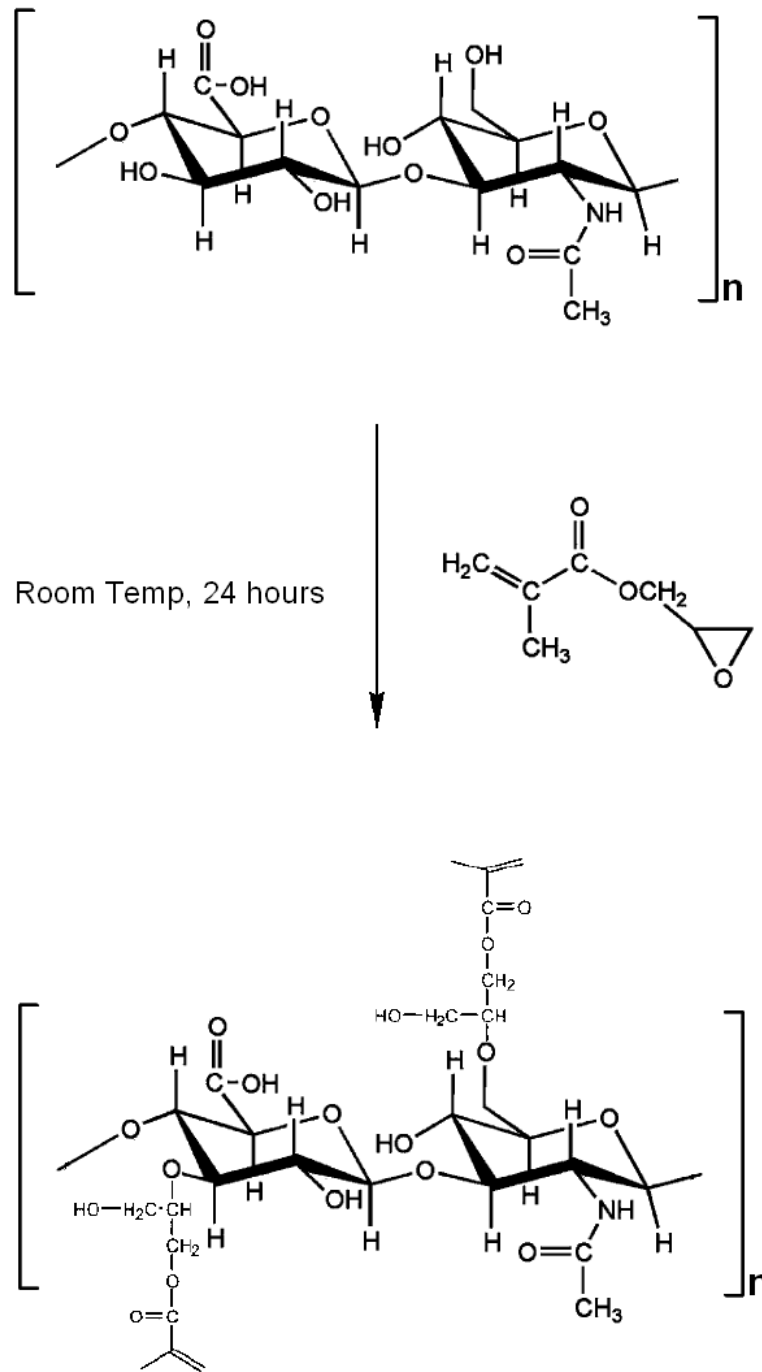


Table 3.1 Hydrogel Biomaterial Composition and Concentration

Group	Hydrogel	PEG	CS	HA	MMP-pep
1	PEG	20%			
2	PEG:MMP-pep	16%			4%
3	CS		20%		
4	PEG:CS	10%	10%		
5	PEG:CS:MMP-pep	9%	9%		2%
6	HA			1%	
7	PEG:HA	19%		1%	
8	PEG:HA:MMP-pep	15%		1%	4%
9	PEG:CS:HA	9.5%	9.5%	1%	
10	PEG:CS:HA:MMP-pep	8.5%	8.5%	1%	2%

Figure 3.6 MALDI-TOF Spectra & NMR of the Crude MMP-pep (A) Peaks at 739 [MH⁺], 761 [MH+Na⁺] and 779 [MH+Na+H₂O⁺] m/z indicating correct molecular weight of peptide. (B) An NMR of the peptide before modification showing that there are no acrylate protons in the region from 5.5 – 6.5ppm.

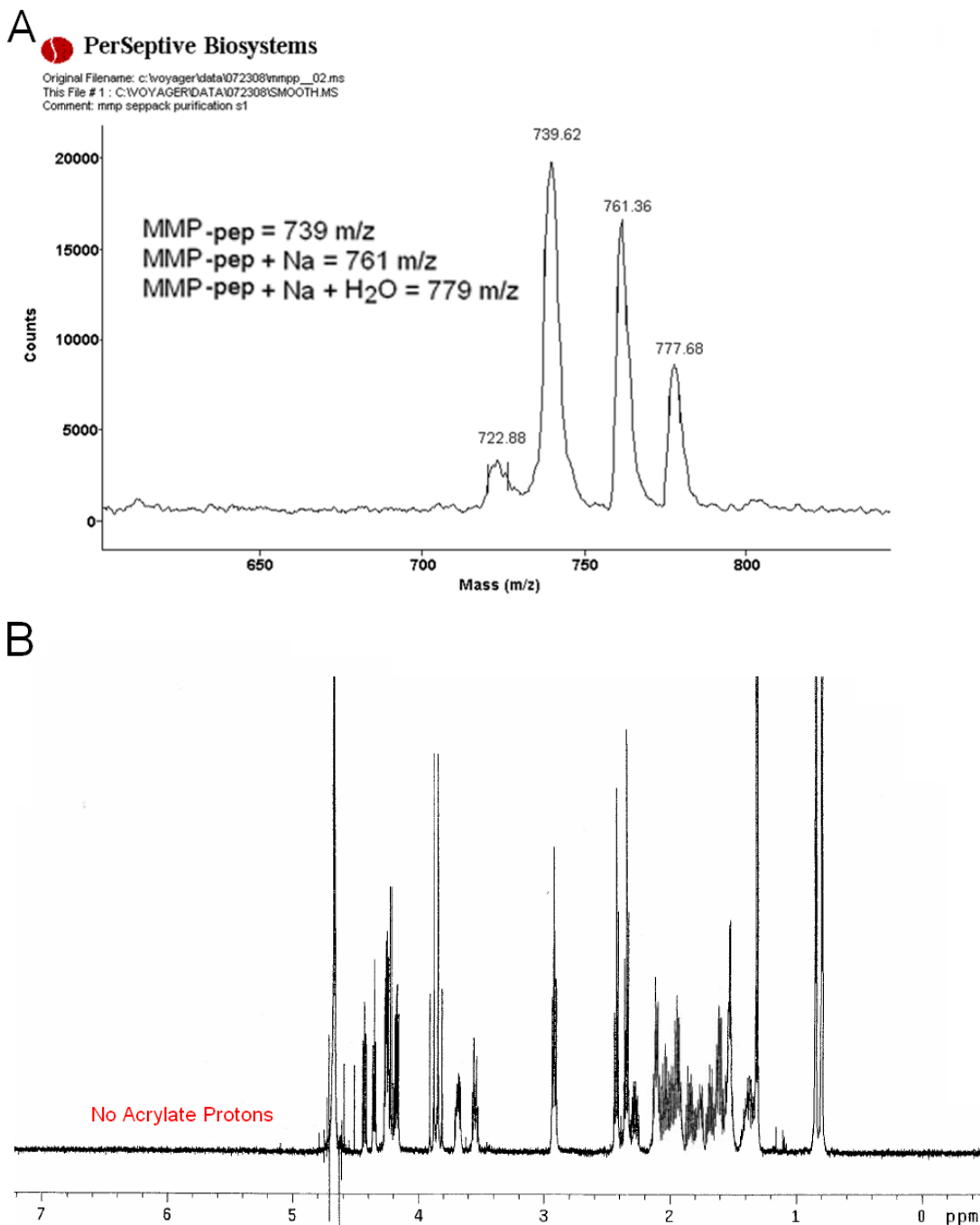
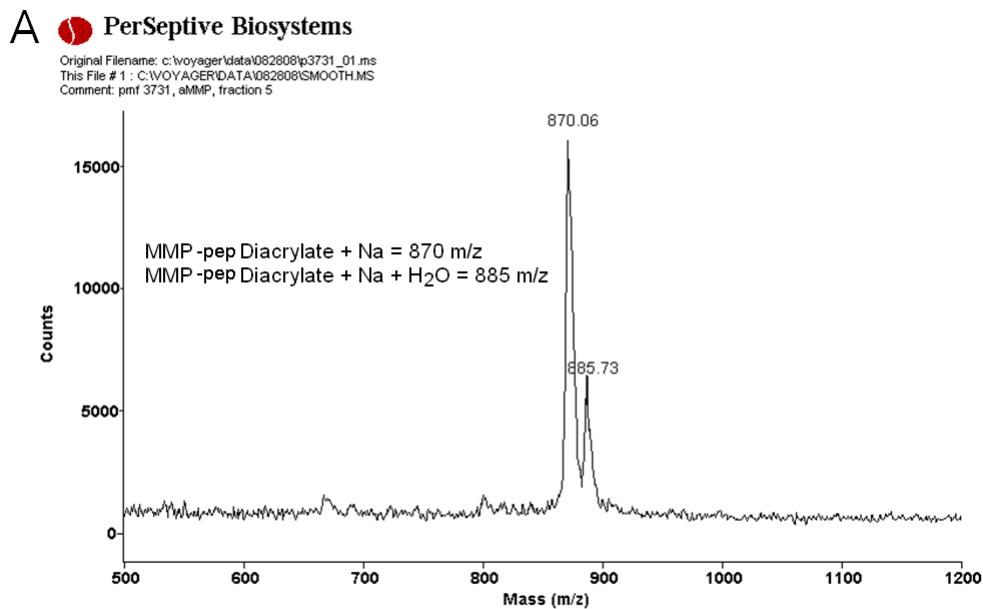


Figure 3.7 MALDI-TOF Spectra & NMR of the Modified MMP-pep (A) Successful acrylation is indicated by MALDI-TOF spectra showing the modified peptide peaks at 870 m/z and 885 m/z with an increase in molecular weight of 110 from the addition of the acrylate groups. (B) NMR of modified peptide further validates successful acrylation. Ratio of the integrals at 5.6 – 5.7 ppm and 6.0 – 6.2 ppm to the integral at 0.75 ppm was obtained verifying with two acrylate groups per peptide sequence.



B

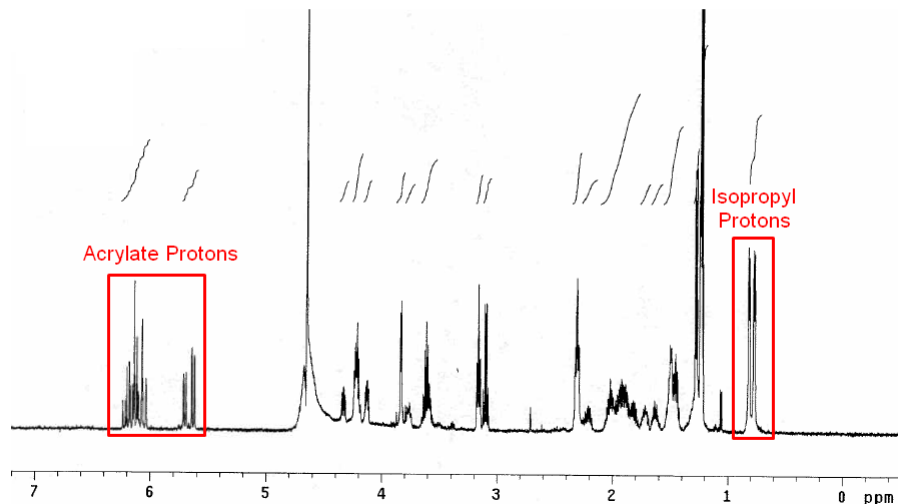


Figure 3.8 Unmodified CS NMR (A) Unmodified CS NMR with an inset of its chemical structure. (B) Expanded NMR of the no methacrylate portions near the anomeric proton peak.

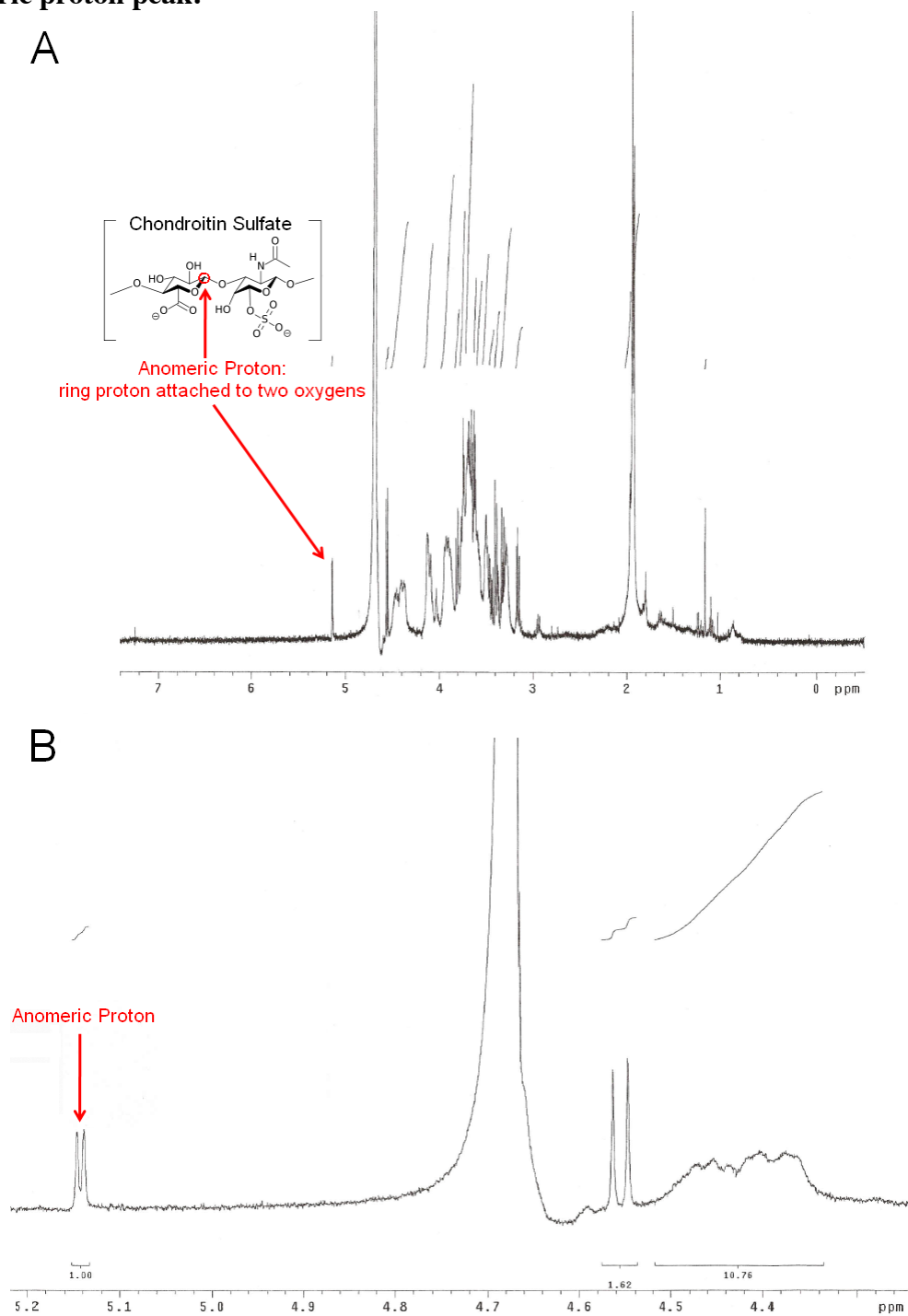


Figure 3.9 Modified CS NMR (A) NMR spectra of acrylated CS showing methacrylate peaks around 6 ppm. (B) Expanded NMR of the methacrylate portion showing the integrals of each individual peak. The ratio of the integral of one of the bound methacrylate proton peak at 5.5 ppm and the anomeric proton peak at 5.1 ppm verified that there is one acrylate group for every two units of CS.

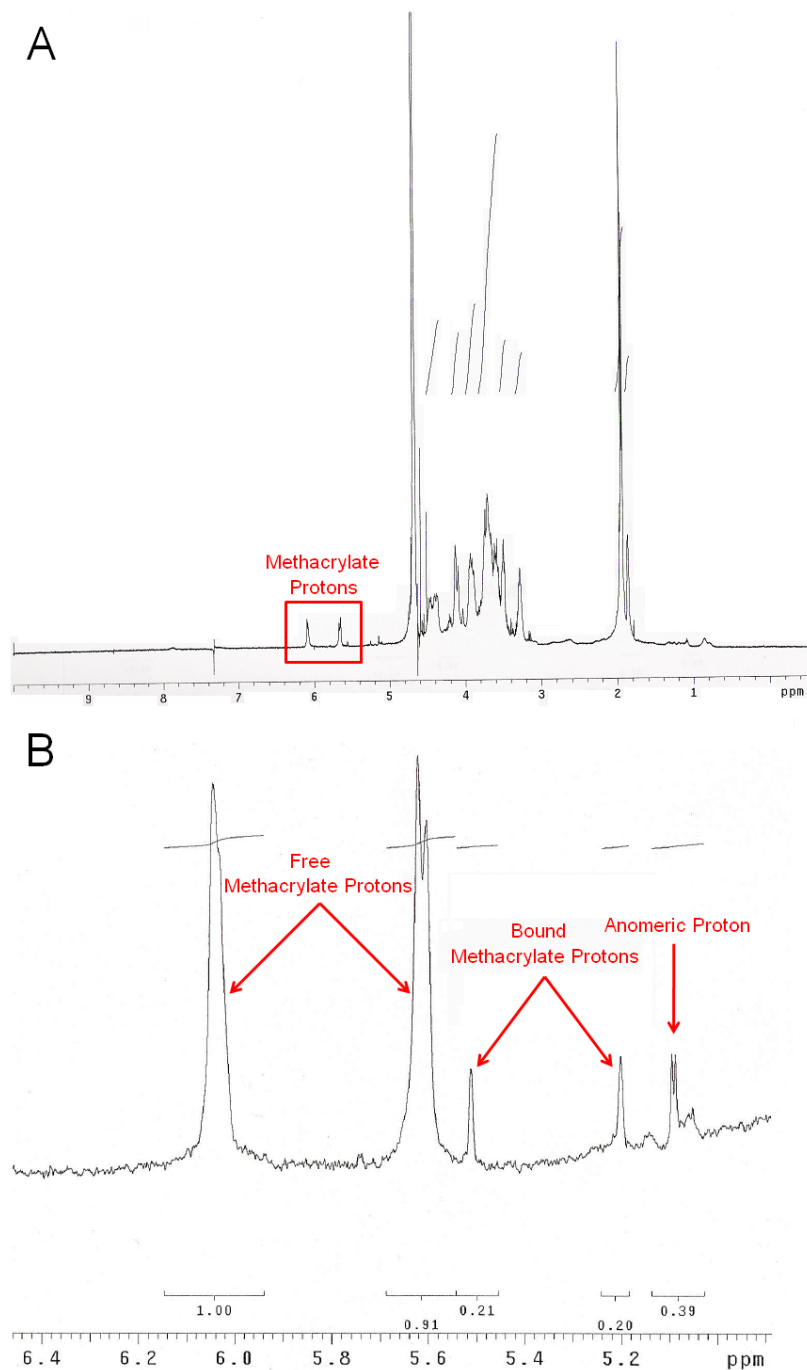


Figure 3.10 Unmodified HA NMR (A) Unmodified HA NMR with an inset of the chemical structure (B) Expanded NMR of the HA methyl protons at 1.84 ppm.

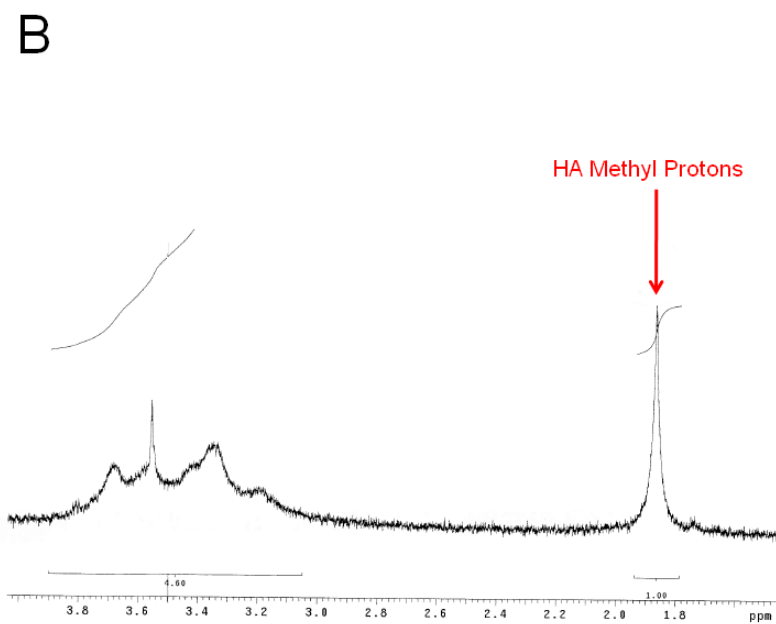
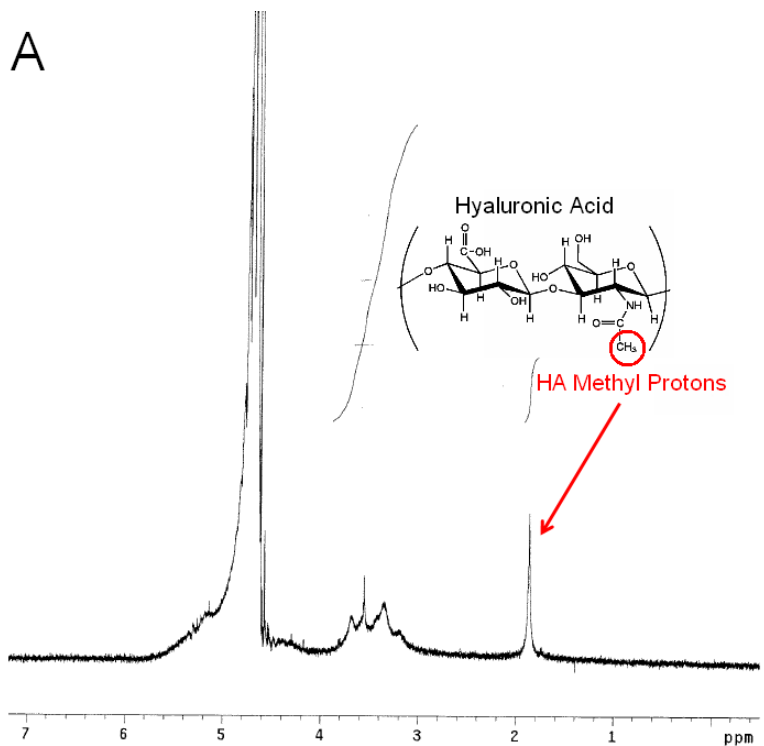


Figure 3.11 Modified HA NMR (A) Acrylated HA (B) Expanded NMR of the methyl protons. The ratio of peaks at 1.92 ppm, which represents the methyl protons of HA, and 1.84 ppm, which represents the methyl protons of the glycidyl methacrylate (GM) that has bounded to HA during acrylation verified that there is one acrylate group for every eight units of HA.

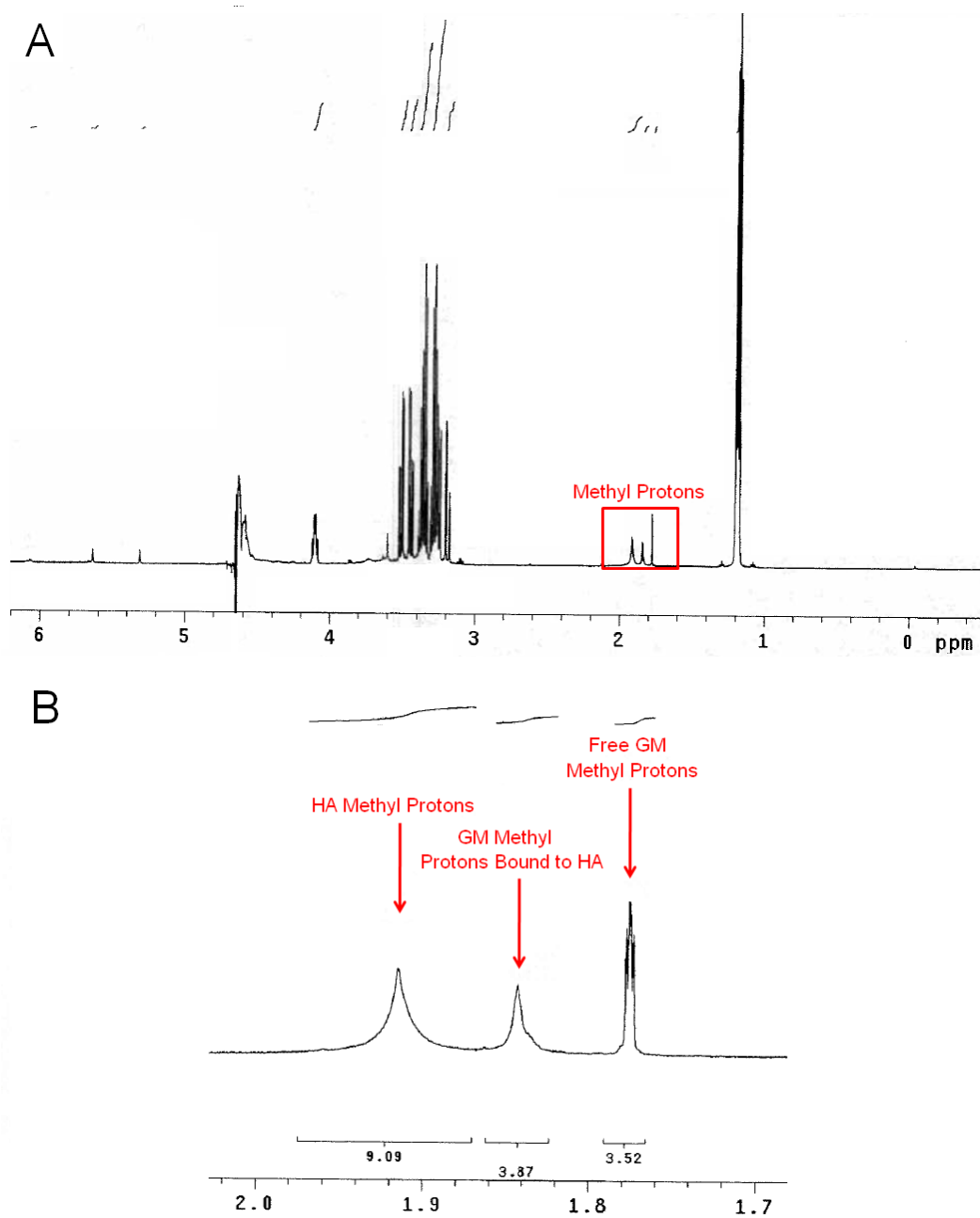


Figure 3.12 Swelling Ratio & EWC (A) Volumetric swelling ratios of various hydrogel constructs correlate to the ability of the hydrogels to absorb water. Pure CS and HA hydrogels exhibit the highest swelling ratio. (B) Equilibrium water content of various constructs illustrates that the incorporation of CS into the hydrogel network increased the water content.

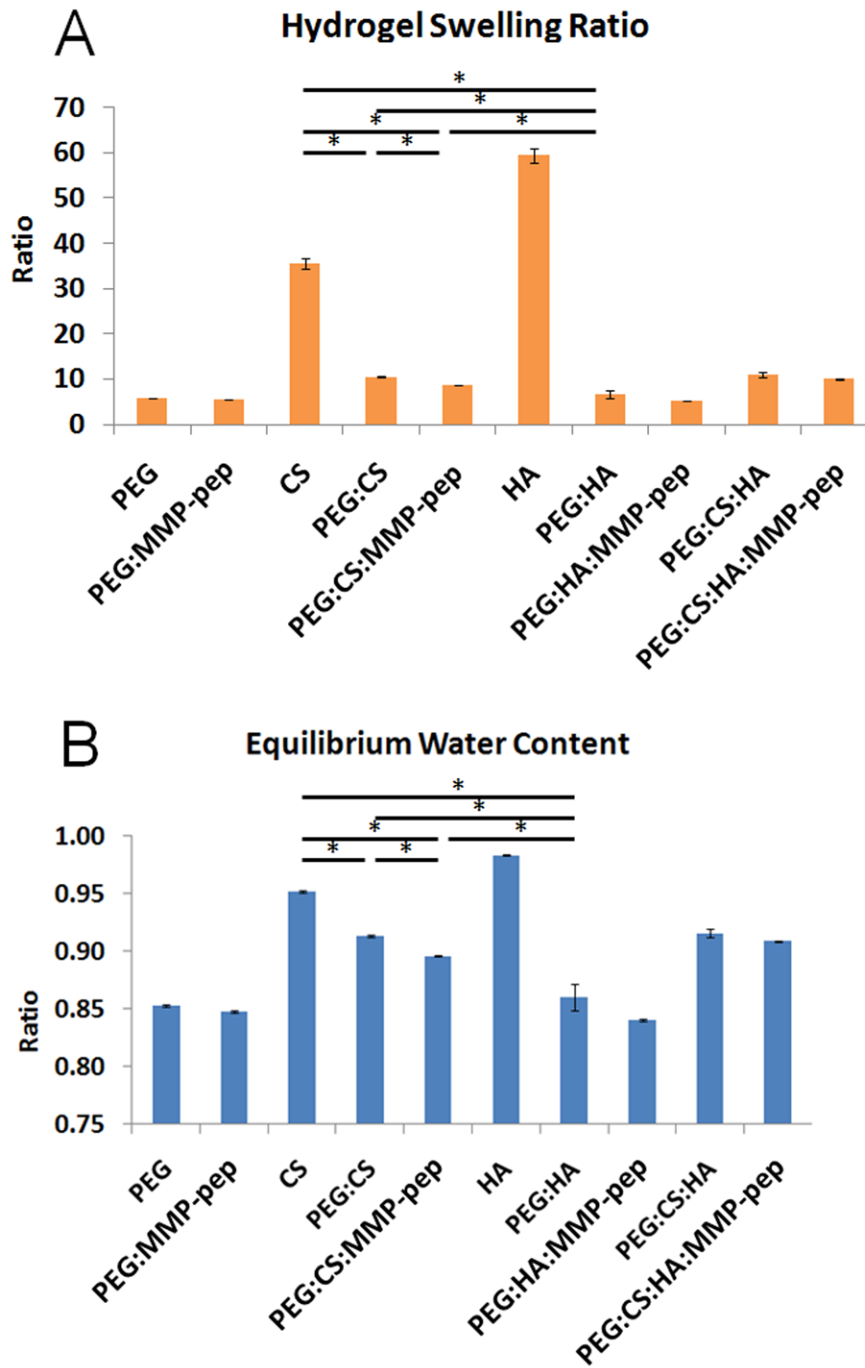
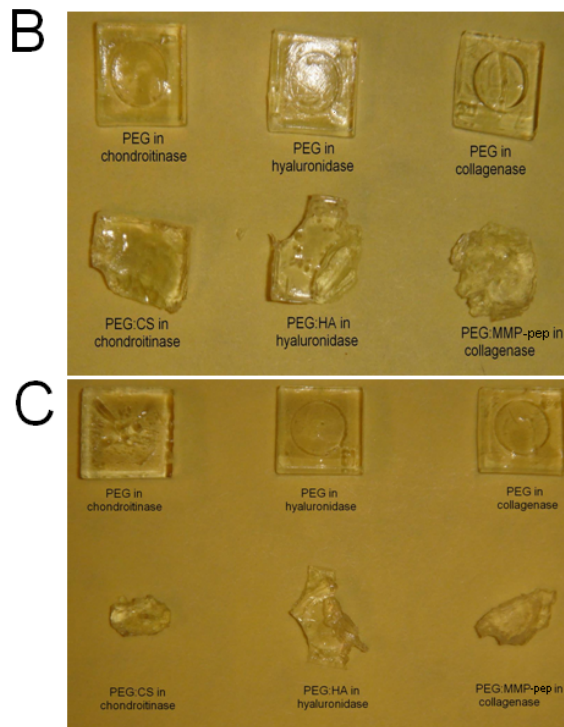
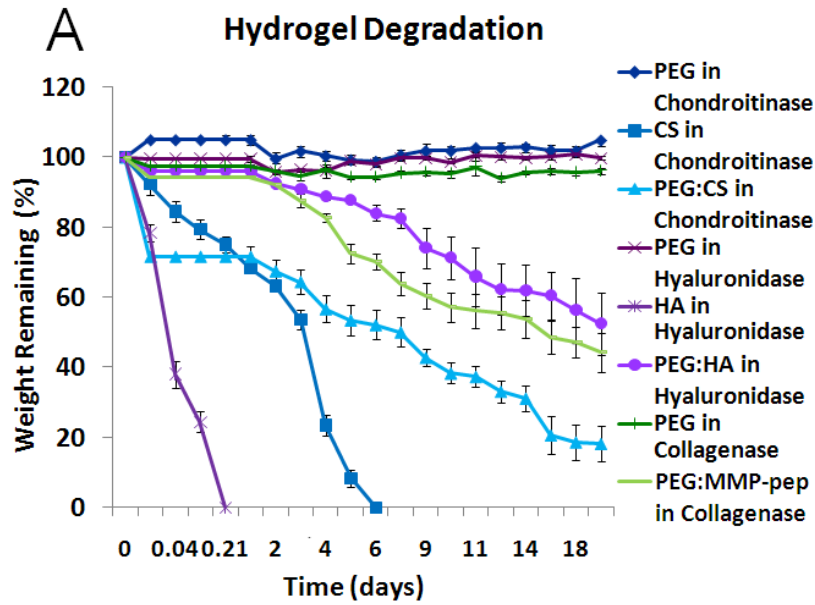


Table 3.2 Compressive Moduli of Blank Hydrogel Constructs

Blanks		
Hydrogel Groups	Moduli (kPa)	Standard Error
PEG	293.21	± 39.18
PEG:MMP-pep	261.88	± 1.51
CS	82.39	± 38.82
PEG:CS	117.8	± 54.46
PEG:CS:MMP-pep	105.78	± 26.89
HA	31.48	± 8.86
PEG:HA	330.6	± 19.13
PEG:HA:MMP-pep	184.28	± 26.76
PEG:CS:HA	74.02	± 11.10
PEG:CS:HA:MMP-pep	67.86	± 2.55

Figure 3.13 Hydrogel Degradation Profiles (A) PEG-based hydrogels incorporating CS, HA, and MMP-pep were determined to see how each component affects degradation kinetics. The addition of CS into PEG-based hydrogels yield the fastest degradation rate whereas the addition of HA yield the lowest degradation rate. Images of the hydrogels at day 10 (B) and 21 (C).



3.6 REFERENCES

1. Peppas, N.A., et al., *Hydrogels in pharmaceutical formulations*. Eur J Pharm Biopharm, 2000. **50**(1): p. 27-46.
2. Nuttelman, C.R., M.C. Tripodi, and K.S. Anseth, *In vitro osteogenic differentiation of human mesenchymal stem cells photoencapsulated in PEG hydrogels*. J Biomed Mater Res A, 2004. **68**(4): p. 773-82.
3. Alcantar, N.A., E.S. Aydil, and J.N. Israelachvili, *Polyethylene glycol-coated biocompatible surfaces*. J Biomed Mater Res, 2000. **51**(3): p. 343-51.
4. Langer, R., *Biomaterials in drug delivery and tissue engineering: one laboratory's experience*. Acc Chem Res, 2000. **33**(2): p. 94-101.
5. Martens, P.J., S.J. Bryant, and K.S. Anseth, *Tailoring the degradation of hydrogels formed from multivinyl poly(ethylene glycol) and poly(vinyl alcohol) macromers for cartilage tissue engineering*. Biomacromolecules, 2003. **4**(2): p. 283-92.
6. Peppas, N.A., et al., *Physicochemical foundations and structural design of hydrogels in medicine and biology*. Annu Rev Biomed Eng, 2000. **2**: p. 9-29.
7. Bryant, S.J. and K.S. Anseth, *Controlling the spatial distribution of ECM components in degradable PEG hydrogels for tissue engineering cartilage*. J Biomed Mater Res A, 2003. **64**(1): p. 70-9.
8. Burdick, J.A. and K.S. Anseth, *Photoencapsulation of osteoblasts in injectable RGD-modified PEG hydrogels for bone tissue engineering*. Biomaterials, 2002. **23**(22): p. 4315-23.

9. Burdick, J.A., et al., *Delivery of osteoinductive growth factors from degradable PEG hydrogels influences osteoblast differentiation and mineralization*. J Control Release, 2002. **83**(1): p. 53-63.
10. Cruise, G.M., et al., *A sensitivity study of the key parameters in the interfacial photopolymerization of poly(ethylene glycol) diacrylate upon porcine islets*. Biotechnol Bioeng, 1998. **57**(6): p. 655-65.
11. Elisseff, J., et al., *Controlled-release of IGF-I and TGF-beta1 in a photopolymerizing hydrogel for cartilage tissue engineering*. J Orthop Res, 2001. **19**(6): p. 1098-104.
12. Williams, C.G., et al., *In vitro chondrogenesis of bone marrow-derived mesenchymal stem cells in a photopolymerizing hydrogel*. Tissue Eng, 2003. **9**(4): p. 679-88.
13. Anseth, K.S., et al., *In situ forming degradable networks and their application in tissue engineering and drug delivery*. J Control Release, 2002. **78**(1-3): p. 199-209.
14. Kim, S., et al., *Synthetic MMP-13 degradable ECMs based on poly(N-isopropylacrylamide-co-acrylic acid) semi-interpenetrating polymer networks. I. Degradation and cell migration*. J Biomed Mater Res A, 2005. **75**(1): p. 73-88.
15. Kim, S. and K.E. Healy, *Synthesis and characterization of injectable poly(N-isopropylacrylamide-co-acrylic acid) hydrogels with proteolytically degradable cross-links*. Biomacromolecules, 2003. **4**(5): p. 1214-23.
16. Seliktar, D., et al., *MMP-2 sensitive, VEGF-bearing bioactive hydrogels for promotion of vascular healing*. J Biomed Mater Res A, 2004. **68**(4): p. 704-16.
17. Chen, G., Ushida, Takashi, Tateishi, Tetsuya, *Scaffold Design for Tissue Engineering*. Macromolecular Bioscience, 2002. **2**: p. 67-77.

18. Li, Q., et al., *Photocrosslinkable polysaccharides based on chondroitin sulfate*. J Biomed Mater Res A, 2004. **68**(1): p. 28-33.
19. Pek, Y.S., et al., *Degradation of a collagen-chondroitin-6-sulfate matrix by collagenase and by chondroitinase*. Biomaterials, 2004. **25**(3): p. 473-82.
20. Hwang, N.S., et al., *Response of zonal chondrocytes to extracellular matrix-hydrogels*. FEBS Lett, 2007. **581**(22): p. 4172-8.
21. Gerecht, S., et al., *Hyaluronic acid hydrogel for controlled self-renewal and differentiation of human embryonic stem cells*. Proc Natl Acad Sci U S A, 2007. **104**(27): p. 11298-303.
22. Leach, B.J., Bivens, K. A. Patrick, C. W., Jr., Schmidt, C. E., *Photocrosslinked hyaluronic acid hydrogels: natural, biodegradable tissue engineering scaffolds*. Biotechnol Bioeng, 2003. **82**(5): p. 578-89.
23. Leach, J.B. and C.E. Schmidt, *Characterization of protein release from photocrosslinkable hyaluronic acid-polyethylene glycol hydrogel tissue engineering scaffolds*. Biomaterials, 2005. **26**(2): p. 125-35.
24. Lee, H. and T.G. Park, *Photo-crosslinkable, biomimetic, and thermo-sensitive pluronic grafted hyaluronic acid copolymers for injectable delivery of chondrocytes*. J Biomed Mater Res A, 2008.
25. Suh, J.K. and H.W. Matthew, *Application of chitosan-based polysaccharide biomaterials in cartilage tissue engineering: a review*. Biomaterials, 2000. **21**(24): p. 2589-98.
26. Yoo, H.S., et al., *Hyaluronic acid modified biodegradable scaffolds for cartilage tissue engineering*. Biomaterials, 2005. **26**(14): p. 1925-33.

27. Butnariu-Ephrat, M., et al., *Resurfacing of goat articular cartilage by chondrocytes derived from bone marrow*. Clin Orthop Relat Res, 1996(330): p. 234-43.
28. Nettles, D.L., et al., *Photocrosslinkable hyaluronan as a scaffold for articular cartilage repair*. Ann Biomed Eng, 2004. **32**(3): p. 391-7.
29. Bryant, S.J., et al., *Crosslinking density influences the morphology of chondrocytes photoencapsulated in PEG hydrogels during the application of compressive strain*. J Orthop Res, 2004. **22**(5): p. 1143-9.
30. Varghese, S., et al., *Chondroitin sulfate based niches for chondrogenic differentiation of mesenchymal stem cells*. Matrix Biol, 2008. **27**(1): p. 12-21.
31. He, X. and E. Jabbari, *Material properties and cytocompatibility of injectable MMP degradable poly(lactide ethylene oxide fumarate) hydrogel as a carrier for marrow stromal cells*. Biomacromolecules, 2007. **8**(3): p. 780-92.
32. Bryant, S.J. and K.S. Anseth, *Hydrogel properties influence ECM production by chondrocytes photoencapsulated in poly(ethylene glycol) hydrogels*. J Biomed Mater Res, 2002. **59**(1): p. 63-72.
33. Poole, A.R., et al., *Composition and structure of articular cartilage: a template for tissue repair*. Clin Orthop Relat Res, 2001(391 Suppl): p. S26-33.
34. Flik, K.R., et al., *Articular Cartilage*, in *Cartilage Repair Strategies*. 2007, Humana Press Inc.: New Jersey. p. 374.
35. Schinagl, R.M., et al., *Depth-dependent confined compression modulus of full-thickness bovine articular cartilage*. J Orthop Res, 1997. **15**(4): p. 499-506.

CHAPTER FOUR

Directed Differentiation of MSCs into Specific Chondrogenic Phenotypes

4.1 INTRODUCTION

The preliminary goal for cartilage tissue engineering is to create a homogeneous tissue type by encapsulating chondrocytes uniformly within a polymer matrix to mimic the overall properties of articular cartilage. However, as discussed in Chapter Two, it is time consuming to isolate chondrocytes and they have the tendency to de-differentiate during *in vitro* culture [1, 2]. To this end, many investigators have utilized hydrogel-based approaches to induce the chondrogenic differentiation of stem cells.

As described in Chapter Two, stem cells are characterized by their capacity for self renewal and their ability to differentiate into a diverse assortment of specialized cell types [3]. Embryonic stem (ES) cells and adult stem cells are distinguished by the cells' differentiation potential. Both embryonic and adult stem cells have shown great potential for cartilage tissue engineering [3-12]. ES cells can serve as an unlimited cell source but; however, it is extremely difficult to control the cells' differentiation and obtain a homogenous cell population [7]. Therefore, researchers have turned to adult stem cells whose differentiation pathways can be better directed. Adult stem cells that are commonly used for cartilage tissue engineering include mesenchymal stem cells (MSC), adipose stem cells (ASC), adipose-derived stem cells (ADSC), and to a lesser extent, synovial-derived stem cells (SDSC) [11-18]. Although MSCs and ADSCs have been widely used in the cartilage tissue engineering field, numerous comparative studies have determined that MSCs have superior chondrogenic potential for tissue engineering [13-

15, 19-21]. Thus the research conducted in this dissertation utilized MSCs for chondrogenesis.

In this chapter, MSCs were encapsulated within PEG-based hydrogel scaffolds containing a combination of CS, HA, and MMP-sensitive peptide (MMP-pep) to investigate the effects of biomaterial compositions on MSC differentiation into chondrocytes. PEG-based hydrogels were used to create the complex biomimetic environment because they have tunable properties, can be functionalized easily, and are non-immunogenic [22-26]. Within the PEG-based hydrogel, an MMP-pep was incorporated because matrix metalloproteases (MMPs) have been shown to be secreted by cells during ECM remodeling, and MMPs are capable of cleaving the α -chains of collagens type I, II and III [27-29]. CS and HA are natural components of the ECM; therefore, their incorporation into the hydrogel network aids in mimicking the natural cartilage environment. CS has the ability to retain water, which allows the diffusion of nutrients. The electrostatic repulsion caused by the sulfated groups of CS contributes to the compressive strength of articular cartilage [30, 31]. Hyaluronic acid (HA) has been shown to contribute to cellular proliferation, migration, and wound healing [32].

The findings of this chapter indicate that biomaterials indeed play an inductive role in the chondrogenesis of MSCs. Furthermore, the results demonstrated that a particular biomaterial composition can induce the differentiation of MSCs into a specific chondrogenic phenotype, which can be correlated to the specific zones of articular cartilage.

4.2 MATERIALS AND METHODS

4.2.1 Cell Encapsulation and In Vitro Culture

To evaluate the affects of biomaterial composition on chondrogenesis, D1 ORL UVA (ATCC, Manassas, VA) cells, a mouse bone marrow stem cell line [33, 34], were encapsulated within each composite hydrogel construct previously listed in **Table 3.1** and cultured for 2, 4, or 6 weeks in a chondrogenic medium containing TGF- β 1 [35, 36]. A progenitor cell line was used instead of isolated primary stromal cells in order to keep the cell properties constant across various experiments in order to be able to better evaluate the influence of the material compositions. A cell density of 20 million cells/mL were mixed with the syringe filtered polymer solution and 125 μ L of the cell/polymer mixed was placed in a square mold (7x7x2mm) and polymerized for 10 minutes using a long-wave ultraviolet lamp (Model B100AP, Blak-Ray) at the intensity of \sim 10 mW/cm². The hydrogels were cultured in serum-free chondrogenic media containing 1% penicillin/streptomycin, 10nM dexamethasone, 50 μ g/mL ascorbic acid-2-phosphate, 40 μ g/mL L-proline, 5 mL ITS+1, and 10 ng/mL TGF- β 1 for 2, 4, and 6 weeks in a 12-well plate. The media was changed every other day.

4.2.2 RNA Isolation and RT-PCR

Chondrogenesis was determined by the gene expression of collagen I, II, X and X I within these hydrogel matrices at 2, 4, and 6 week time points. The hydrogel matrices were removed from culture and the gene expressions of encapsulated cells were analyzed. The hydrogels were placed into individual 2mL microcentrifuge tubes, and 200 μ L of TRIzol[®] was added to the tubes. The hydrogels were then crushed using a

homogenizer (Wheaton, Millville, NJ). After complete homogenization, another 800 μ L of TRIzol[®] was added to each tube.

The RNA isolation of the homogenized scaffolds was performed following the manufacturer's protocol. Briefly, the crushed scaffolds were incubated on ice for 45 minutes. 200 μ L of chloroform was added to each tube and then agitated vigorously for 15 seconds. The tubes were then incubated again at room temperature for 3 minutes and centrifuged at 12,000 RCF for 15 minutes at 4 °C. The aqueous layer was transferred to new tubes containing 400 μ L of new chloroform and centrifuged again at 12,000 RCF for 15 minutes at 4 °C. The aqueous layer was transferred into a new tube, this time containing 500 μ L of 100% isopropanol and 20 μ L of glycogen (5mg/mL, Ambion, Austin, TX) in each tube, for the visibility of the RNA pellet. After the addition of the glycogen, the tubes were manually rotated for 4 minutes and incubated for 6 minutes at room temperature. The tubes were then centrifuged at 12,000 RCF for 10 minutes at 4 °C, the isopropanol was poured out, and 1mL of 80% ethanol was added to each tube to re-suspend the RNA pellet. The tubes were then centrifuged again at 7,500 RCF for 10 minutes at 4 °C. The ethanol was poured out and the tubes were air dried for 10 minutes. Then, 21 μ L of nuclease free water was added to each tube and incubated at 55 °C for 10 minutes. After the incubation, the RNA concentration for each hydrogel sample was determined using a NanoDrop with the ND-1000 software.

Genomic DNA was removed using Deoxyribonuclease I (Invitrogen, Carlsbad, CA). First a strand of cDNA was synthesized by reverse transcription (RT) using Superscript[™] III kit (Invitrogen, Carlsbad, CA), following the manufacturer's instructions. The RT reaction was performed at 25°C for 10 minutes, 50°C for 50 minutes, and terminated after 5 minutes at 85°C.

Quantitative polymerase chain reaction (PCR) was performed using an ABI Prism® 7900 Real Time thermal cycler and HotStartTaq DNA Polymerase with SYBR green/ROX PCR master mix (SA Biosciences, Fredrick, MD). Primers for the housekeeping gene (GAPDH), collagen type II, type X and type I (SA Biosciences, Fredrick, MD) are listed in **Table 4.1**. GAPDH was used as the housekeeping gene because it is expressed in both differentiated and undifferentiated MSCs. As discussed in chapter two, collagen type II is a standard genetic marker to determine chondrogenesis because collagen type II is the most abundant type of collagen in articular cartilage. The expression of type X collagen is a genetic marker for hypertrophic chondrocytes, thus type X collagen expression indicates terminal differentiation. MSCs have a basal level expression of type I collagen, therefore the early expression of type I collagen is expected. However, type I collagen expression at later time points is an indication of either fibrocartilage formation or de-differentiation. During the PCR reactions, the HotStartTaq DNA Polymerase was first activated at 95°C for 10 minutes then the next 40 cycles ran at 95°C for of 15 seconds per cycle. After the DNA strand was denatured, it was then elongated with 2 cycles. The first cycle was 60 seconds at 60°C and the second for 60 seconds at 72°C.

Threshold cycle (C_T) values were determined using the ABI PRISM® 7700 Sequence Detection System software and also used to analyze the total product. The housekeeping gene, GAPDH, was used to normalize relative gene expression through the $2^{-\Delta\Delta CT}$ method [37]. GAPDH was used to normalize the genes of interest since this gene remains proportional to the amount of starting total RNA that was initially isolated from each sample. Gene expression fold differences were then determined via $2^{-\Delta\Delta CT}$ method, and the derivation of this analysis were described in detail by Livak and Schmittgen [37, 38]. Negative controls to assess the quality of the primers and total

RNA was also assessed, which consisted of running samples without templates and synthesizing cDNA without reverse transcriptase, respectively. All samples were run in triplicate within the assay.

4.2.3 Endpoint RT-PCR

End-point RT-PCR was performed to verify the results from the quantitative real time PCR. The cDNA was fragmented via gel electrophoresis. Briefly, 2.25g of agarose was added to 150 mL of Tris borate EDTA (TBE) buffer to create a 1.5% agarose gel. The agarose solution was covered with saran wrap and heated for 3 minutes in a microwave until the agarose was completely dissolved. The solution was allowed to cool for 10 minutes at room temperature before being poured into a gel frame. A well-comb was placed at one end of the gel and the agarose solution was allowed to stand in room temperature for 1 hour to harden and cool. Meanwhile, 5 μ L of amplicons for each hydrogel group were obtained from the previous real time PCR experiment and added to 1 μ L of DNA loading buffer. An aliquot of 5 μ L of the DNA ladder was also added to 1 μ L of the loading buffer. Once the gel hardened, the cDNA and DNA ladder were loaded into individual lanes. The gel ran for 1 hour and 30 minutes at 100V and then images were taken with the alpha imager software.

4.2.4 Histology and Immunohistochemistry

Histology of these hydrogel matrices was performed to investigate the chondrogenic differentiation and verify the quantitative real time data. At 2, 4, and 6 week time points, hydrogels were removed from culture and fixed in 4% paraformaldehyde at 4°C for an overnight period. Fixed hydrogels were then dehydrated for paraffin embedding using 1-hr sequential steps in the following order: 80%, 95%,

95% ethanol in dH₂O, 100% ethanol, 50/50 ethanol/CitriSolv, 100% CitriSolv, 100% CitriSolv, 60°C molten paraffin, and 60°C molten paraffin for an overnight period. Paraffin-embedded hydrogels were sliced in transverse sections at 10µm using a rotary microtome (Labmaster). Sections were stained for differentiation markers.

Double Sequential immunohistochemistry was performed to stain for collagen II (green) and collagen X (red) using rabbit polyclonal primary antibodies (Abcam, Cambridge, MA) and Texas red (collagen II) or FITC (collagen X) conjugated secondary antibodies. Slides containing sectioned hydrogels were blocked for unspecific binding for 30 minutes at 37 °C using 3% (w/v) bovine serum albumin (BSA) in PBS (pH 7.4). The slides were rinsed with 0.05% tween 20 in PBS solution three times. Washed slides were incubated with primary antibody for 30 minutes at 37 °C. The slides were rinsed again before the second incubation with the secondary antibody for 30 minutes at 37 °C. These steps were repeated for collagen X on the same slides. The slides were imaged using a confocal fluorescence microscope (Leica SP2 AOBS, 63X).

4.2.5 Biochemical Characterization

Glycosaminoglycan (GAG) production within each hydrogel group was determined using the Dimethylmethylene blue (DMMB) assay. Briefly, at 2, 4, and 6 week time points, hydrogels were removed from culture. Wet weights (*ww*) and dry weights (*dw*) after 48 hours of lyophilization were obtained for each construct (n=3). The dry constructs were then digested in 1 mL of papinase (papain, 125 µg/mL; Sigma, St. Louis, MO) at 60°C overnight. 200 µL of the DMMB solution was added to each well of the 96 well plates; then 50 µL of standard solution and sample solutions were added. The plate was shaken for 10 seconds before reading the absorbance at 525nm. To

account for the hydrogel material, absorbance of blank hydrogels was subtracted from the sample values.

The DNA content was determined using Sigma's DNA quantification kit (DNA-QF) in order to normalize the GAG production. The assay was carried out following the manufacture's protocol for multiwell assay. Briefly, 50 μL of sample was added to 1 mL of the bisbenzimidazole H 33258 dye solution (0.1 $\mu\text{g}/\text{mL}$). Then 200 μL of sample-dye solution was pipetted in triplicate into a 96 well plate. The fluorescence was read at 360 excitation and 460 emissions. The calibration curve was obtained by plotting the total DNA concentration versus the relative fluorescence units.

4.2.6 Mechanical Compression of Cell Laden Hydrogels

The compressive modulus of the various cell-laden swollen hydrogels were determined at room temperature on an In-spec 2200 Instron mechanical tester with a 125 N loading cell using a parallel plate apparatus and loading of 20% of the initial thickness per second (0.1 mm/sec). The pre-sterilized cell-polymer solution was polymerized in a square mold (2 mm x 7 mm x 7 mm) for 10 minutes using a long-wave ultraviolet lamp (Model B100AP, Blak-Ray) at the intensity of $\sim 10 \text{ mW}/\text{cm}^2$. The polymerized hydrogel constructs were then used for mechanical testing and were compressed to the maximum thickness of 2 mm. The compressive modulus of the cell-laden hydrogels were determined by analyzing the linear region of the stress versus the strain curve of the samples at low deformations (<20% strain).

4.2.7 Statistical Analysis

All quantitative data were expressed as mean \pm standard deviation and were verified by analysis of variance using student T-Test with equal variance. P values of less than 0.05 were considered statistically significant.

4.3 RESULTS

4.3.1 Chondrogenic Differentiation of MSCs

The gene expression of type II collagen was used to verify chondrogenesis since collagen II makes up approximately 90% of the collagen in articular cartilage. Type X collagen was used to determine chondrocyte hypertrophy. Only the hypertrophic chondrocytes in the calcified cartilage zone produce type X collagen. The gene expression of type I collagen indicates fibrocartilage formation or chondrocyte de-differentiation. The average fold difference as compared to undifferentiated cells encapsulated within PEG-only hydrogels for collagen II and X for each hydrogel construct are shown in **Figures 4.1A** and **4.1B** respectively. Average fold difference for collagen type I is shown in **Figure 4.2A** and **Figure 4.2B** is an expansion of type I collagen expression at 6 weeks. **Figure 4.3** are the gel images of endpoint RT-PCR for GAPDH, collagen II, and collagen X at 2, 4, and 6 weeks.

At all time points, the various hydrogel matrices exhibited similar trends in type II collagen expression. The collagen II expression increased between week 2 and week 4 but decreased by week 6 in all of the hydrogel matrices. The addition of CS to the PEG hydrogels only significantly increased collagen II expression at the 2 week time point. However, at all time points, the combined addition of CS and MMP-pep into the PEG hydrogels significantly increased collagen II expression indicating that the combination

of CS and MMP-pep enhanced chondrogenesis. The addition of HA alone to the PEG hydrogels had no significant effect on the collagen II expression, however the combined addition of HA and MMP-pep to PEG hydrogels significantly increased the collagen II expression at all time points. Although the combined addition of CS and MMP-pep as well as HA and MMP-pep to the PEG hydrogels, significantly increased the collagen II expression, the PEG:CS:MMP-pep hydrogels had significantly higher collagen II expression than the PEG:HA:MMP-pep hydrogels at 2 weeks. The results from this study demonstrate that the interactions of CS and MMP-pep are initially more favorable than the HA and MMP-pep interaction for chondrogenesis.

At 2 weeks, collagen X expression was very low for all the hydrogel matrices with the exception of CS-only hydrogel matrices. Collagen X expression increased in all hydrogel groups at 4 weeks. The CS-only hydrogel group exhibited the greatest collagen X expression, which was significantly ($p < 0.05$) higher than all other hydrogel groups for both 2 and 4 weeks. At 6 weeks the collagen X expression decreased in all groups except those that contained CS in their hydrogel composition, where collagen X expression continued to increase. This implies that CS may play an inductive role in differentiating MSCs into the hypertrophic phenotype by accelerating differentiation into the terminal state.

Relatively low levels of type I collagen expression were present in all hydrogel groups at 2 weeks and steadily decreased to a non-detectable level at 6 weeks. At 2 and 4 weeks, the PEG:CS hydrogel group had significantly higher collagen I expression than almost all other hydrogel groups. Both the pure CS and HA hydrogel groups had collagen I expression that were significantly lower than almost all other hydrogel groups. The down regulation of type I collagen expression at 6 weeks verified that chondrogenesis was directed towards the articular cartilage and not the fibrocartilage

phenotype. Additionally, the lack of type I collagen expression signifies that the differentiated chondrocytes did not de-differentiate into the fibroblastic form at 6 weeks.

4.3.2 Histological Analysis of Imaged Hydrogels

For further verification of chondrogenesis and to validate the quantitative data, immunohistochemical staining was performed to determine the cells' production of collagen II and collagen X. At all time points, positive staining for both collagen II and X was observed in the fluorescent images shown in **Figure 4.4**. At 2 weeks the PEG:CS and the PEG:MMP-pep hydrogels showed more positive staining for collagen II than the PEG hydrogels, which was consistent with the gene expression analysis. The PEG:CS:MMP-pep hydrogel matrix exhibited the most collagen II staining. The CS-only hydrogels also showed the greatest amount of collagen X staining at 2 weeks, but the distribution appears to be clustered. At 4 weeks, large aggregates of collagen X staining were observed with increased intensity shown in the CS-only hydrogel group. The collagen II staining at 4 weeks became more clustered in the PEG:MMP-pep and the PEG:CS:HA hydrogel groups but remained evenly distributed for the other hydrogel groups. At 6 weeks the collagen X staining intensified while the collagen II staining decreased for all hydrogel groups, which were again consistent with our gene expression data at 6 weeks. Due to the low levels of type I collagen gene expression; immunohistochemical staining was not performed for this gene.

4.3.3 Protein Analysis for Total GAG Production

Biochemical composition, specifically DNA and GAG concentration of the hydrogel matrices, was observed to be dependent on matrix composition and time spent in culture. Given the differences in material composition and cell density of the

hydrogels, blank (without cells) hydrogels were subtracted as background and matrix accumulation was normalized to the DNA content. Thus, the observed differences are indications of the biosynthetic activity of the cells within each hydrogel group. The GAG/DNA ratios of all the hydrogel groups are shown in **Figure 4.5**. At 2 weeks, the addition of CS to the PEG hydrogels significantly increased the GAG production. HA-only hydrogels produced significantly less GAG than the PEG:HA and PEG:HA:MMP-pep groups, at 2 weeks. For all hydrogel groups the GAG production increased from 2 to 4 weeks. Interestingly though, greater matrix accumulation was observed in hydrogel groups containing HA compared to hydrogel groups that did not contain HA, at all time points. At six weeks the GAG production in most of the hydrogel groups decreased, with the exception of pure CS and HA hydrogels which increased in matrix accumulation.

4.3.4 Mechanical Strength of Hydrogel Constructs

The compressive modulus of each hydrogel group at 2, 4, and 6 weeks was also determined and listed in **Table 4.2**. The results indicate that the compressive modulus increased with time for all hydrogel groups with the exception of the HA-only hydrogels. The HA-only hydrogel group is the only group that showed a decrease in compressive modulus from 2 to 4 weeks. At 6 weeks the compressive modulus of the pure HA hydrogel group could not be obtained due to the complete degradation of the hydrogels. The CS-only hydrogel constructs, exhibited the lowest compressive modulus at 2 weeks, but continued to increase at both 4 and 6 weeks. The PEG:HA hydrogel group exhibited the highest compressive modulus at all time points. Similar to the findings from Chapter Three, it was observed that the addition of MMP-pep or CS to the hydrogel constructs lowered the compressive modulus while adding HA to the matrices increased the modulus.

4.4 DISCUSSION

To evaluate chondrogenesis, D1 mouse progenitor cells were encapsulated within each hydrogel group and cultured for 2, 4, and 6 weeks. At each time point the GAG production as well as the gene expression for type II, X, and I collagen was determined. RT-PCR results for the gene expression of type I, II, and X collagens were in accordance with previous studies conducted by Barry et al. [39]. Barry et al. demonstrated that the encapsulated MSCs showed a temporal expression of the different kinds of collagen, with early expression of type I, followed by the expression of collagen II and terminating with the increasing expression of collagen X [39]. Undifferentiated MSCs have been shown to uniformly express type I collagen [39, 40]. Additionally, type I collagen is a genetic marker for fibrocartilage because it is the only type of cartilage that contains type I collagen in addition to the normal type II collagen [41]. Therefore, type I collagen expression was used to determine cell de-differentiation and formation of fibrocartilage. For all hydrogel groups, type I collagen was present at low levels at 2 weeks and steadily decreased to an almost undetectable level at 6 weeks. The decrease in type I collagen is an indication that the initial type I collagen expression at two weeks is from undifferentiated cells and not from fibrocartilage. If the MSCs were differentiating into fibrocartilage, the type I collagen expression would increase with time instead of decrease.

Type II collagen is a common genetic marker used to determine chondrogenesis because it makes up approximately 90% of the collagen in articular cartilage. Collagen II expression for all hydrogel compositions was relatively high at 2 weeks and continued to increase at 4 weeks for most hydrogel groups. However, by 6 weeks type II collagen expression decreased, while type X collagen increased in all hydrogel groups. At all time points, the addition of CS:MMP-pep or HA:MMP-pep into PEG hydrogels significantly

increased collagen II expression, while the addition of CS or HA alone had only a modest effect. At 2 and 4 weeks, PEG:CS:MMP-pep scaffolds had significantly higher collagen II expression than PEG:HA:MMP-pep hydrogels.

Type X collagen is only produced by hypertrophic chondrocytes. The increase in type X collagen indicated that chondrogenesis during this study occurred up to 4 weeks, and by the 6 week time point all the chondrocytes became hypertrophic. Hypertrophic chondrocytes terminally differentiate and either begin endochondral ossification resulting in the creation of bone tissue [42] or undergo apoptosis [43-45] depending on their location. According to the mRNA results, the MSCs within all hydrogel groups began differentiation at 2 weeks and continued to differentiate into chondrocytes up to 4 weeks. At 6 weeks there were very few undifferentiated cells and the majority of the chondrocytes had undergone terminal differentiation into the hypertrophic phenotype.

Histology and immunohistochemistry confirmed the mRNA results and revealed that cartilage-specific proteins were produced within the hydrogel matrices. Immunohistochemical staining for types II and X collagen (**Figure 4.4**) indicated significant differences between 2 and 6 weeks. At week 2 the MSCs in all hydrogel groups produced more type II collagen, but after 6 weeks of culture, type X collagen production dominated in all hydrogel groups, which agreed with the RT-PCR data. At 2 weeks the observed collagen II staining were high in PEG:CS:MMP-pep, PEG:CS:HA, and PEG:MMP-pep hydrogels, while CS-only hydrogels exhibited the highest amount of collagen X staining. At week 4, PEG:CS:MMP-pep and PEG:CS:HA hydrogel constructs continued to express high levels of collagen II and low levels of collagen X staining, while CS-only hydrogels still showed very high collagen X expression. However, PEG:MMP-pep hydrogel constructs also showed significantly higher levels of collagen X expression at 4 weeks compared to week 2. Cells cultured up to 6 weeks

exhibited higher levels of collagen X staining in all formulations, indicating that prolonged in-vitro culture of MSC-derived chondrocytes resulted in a hypertrophic phenotype [45].

Biochemical analysis for total GAG production (normalized to DNA content; blank hydrogels as background control) indicated that proteoglycan synthesis and matrix remodeling are significantly influenced by biomaterial composition. The GAG/DNA ratios for all hydrogel groups are shown in **Figure 4.5**. GAG production appears to be time dependent, increasing from 2 to 4 weeks and then decreasing at week 6, once terminal MSC differentiation is achieved. In addition, matrices incorporating HA showed significant increases in GAG production compared to PEG-only hydrogels at 4 weeks. The greater matrix accumulation observed in hydrogel groups containing HA compared to those that did not contain HA, may be an indication that the presence of HA within the hydrogel matrix enhances GAG production. The GAG production increased between 2 and 4 weeks for all hydrogel groups but dropped off at 6 weeks with the exception of the pure CS and HA groups. The cause for the continued increase in GAG production in these two hydrogel groups is unclear, but the structural integrity of these hydrogels at 6 weeks may play a role. The degradation results from Chapter Three determined that the pure CS and HA hydrogels degraded very rapidly. This rapid degradation was observed during the differentiation studies, where both pure CS and HA hydrogels degraded by 6 weeks.

Hydrogels without PEG lacked mechanical stability as shown by the hydrogels' compressive modulus listed in **Table 4.2**. Mechanical strength is important for the structural support of the cells within these matrices. As discussed in Chapter Two, chondrocytes are responsible for the maintenance of the cartilage ECM [46] and therefore they are extremely sensitive to their external surroundings. Without structural

support, chondrocytes will attempt to compensate by synthesizing their own ECM, which could be a reason for the increased GAG production at 6 weeks within the CS and HA hydrogels. The cells within the other hydrogel groups showed a decrease in GAG production once they reached their GAG production threshold, which has been shown to occur by Day 21 [39]. Barry et al. demonstrated that during the hMSC differentiation pathway, matrix accumulation occurs until the ratio of chondroitin-6-sulfate and chondroitin-4-sulfate reaches approximately 4 (CS6:CS4), which is the GAG production threshold [39]. Once the threshold has been reached, chondrocytes stop synthesizing additional GAG and begin to turn-over the GAG during remodeling [39, 46]. The findings of this study illustrate the capacity of MSCs for biochemical activity within the various hydrogel compositions. Additionally, the mRNA and biochemical results indicated that specific hydrogel compositions have unique regulation of chondrogenic genes and GAG production that correlate to the specific zones of articular cartilage.

The results of this study demonstrate that biomaterial composition not only induces the chondrogenic differentiation of MSCs but that the differentiation can be correlated to the specific zones of articular cartilage. **Figure 4.6** illustrates the correlations between the various composite hydrogel constructs and the specific zones of articular cartilage. In particular, the PEG:CS:MMP-pep hydrogel composition had the highest collagen II expression as well as the lowest GAG production at 2, 4, and 6 weeks, which can be correlated to the superficial zone of articular cartilage. The PEG:CS composition had midrange expression of collagen II and GAG content for all time points, which is similar to that of the transitional zone. The PEG:HA hydrogel composition can be correlated to the deep zone of articular cartilage because of its high GAG content and low expression of collagen II. The MSCs within the CS-only hydrogel composition differentiated into hypertrophic chondrocytes with very high expression of

collagen X; thus, the CS-only hydrogel composition can be used to induce chondrogenesis specific to the calcified cartilage zone.

As discussed in Chapter Two, the mechanical properties of each articular cartilage zone is dependent on the matrix composition within each zone [47]. The compressive modulus of articular cartilage increased significantly from the articular surface to the deep zone [48]. The compressive modulus of the cell-laden hydrogel matrices from this study can also be correlated to each zone of articular cartilage, with PEG:CS:MMP-pep having the lowest compressive modulus, followed by PEG:CS. PEG:HA has the highest compressive modulus.

In summary, this chapter has demonstrated that hydrogels incorporating both synthetic and natural polymers as well as cell-induced degradability are suitable for the generation of zone-specific chondrogenic phenotypes from a single MSC population. Furthermore, this study is the first to report that specific biomaterial compositions have the capability of inducing MSC differentiation into a specific chondrogenic phenotype that can be correlated to the various zones of articular cartilage. Based on these specific correlations determined in this chapter, Chapter Five discusses the fabrication of a single multi-layered hydrogel construct and examines its ability to simultaneously differentiate the MSCs into the specific zones of articular cartilage.

4.5 FIGURES

Table 4.1 Sequences and Primers used in Real-Time PCR Assays

Gene/ Species	NCBI Reference Sequence	Size (in base pairs)	Primer Sequence
GAPDH Mouse	NM_008084.2	140	(F) 5'-GGCATTGCTCTCAATGACAA-3' (R) 5'-AGGGTGCAGGGAACCTTTATT-3'
Type II Collagen Mouse	NM_031163.3	138	(F) 5'-GATGGCTCTAATGGAATCCC-3' (R) 5'-CATCGCCATAGCTGAAGTG-3'
Type X Collagen Mouse	NM_009925.4	94	(F) 5'-GTTCTCCTCTTACTGGAATCCCTTA-3' (R) 5'-TTATGCTGAACGGTACCAAACG-3'
Type I Collagen Mouse	NM_007742.3	66	(F) 5'-GGTCCTCGTGGTGCTGCT-3' (R) 5'-ACCTTTGCCCCCTTCTTTG-3'

Figure 4.1 Collagen II and X Gene Expression shown as average fold difference compared to undifferentiated D1 cells with PEG hydrogels for (A) collagen type II and (B) collagen type X.

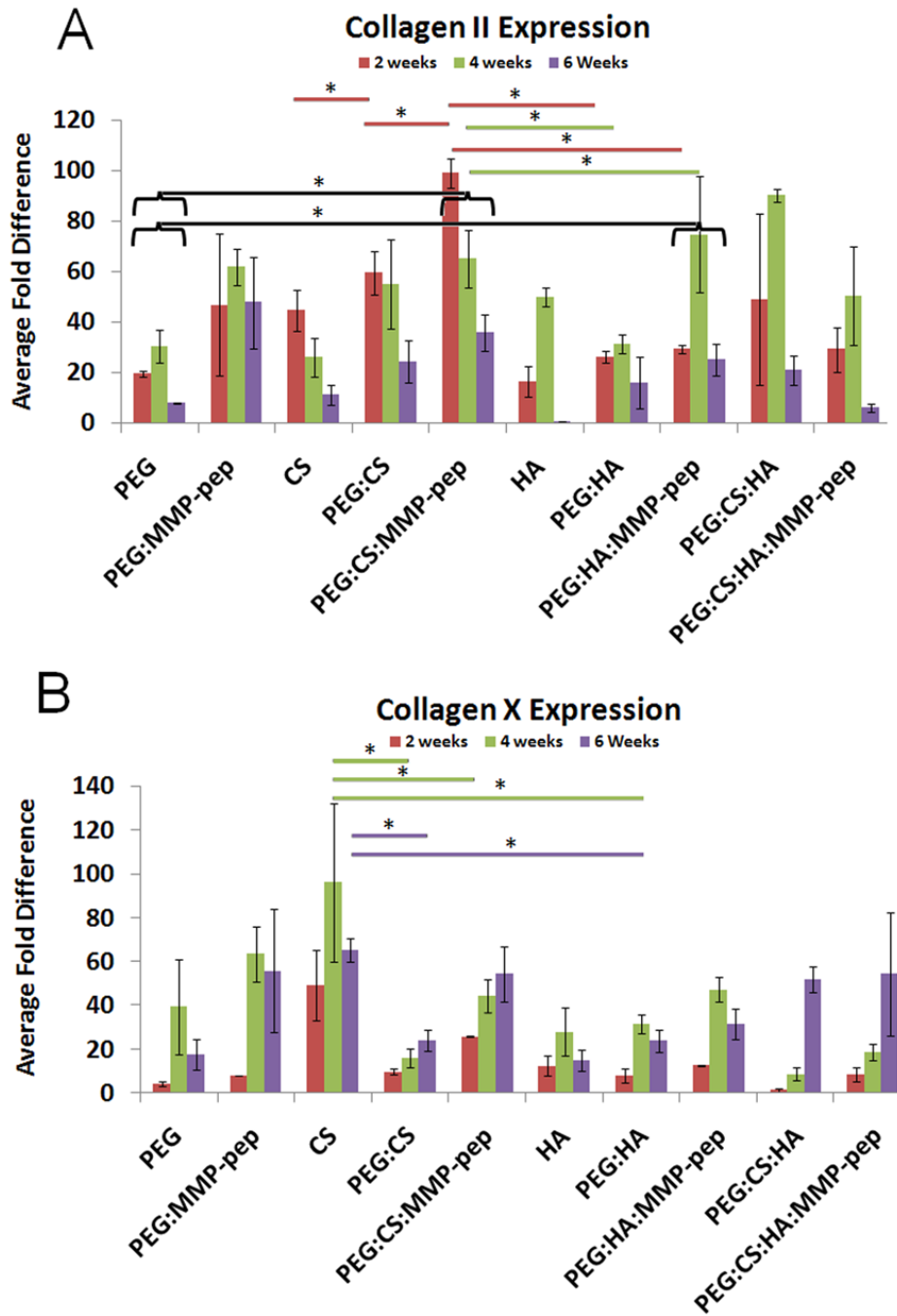


Figure 4.2 Collagen I Gene Expression shown as average fold difference compared to undifferentiated D1 cells with PEG hydrogels for (A) collagen type I and (B) the expanded collagen type I expression at 6 weeks.

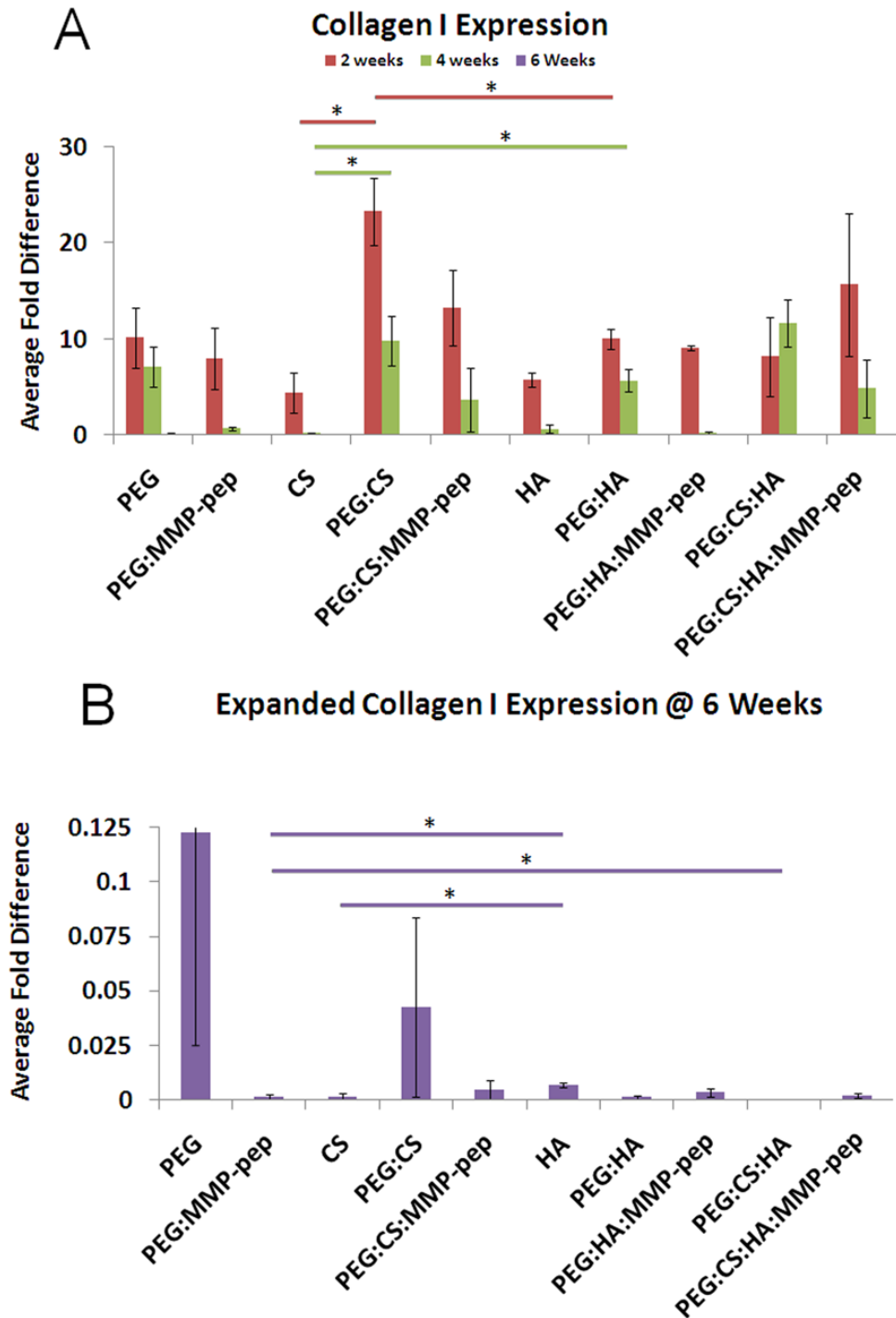


Figure 4.3 End-point Agarose Gels for collagen type II, type X and GAPDA for 2, 4 and 6 weeks

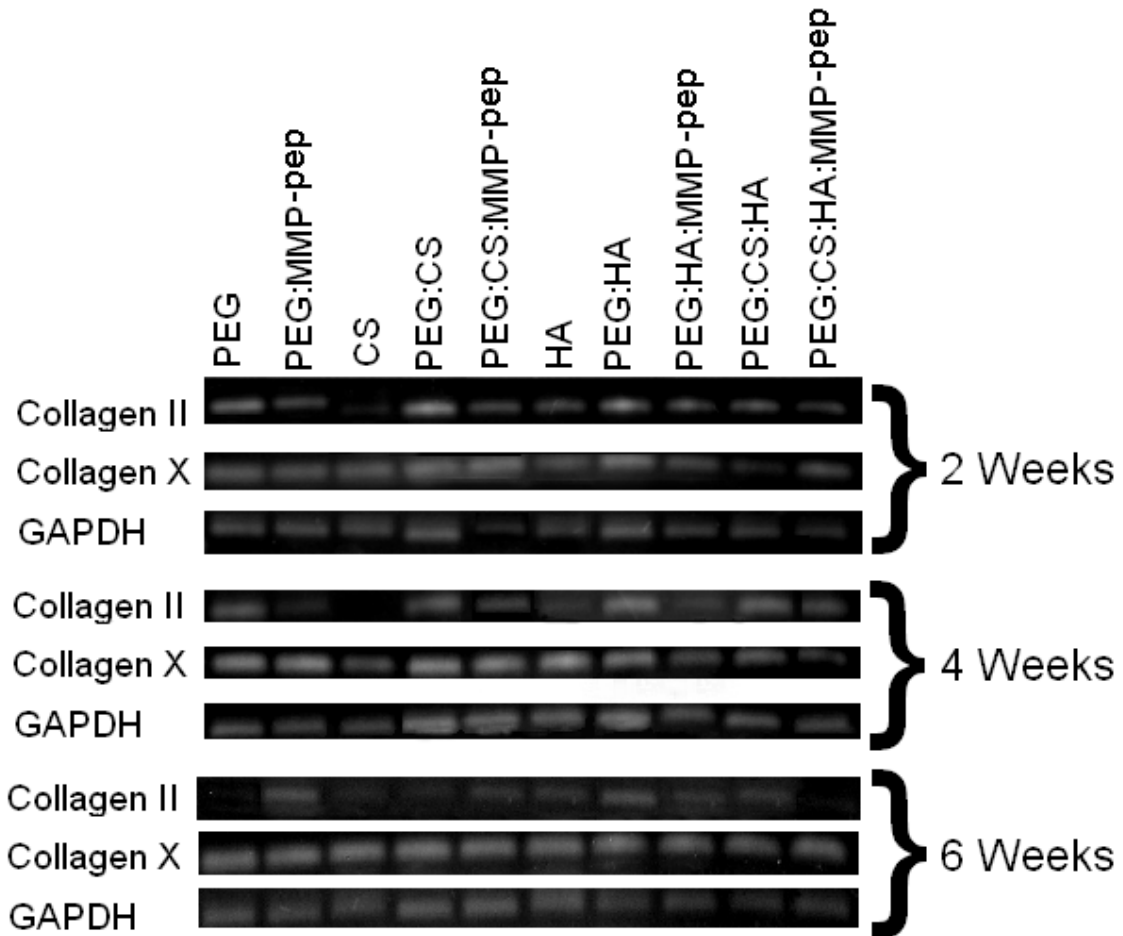


Figure 4.4 Immunohistochemical Staining of paraffin-embedded sections of all hydrogels constructs at 2, 4 and 6 weeks for collagen II (green) and X (red) (63X objective, Leica SP2 AOBS). At all time points, the fluorescent images showed positive staining for both collagen II and X.

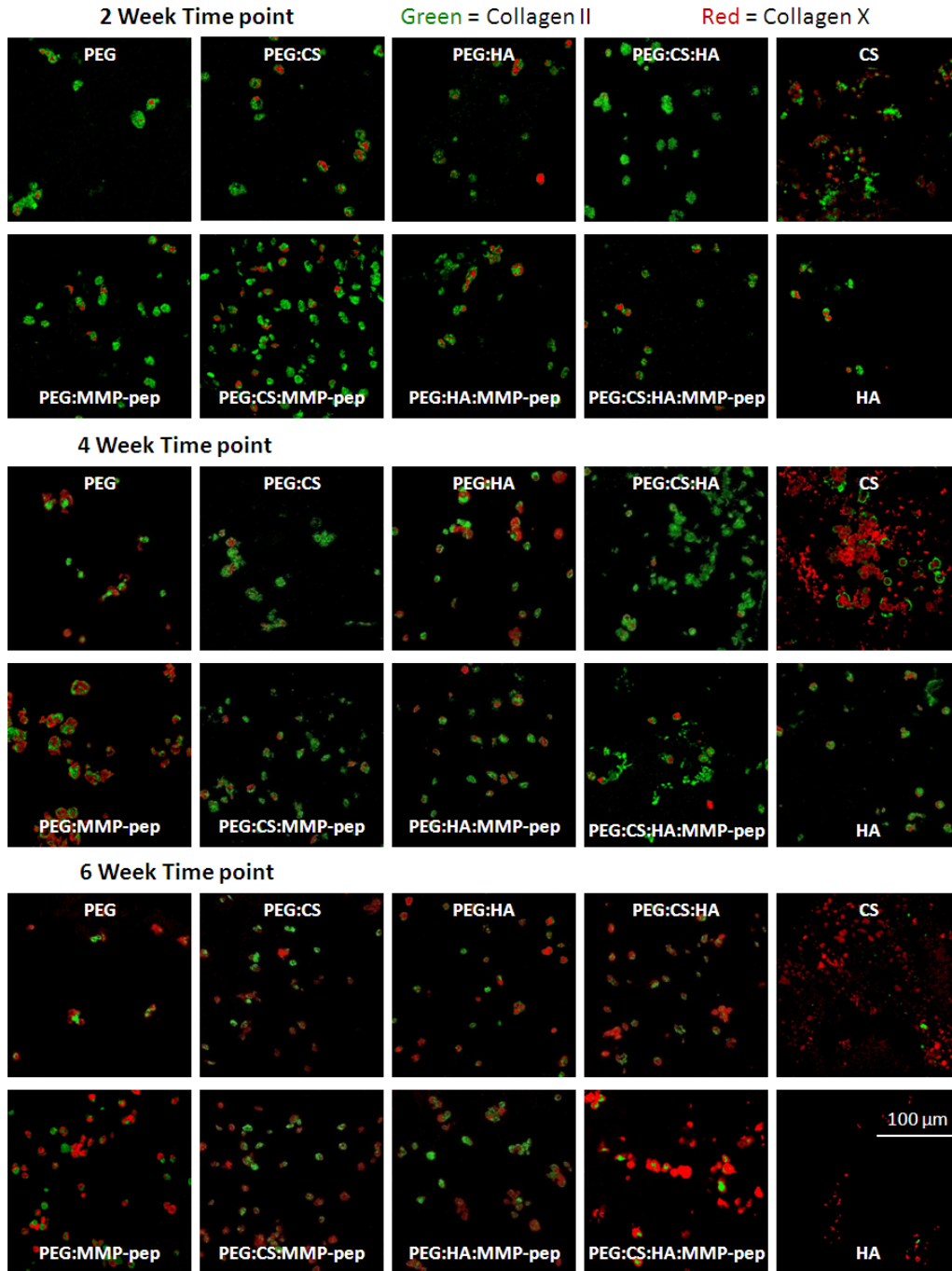


Figure 4.5 GAG Concentrations of the hydrogel constructs is dependent on matrix composition and time point of assay. Given the differences in material composition and cell density of the hydrogels, GAG content of blank (no cells) hydrogels were subtracted as background and matrix accumulation was normalized to DNA content to observe differences in the biosynthetic activity of the cells within each hydrogel group.

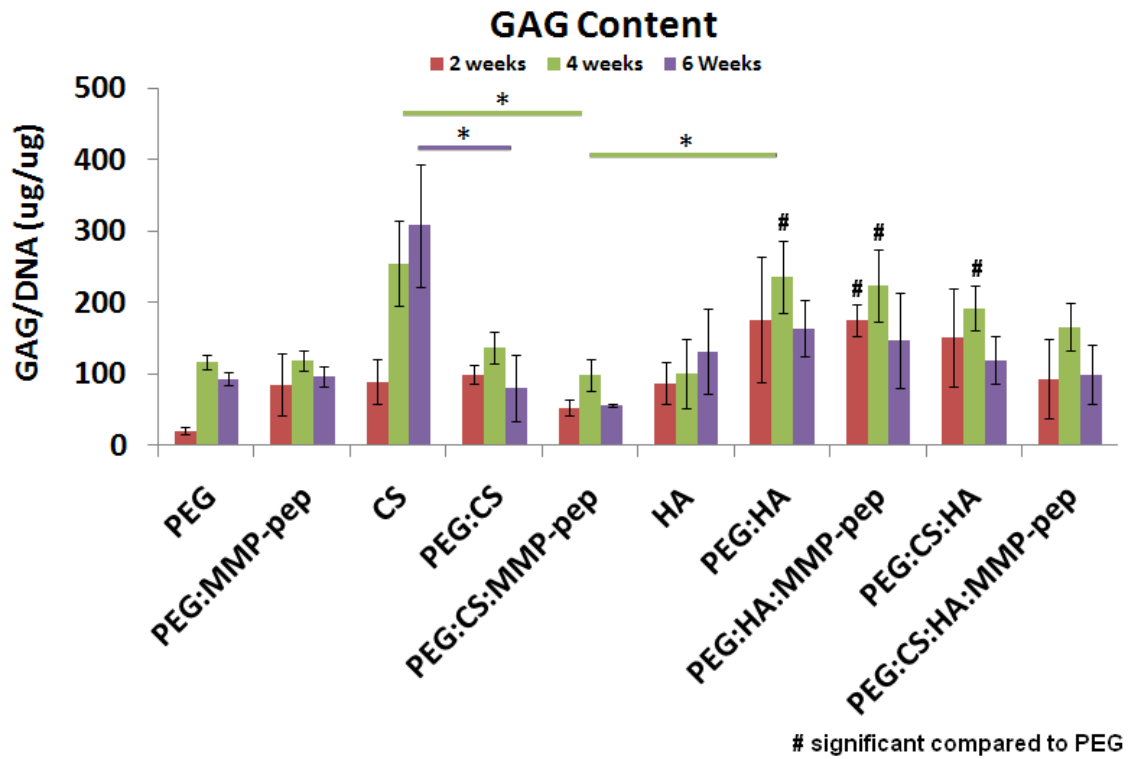
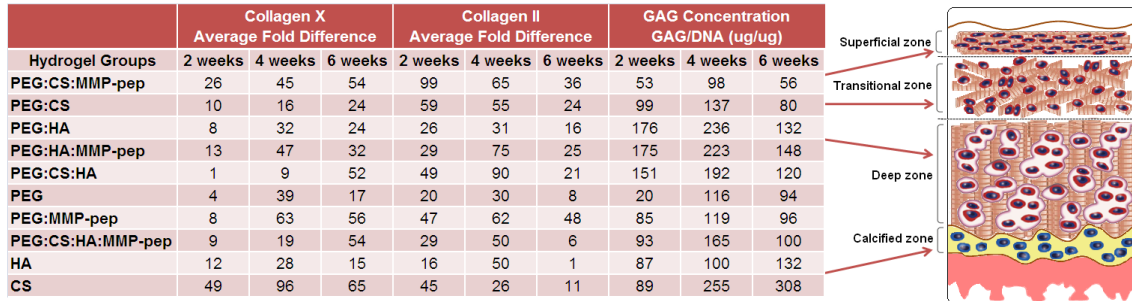


Table 4.2 Compressive Moduli of Cell Laden Hydrogel Constructs

Hydrogel Groups	2 Weeks		4 Weeks		6 Weeks	
	Moduli (kPa)	Standard Error	Moduli (kPa)	Standard Error	Moduli (kPa)	Standard Error
PEG	197.65	± 25.51	512.59	± 96.62	751.18	± 54.86
PEG:MMP-pep	244.41	± 37.00	492.34	± 40.47	603.99	± 64.26
CS	26.42	± 5.80	65.03	± 9.98	68.18	± 37.37
PEG:CS	121.14	± 36.00	284.00	± 89.96	270.87	± 31.55
PEG:CS:MMP-pep	120.33	± 28.62	147.88	± 21.01	209.1	± 38.16
HA	41.66	± 14.12	11.60	± 4.68		
PEG:HA	271.57	± 64.21	435.07	± 59.52	1227.9	± 102.14
PEG:HA:MMP-pep	201.41	± 4.77	360.63	± 54.56	666.73	± 118.35
PEG:CS:HA	92.19	± 10.47	204.50	± 77.75	521.79	± 31.39
PEG:CS:HA:MMP-pep	80.30	± 13.46	159.96	± 17.85	389.44	± 59.70

Figure 4.6 Correlations of Hydrogel Compositions to the Zones of Articular Cartilage. PEG:CS:MMP-pep corresponding to the superficial zone, PEG:CS to the transitional zone, PEG:HA:MMP-pep to the deep zone and CS corresponding to the calcified cartilage zone.



4.6 REFERENCES

1. Benya, P.D. and J.D. Shaffer, *Dedifferentiated chondrocytes reexpress the differentiated collagen phenotype when cultured in agarose gels*. Cell, 1982. **30**(1): p. 215-24.
2. Thirion, S. and F. Berenbaum, *Culture and phenotyping of chondrocytes in primary culture*. Methods Mol Med, 2004. **100**: p. 1-14.
3. Caplan, A.I., *Mesenchymal stem cells*. J Orthop Res, 1991. **9**(5): p. 641-50.
4. Varghese, S., et al., *Chondrogenic differentiation of human embryonic germ cell derived cells in hydrogels*. Conf Proc IEEE Eng Med Biol Soc, 2006. **1**: p. 2643-6.
5. Hwang, N.S., et al., *Chondrogenic differentiation of human embryonic stem cell-derived cells in arginine-glycine-aspartate-modified hydrogels*. Tissue Eng, 2006. **12**(9): p. 2695-706.
6. Hwang, N.S., S. Varghese, and J. Elisseeff, *Derivation of chondrogenically-committed cells from human embryonic cells for cartilage tissue regeneration*. PLoS ONE, 2008. **3**(6): p. e2498.
7. Hwang, N.S., et al., *Effects of three-dimensional culture and growth factors on the chondrogenic differentiation of murine embryonic stem cells*. Stem Cells, 2006. **24**(2): p. 284-91.
8. Kramer, J., et al., *Embryonic stem cell-derived chondrogenic differentiation in vitro: activation by BMP-2 and BMP-4*. Mech Dev, 2000. **92**(2): p. 193-205.
9. Hwang, N.S., et al., *Enhanced chondrogenic differentiation of murine embryonic stem cells in hydrogels with glucosamine*. Biomaterials, 2006. **27**(36): p. 6015-23.

10. Wakitani, S., et al., *Mesenchymal cell-based repair of large, full-thickness defects of articular cartilage*. J Bone Joint Surg Am, 1994. **76**(4): p. 579-92.
11. Song, L., D. Baksh, and R.S. Tuan, *Mesenchymal stem cell-based cartilage tissue engineering: cells, scaffold and biology*. Cytotherapy, 2004. **6**(6): p. 596-601.
12. Chen, F.H. and R.S. Tuan, *Mesenchymal stem cells in arthritic diseases*. Arthritis Res Ther, 2008. **10**(5): p. 223.
13. Jakobsen, R.B., et al., *Chondrogenesis in a hyaluronic acid scaffold: comparison between chondrocytes and MSC from bone marrow and adipose tissue*. Knee Surg Sports Traumatol Arthrosc, 2009.
14. Diekman, B.O., et al., *Chondrogenesis of adult stem cells from adipose tissue and bone marrow: induction by growth factors and cartilage-derived matrix*. Tissue Eng Part A, 2010. **16**(2): p. 523-33.
15. Kim, H.J. and G.I. Im, *Chondrogenic differentiation of adipose tissue-derived mesenchymal stem cells: greater doses of growth factor are necessary*. J Orthop Res, 2009. **27**(5): p. 612-9.
16. Awad, H.A., et al., *Chondrogenic differentiation of adipose-derived adult stem cells in agarose, alginate, and gelatin scaffolds*. Biomaterials, 2004. **25**(16): p. 3211-22.
17. Mahmoudifar, N. and P.M. Doran, *Chondrogenic differentiation of human adipose-derived stem cells in polyglycolic acid mesh scaffolds under dynamic culture conditions*. Biomaterials, 2010. **31**(14): p. 3858-67.
18. Pei, M., F. He, and G. Vunjak-Novakovic, *Synovium-derived stem cell-based chondrogenesis*. Differentiation, 2008. **76**(10): p. 1044-56.

19. Winter, A., et al., *Cartilage-like gene expression in differentiated human stem cell spheroids: a comparison of bone marrow-derived and adipose tissue-derived stromal cells*. *Arthritis Rheum*, 2003. **48**(2): p. 418-29.
20. Huang, J.I., et al., *Chondrogenic potential of progenitor cells derived from human bone marrow and adipose tissue: a patient-matched comparison*. *J Orthop Res*, 2005. **23**(6): p. 1383-9.
21. Afizah, H., et al., *A comparison between the chondrogenic potential of human bone marrow stem cells (BMSCs) and adipose-derived stem cells (ADSCs) taken from the same donors*. *Tissue Eng*, 2007. **13**(4): p. 659-66.
22. Burdick, J.A. and K.S. Anseth, *Photoencapsulation of osteoblasts in injectable RGD-modified PEG hydrogels for bone tissue engineering*. *Biomaterials*, 2002. **23**(22): p. 4315-23.
23. Bryant, S.J., et al., *Encapsulating chondrocytes in degrading PEG hydrogels with high modulus: engineering gel structural changes to facilitate cartilaginous tissue production*. *Biotechnol Bioeng*, 2004. **86**(7): p. 747-55.
24. Bryant, S.J., et al., *Crosslinking density influences the morphology of chondrocytes photoencapsulated in PEG hydrogels during the application of compressive strain*. *J Orthop Res*, 2004. **22**(5): p. 1143-9.
25. Bryant, S.J. and K.S. Anseth, *Controlling the spatial distribution of ECM components in degradable PEG hydrogels for tissue engineering cartilage*. *J Biomed Mater Res A*, 2003. **64**(1): p. 70-9.
26. Alcantar, N.A., E.S. Aydil, and J.N. Israelachvili, *Polyethylene glycol-coated biocompatible surfaces*. *J Biomed Mater Res*, 2000. **51**(3): p. 343-51.

27. Park, Y., et al., *Bovine primary chondrocyte culture in synthetic matrix metalloproteinase-sensitive poly(ethylene glycol)-based hydrogels as a scaffold for cartilage repair*. Tissue Eng, 2004. **10**(3-4): p. 515-22.
28. Reboul, P., et al., *The new collagenase, collagenase-3, is expressed and synthesized by human chondrocytes but not by synoviocytes. A role in osteoarthritis*. J Clin Invest, 1996. **97**(9): p. 2011-9.
29. Mengshol, J.A., et al., *Interleukin-1 induction of collagenase 3 (matrix metalloproteinase 13) gene expression in chondrocytes requires p38, c-Jun N-terminal kinase, and nuclear factor kappaB: differential regulation of collagenase 1 and collagenase 3*. Arthritis Rheum, 2000. **43**(4): p. 801-11.
30. Li, Q., et al., *Photocrosslinkable polysaccharides based on chondroitin sulfate*. J Biomed Mater Res A, 2004. **68**(1): p. 28-33.
31. Varghese, S., et al., *Chondroitin sulfate based niches for chondrogenic differentiation of mesenchymal stem cells*. Matrix Biol, 2008. **27**(1): p. 12-21.
32. Yoo, H.S., et al., *Hyaluronic acid modified biodegradable scaffolds for cartilage tissue engineering*. Biomaterials, 2005. **26**(14): p. 1925-33.
33. Dahir, G.A., et al., *Pluripotential mesenchymal cells repopulate bone marrow and retain osteogenic properties*. Clin Orthop Relat Res, 2000(379 Suppl): p. S134-45.
34. Hsiong, S.X., et al., *Cyclic arginine-glycine-aspartate peptides enhance three-dimensional stem cell osteogenic differentiation*. Tissue Eng Part A, 2009. **15**(2): p. 263-72.
35. Chimal-Monroy, J., M.T. Bravo-Ruiz, and L. Diaz de Leon, *Regulation of chondrocyte differentiation by transforming growth factors beta 1, beta 2, beta 3, and beta 5*. Ann N Y Acad Sci, 1996. **785**: p. 241-4.

36. Chimal-Monroy, J. and L. Diaz de Leon, *Differential effects of transforming growth factors beta 1, beta 2, beta 3 and beta 5 on chondrogenesis in mouse limb bud mesenchymal cells*. Int J Dev Biol, 1997. **41**(1): p. 91-102.
37. Livak, K.J. and T.D. Schmittgen, *Analysis of relative gene expression data using real time quantitative PCR and the 2^{-ΔΔCT} method*. . 2001. p. 402-408.
38. Mapili Call, G., *Microfabrication of Spatially-Patterned, Polymer Scaffolds for Applications in Stem Cell and Tissue Engineering*, in *Biomedical Engineering*. 2007, University of Texas at Austin: Texas. p. 201.
39. Barry, F., et al., *Chondrogenic differentiation of mesenchymal stem cells from bone marrow: differentiation-dependent gene expression of matrix components*. Exp Cell Res, 2001. **268**(2): p. 189-200.
40. Williams, C.G., et al., *In vitro chondrogenesis of bone marrow-derived mesenchymal stem cells in a photopolymerizing hydrogel*. Tissue Eng, 2003. **9**(4): p. 679-88.
41. Eyre, D.R. and J.J. Wu, *Collagen of fibrocartilage: a distinctive molecular phenotype in bovine meniscus*. FEBS Lett, 1983. **158**(2): p. 265-70.
42. Harper, J. and M. Klagsbrun, *Cartilage to bone--angiogenesis leads the way*. Nat Med, 1999. **5**(6): p. 617-8.
43. Hall, B.K., *Bones and Cartilage Developmental and Evolutionary Skeletal Biology*. 2005, San Diego: Elsevier Academic Press. 760.
44. Oyajobi, B.O., et al., *Expression of type X collagen and matrix calcification in three-dimensional cultures of immortalized temperature-sensitive chondrocytes derived from adult human articular cartilage*. J Bone Miner Res, 1998. **13**(3): p. 432-42.

45. Pacifici, M., et al., *Cell hypertrophy and type X collagen synthesis in cultured articular chondrocytes*. *Exp Cell Res*, 1991. **192**(1): p. 266-70.
46. Flik, K.R., et al., *Articular Cartilage*, in *Cartilage Repair Strategies*. 2007, Humana Press Inc.: New Jersey. p. 374.
47. Williams, R.J., L. Peterson, and B. Cole, *Cartilage Repair Strategies*. 2007, New Jersey: Humana Press Inc. 374.
48. Schinagl, R.M., et al., *Depth-dependent confined compression modulus of full-thickness bovine articular cartilage*. *J Orthop Res*, 1997. **15**(4): p. 499-506.

CHAPTER FIVE

Simultaneous Differentiation of MSCs into Zonally Organized Articular Cartilage within a Multi-layered Hydrogel

5.1 INTRODUCTION

Although tissue engineered cartilage offers a promising solution, most efforts to date have focused on generating homogenous tissues whose bulk properties are similar to native articular cartilage [1-7]. However, anatomically and functionally, articular cartilage consists of four, spatially distinct regions; the superficial, transitional, deep, and calcified zones [8].

As discussed in Chapter Two, each zone is characterized by unique extra-cellular matrix (ECM) compositions, mechanical properties, and cellular organization. The cartilage ECM is primarily composed of type II collagen and glycosaminoglycans (GAGs) whose relative concentrations vary spatially from the superficial to the deep zone leading to varying mechanical properties [9]. The superficial zone contains high levels of collagen II and low levels of GAG [10]. The transitional zone has lower collagen II content while the GAG concentration increases [11]. The deep zone contains the highest concentration of GAGs and the lowest level of collagen II fibers [8]. Finally, the calcified cartilage zone contains high levels of collagen X and integrates the cartilage to the subchondral bone [8, 10, 11]. The mechanical properties of articular cartilage are sensitive to changes in the ECM composition because any compressive forces that are experienced by the tissue, stimulates GAG synthesis and ECM remodeling [12, 13]. Specifically, the compressive modulus increases significantly from the articular surface to the deep zone and is dictated by the varying ECM composition of the various zones and the structural organization of the ECM molecules [9].

Since the properties of articular cartilage are dictated by its structural organization, it is important to reproduce this zonal architecture and function when attempting to generate articular cartilage substitutes. The classical approach of creating homogenous tissue replacements has failed to achieve widespread clinical effectiveness because the bulk properties of the homogenous tissue cannot mimic native articular cartilage function. Thus the goal of this dissertation and the focus of this chapter were to create zonally organized articular cartilage that can function as proper mechanical substitutes.

Chapter Four demonstrated that biomaterials can be used to direct stem cell differentiation into specific chondrocytes, within single layer hydrogels. Building on the findings of Chapter Four, a multi-layered hydrogel with the specific biomaterials was created in Chapter Five. The multi-layered hydrogel construct (MLHC) was fabricated for the purpose of simultaneously differentiating a single stem cell population into the specific zones of articular cartilage. The specific correlations determined in Chapter Four for each layer of the multi-layer construct are as follows: PEG:CS:MMP-pep, PEG:CS, and PEG:HA, representing the superficial, transitional, and deep zone respectively. The findings indicate that three-dimensional matrices composed of both synthetic and natural biopolymers may provide specific environmental cues necessary for differentiating MSCs and directing them to develop into zone-specific cartilage phenotypes.

5.2 MATERIALS AND METHODS

5.2.1 Multi-Layered Hydrogel Fabrication

The fabrication of the MLHC was performed from the bottom layer upward. The specific biomaterial compositions and concentrations of each layer are listed in **Table 5.1**. Briefly, 100 μL of PEG:HA-MSM mixture was polymerized under UV for 3 minutes to represent the deep zone. Then 100 μL of PEG:CS-MSM mixture was added on top of the partially polymerized bottom layer and placed under UV for an additional 3 minutes to represent the transitional zone. Finally, for the superficial zone, 100 μL of PEG:CS:MMP-pep-MSM mixture was placed under UV on top of the previous two layers for 5 minutes to fully polymerize the entire multi-layered hydrogel. A schematic of the multi-layered hydrogel fabrication technique is illustrated in **Figure 5.1A**, S representing the superficial layer, T representing the transitional layer, and D representing the deep layer. This multi-layered scaffold was cultured in serum-free chondrogenic media containing 1% penicillin/streptomycin, 10nM Dexamethasone, 50 $\mu\text{g}/\text{mL}$ ascorbic acid-2-phosphate, 40 $\mu\text{g}/\text{mL}$ L-proline, 5 mL ITS+1, and 10 ng/mL TGF- β 1 for 2, 4, and 6 weeks in a 12-well plate [14]. **Figure 5.1D** showed the cell laden multi-layered hydrogel construct exhibiting distinct chondron formations, which are chondrocytes surrounded by a proteoglycan matrix, after 2 weeks in culture.

5.2.2 Single Layer Hydrogel Fabrication and Cell Culture

As illustrated in **Figure 5.1B**, single layer hydrogels were fabricated and cultured as controls for replication of previous experiments performed in Chapter Four. D1 bone marrow progenitor cells were encapsulated within polymer solutions of PEG:CS:MMP-pep, PEG:CS, and PEG:HA as single layered hydrogel constructs. 20 million cells/mL were mixed with the syringe-filtered polymer solution of each layer and 100 μL of the cell/polymer mixed was polymerized for 10 minutes using a long-

wave ultraviolet lamp (Model B100AP, Blak-Ray) at an intensity of ~ 10 mW/cm². The hydrogels were cultured in serum-free chondrogenic media as detailed in Section 5.2.1. The media was changed every other day.

5.2.3 Cell Viability

Viability of encapsulated cells in the multi-layered hydrogel constructs was determined after 2, 4, and 6 weeks of culture. At each time, the media were discarded, and the constructs were washed with PBS (Gibco, Carlsbad, CA) twice for 5 minutes. The MLHC were thinly sliced transversely with a razor. Cell viability was assessed based on previously published methods by Lee et al. [15]. Briefly, the Live/Dead Viability/Cytotoxicity Kit (Molecular Probes, Eugene, OR) that contains calcein-AM (“live” dye) and ethidium homodimer-1 (“dead” dye) was used to assess the integrity of the cellular membrane. Dye solution was made with 0.5 μ L of calcein-AM dye and 2 μ L of ethidium homodimer-1 dye in 1 mL of DMEM. A transverse slice of the construct was incubated in 500 μ L of the “Live/Dead” dye solution for 30 minutes. Fluorescence microscopy (Olympus, 4X) was performed using a fluorescein optical filter (485 ± 10 nm) for calcein-AM and a rhodamine optical filter (530 ± 12.5 nm) for ethidium homodimer-1.

5.2.4 RNA Isolation and RT-PCR

Chondrogenesis was determined by the gene expression of collagen I, II, and X within these multi-layered hydrogel constructs at 2, 4, and 6 week time points. The hydrogel constructs were removed from culture, and the gene expressions of encapsulated cells were analyzed. The single-layered hydrogels were homogenized, as detailed in Section 4.2.2. The MLHC was first sliced with a razor to separate the layers

as illustrated in **Figure 5.1C** and the interface was used to determine the modulus. The individual layers were placed into individual 2mL microcentrifuge tubes, and 200 μ L of TRIzol[®] was added to the tubes. Each layer was then crushed using a homogenizer (Wheaton). After complete homogenization, another 800 μ L of Trizol[®] was added to the tube. The RNA isolation of the homogenized scaffolds was performed following the manufacture's protocol, as detailed in Section 4.2.2. Genomic DNA was removed using Deoxyribonuclease I (Invitrogen, Carlsbad, CA). The first strand of cDNA was synthesized by reverse transcription (RT) using Superscript[™] III kit (Invitrogen, Carlsbad, CA), following the manufacturer's instructions, as detailed in Section 4.2.2. Quantitative polymerase chain reaction (PCR) was performed using an ABI Prism[®] 7900 Real Time thermal cycler and HotStartTaq DNA Polymerase with SYBR green/ROX PCR master mix (SA Biosciences, Fredrick, Maryland). Primers for the housekeeping gene (GAPDH), collagen type II, type X and type I (SA Biosciences, Frederick, MD) are listed in **Table 4.1**.

5.2.5 Histology and Immunohistochemistry

Histology of these hydrogel matrices was performed to determine the chondrogenic differentiation within the MLHC and for verification of the quantitative real time data. At 2, 4, and 6 week time points, hydrogels were removed from culture and fixed in 4% paraformaldehyde at 4°C for an overnight period. Fixed hydrogels were then dehydrated for paraffin embedding using 1-hr sequential steps in the following order: 80%, 95%, 95% ethanol in dH₂O, 100% ethanol, 50/50 ethanol/CitriSolv, 100% CitriSolv, 100% CitriSolv, 60°C molten paraffin, and 60°C molten paraffin for an overnight period. Paraffin-embedded hydrogels were sliced in transverse sections at 10 μ m using a rotary microtome. Sections were stained for differentiation.

Double sequential immunohistochemistry was performed to stain for collagen II (green) and collagen X (red) using rabbit polyclonal primary antibodies (Abcam, Cambridge, MA) and Texas red (collagen II) or FITC (collagen X) conjugated secondary antibodies. Slides containing sectioned hydrogels were blocked for nonspecific binding for 30 minutes at 37 °C using 3% (w/v) bovine serum albumin (BSA) in PBS (pH 7.4). The slides were rinsed with 0.05% tween 20 in PBS solution three times. The washed slides were incubated with primary antibody for 30 minutes at 37 °C. The slides were rinsed again before the second incubation with the secondary antibody for 30 minutes at 37 °C. These steps were repeated for collagen X on the same slides. The slides were imaged using a confocal fluorescence microscope (Leica SP2 AOBS, 63X).

5.2.6 Biochemical Characterization

Glycosaminoglycan (GAG) production within each layer of the MLHC was determined using the Dimethylmethylene blue (DMMB) assay. Briefly, at 2, 4, and 6 week time points, hydrogels were removed from culture. Wet weights (ww) and dry weights (dw) after 48 hours of lyophilization were obtained for each construct (n=3). The dry constructs were then digested in 1 mL of papinase (papain, 125 μ g/mL; Sigma, St. Louis, MO) at 60°C overnight. 200 μ L of the DMMB solution was added to each well of the 96 well plates; then 50 μ L of standard and samples were added. The plate was shaken for 10 seconds before reading the absorbance at 525nm. To account for the hydrogel material, absorbance of blank hydrogels was subtracted from the sample values. The DNA content was determined using Sigma's DNA quantification kit (DNA-QF) in order to normalize the GAG production. The assay was carried out following the manufacture's protocol for multiwall assay, as detailed in Section 4.25.

5.2.7 Compression Studies of the MLHC

The compressive modulus of the individual layers and the interfaces between layers of the MLHC were determined at room temperature on an In-spec 2200 Instron mechanical tester with a 125 N loading cell using a parallel plate apparatus and loading of 20% of the initial thickness per second (0.1 mm/sec). The compressive modulus of the individual layers as well the interface between were determined by analyzing the linear region of the stress versus the strain curve of the samples at low deformations (<20% strain).

5.2.8 Statistical Analysis

All quantitative data were expressed as mean \pm standard error and were verified by analysis of variance using one way ANOVA Fixed Effects Model [16]. P values of less than 0.05 were considered statistically significant. Error bars in all figures represent standard error.

5.3 RESULTS

5.3.1 Viability of Encapsulated MSCs

A cytotoxicity assay was performed to test for the viability of the MSCs encapsulated within the multi-layered hydrogel constructs at 2, 4, and 6 weeks. As shown in **Figure 5.2**, the majority of the cells stained green, indicating that there are more live cells than dead cells, which are stained red, at all time points. At 2 weeks, the transitional layer exhibited the greatest amount of live cells, while the deep layer contained the largest amount of dead cells. At 4 weeks, the cell density appears to be more evenly distributed within all the layers of the multi-layered construct with very few

dead cells. At 6 weeks, all the dead cells appear at the edge of the hydrogel construct with the greatest amount of dead cells in the deep layer. Additionally, the deep layer also contains the highest cell density at 6 weeks.

5.3.2 Chondrogenic Differentiation of MSCs

The purpose of this chapter was to investigate the potential of a MLHC to simultaneously differentiate MSCs into zone specific chondrocytes. Again, gene expression of collagen type II, X, and I were used to verify chondrogenesis. The average fold difference as compared to undifferentiated cells encapsulated within PEG-only hydrogels for collagen II, X, and I of each layer of the MLHC and single layer controls (SLC) are shown in **Figures 5.3, 5.4, and 5.5**, respectively. Again, the PEG:CS:MMP-pep composition represents the superficial layer, the PEG:CS composition represents the transitional layer, and the PEG:HA composition represents the deep layer for the SLC.

Collagen II expression in the superficial layer was significantly ($p < 0.05$) higher compared to the deep layer at all time points as (**Figure 5.3A**). Similarly, the SLC (**Figure 5.3B**) demonstrated significantly higher collagen II expression at all time points in the superficial composition (PEG:CS:MMP-pep) as compared to the deep composition (PEG:HA). Additionally, at 2 weeks both the superficial and deep layer of the MLHC exhibited significantly higher collagen II expressed as compared to the PEG:CS:MMP-pep and PEG:HA SLC, respectively.

Collagen X expression within the MLHC was significantly higher in the deep layer as compared to the superficial layer (**Figure 5.4A**) for both 4 and 6 weeks. The SLC (**Figure 5.4B**) exhibited a trend of increasing collagen X expression from the superficial to the deep composition at all time points, but was only statistically different between the PEG:CS:MMP-pep and the PEG:HA at 2 weeks. Although the transitional

layer and the PEG:CS composition showed a trend of lower collagen II and higher collagen X when compared to the superficial layer and the PEG:CS:MMP-pep composition, the values were not statistically significant for both the SLC and between the layers of the MLHC.

The expression of type I collagen was again very low for both the SLC as well as within the individual layers of the MLHC. As shown in **Figure 5.5A**, at 2 weeks, the transitional layer of the multi-layered construct had significantly higher collagen I expression than the superficial layer. While at 6 weeks, both the superficial and transitional layer of the MLHC exhibited significantly lower collagen I expression compared to the deep layer. **Figure 5.5B** shows the collagen I expression of the SLC. At both 4 and 6 weeks the PEG:HA composition had significantly higher collagen I expression than the PEG:CS:MMP-pep composition. At 4 weeks, the PEG:CS:MMP-pep composition has significantly lower collagen I expression compared to the superficial layer of the multi-layered construct. At 4 weeks the superficial, the transitional, and the deep layers of the multi-layered construct had higher collagen I expression than their opposing SLC.

5.3.3 Histological Analysis of Imaged Hydrogels

For further verification of chondrogenesis, immunohistochemical staining was performed to determine if the cells were producing collagen II and collagen X. At all time points, the fluorescent images showed positive staining for both collagen II and X within all layers (**Figure 5.6**). The collagen II staining increased with time and exhibited the highest intensity at 6 weeks. At 2 weeks the collagen II staining appeared more evenly dispersed within the superficial and transitional layer but within the deep layer the collagen II staining appear to be aggregated into clusters. At 4 and 6 weeks the

spatial organization of both collagen II appeared to correspond to native articular cartilage [8]. In the superficial layer the collagen II staining appeared to be relatively high and the collagen diameter appeared to be smaller, less clustered and aligned parallel to the top surface (articular surface). In the transitional layer the collagen II staining appeared to be higher than the collagen X staining and collagen diameters are larger and more clustered with a random orientation. Finally, in the deep layer the collagen X were the most intense at all time points, with larger collagen diameter and clusters, which are aligned perpendicular to the bottom surface (subchondral plate). Again immunohistochemical staining was not performed for type I collagen due to low mRNA expression.

5.3.4 Protein Analysis for Total GAG Production

The GAG/DNA ratio for each layer of the MLHC is shown in **Figure 5.7A**. GAG production increased with time in all layers of the MLHC with cells in the deep layer exhibiting significantly higher GAG levels compared to the superficial layer at all time points. The transitional layer also had significantly lower GAG production compared to the deep layer at both 2 and 4 weeks. **Figure 5.7B** shows the GAG concentration of the SLC and at all time points the PEG:HA composition had significantly higher GAG production compared to the PEG:CS:MMP-pep composition. At 2 and 6 weeks, the superficial layer of the multi-layered construct had significantly higher GAG production when compared to the PEG:CS:MMP-pep single layer control. However, the PEG:CS single layer composition exhibited significantly higher GAG production than the transitional layer of the multi-layered construct. At 4 weeks there were no significant differences between the layers of the multi-layered construct and the SLC.

5.3.5 Compressive Strength of the Individual Layers

Table 5.2 and **Table 5.3** list the compressive moduli of the individual layers of the blank and cell-laden MLHC, including the interface, respectively. **Table 5.4** lists the compressive modulus of the SLC. The compressive modulus of the interface shows a gradual increase between the superficial and transitional layer, as well as between the transitional and the deep layer within the MLHC. **Figure 5.8** shows the compressive modulus of the individual layers as a bar graph for easy comparison. Similar to our single layer results discussed in Chapter Four and the SLC, the MLHC showed increasing compressive strength from the superficial to the deep layer. The compressive moduli of the individual layers as well as the interface all increased with time, with 6 weeks exhibiting the highest modulus of all layers and interfaces. The compressive modulus of the deep layer was significantly higher than the superficial layer at all time points. Additionally, at 2 and 4 weeks the modulus of the deep layer was also significantly higher than that of the transitional layer. The compressive modulus of the superficial layer was not significantly different from the transitional layer at all time points. The compressive modulus of the superficial layer at both 2 and 4 weeks is significantly higher than the modulus of the PEG:CS:MMP-pep composition found in chapter four and the SLC. The 4 week modulus of the deep layer was also significantly higher than the modulus of the PEG:HA composition determined in chapter four. Additionally, at 4 weeks the moduli of all layers within the MLHC were significantly higher than the SLC. At 6 weeks, the modulus of the transitional layer of the MLHC was significantly higher than the modulus of the PEG:CS composition obtained in Chapter Four. Furthermore, the modulus of the deep layer of the MLHC is significantly higher than that of the SLC.

5.3 DISCUSSION

Chapter Four directly compared the effects of CS and HA incorporation as well as MMP-pep for matrix degradation within a PEG-based hydrogel network for chondrogenesis from MSCs. Collectively, the single layer results demonstrated that these hydrogels not only induce MSCs to differentiate into chondrocytes, but also that the differentiated phenotype and matrix production can be tailored to specific zones of articular cartilage by altering the material composition. Specifically, the PEG:CS:MMP-pep composition exhibited the highest collagen II expression as well as the lowest GAG production, which can be correlated to the superficial zone of articular cartilage. Both the PEG:CS and PEG:MMP-pep compositions had midrange expression of collagen II as well as GAG content, which can be correlated to the transitional zone of articular cartilage. At the same time, the PEG:HA composition can be correlated to the deep zone because of its high GAG content and low expression of collagen II. Although both PEG:MMP-pep and PEG:CS can be correlated to the transitional zone, PEG:CS was used to formulate the transitional layer of the multi-layered construct because it exhibited less collagen X expression at both 4 and 6 weeks. Based on these specific correlations, this chapter evaluated the ability of a MLHC to simultaneously differentiate the MSCs into the specific zones of articular cartilage.

To ensure that the MSCs survived the fabrication process, the cell viability of the MLHC was assessed at 2, 4, and 6 weeks. The images shown in **Figure 5.2** demonstrate that the majority of the cells survived at all time points and within all layers of the multi-layered construct. Additionally, the cells also appeared to have proliferated, increasing in cell density from 2 to 6 weeks.

The gene expressions of type I, II, and X collagens within the MLHC are in accordance with the single layer results found in Chapter Four. There was high collagen

II expression in the superficial layer and high collagen X expression in the deep layer. The transitional zone did not exhibit any significant differences in the expression of collagen II or X to either the superficial or the deep layer. Additionally, type I collagen, a marker for fibrocartilage [17], remained low within all layers at all time points. The low-level expression of collagen I indicates that the MSCs were differentiating down the articular cartilage pathway and not towards fibrocartilage formation. The formation of fibrocartilage is the major limitation of all previous cartilage repair strategies.

Histology and immunohistochemistry confirmed the RT-PCR findings and revealed that cartilage-specific proteins were produced within each layer of the multi-layered hydrogel constructs. Immunohistochemical staining for types II and X collagen showed significant differences between 2 and 6 weeks as shown in **Figure 5.6**. At 2 weeks the collagen II expression was spatially scattered with a few clusters within the deep layer. However, there was a significant increase in collagen II expression at 4 and 6 weeks compared to the week 2 images. Furthermore, the collagen staining at 4 and 6 weeks showed larger clusters, especially in the deep layer with the majority of the clusters aligning perpendicular to the articular surface. The size, clustering of the collagen and the alignment seen in the fluorescent images are similar to the structural organization of native articular cartilage.

Greater matrix accumulation was observed in the deep layers of the MLHC at all time points, indicating that the PEG:HA formulation still enhances GAG production. The GAG production increases with time but appears to level off within the deep layer. The leveling off of GAG production at the 6 week time point is most likely due to the fact that the GAG accumulation has reached its threshold as discussed in Chapter Four. Once the threshold is reached, the cells begin to remodel the ECM and turnover the

ECM components, including GAG, resulting in the relatively same GAG concentration at both the 4 and 6 week time point.

Similar to the SLC, the multi-layered hydrogel constructs showed increasing compressive strength from the superficial to the deep layer. Since the primary function of articular cartilage is to resist compression it is critical that the multi-layered, composite cartilage-tissue, have comparable and spatially varying compressive strength, similar to native cartilage. Armstrong et al. obtained small, cylindrical plugs of human cartilage to study their mechanical properties and found that out of 103 samples of varying ages, the average compressive modulus was 790 kPa with a maximum value of 1,910 kPa [18]. Shown in **Figure 5.8** and **Table 5.3** are the compressive moduli of the individual layers of the engineered MLHC. The compressive modulus increased from the superficial (239 – 472 kPa) to the deep layer (534 – 1712 kPa) ($p < 0.05$) at all time points, with the deep layer exhibiting the highest modulus (1,712 kPa) at 6 weeks, similar to the maximum value obtained by Armstrong et al. [18]. Averaging the compressive modulus of all the individual layers at 6 weeks, we obtain a value of 950 kPa (± 216 kPa, standard error), which is consistent with the average modulus of human cartilage plugs [18]. Additionally, the modulus of each layer within the MLHC increased with time, which is comparable to the SLC.

Although the moduli of the individual layers of the MLHC exhibit the same trend as seen in the SLC, their compressive strength is significantly higher when compared to their corresponding SLC. At 2 weeks, the superficial layer of the MLHC had significantly higher modulus than the PEG:CS:MMP-pep composition of the SLC, and at 6 weeks the modulus of the deep layer was significantly higher than the PEG:HA composition of the SLC. At 4 weeks, the moduli of all the layers of the MLHC were significantly higher than the SLC. The significant increase in compressive modulus of

each layer of the MLHC over their single-layer counterparts may be an indication that there is a synergistic effect between the layers that leads to enhanced ECM remodeling, resulting in improved mechanical properties.

In summary, the findings of this chapter provides evidence that spatially varying biomaterial compositions within a MLHC can be used to induce differentiation of MSCs into a single and zonally organized 3D articular cartilage-like tissue. Chapter Six discusses the possible clinical applications of these findings. The ability to create native-like, mechanically relevant articular cartilage consisting of zone specific layers provides a new direction in cartilage tissue engineering and could be invaluable for cartilage repair if incorporated with current minimally invasive surgical techniques.

5.4 FIGURES

Table 5.1 Biomaterial Composition of Each Layer

Zone	Material	PEG	CS	HA	MMP-pep
Superficial	PEG:CS:MMP-pep	9%	9%		2%
Transitional	PEG:CS		10%	10%	
Deep	PEG:HA		19%		1%

Figure 5.1 MLHC Fabrication (A) Multi-layered scaffold composed of three distinctive layers each corresponding to the superficial, middle, and deep zone of articular cartilage. (B) Single layer hydrogels of same compositions were used as controls. Individual layers were fabricated using 100 μL of the layer specific composition polymerized for 5 minutes. (C) To analyze the MLHC, each layer was carefully separated and the interface discarded. The separated layers were analyzed individually. (D) After 2 weeks of culture, the cell laden multi-layered hydrogel showed distinct formations of chondrons, which are chondrocytes surrounded by a proteoglycan matrix.

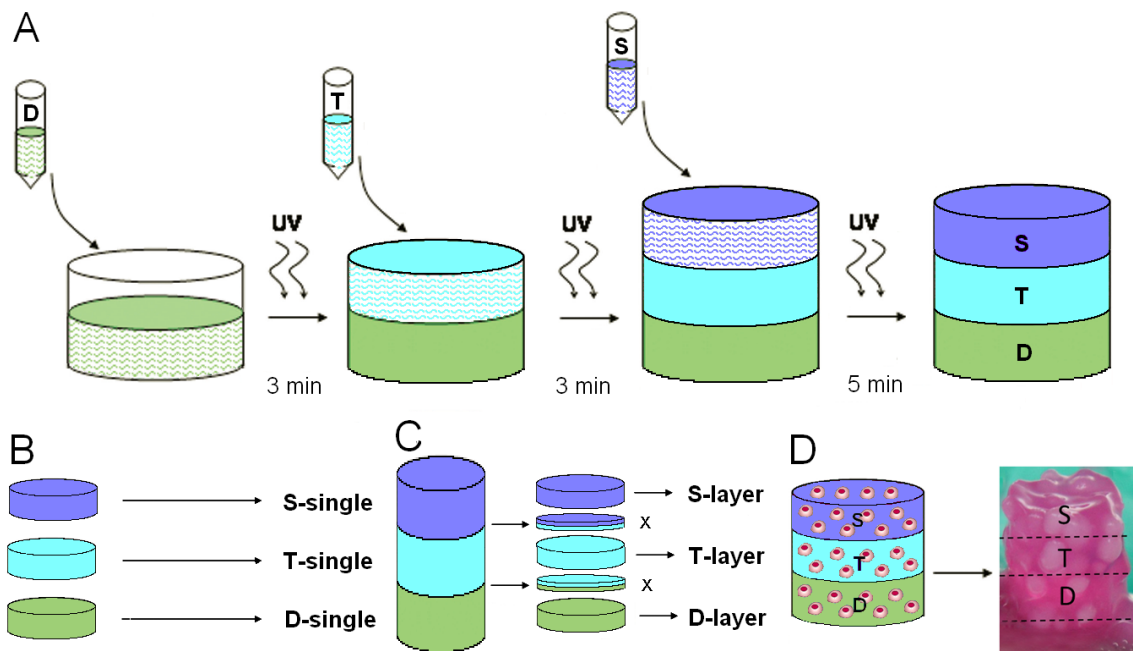


Figure 5.2 MLHC Live/Dead Staining of razor sliced sections of the MHLHC at 2, 4, and 6 weeks (4X objective, Leica SP2 AOBS). At all time points, the majority of the cells are alive (green) with very few dead cells (red).

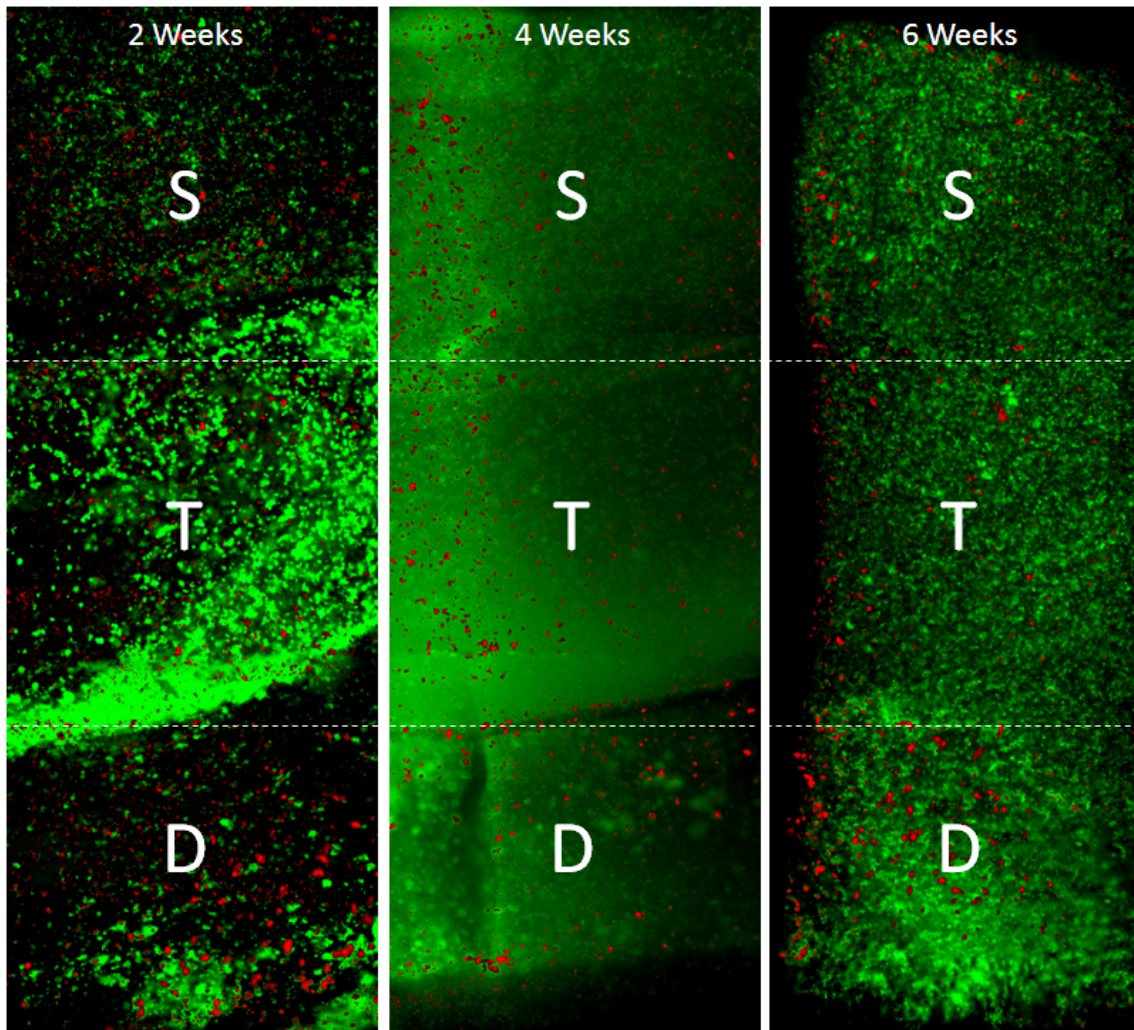


Figure 5.3 MLHC & SLC Collagen II Gene Expression shown as average fold difference at 2, 4, and 6 weeks for gene expression of Collagen II of the (A) Individual layers of the MLHC, showing significantly higher ($p < 0.05$, error bars represent standard error) collagen II expression in the superficial layer than in the deep layer of the MLHC at all time points. (B) Collagen II expression of the SLC.

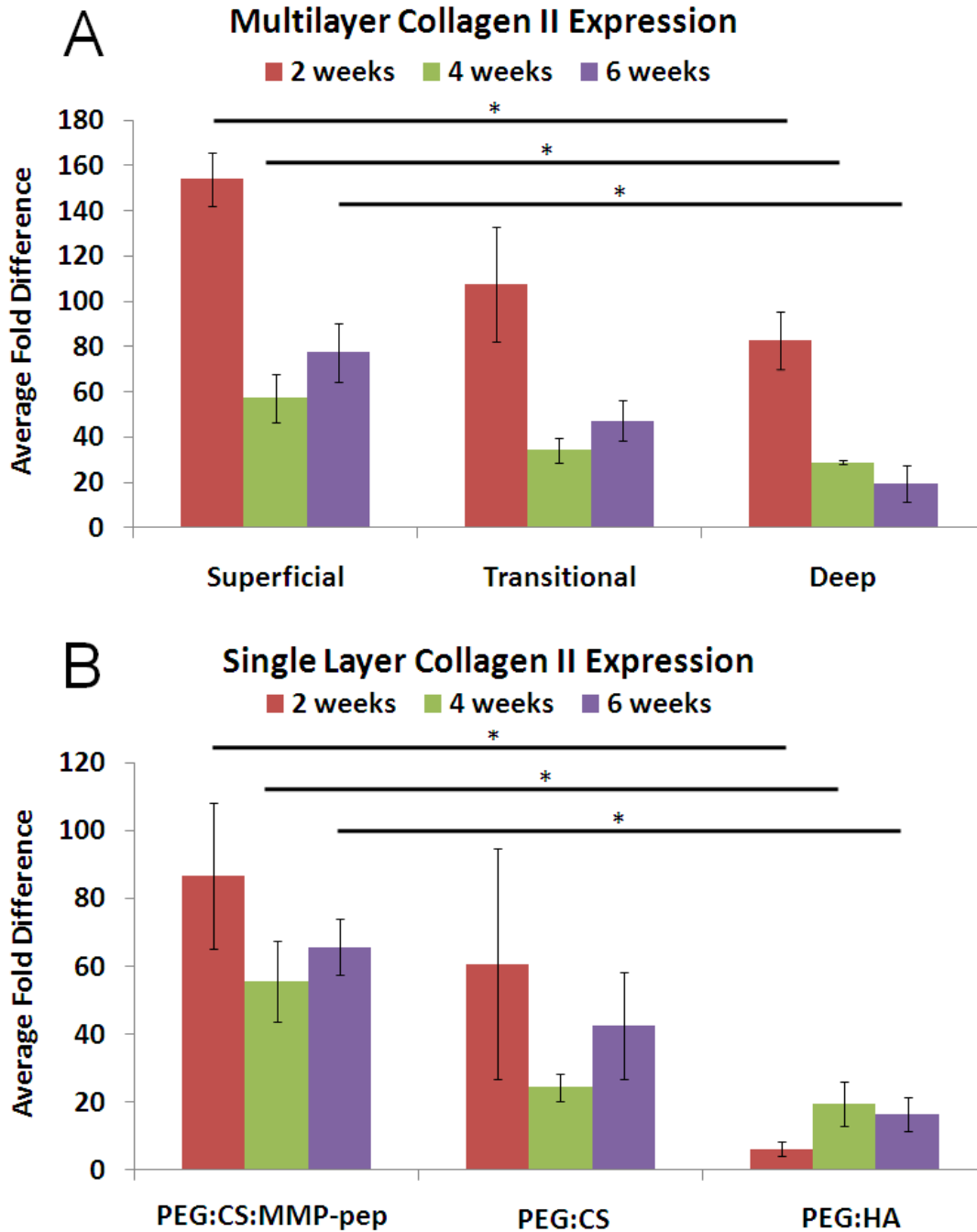


Figure 5.4 MLHC & SLC Collagen X Gene Expression shown as average fold difference at 2, 4, and 6 weeks for gene expression of Collagen X of the (A) Individual layers of the MLHC, showing significantly lower collagen X expression in the superficial layer than the deep layer at 4 and 6 weeks. (B) Collagen X expression of the SLC.

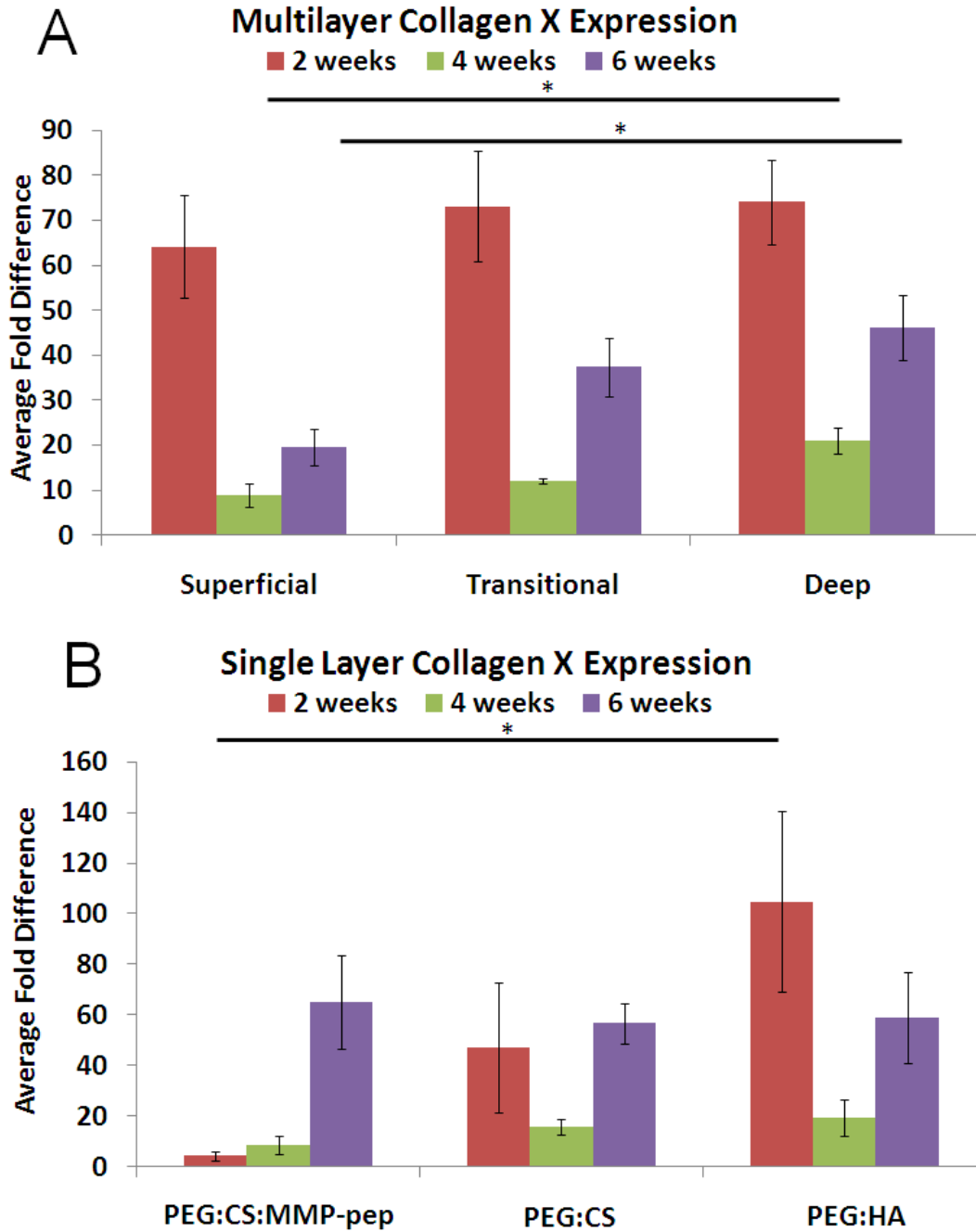


Figure 5.5 MLHC & SLC Collagen I Gene Expression shown as average fold difference at 2, 4, and 6 weeks for gene expression of Collagen I of the (A) Individual layers of the MLHC, showing Collagen I expression remaining relative low within the multi-layered hydrogel constructs at all time points. (B) Collagen X expression of the SLC.

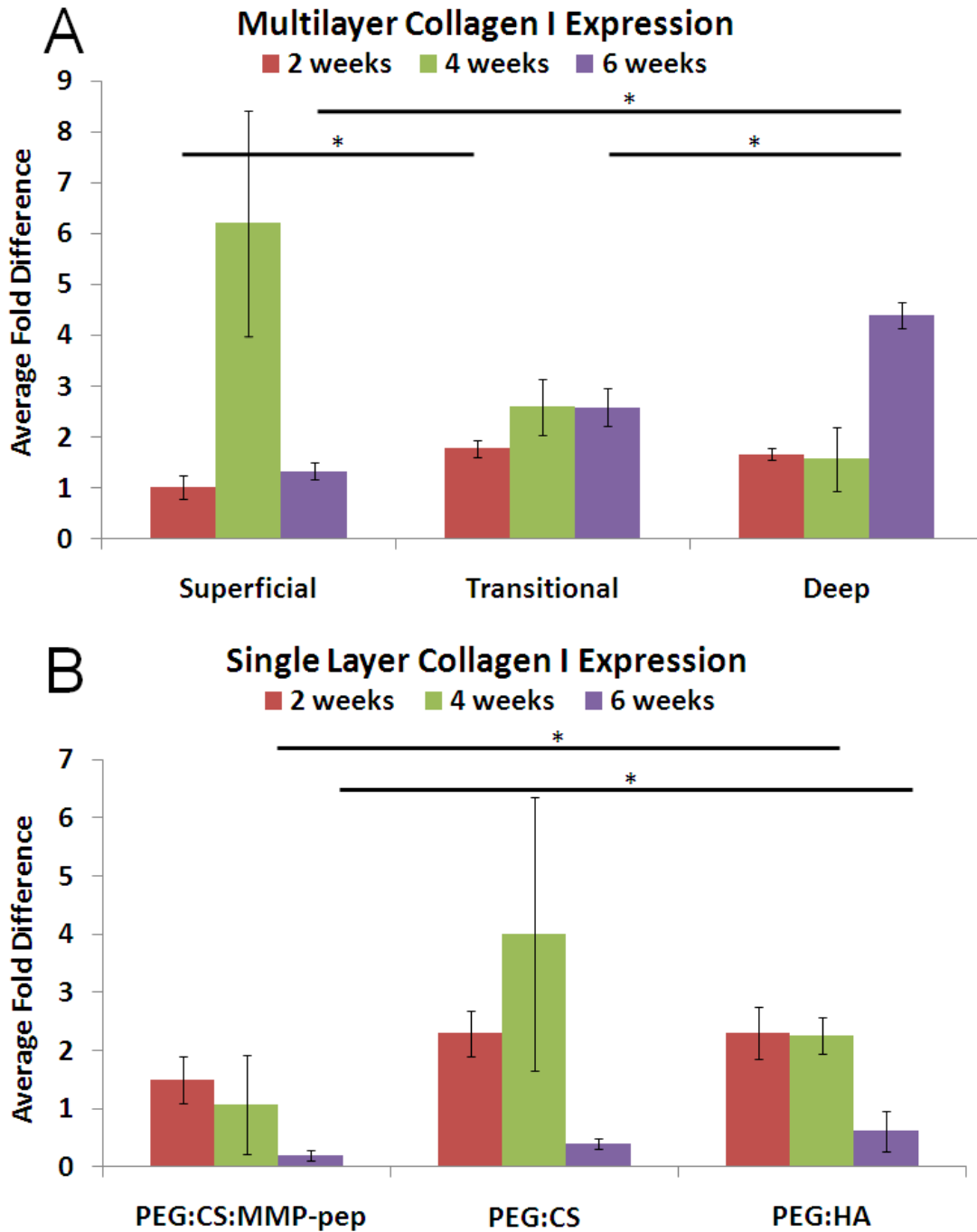


Figure 5.6 MLHC Immunohistochemical Staining of paraffin-embedded sections of the MLHC at 2, 4, and 6 weeks for collagen II (green) and X (red) (10X objective, Leica SP2 AOBS). At all time points, the fluorescent images showed positive staining for both collagen II and X.

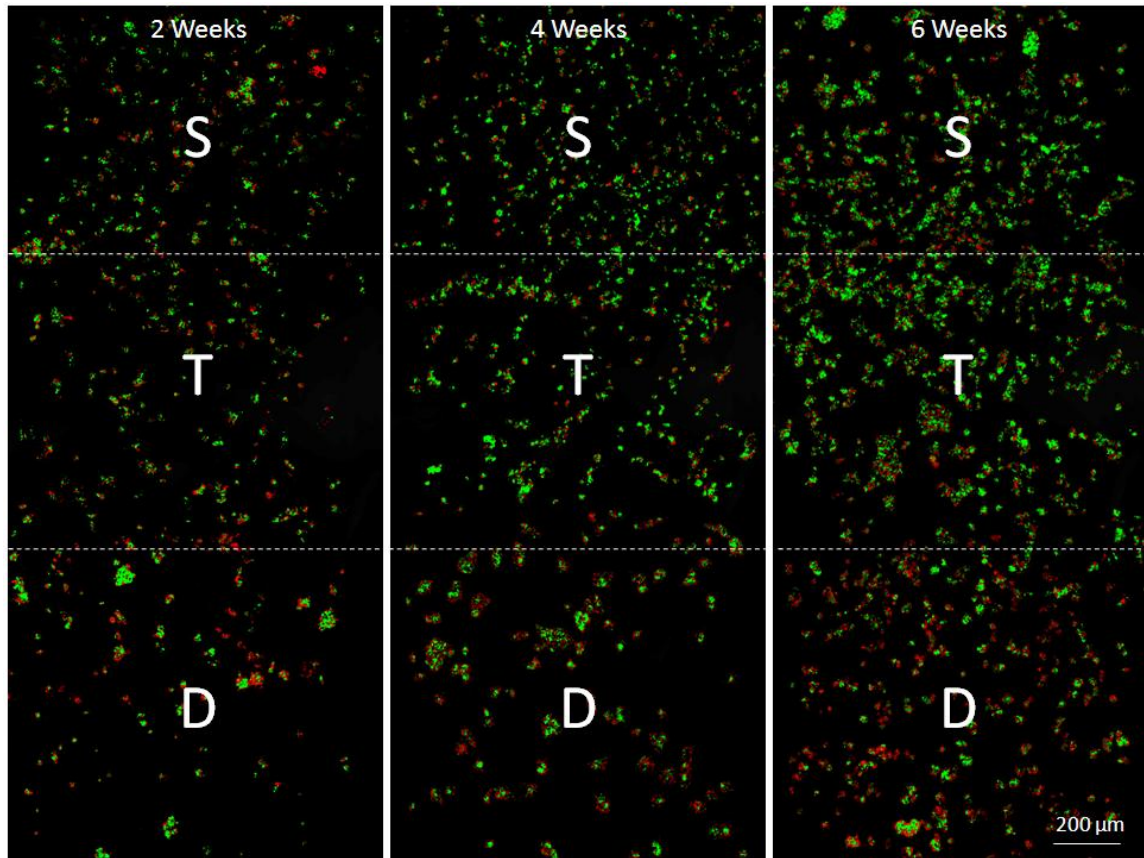


Figure 5.7 MLHC GAG Concentrations for (A) MLHC and (B) SLC. The deep layer showed significantly higher GAG content than the superficial layer at all time points.

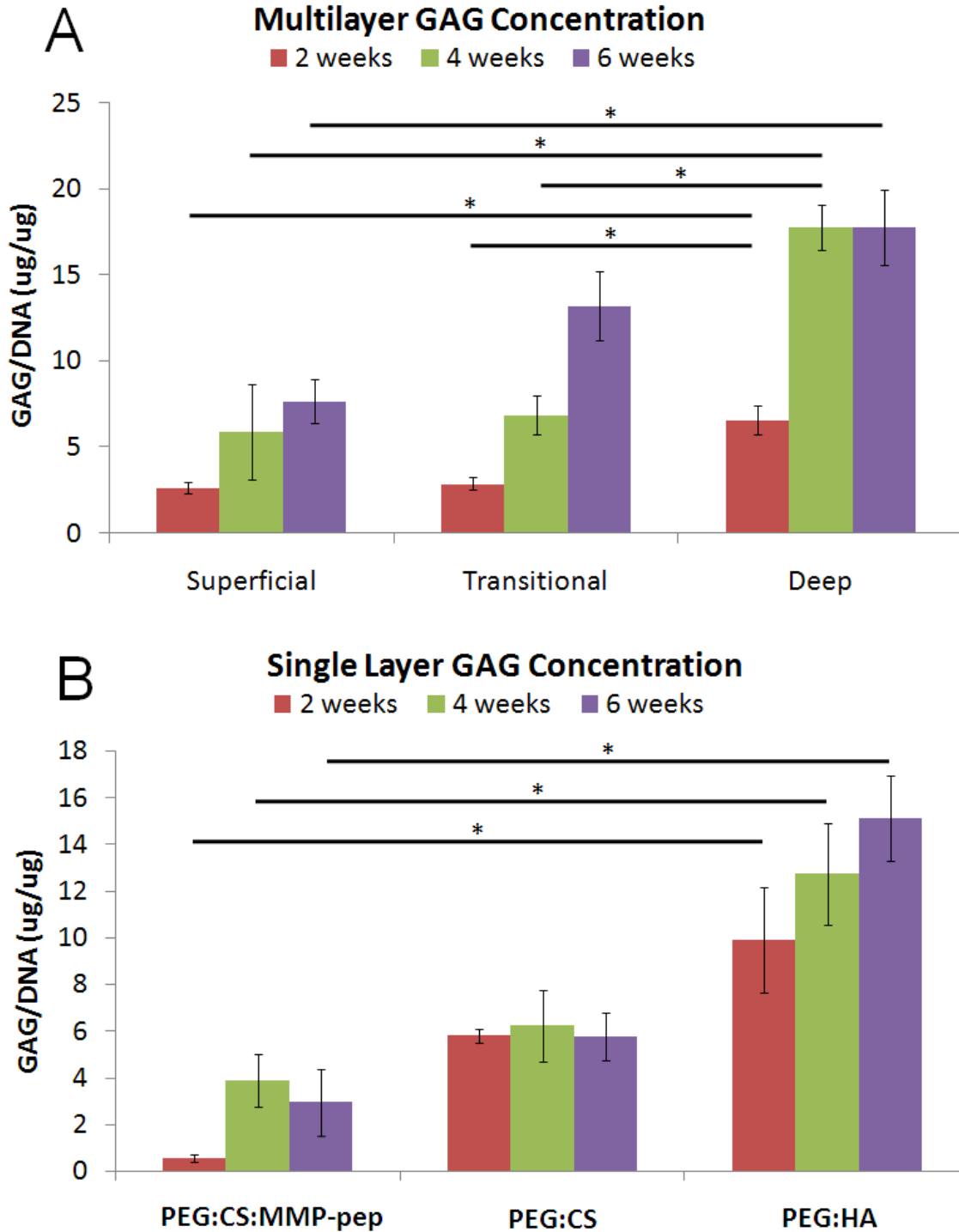


Figure 5.8 MLHC Moduli Graph showing that the compressive strength increases with time and corresponds with the GAG concentration of each zone at all time points. The compressive modulus of the superficial layer and the transitional layer at both 2 and 4 weeks do not significantly differ. The deep layer, which has much higher GAG content, showed significantly higher compressive modulus than the superficial layer for all time points.

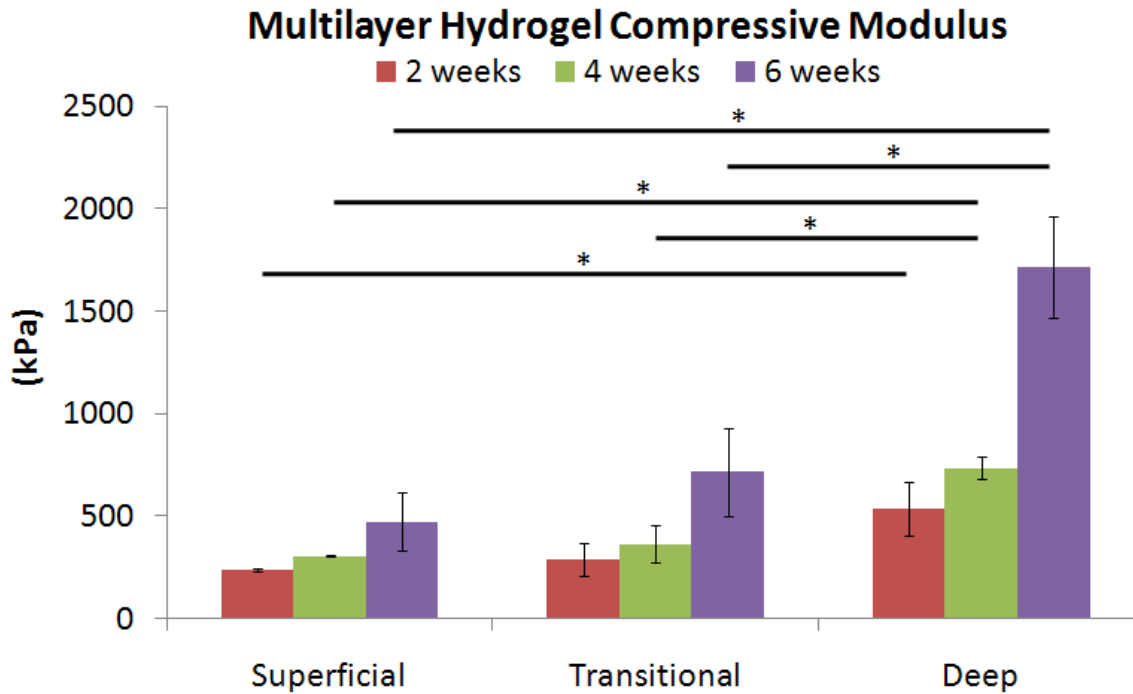


Table 5.2 Compressive Moduli for Blank MLHC

Blanks		
Hydrogel Layer	Moduli (kPa)	Standard Error
Superficial	199.71	± 89.60
ST Interface	200.9	± 63.6
Transitional	203.95	± 65.35
TD Interface	273.33	± 122.18
Deep	942.83	± 66.68

Table 5.3 Compressive Moduli for Cell-Laden MLHC

	2 Weeks		4 Weeks		6 Weeks	
Hydrogel Layer	Moduli (kPa)	Standard Error	Moduli (kPa)	Standard Error	Moduli (kPa)	Standard Error
Superficial	239.1	± 7.10	305.69	± 3.47	472.16	± 141.77
ST Interface	262.95	± 40.1	320.86	± 6.8	521.64	± 54.38
Transitional	286.5	± 81.3	364.45	± 92.54	715.44	± 215.49
TD Interface	307.24	± 6.075	401.56	± 6.35	816.46	± 76.53
Deep	534.43	± 129.1	734.43	± 53.95	1712.8	± 248.33

Table 5.4 Compressive Moduli of the SLC

Single Layer Controls (SLC)	2 weeks		4 weeks		6 weeks	
	Moduli (kPa)	Standard Error	Moduli (kPa)	Standard Error	Moduli (kPa)	Standard Error
PEG:CS:MMP-pep	98.11	± 37.39	125.69	± 5.31	227.57	± 53.51
PEG:CS	154.85	± 51.41	117.51	± 4.06	625.14	± 63.06
PEG:HA	296.55	± 72.72	144.08	± 13.45	836.45	± 61.79
PEG Control	257.49	± 30.67	218.58	± 17.26	734.43	± 53.95

5.5 REFERENCES

1. Elisseeff, J., et al., *Photoencapsulation of chondrocytes in poly(ethylene oxide)-based semi-interpenetrating networks*. J Biomed Mater Res, 2000. **51**(2): p. 164-71.
2. Klein, T.J., et al., *Tissue Engineering of Articular Cartilage with Biomimetic Zones*. Tissue Eng Part B Rev, 2009.
3. Bryant, S.J., et al., *Encapsulating chondrocytes in degrading PEG hydrogels with high modulus: engineering gel structural changes to facilitate cartilaginous tissue production*. Biotechnol Bioeng, 2004. **86**(7): p. 747-55.
4. Fisher, J.P., et al., *Thermoreversible hydrogel scaffolds for articular cartilage engineering*. J Biomed Mater Res A, 2004. **71**(2): p. 268-74.
5. Temenoff, J.S. and A.G. Mikos, *Review: tissue engineering for regeneration of articular cartilage*. Biomaterials, 2000. **21**(5): p. 431-40.
6. Varghese, S., et al., *Chondroitin sulfate based niches for chondrogenic differentiation of mesenchymal stem cells*. Matrix Biol, 2008. **27**(1): p. 12-21.
7. Vunjak-Novakovic, G., et al., *Bioreactor studies of native and tissue engineered cartilage*. Biorheology, 2002. **39**(1-2): p. 259-68.
8. Poole, A.R., et al., *Composition and structure of articular cartilage: a template for tissue repair*. Clin Orthop Relat Res, 2001(391 Suppl): p. S26-33.
9. Schinagl, R.M., et al., *Depth-dependent confined compression modulus of full-thickness bovine articular cartilage*. J Orthop Res, 1997. **15**(4): p. 499-506.
10. Bhosale, A.M. and J.B. Richardson, *Articular cartilage: structure, injuries and review of management*. Br Med Bull, 2008. **87**: p. 77-95.

11. Einhorn, T.A., R.J. O'Keefe, and J.A. Buckwalter, *Orthopaedic Basic Science Foundations of Clinical Practice*. 3 ed. 2007: American Academy of Orthopaedic Surgeons.
12. Boschetti, F. and G.M. Peretti, *Tensile and compressive properties of healthy and osteoarthritic human articular cartilage*. *Biorheology*, 2008. **45**(3-4): p. 337-44.
13. Hall, B.K., *Bones and Cartilage Developmental and Evolutionary Skeletal Biology*. 2005, San Diego: Elsevier Academic Press. 760.
14. Awad, H.A., et al., *Chondrogenic differentiation of adipose-derived adult stem cells in agarose, alginate, and gelatin scaffolds*. *Biomaterials*, 2004. **25**(16): p. 3211-22.
15. Lee, H.J., et al., *Collagen mimetic peptide-conjugated photopolymerizable PEG hydrogel*. *Biomaterials*, 2006. **27**(30): p. 5268-76.
16. Rosener, B., *Fundamentals of Biostatistics*. Sixth ed, ed. L. Purrinton. 2006, Belmont: Duxbury Press. 896.
17. Eyre, D.R. and J.J. Wu, *Collagen of fibrocartilage: a distinctive molecular phenotype in bovine meniscus*. *FEBS Lett*, 1983. **158**(2): p. 265-70.
18. Armstrong, C.G. and V.C. Mow, *Variations in the intrinsic mechanical properties of human articular cartilage with age, degeneration, and water content*. *J Bone Joint Surg Am*, 1982. **64**(1): p. 88-94.

CHAPTER SIX

Overall Summary, Conclusions and Future Direction

6.1 OVERALL SUMMARY

The simultaneous differentiation of MSCs into zonal articular cartilage within a MLHC represents a novel approach for engineering articular cartilage tissue. The multi-layer approach discussed in this dissertation represents a fundamental advance in tissue engineering that will encourage future research efforts to move away from creating homogenous tissue structures with bulk properties and turn towards engineering more physiologically and functionally relevant tissue substitutes with native-like and spatially varying properties.

6.2 CONCLUSIONS

This dissertation outlined the process of creating tissue substitutes that mimic the structure and function of native articular cartilage. Chapter Three first introduced a novel technique to modify an enzymatically degradable synthetic peptide. Chapter Four then demonstrated that a unique combination of the synthetic peptide and biopolymers could successfully induce the differentiation of MSCs into distinctive chondrogenic phenotypes. Finally, Chapter Five incorporated the findings of the previous two chapters to create a multi-layered hydrogel of varying biomaterial compositions to simultaneously induce the differentiation of MSCs into articular cartilage-like tissue with zonal structure and properties.

6.2.1 Chapter Three Research Findings

Chapter Three discussed the synthesis and modification of a matrix metalloproteases sensitive peptide (MMP-pep) as well as the modification of biopolymers, including chondroitin sulfate (CS) and hyaluronic acid (HA). These synthetic and natural materials were used in combination with poly(ethylene glycol) (PEG) to create hydrogel constructs of varying concentrations. The physical properties of the hydrogel constructs—including the water content, swelling ratio, degradation rate, and compressive modulus—were found to be dependent on their material composition. Hydrogel constructs containing the MMP-pep had a lower compressive modulus than the hydrogels without the peptide. The hydrogels containing the MMP-pep degraded faster than hydrogels containing HA but slower than hydrogels contain CS. Pure CS and HA hydrogel degraded the fastest. CS was found to increase water content and swelling ratio when incorporated into the hydrogel construct. Hydrogels containing CS also exhibited higher degradation rates than those containing the MMP-pep or HA. HA provided great mechanical strength when incorporated into the hydrogel construct, which resulted in the slowest degradation profile. The conclusion of Chapter Three is that hydrogels' physical properties can be tailored through manipulation of material compositions and concentrations.

6.2.2 Chapter Four Research Findings

Chapter Four described the use of material compositions, evaluated in Chapter Three, to induce the chondrogenic differentiation of mesenchymal stem cells (MSCs). The purpose of this study was to determine which material composition had the most inductive effect on the MSC differentiation into the chondrogenic phenotype. It was determined that the combination of the MMP-pep and CS within the PEG-based

hydrogel had a high inductive effect for the genetic expression of collagen II. The incorporation of HA into the PEG-based hydrogel was found to be conducive for glycosaminoglycan (GAG) production. Furthermore, plain CS hydrogels induced chondrocyte hypertrophy. Chapter Four concludes that specific biomaterial compositions can induce the differentiation of MSCs into specific chondrogenic phenotypes, which can be correlated to the specific zones of articular cartilage.

6.2.3 Chapter Five Research Findings

Based on the findings of Chapter Four, Chapter Five discussed the fabrication of a multi-layered hydrogel construct (MLHC) for the simultaneous differentiation of MSCs into zone-specific chondrocytes. The results demonstrated that the MLHC had the capability of creating zonal articular cartilage-like tissue. MSCs within the PEG:CS:MMP-pep composition differentiated into chondrocytes that exhibited high gene expression and production of type II collagen as well as lower GAG production, which are characteristic of the superficial zone. The PEG:CS biomaterial composition induced the differentiation of MSCs into chondrocytes that exhibited characteristic similar to the transitional zone, with mid-level type II collagen and GAG production. Due to the structural stability provided by the PEG:HA composition, MSCs within the PEG:HA layer differentiated into chondrocytes that exhibited low type II collagen gene expression and high GAG production, characteristic of the deep zone.

Furthermore, the overall multi-layered construct exhibited spatially varying properties similar to native cartilage. The level of collagen II gene expression and production decreased from the superficial layer to the deep layer. The GAG production and mechanical modulus increased from the superficial layer to the deep layer. The chondrocytes appeared to be more elongated, with collagen fibers within the superficial

layer aligned parallel to the articular surface. Additionally, the chondrocytes in the transitional layer had a more spherical morphology, while collagen fibers in this layer exhibited a random orientation. In the deep layer, both the chondrocytes and collagen fibers formed large clusters that were perpendicular to the subchondral plate. Chapter Five concluded that a MLHC with varying biomaterial composition can effectively induce the simultaneous differentiation of MSCs into zonal articular cartilage-like tissue.

6.3 FUTURE DIRECTIONS

The goal of this dissertation research was to develop a methodology to tissue engineer an articular cartilage substitute that could subsequently eliminate the need for cartilage donor tissue. The reported results are relevant because they clearly demonstrate that MSCs cultured within a MLHC with a varying biomaterial composition can be used to engineer zonally organized cartilage when provided with the appropriate inductive agents.

The clinical relevance of this research is dependent on complementary *in vivo* studies that will determine some of the criteria for translating the *in vitro* results into animal models. After animal studies, the next step is to translate this MLHC approach into a human system by using human stem cells.

6.3.1 Pre-Clinical Studies: Animal Models

Pre-clinical studies involving *in vivo* animal models are essential in closing the gap between *in vitro* experiments and human clinical trials [1]. However, there is no such thing as a perfect pre-clinical animal model that exactly mimics human articular cartilage. Therefore, researchers must carefully choose an animal model that most accurately represents the human condition being investigated in order to avoid

inaccurate generalizations caused by extrapolating findings from such animal models to human models.

Anatomically, the thickness of human articular cartilage on the medial femoral condyle ranges from about 1.65 to 2.65 mm [2], and the average volume of human cartilage defects is approximately 550 mm³, with lesions that require treatment measuring 10mm or more in diameter [3]. Additionally, human articular cartilage has very low intrinsic repair capabilities. The ideal animal model would imitate human cartilage by having similar cartilage thickness, appropriately sized defects, and limited capacity for spontaneous repair. Every available animal model has its benefits and limitations, both of which will be outlined in this section to provide a comparative analysis of various available species for *in vivo* studies. Each species will be discussed in order of size.

Murine models, including rodents such as mice and rats, are generally used to provide proof-of-concept data and serve as a bridge between *in vitro* studies and larger animal studies. The major advantage of using a murine model is that it is a cost effective method to obtain mechanistic information on cartilage repair [4]. There are immunocompromised rodent strains including athymic, transgenic, and knockout that are readily available for implanting xenogenic cells and tissues. Furthermore, the use of murine models provides researchers access to a larger array of probes, antibodies, and reagents that can enhance their studies [4]. The small size of the joint and thinness of the cartilage layer are the two main limitations of the murine model [5]. Additionally, rats have a better intrinsic repair capacity due to their long-term open growth plate [6], thereby limiting the transferability of findings to humans whose repair capabilities are much more limited.

Rabbits, a lapine model, are popular for research on cartilage regeneration because New Zealand White Rabbits have joints that are large enough to create 3-4 mm defects [4]. However, upon examining the thickness of rabbit cartilage, Rasanen determined that the average trochlear groove was only 0.44 ± 0.08 mm thick, and the anteromedial femoral condyle was only 0.3 ± 0.07 mm [7]. The thinness of the rabbit's cartilage limits the size and depth of defects that can be made, since the average experimental defect is about 3 mm in depth [8-10]. If 3 mm defects are created, the majority of the defect volume will be within the subchondral bone layer and therefore will not be representative of human defects. Similar to the murine model, the advantage of utilizing the rabbit model is that large quantities of genetically modified rabbits are available. The rabbits are easy to handle, with a relatively low cost associated with their purchase and care [11-13]. However, similar to rats, rabbits have the high potential for spontaneous healing, which is mediated by proliferation and differentiation of mesenchymal cells from the bone marrow [14]. Finally, the mechanical loading conditions for rabbit cartilage are significantly different from that of humans, making it impractical to translate rabbit models to human models.

Canine models more closely resemble humans than murine or lapine models because dogs naturally suffer from cartilage defects such as osteoarthritis [15] and lack the intrinsic ability for cartilage repair [16-18]. Additionally, dogs can be used to study rehabilitation protocols or specific exercise programs since dogs can be easily trained to use treadmills [4]. The major drawback of using dogs in research is that there are significant ethical concerns due their societal status as family companions and pets [4]. The canine model is also limited by cartilage size and thickness. Dogs' cartilage thickness ranges from 0.95 mm to 1.3 mm, with an average defect size of 4 mm [5]. This

average is significantly smaller than the average human defects, which are greater than 10 mm [3].

A goat, otherwise referred to as a caprine model, offers advantages over the previously mentioned models because of larger joints and thicker cartilage, which more closely resemble the human joint [4]. The average size of a goat defect is about 6 mm [5] in diameter, which approaches the average size of a human defect, and does not show spontaneous healing [19]. Additionally, the goat's larger joint size allows accessibility for arthroscopic procedures, while the thicker cartilage range of 0.8 to 2.0 mm [20] allows for the evaluation of the healing response to both partial and full thickness defects. Niederauer et al. have successfully used a caprine model to examine the treatment of osteochondral defects using various implantable constructs, thereby showing that repair was achieved with hyaline-like cartilage and the underlying bone [21]. When compared to larger animal models, goats are relatively inexpensive and easy to care for if housed in appropriate facilities. Although the larger goat joint allows for the creation of larger defects, when compared to the size of human defects, goat defects still fall in the lower end of what is considered clinically relevant in humans [4].

The porcine model is rarely used in cartilage research even though a pig's joint size, cartilage thickness, and weight-bearing requirements more closely mimic the human condition [22-24]. Pigs are rarely used in research because they are large and aggressive animals, which make them difficult to deal with in a research environment [25, 26]. Due to this limitation, mini-pig strains have been bred to be docile with controlled weight and size. The mini-pig stifle joint, although still smaller than human joints, can be used to study cartilage repair because defects of 6-8 mm in diameter can be created in their femoral condyles or their trochlear grooves [1]. It is important to note that only skeletally mature pigs with full closure of the growth plate have a limited

endogenous repair response. Therefore, only skeletally mature mini-pigs between 18-22 months of age are used in experimental models [24]. Similar to the caprine model, cartilage thickness is also an advantage of the porcine model. The 1.5 mm [27] thickness of swine cartilage allows for the creation of partial and full thickness defects as well as arthroscopic evaluation after treatment [28, 29]. However, since mini-pigs are specially bred pigs, they can be costly to acquire and maintain [4].

The equine model is the largest of the animal models that are available for cartilage research [4]. Horse articular cartilage injury and repair are much better understood than in other animal models, due to the horse racing industry which has resulted in the need for clinical treatment of chondral or osteochondral injuries in horses [30]. Translating basic research into pre-clinical studies with horses can be smoother due to the amount of clinical treatment data that is available, making the equine model appealing to researchers. Horses are similar to humans in that they suffer from cartilage injuries and osteoarthritis with no real intrinsic ability for self-repair [31, 32] of the cartilage. The equine model is highly beneficial for pre-clinical evaluation of new cartilage repair techniques because the horse's large joint size permits arthroscopic assessment [4]. Additionally, the lesions found in horses are approximately the same size and depth as seen in humans [5]. The horse stifle joint has a cartilage thickness of about 1.75 mm [27], which is the closest to that of human cartilage (2.35 mm) out of all the previously mentioned species. Therefore, clinically relevant-sized defects in human cartilage correlate closely to full or partial thickness defects found in horses [5, 33-35].

However, horses have distinctly different loading conditions than humans which result in a much harder subchondral bone layer than that of humans [36]. Thus, the major disadvantage of the equine model is that any treatment used for horse cartilage defect will be subjected to greater loading conditions than in humans, due to the horse's

weight and physiology [4]. Other disadvantages include the extremely high cost of obtaining and caring for these animals. In addition to needing the appropriate facilities to house the animals, veterinary support for surgical procedures as well as perioperative care are also required when working with horses [4]. Although factors such as joint size, cartilage morphology, and available clinical data make the equine model attractive for pre-clinical studies, high joint loading conditions, high cost, and the need for highly specialized facilities prevent most researchers from being able to use the equine model. Even though horses are a logical translational model for establishing the efficacy and safety of new cartilage treatments, the application of the equine model is not always readily available to all researchers.

In summary, there are multiple factors that need to be considered when selecting the appropriate animal model. Since costs increase with animal size, researchers with limited funding tend to conduct initial studies using smaller animal models to show proof-of concept. Smaller animals offer the advantage of having genetically similar populations, which can significantly reduce variances in results, but the genetic diversity of large animals better mimic the human population. While the disadvantage of small animal models is that they do not adequately mimic the human condition, the use of large animals requires larger sets of experimental animals due to their genetic variance which lead to different levels of healing responses. As mentioned at the start of this section, no animal model is ideal for cartilage research since each animal species has its advantages as well as its disadvantages. Therefore, when planning an animal study, research investigators must perform a detailed comparative analysis of cost effectiveness, anatomy, maturity, joint biomechanics, and postsurgical protocols associated with each species.

6.3.2 Clinical Application

As illustrated in **Fig. 6.1**, cartilage defects are separated into two categories, partial thickness and full thickness defects. Partial thickness defects that do not penetrate the subchondral bone do not heal spontaneously. Full thickness defects that do penetrate the subchondral bone elicit an intrinsic repair response that results in the formation of fibrocartilaginous tissue, which is a mechanically poor replacement for hyaline articular cartilage. Over time the repaired tissue will degenerate due to repeated mechanical stress, leading to the continued degeneration of the articular cartilage.

A number of clinical strategies for cartilage repair were discussed in Section 2.5, but each repair strategy has its drawbacks. Arthroscopic procedures such as lavage and debridement are temporary solutions used to manage pain but these procedures do not repair the cartilage defect. Microfracture surgery is an easy procedure that involves drilling into the subchondral bone to induce the natural healing response, but the surgery results in the formation of mechanically inferior fibrocartilage. Due to the mechanical instability of fibrocartilage, continuous degeneration of the remaining articular cartilage will occur over time. Autologous chondrocyte implantation (ACI) and matrix-induced or matrix-associated ACI involve the isolation and expansion of the patient's own chondrocytes for re-implantation at a later stage. The first generation ACI required harvesting a periosteal graft from the patient's medial tibia. The usage of the periosteal grafts became problematic due to graft hypertrophy and harvest site morbidity. Thus, the 3rd generation MACI was developed to eliminate the need for a periosteal graft by using biomaterials as cell carriers. The matrices used for this technique include protein-based polymers such as fibrin or collagen and carbohydrate-based matrices such as Hyleron and artificial polymers [37]. Although the third generation MACI has been proven to be superior to microfracture surgery [38], it is still not the preferred choice for

surgeons because the technique induces fibrocartilage formation [39]. Osteochondral transplants offer the unique advantage of using native cartilage tissue for replacement and repair. Allogenic tissue from cadavers is a feasible tissue choice and can be successful in treating large cartilage defects [40]; however, it has been shown that fresh tissue has a better success rate than frozen tissue in terms of cell death and mechanical stability [41]. Additionally, immune rejection is still a potential problem when using allogenic tissues [42]. Osteochondral autologous grafts (OATS) are a better alternative to allogenic grafts, in terms of being fresh and non-immunogenic, but autologous grafts are limited in quantity and can cause donor site morbidity [43]. Lastly, matrix scaffolds of both synthetic and natural materials have been successfully used to develop functional tissue substitutes for the treatment of cartilage defects [44].

The research findings of this dissertation could translate into clinical applications that offer a number of advantages over current cartilage repair strategies. First, the use of a stem cell population eliminates the need for chondrocyte isolation and expansion, saving time and avoiding immune rejection problems. Adult stem cells are highly proliferative and are easily obtainable. The results discussed in this dissertation demonstrate the feasibility of differentiating a single stem cell population into specific chondrogenic phenotypes, which correlate to distinctive zones of articular cartilage.

Secondly, the use of biomaterials enables researchers to fine-tune characteristics such as water absorption, nutrient diffusion, biodegradation, and mechanical stability. The various biomaterials discussed in this dissertation were shown to have different swelling capacities, degradation rates, and mechanical moduli, which can be modulated by changing the material composition and material concentration to match the properties of native articular cartilage.

Finally, the layer-by-layer fabrication technique described in this dissertation provides the capability to treat both partial and full thickness cartilage defects. The multi-layer hydrogel fabrication can be used to selectively engineer only the relevant zones of the damaged cartilage or to create layered osteochondral junctions. For partial thickness injuries, the multi-layered fabrication technique can be used to create a construct consisting of only the layers that correspond to the thickness of the injury. The MLHC can easily be implanted via an arthroscopic technique with fibrin glue, which is also used in both ACI and MACI. The fibrin glue can be applied to secure the construct within the defect area and eliminate the need to create a full thickness defect for construct integration. For full thickness defects, the multi-layered construct can be fabricated to include a subchondral bone layer for easy integration. Additionally, the cell-mediated degradability allows for matrix remodeling as well as chondrocyte ECM deposition.

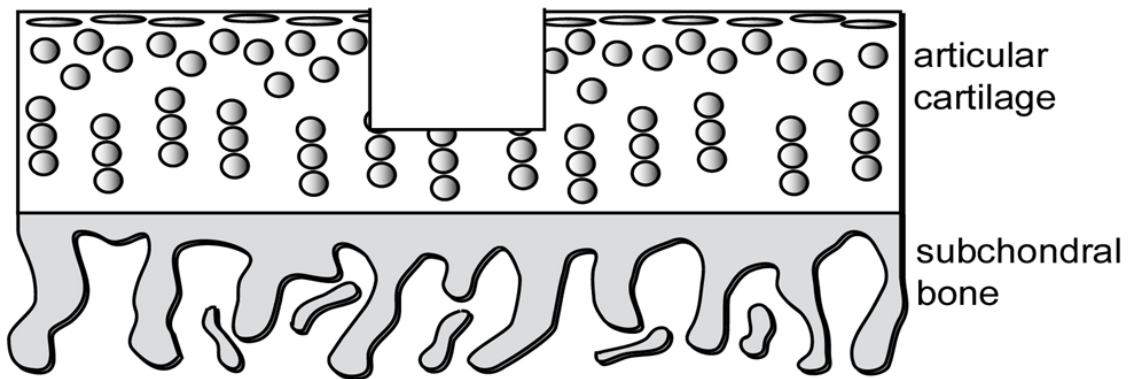
There are many advantages of using MLHC to clinically treat articular cartilage defects in humans, however, clinical trials are required to be conducted before hand to ensure that the MLHC are safe and to identify any side effects that may be associated with its use. Clinical Trials are broken down into four phases. Clinical feasibility is Phase I assesses safety, determine proper dosage and identify any side effects [45]. Phase II involves clinical research to verify effectiveness of treatment [45]. Clinical validation occurs in Phase III in which multiple clinical centers evaluate and attempt to reproduce the results of the initial studies. Phase IV is for clinical acceptance in which the treatment is surveillance in the market to determine long term performance and possible adverse effects [45]. The time and cost that is required to conduct a clinical trial varies by the type of treatment or device. In addition, the time requirement is also dependent on the number of patients available who meet the specific criteria and the

number of patients needed to achieve statistical significance accepted by the Food and Drug Administration (FDA) [45]. In general, clinical trials for orthopedic implants require a total of about 200 to 300 patients, which can take up to three years to acquire [45]. In addition, the FDA also requires a two-year follow-up period for orthopedic implants. Therefore, it can take up to seven years and cost from \$700,000 to \$1 million dollars for preclinical and clinical studies of orthopedic implants that are classified as significant-risk [45].

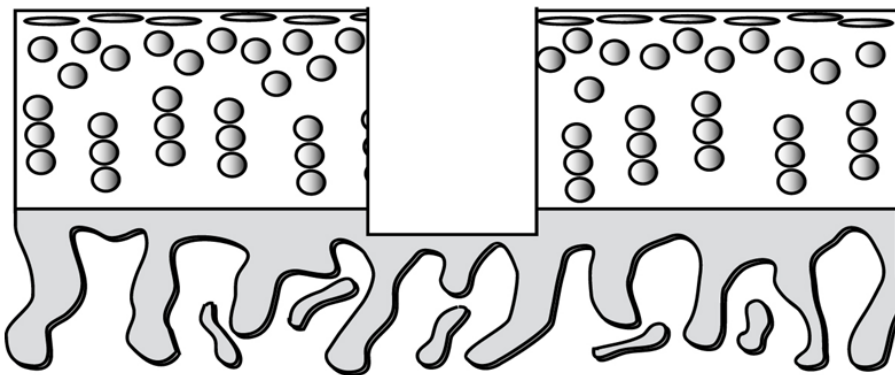
6.4 FIGURES

Figure 6.1 Partial & Full Thickness Articular Cartilage Defect Illustration (A) Partial thickness articular cartilage defect and (B) Full thickness defect that penetrates the subchondral bone [46].

A: partial thickness defect



B: full thickness defect



6.5 REFERENCES

1. Gotterbarm, T., et al., *The minipig model for experimental chondral and osteochondral defect repair in tissue engineering: retrospective analysis of 180 defects*. Lab Anim, 2008. **42**(1): p. 71-82.
2. Shepherd, D.E. and B.B. Seedhom, *Thickness of human articular cartilage in joints of the lower limb*. Ann Rheum Dis, 1999. **58**(1): p. 27-34.
3. Hjelle, K., et al., *Articular cartilage defects in 1,000 knee arthroscopies*. Arthroscopy, 2002. **18**(7): p. 730-4.
4. Chu, C.R., M. Szczodry, and S. Bruno, *Animal models for cartilage regeneration and repair*. Tissue Eng Part B Rev, 2010. **16**(1): p. 105-15.
5. Ahern, B.J., et al., *Preclinical animal models in single site cartilage defect testing: a systematic review*. Osteoarthritis Cartilage, 2009. **17**(6): p. 705-13.
6. Libbin, R.M. and M.E. Rivera, *Regeneration of growth plate cartilage induced in the neonatal rat hindlimb by reamputation*. J Orthop Res, 1989. **7**(5): p. 674-82.
7. Rasanen, T. and K. Messner, *Regional variations of indentation stiffness and thickness of normal rabbit knee articular cartilage*. J Biomed Mater Res, 1996. **31**(4): p. 519-24.
8. Buma, P., et al., *Cross-linked type I and type II collagenous matrices for the repair of full-thickness articular cartilage defects--a study in rabbits*. Biomaterials, 2003. **24**(19): p. 3255-63.
9. Han, C.W., et al., *Analysis of rabbit articular cartilage repair after chondrocyte implantation using optical coherence tomography*. Osteoarthritis Cartilage, 2003. **11**(2): p. 111-21.

10. Wei, X., J. Gao, and K. Messner, *Maturation-dependent repair of untreated osteochondral defects in the rabbit knee joint*. J Biomed Mater Res, 1997. **34**(1): p. 63-72.
11. Chu, C.R., et al., *Osteochondral repair using perichondrial cells. A 1-year study in rabbits*. Clin Orthop Relat Res, 1997(340): p. 220-9.
12. Furukawa, T., et al., *Biochemical studies on repair cartilage resurfacing experimental defects in the rabbit knee*. J Bone Joint Surg Am, 1980. **62**(1): p. 79-89.
13. Kawamura, S., et al., *Articular cartilage repair. Rabbit experiments with a collagen gel-biomatrix and chondrocytes cultured in it*. Acta Orthop Scand, 1998. **69**(1): p. 56-62.
14. Shapiro, F., S. Koide, and M.J. Glimcher, *Cell origin and differentiation in the repair of full-thickness defects of articular cartilage*. J Bone Joint Surg Am, 1993. **75**(4): p. 532-53.
15. Shortkroff, S., et al., *Healing of chondral and osteochondral defects in a canine model: the role of cultured chondrocytes in regeneration of articular cartilage*. Biomaterials, 1996. **17**(2): p. 147-54.
16. Breinan, H.A., et al., *Autologous chondrocyte implantation in a canine model: change in composition of reparative tissue with time*. J Orthop Res, 2001. **19**(3): p. 482-92.
17. Breinan, H.A., et al., *Effect of cultured autologous chondrocytes on repair of chondral defects in a canine model*. J Bone Joint Surg Am, 1997. **79**(10): p. 1439-51.
18. Cook, S.D., et al., *Repair of articular cartilage defects with osteogenic protein-1 (BMP-7) in dogs*. J Bone Joint Surg Am, 2003. **85-A Suppl 3**: p. 116-23.

19. Jackson, C.E., et al., *A preliminary evaluation of a prospective study of pulmonary function studies and symptoms of hypoventilation in ALS/MND patients*. J Neurol Sci, 2001. **191**(1-2): p. 75-8.
20. Brehm, W., et al., *Repair of superficial osteochondral defects with an autologous scaffold-free cartilage construct in a caprine model: implantation method and short-term results*. Osteoarthritis Cartilage, 2006. **14**(12): p. 1214-26.
21. Niederauer, G.G., et al., *Evaluation of multiphase implants for repair of focal osteochondral defects in goats*. Biomaterials, 2000. **21**(24): p. 2561-74.
22. Chiang, H., et al., *Repair of porcine articular cartilage defect with autologous chondrocyte transplantation*. J Orthop Res, 2005. **23**(3): p. 584-93.
23. Jiang, C.C., et al., *Repair of porcine articular cartilage defect with a biphasic osteochondral composite*. J Orthop Res, 2007. **25**(10): p. 1277-90.
24. Vasara, A.I., et al., *Immature porcine knee cartilage lesions show good healing with or without autologous chondrocyte transplantation*. Osteoarthritis Cartilage, 2006. **14**(10): p. 1066-74.
25. Newman, E., A.S. Turner, and J.D. Wark, *The potential of sheep for the study of osteopenia: current status and comparison with other animal models*. Bone, 1995. **16**(4 Suppl): p. 277S-284S.
26. Swindle, M.M., A.C. Smith, and B.J. Hepburn, *Swine as models in experimental surgery*. J Invest Surg, 1988. **1**(1): p. 65-79.
27. Frisbie, D.D., M.W. Cross, and C.W. McIlwraith, *A comparative study of articular cartilage thickness in the stifle of animal species used in human pre-clinical studies compared to articular cartilage thickness in the human knee*. Vet Comp Orthop Traumatol, 2006. **19**(3): p. 142-6.

28. Pan, Y., et al., *Hand-held arthroscopic optical coherence tomography for in vivo high-resolution imaging of articular cartilage*. J Biomed Opt, 2003. **8**(4): p. 648-54.
29. Zelle, S., et al., *Arthroscopic techniques for the fixation of a three-dimensional scaffold for autologous chondrocyte transplantation: structural properties in an in vitro model*. Arthroscopy, 2007. **23**(10): p. 1073-8.
30. Nixon, A.J., et al., *Arthroscopic reattachment of osteochondritis dissecans lesions using resorbable polydioxanone pins*. Equine Vet J, 2004. **36**(5): p. 376-83.
31. Convery, F.R., W.H. Akeson, and G.H. Keown, *The repair of large osteochondral defects. An experimental study in horses*. Clin Orthop Relat Res, 1972. **82**: p. 253-62.
32. Koch, T.G. and D.H. Betts, *Stem cell therapy for joint problems using the horse as a clinically relevant animal model*. Expert Opin Biol Ther, 2007. **7**(11): p. 1621-6.
33. Hendrickson, D.A., et al., *Chondrocyte-fibrin matrix transplants for resurfacing extensive articular cartilage defects*. J Orthop Res, 1994. **12**(4): p. 485-97.
34. Hidaka, C., et al., *Acceleration of cartilage repair by genetically modified chondrocytes over expressing bone morphogenetic protein-7*. J Orthop Res, 2003. **21**(4): p. 573-83.
35. Strauss, E.J., et al., *Biochemical and biomechanical properties of lesion and adjacent articular cartilage after chondral defect repair in an equine model*. Am J Sports Med, 2005. **33**(11): p. 1647-53.

36. Murray, R.C., et al., *Subchondral bone thickness, hardness and remodelling are influenced by short-term exercise in a site-specific manner*. J Orthop Res, 2001. **19**(6): p. 1035-42.
37. Trattinig, S., et al., *Matrix-based autologous chondrocyte implantation for cartilage repair: noninvasive monitoring by high-resolution magnetic resonance imaging*. Magn Reson Imaging, 2005. **23**(7): p. 779-87.
38. Basad, E., et al., *Matrix-induced autologous chondrocyte implantation versus microfracture in the treatment of cartilage defects of the knee: a 2-year randomised study*. Knee Surg Sports Traumatol Arthrosc, 2010. **18**(4): p. 519-27.
39. Horas, U., et al., [*Osteochondral transplantation versus autogenous chondrocyte transplantation. A prospective comparative clinical study*]. Chirurg, 2000. **71**(9): p. 1090-7.
40. Czitrom, A.A., et al., *Bone and cartilage allotransplantation. A review of 14 years of research and clinical studies*. Clin Orthop Relat Res, 1986(208): p. 141-5.
41. Tomford, W.W., D.S. Springfield, and H.J. Mankin, *Fresh and frozen articular cartilage allografts*. Orthopedics, 1992. **15**(10): p. 1183-8.
42. Langer, F., et al., *The immunogenicity of allograft knee joint transplants*. Clin Orthop Relat Res, 1978(132): p. 155-62.
43. Hangody, L., et al., *Autologous osteochondral grafting--technique and long-term results*. Injury, 2008. **39 Suppl 1**: p. S32-9.
44. Tuli, R., W.J. Li, and R.S. Tuan, *Current state of cartilage tissue engineering*. Arthritis Res Ther, 2003. **5**(5): p. 235-8.
45. Fuson, R.L., et al., *The conduct of orthopaedic clinical trials*. J Bone Joint Surg Am, 1997. **79**(7): p. 1089-98.

46. Redman, S.N., S.F. Oldfield, and C.W. Archer, *Current strategies for articular cartilage repair*. Eur Cell Mater, 2005. **9**: p. 23-32; discussion 23-32.

APPENDIX A

MSC Differentiation within Bi-Layer Hydrogels

A.1 INTRODUCTION

Many investigators have applied the concept of creating bi-layered matrix materials in cartilage regeneration [1-4]. Specifically, Bartlett et al. used porcine type-I/III collagen bi-layer seeded with chondrocytes in the matrix-induced autologous chondrocyte implantation (MACI) procedure to replace the need to harvest periosteal flaps [1, 2]. Additionally, both Sharma et al. and Ng et al. demonstrated that, when cultured in a bi-layer hydrogel, chondrocytes isolated from the superficial and deep zone improved chondrogenic properties over single layer controls [3, 4].

Even though the findings of Chapter Four demonstrate the feasibility of MSC differentiation into zonal chondrocytes, translating these findings by creating a multi-layered construct with varying biomaterial composition may be difficult due to the complex nature of combining four different layers into one hydrogel construct. As proof-of-concept for the simultaneous differentiation of MSCs, bi-layered hydrogels were created since there have been a number of reported successes with bi-layered constructs. The fabricated bi-layer consists of biomaterials established in Chapter Four, PEG:CS:MMP-pep representing the superficial layer and PEG:HA representing the deep layer.

A.2 MATERIALS AND METHODS

A.2.1 Bi-layered Hydrogel Fabrication

The fabrication of the bi-layered hydrogel was performed from the bottom layer upward. The specific biomaterial compositions and concentrations of each layer are listed in **Table A.1**. First, 100 μL of PEG:HA-MSD mixture was polymerized under UV for 3 minutes to represent the deep zone. Then 100 μL of PEG:CS:MMP-pep-MSD mixture, representing the superficial zone, was added on top of the partially polymerized bottom layer and placed under UV for an additional 5 minutes to fully polymerize the entire hydrogel. This bi-layered scaffold was cultured in serum-free chondrogenic media containing 1% penicillin/streptomycin, 10nM Dexamethasone, 50 $\mu\text{g}/\text{mL}$ ascorbic acid-2-phosphate, 40 $\mu\text{g}/\text{mL}$ L-proline, 5 mL ITS+1, and 10 ng/mL TGF- β 1 for 2, 4, and 6 weeks in a 12-well plate [5].

A.2.2 Cell Viability

Viability of encapsulated cells in the bi-layered hydrogel constructs was determined after 2, 4, and 6 weeks of culture. At each time, the media were discarded and the constructs were washed with PBS (Gibco, Carlsbad, CA) twice for 5 minutes. The bi-layered hydrogels were thinly sliced transversely with a razor. Cell viability was assessed based on previously published methods by Lee et al. [6]. Briefly, the Live/Dead Viability/Cytotoxicity Kit (Molecular Probes, Eugene, OR) that contains calcein AM (“live” dye) and ethidium homodimer-1 (“dead” dye) was used to assess the integrity of the cellular membrane. Dye solution was made with 0.5 μL of calcein AM dye and 2 μL of ethidium homodimer-1 dye in 1 mL of DMEM. A transverse slice of the construct was incubated in 500 μL of the “Live/Dead” dye solution for 30 minutes. Fluorescence microscopy (Olympus, 4X) was performed using a fluorescein optical filter (485 ± 10

nm) for calcein AM and a rhodamine optical filter (530 ± 12.5 nm) for ethidium homodimer-1.

A.2.3 RNA Isolation and RT-PCR

Chondrogenesis was determined by the gene expression of collagen II, X, and I within these bi-layered hydrogel constructs at 2, 4, and 6 week time points. The hydrogel constructs were removed from culture and the gene expressions of encapsulated cells were analyzed. The single-layered hydrogels were homogenized as detailed in Section 4.2.2. The bi-layered hydrogels were first sliced with a razor to separate the layers. The individual layers were placed into individual 2mL microcentrifuge tubes and 200 μ L of TRIzol[®] was added to the tubes. Each layer was then crushed using a homogenizer (Wheaton). After complete homogenization, another 800 μ L of TRIzol[®] was added to the tube. The RNA isolation of the homogenized scaffolds was performed following the manufacturer's protocol, as detailed in Section 4.2.2. Genomic DNA was removed using Deoxyribonuclease I (Invitrogen, Carlsbad, CA). The first strand of cDNA was synthesized by reverse transcription (RT) using Superscript[™] III kit (Invitrogen, Carlsbad, CA), following the manufacturer's instructions, as detailed in Section 4.2.2. Quantitative polymerase chain reaction (PCR) was performed using an ABI Prism[®] 7900 Real Time thermal cycler and HotStartTaq DNA Polymerase with SYBR green/ROX PCR master mix (SA Biosciences, Fredrick, MD). Primers for the housekeeping gene (GAPDH), collagen type II, type X, and type I (SA Biosciences, Fredrick, MD) are listed in **Table 4.1**.

A.2.4 Histology and Immunohistochemistry

Histology of these hydrogel matrices was performed to determine the chondrogenic differentiation within the bi-layered constructs and for verification of the quantitative real time data. At 2, 4, and 6 week time points, hydrogels were removed from culture and fixed in 4% paraformaldehyde at 4°C for an overnight period. Fixed hydrogels were then dehydrated for paraffin embedding using 1-hr sequential steps in the following order: 80%, 95%, 95% ethanol in dH₂O, 100% ethanol, 50/50 ethanol/CitriSolv, 100% CitriSolv, 100% CitriSolv, 60°C molten paraffin, and 60°C molten paraffin for an overnight period. Paraffin-embedded hydrogels were sliced in transverse sections at 10µm using a rotary microtome. Sections were stained for differentiation.

Double sequential immunohistochemistry was performed to stain for collagen II (green) and collagen X (red) using rabbit polyclonal primary antibodies (Abcam, Cambridge, MA) and Texas red (collagen II) or FITC (collagen X) conjugated secondary antibodies. Slides containing sectioned hydrogels were blocked for unspecific binding for 30 minutes at 37 °C using 3% (w/v) bovine serum albumin (BSA) in PBS (pH 7.4). The slides were rinsed with 0.05% tween 20 in PBS solution three times. After washing, the slides were incubated with primary antibody for 30 minutes at 37 °C. The slides were rinsed again before the second incubation with the secondary antibody for 30 minutes at 37 °C. These steps were repeated for collagen X on the same slides. The slides were imaged using a confocal fluorescence microscope (Leica SP2 AOBS, 63X).

A.2.5 Biochemical Characterization

Glycosaminoglycan (GAG) production within each layer of the bi-layered construct determined using the Dimethylmethylene blue (DMMB) assay. Briefly, at 2, 4, and 6 week time points, hydrogels were removed from culture. Wet weights (ww) and dry weights (dw) after 48 hours of lyophilization were obtained for each construct (n=3). The dry constructs were then digested in 1 mL of papinase (papain, 125 $\mu\text{g}/\text{mL}$; Sigma) at 60°C overnight. 200 μL of the DMMB solution was added to each well of the 96 well plates and then 50 μL of standard and samples were added. The plate was shaken for 10 seconds before reading the absorbance at 525nm. To account for the hydrogel material, absorbance of blank hydrogels was subtracted from the sample values. The DNA content was determined using Sigma's DNA quantification kit (DNA-QF) in order to normalize the GAG production. The assay was carried out following the manufacturer's protocol for multiwall assay, as detailed in Section 4.2.5.

A.2.6 Compression Studies of Bi-layered Hydrogels

The compressive modulus of the individual layers and the interfaces between layers of the bi-layered hydrogel constructs were determined at room temperature on an In-spec 2200 Instron mechanical tester with a 125 N loading cell using a parallel plate apparatus and loading of 20% of the initial thickness per second (0.1 mm/sec). The compressive modulus of the individual layers as well the interface between were determined by analyzing the linear region of the stress versus the strain curve of the samples at low deformations (<20% strain).

A.2.7 Statistical Analysis

All quantitative data were expressed as mean \pm standard deviation and were verified by analysis of variance using student T-Test with equal variance. P values of less than 0.05 were considered statistically significant.

A.3 RESULTS

A.3.1 Viability of Encapsulated MSCs

Cytotoxicity was performed to test for the viability of the MSCs encapsulated within the bi-layered hydrogel constructs at 2, 4, and 6 weeks. As shown in **Figure A.1**, the majority of the cells stained green, indicating that there are more live cells than dead cells. Dead cells are stained red at all time points. At 2 weeks, there appeared to be more cells in the superficial than the deep layer. At 4 weeks, the cell density appeared to be more evenly distributed within both layers with very few dead cells. At 6 weeks, the deep layer had the greatest amount of cells which appeared to form clusters perpendicular to the interface.

A.3.2 Chondrogenic Differentiation of MSCs

The purpose of this study was to provide proof-of-concept of the potential to simultaneously differentiate MSCs into chondrocytes of the superficial and deep zone. Gene expression of collagen type II, X, and I was used to verify chondrogenesis. The average fold difference as compared to undifferentiated cells encapsulated within PEG-only hydrogels for collagen II, X, and I of each layer of the bi-layered constructs are shown in **Figures A.2A, A.2B, and A.2C**, respectively. Although the results indicate that the collagen II expression is higher in the superficial zone and the collagen X

expression is higher in the deep zone at all time points, there were no significant differences between the two layers for gene expression. The expression of collagen I was relatively low in both layers at all time points.

A.3.3 Histological Analysis of Imaged Hydrogels

To verify the quantitative gene expression results, immunohistochemical staining was performed to determine if the cells were producing collagen II and collagen X within the bi-layered constructs. At all time points, the fluorescent images showed positive staining for both collagen II and X within both layers, as shown in **Figure A.3**. The collagen II staining is consistent with the mRNA data. At 2 weeks the collagen II staining appeared more evenly dispersed within both layers. However, at 4 weeks the collagen II staining appeared to decrease in both layers while the collagen X staining increased in deep layer. At 6 weeks the spatial organization of collagen appeared to correspond to native articular cartilage [7]. In the superficial layer, the collagen II staining appeared to be aligned somewhat parallel to the top surface (articular surface). In the deep layer, collagen X levels were the highest at all time points, with larger collagen diameter and clusters, which were aligned perpendicular to the bottom surface (subchondral plate). Again, immunohistochemical staining was not performed for type I collagen due to low mRNA expression.

A.3.4 Protein Analysis for Total GAG Production

The GAG/DNA ratio for each layer of the bi-layered hydrogels is shown in **Figure A.4**. GAG production increased with time in both layers of the bi-layered constructs, with cells in the deep layer exhibiting significantly higher GAG levels compared to the superficial layer at 6 weeks.

A.3.5 Compressive Strength of the Individual Layers

Table A.2 lists the compressive moduli of the individual layers of the bi-layered hydrogel constructs, including the interface. The compressive modulus of the deep layer was significantly higher than the modulus of the superficial layer at all time points.

A.4 DISCUSSION

Chapter Four demonstrated that biomaterial composition can direct MSC differentiation in specific chondrogenic phenotypes. It was determined that the PEG:CS:MMP-pep and PEG:HA composition differentiated chondrocytes with similar characteristics to the superficial and deep zone of articular cartilage, respectively. Thus, as proof of concept, bi-layer hydrogels were created using these specific biomaterial combinations to differentiate MSCs into chondrocytes with varying phenotypes.

The cytotoxicity test indicated that the majority of the cells survive the fabrication process and are proliferating. At 6 weeks, the cells appeared to be aligned perpendicular to the interface, which indicated that they had remodeled the hydrogel network and structurally organized themselves in a similar orientation to that observed in the deep layer of native articular cartilage. Expression of collagen II, X, and I was used to determine MSC chondrogenic differentiation. The results demonstrated that there was higher collagen II expression in the superficial layer and higher collagen X expression in the deep layer at all time points. However, statistical analysis revealed that there were no significant differences between the layers for both collagen II and X expression. As mentioned in Chapters Four and Five, the expression of collagen I was used to determine fibrocartilage formation or de-differentiation of chondrocytes. The relatively low expression of collagen I within both layers indicated that the MSCs did not differentiate into fibrocartilage nor did they de-differentiate. GAG production was

higher in the deep layer than the superficial layer at all time points, but a significant difference was only observed between both layers at 6 weeks. Lastly, the mechanical strength of the deep layer was significantly greater than that of the superficial layer at all time points.

Gene expression, biochemical analysis, and histochemical analysis showed spatially varying ECM composition and mechanical properties similar to the native articular cartilage tissue. The findings of this study provide proof of concept of the ability to direct a single stem cell population to different chondrogenic phenotypes within a single 3D bi-layered structure.

A.5 FIGURES

Table A.1 Biomaterial Composition of each Layer

Zone	Material	PEG	CS	HA	MMP-pep
Superficial	PEG:CS:MMP-pep	9%	9%		2%
Deep	PEG:HA	19%		1%	

Figure A.1 Bi-Layer Live/Dead Staining of razor sliced sections of the bi-layered hydrogels constructs at 2, 4, and 6 weeks (4X objective, Leica SP2 AOBS). At all time points, the majority of the cells are alive (green) with very few dead cells (red).

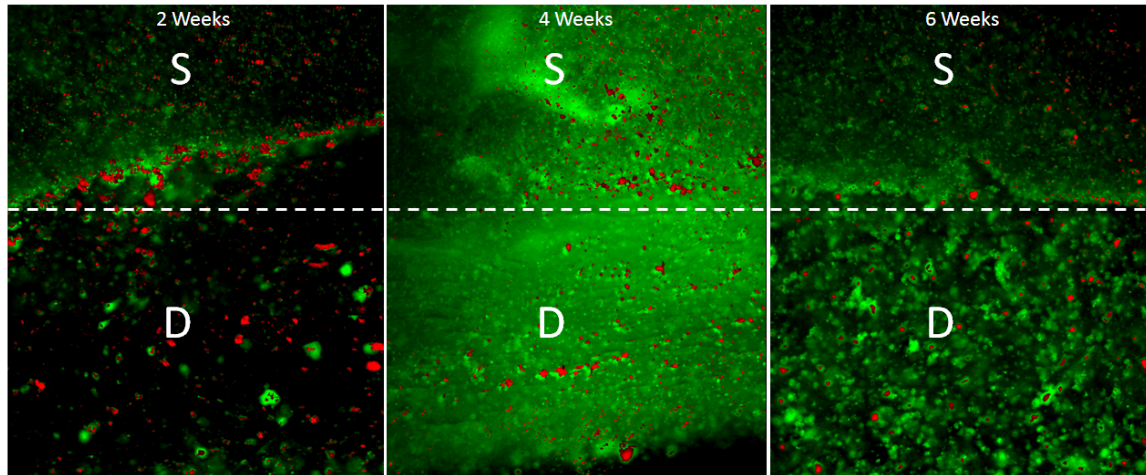


Figure A.2 Bi-Layer Collagen II, X, and I Gene Expression Average fold difference for gene expression of (A) Collagen II, (B) Collagen X, and (C) Collagen I of the bi-layered constructs at 2, 4, and 6 weeks. No significant differences are seen in all three gene expression between the superficial and the deep layer at all time points. Collagen I expression still remains relative low within the bi-layered hydrogel constructs at all time points.

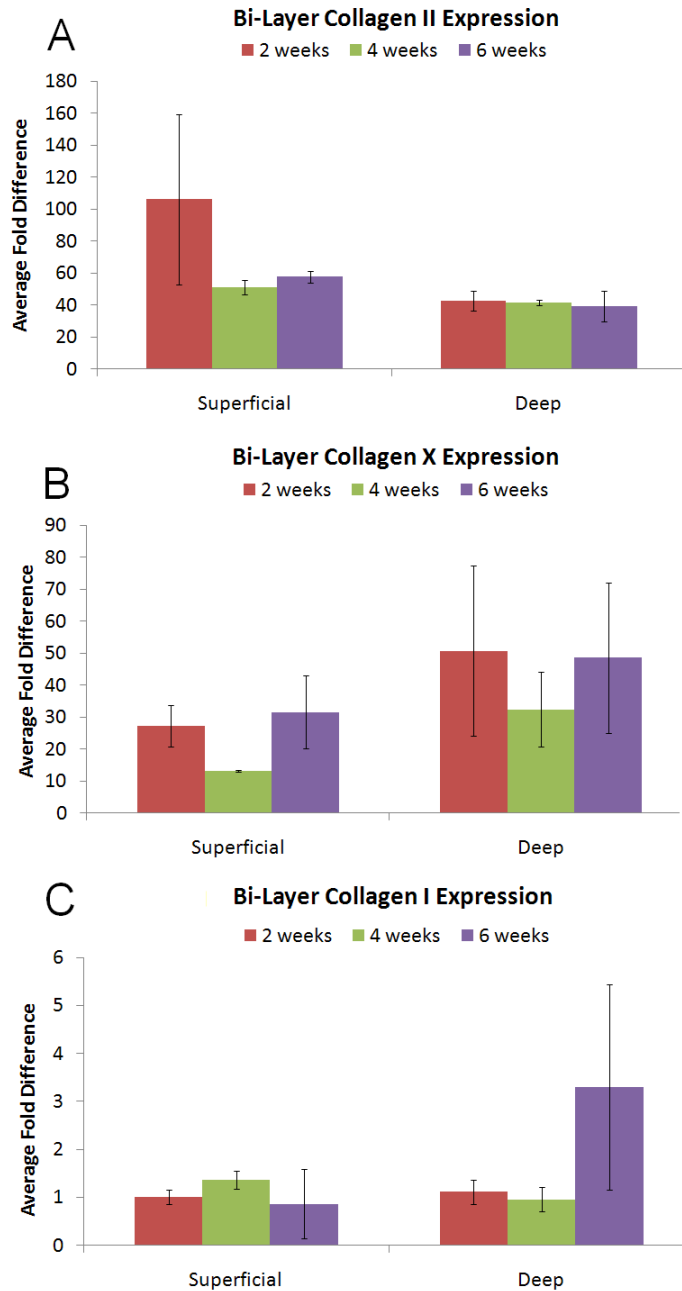


Figure A.3 Bi-Layer Immunohistochemical Staining of paraffin-embedded sections of bi-layered hydrogels constructs at 2, 4, and 6 weeks for collagen II (green) and X (red) (10X objective, Leica SP2 AOBS). At all time points, the fluorescent images showed positive staining for both collagen II and X.

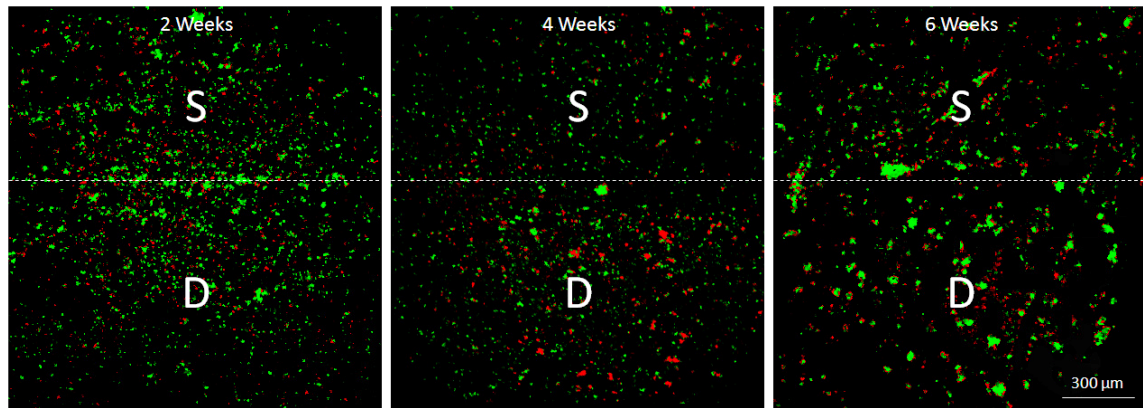


Figure A.4 Bi-Layer GAG Concentrations. The deep layer showed significantly higher GAG content than the superficial layer at all time points.

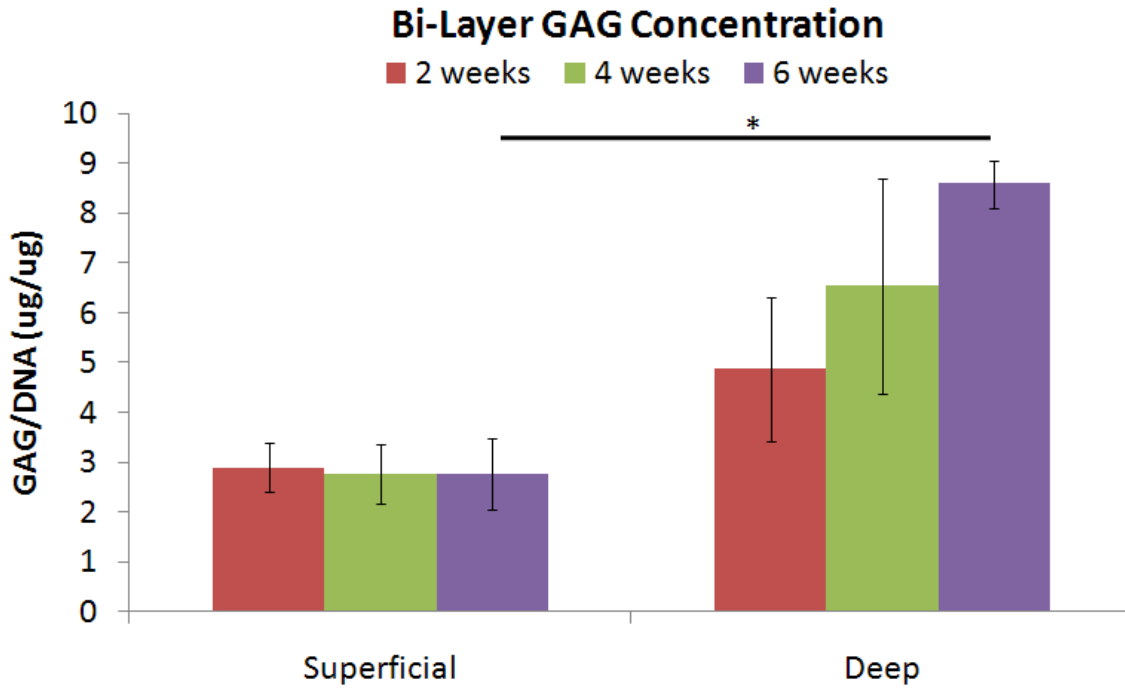


Table A.2 Compressive Moduli of Bi-Layer Hydrogels

Bi-layered Hydrogels	2 weeks		4 weeks		6 weeks	
	Moduli (kPa)	Standard Error	Moduli (kPa)	Standard Error	Moduli (kPa)	Standard Error
Superficial	120.38	± 9.49	99.51	± 13.5	445.42	± 97.97
Interface	127.20	± 8.62	172.17	± 28.16	409.99	± 60.67
Deep	396.97	± 21.12	197.14	± 40.8	925.79	± 93.46

A.6 REFERENCES

1. Bartlett, W., et al., *Autologous chondrocyte implantation at the knee using a bilayer collagen membrane with bone graft. A preliminary report.* J Bone Joint Surg Br, 2005. **87**(3): p. 330-2.
2. Bartlett, W., et al., *Autologous chondrocyte implantation versus matrix-induced autologous chondrocyte implantation for osteochondral defects of the knee: a prospective, randomised study.* J Bone Joint Surg Br, 2005. **87**(5): p. 640-5.
3. Sharma, B., et al., *Designing zonal organization into tissue-engineered cartilage.* Tissue Eng, 2007. **13**(2): p. 405-14.
4. Ng, K.W., G.A. Ateshian, and C.T. Hung, *Zonal chondrocytes seeded in a layered agarose hydrogel create engineered cartilage with depth-dependent cellular and mechanical inhomogeneity.* Tissue Eng Part A, 2009. **15**(9): p. 2315-24.
5. Awad, H.A., et al., *Chondrogenic differentiation of adipose-derived adult stem cells in agarose, alginate, and gelatin scaffolds.* Biomaterials, 2004. **25**(16): p. 3211-22.
6. Lee, H.J., et al., *Collagen mimetic peptide-conjugated photopolymerizable PEG hydrogel.* Biomaterials, 2006. **27**(30): p. 5268-76.
7. Poole, A.R., et al., *Composition and structure of articular cartilage: a template for tissue repair.* Clin Orthop Relat Res, 2001(391 Suppl): p. S26-33.

APPENDIX B

Supplementary Mechanical Studies for Future Work

B.1 INTRODUCTION

In Chapter Four, the modulus of pure HA hydrogels at 6 weeks could not be obtained due to their poor mechanical stability, which led them to the hydrogels collapse during culture before. Additionally, Chapter Four results indicated that pure CS hydrogels were a good candidate to represent the calcified zone of articular cartilage. However, in Chapter Five, all attempts to utilize the pure CS formulation as the fourth layer of the multi-layered hydrogel construct (MLHC) failed because the structural integrity of the pure CS hydrogel prevented quantitative and qualitative analysis of chondrogenesis within this layer. Therefore, the purpose of this study was to determine the 6 week compressive modulus of pure HA hydrogels and to determine the CS concentration that would provide the optimal compressive strength for future multi-layer studies.

B.2 MATERIALS AND METHODS

B.2.1 Compression Studies of Bi-Layered Hydrogels

The compressive modulus of the cell-laden swollen hydrogels were determined at room temperature on an In-spec 2200 Instron mechanical tester with a 125 N loading cell using a parallel plate apparatus and loading 20% of the initial thickness per second (0.1 mm/sec). The pre-sterilized cell-polymer solution was polymerized in a square mold (2 mm x 7 mm x 7 mm) for 10 minutes using a long-wave ultraviolet lamp (Model

B100AP, Blak-Ray) at the intensity of ~ 10 mW/cm². The polymerized hydrogel constructs were then used for mechanical testing and were compressed to the maximum thickness of 2 mm. The compressive modulus of cell-laden hydrogels were determined by analyzing the linear region of the stress versus the strain curve of the samples at low deformations (<20% strain).

B.2.2 Hydrogel Culture

The hydrogels cell-laden hydrogels were cultured in serum-free chondrogenic media containing 1% penicillin/streptomycin, 10nM dexamethasone, 50 μ g/mL ascorbic acid-2-phosphate, 40 μ g/mL L-proline, 5 mL ITS+1, and 10 ng/mL TGF- β 1 for 2, 4, and 6 weeks in a 12-well plate. The media were changed every other day. Extreme care was taken during media changes in order to prevent hydrogel collapse. The hydrogels were handled as minimally as possible and the medial was carefully aspirated from the well plates.

B.2.3 Statistical Analysis

All quantitative data were expressed as mean \pm standard error and were verified by analysis of variance using student T-Test with equal variance. P values of less than 0.05 were considered statistically significant.

B.3 RESULTS

B.3.1 Compressive Strength of CS and HA Hydrogels

Table B.1 lists the compressive modulus of the first CS studying with high concentrations. **Table B.2** lists the compressive modulus of the second CS study with

lower CS concentrations. **Table B.3** lists the compressive modulus of CS, HA, and PEG:HA from previous studies conducted in Chapter Four and the modulus of the CS and HA hydrogels determined in this study.

B.4 DISCUSSION

Two studies were conducted to find the optimal CS concentration with the most appropriate compressive modulus for future multi-layer studies. First, higher concentrations of CS were used due to the low mechanical strength of the 20% (w/v) concentration. During this study the polymer solutions for the 75% (w/v) and the 100% (w/v) were too viscous to accurately pipet the correct volume. Therefore, the thick polymer solutions were scooped out of the microcentrifuge tube into the mold for polymerization. The modulus for all concentrations above 20% (w/v) was extremely high. Therefore, a second study was done with lower CS concentrations. The results of the second study indicated that the 30% (w/v) CS concentration had a blank modulus of 511.97 kPa, which is the most appropriate modulus, being reasonably higher than the blank modulus of PEG:HA formulation in Chapter Four.

The 30% (w/v) CS concentration was used to determine the modulus of the cell-laden hydrogels at 2, 4, and 6 weeks. The modulus of 1% HA (w/v) was also determined in the same study. By taking extreme care during HA hydrogel culture, the modulus was obtained at all time points. The results indicate that the modulus 1% (w/v) HA is higher than 20% (w/v) CS hydrogels from the previous study at all time points. Additionally, 1% (w/v) HA hydrogels showed an increase in compressive strength with time, which is most likely due to the GAG production. Furthermore, the modulus of 30% (w/v) CS hydrogels also increased with time and was consistently higher than the PEG:HA formulation at all time points. These results indicate that 30% (w/v) CS has

the mechanical stability to be incorporated at the fourth layer in future multi-layer studies.

B.5 FIGURES

Table B.1 Compressive Moduli of High % (w/v) Blank CS Hydrogels

05/06/10		
Without Cells		
Hydrogel Concentration	Modulus (kPa)	Standard Error
20% (w/v) CS	131.15	± 7.70
50% (w/v) CS	713.29	± 53.59
75% (w/v) CS	1171.90	± 80.64
100% (w/v) CS	1848.10	± 123.16

Table B.2 Compressive Moduli of Low % (w/v) Blank CS Hydrogels

05/18/10	Without Cells	
Hydrogel Concentration	Moduli (kPa)	Standard Error
20% (w/v) CS	240.12	± 66.54
25% (w/v) CS	312.06	± 29.9
30% (w/v) CS	511.97	± 41.26
35% (w/v) CS	669.82	± 61.02
40% (w/v) CS	727.00	± 23.6
45% (w/v) CS	813.39	± 19.17
50% (w/v) CS	889.25	± 21.42

Table B.3 Compressive Moduli of Cell-Laden CS and HA Hydrogels

		2 Weeks		4 Weeks		6 Weeks	
	Hydrogel Composition	Moduli (kPa)	Standard Error	Moduli (kPa)	Standard Error	Moduli (kPa)	Standard Error
Previous Study 10/23/09	1 % (w/v) HA	41.66	± 14.12	11.60	± 4.68		
	20 % (w/v) CS	26.42	± 5.80	65.03	± 9.98	68.18	± 37.37
	20 % (w/v) PEG:HA	271.57	± 64.21	435.07	± 59.52	1227.9	± 102.14
Current Study 6/14/10	1 % (w/v) HA	38.54	± 3.82	45.95	± 3.89	81.465	± 11.31
	30 % (w/v) CS	445.46	± 123.93	606.56	± 85.58	1428.9	± 223.73

APPENDIX C

List of Abbreviations

ACI	Autologous chondrocyte implantation
ADSC	Adipose-derived stem cell
ASC	Adipose stem cell
ATCC	American type culture collection
bFGF	basic Fibroblast growth factor
BMSC	Bone marrow stromal cell
BSA	Bovine serum albumin
COMP	Cartilage oligomeric matrix protein
CS	Chondroitin Sulfate
DCM	Dichloromethane
DMEM	Dulbecco's modified eagle medium
DMMB	Dimethylmethylene blue
DNA	Deoxyribonucleic acid
DS	Dermatan sulfate
EB	Embryoid body
ECM	Extracellular matrix
EDTA	Ethylene diamine tetra acetic acid
EGF	Epidermal growth factor
ES	Embryonic stem cell
EWC	Equilibrium water content
FBS	Fetal bovine serum
FDA	Food and Drug Administration
FITC	Fluorescein isothiocyanate
GAG	Glycosaminoglycan
GAPDH	Glyceraldehyde 3-phosphate dehydrogenase
GM	Glycidyl methacrylate
GMHA	Glycidyl methacrylate hyaluronic acid
HA	Hyaluronic Acid
hMSC	Human mesenchymal stem cell
HPLC	High performance liquid chromatography
kPa	Kilo Pascals

KS	Keratin sulfate
LC	Liquid chromatography
MAA	Methacrylic acid
MACI	Matrix-induced autologous chondrocyte implantation
MALDI-TOF	Matrix assisted laser de-ionization time of flight
MLHC	Multi-layered hydrogel construct
MMP	Matrix metalloproteinase
MMP-pep	Matrix metalloproteinase sensitive peptide
MS	Mass spectrometry
MSC	Mesenchymal stem cell
NMP	N-methylpyrrolidone
NMR	Nuclear magnetic resonance
OA	Osteoarthritis
OATS	Osteochondral autograft transfer system
p(NIPAAm-co-AAc)	N-isopropylacrylamide-acrylic acid copolymer
PBS	Phosphate buffered saline
PCL	Poly(ϵ -caprolactone)
PCR	Polymerase chain reaction
PEG	Poly(ethylene glycol)
PEG:CS	PEG:Chondroitin Sulfate
PEG:CS:MMP-pep	PEG:Chondroitin Sulfate:MMP-sensitive peptide
PEG:HA	PEG:Hyaluronic Acid
PEG:HA:MMP-pep	PEG:Hyaluronic Acid:MMP-sensitive peptide
PEGDA	Poly(ethylene glycol) Diacrylate
PEGDMA	Poly(ethylene glycol) Dimethacrylate
PG	Proteoglycan
PGA	Polyglycolic acid
Phos-PEG	Phosphoester-poly(ethylene glycol)
PLA	Processed lipoaspirate
PLEOF	Poly(lactide ethylene oxide fumarate)
PLGA	Poly(lactic-co-glycolic acid)
PRG4	Proteoglycan 4 or lubricin
qPCR	Quantitative polymerase chain reaction
QPQGLAK	Gln-Pro-Gln-Gly-Leu-Ala-Lys (MMP-sensitive peptide)
RA	Rheumatoid arthritis
RGD	Arginine-glycine-aspartate peptide
RT	Reverse transcription
SA	Super Array

SDS	Sodium dodecyl Sulfate
SDSC	Synovial-derived stem cell
SEM	Scanning electron microscope
SFB	Synovial fibroblasts
sIPN	Semi-interpenetrating polymer network
SLC	Single layer control
TBE	Tris borate EDTA
TES	Tris-EDTA
TGF β	Transforming growth factor beta

Bibliography

- Abboudi, J.et al., 'Cartilage Injuries and Restoration' Available from www.orthspec.com/cartilage_sports_injuries.htm. January 6, 2010, 2010. Accessed June 23 2010.
- Adamietz, P. 'Synergy of Transforming Growth Factor B-1 and Insulin-Like Growth Factor in Stimulating Formation of Neocartilage by Pig Articular Chondrocyte Pellet Culture'. In 2nd Fribourg International Symposium on Cartilage Repair Fribourg, Switzerland: 1997.
- Afizah, H.et al., A Comparison between the Chondrogenic Potential of Human Bone Marrow Stem Cells (BMSCs) and Adipose-Derived Stem Cells (ADSCs) Taken from the Same Donors. *Tissue Eng*, 2007. **13**(4): p. 659-66.
- Ahern, B. J.et al., Preclinical Animal Models in Single Site Cartilage Defect Testing: A Systematic Review. *Osteoarthritis Cartilage*, 2009. **17**(6): p. 705-13.
- Ahmed, T. A.et al., Fibrin: A Versatile Scaffold for Tissue Engineering Applications. *Tissue Eng Part B Rev*, 2008.
- Alcantar, N. A.et al., Polyethylene Glycol-Coated Biocompatible Surfaces. *J Biomed Mater Res*, 2000. **51**(3): p. 343-51.
- Allard, S. A.et al., Cells and Matrix Expressing Cartilage Components in Fibroblastic Tissue in Rheumatoid Pannus. *Scand J Rheumatol Suppl*, 1988. **76**: p. 125-9.
- Anseth, K. S.et al., In Situ Forming Degradable Networks and Their Application in Tissue Engineering and Drug Delivery. *J Control Release*, 2002. **78**(1-3): p. 199-209.
- Armstrong, C. G.et al., Variations in the Intrinsic Mechanical Properties of Human Articular Cartilage with Age, Degeneration, and Water Content. *J Bone Joint Surg Am*, 1982. **64**(1): p. 88-94.
- Augst, A.et al., Effects of Chondrogenic and Osteogenic Regulatory Factors on Composite Constructs Grown Using Human Mesenchymal Stem Cells, Silk Scaffolds and Bioreactors. *J R Soc Interface*, 2008. **5**(25): p. 929-39.

- Awad, H. A.et al., Chondrogenic Differentiation of Adipose-Derived Adult Stem Cells in Agarose, Alginate, and Gelatin Scaffolds. *Biomaterials*, 2004. **25**(16): p. 3211-22.
- Barry, F.et al., Chondrogenic Differentiation of Mesenchymal Stem Cells from Bone Marrow: Differentiation-Dependent Gene Expression of Matrix Components. *Exp Cell Res*, 2001. **268**(2): p. 189-200.
- Bartlett, W.et al., Autologous Chondrocyte Implantation at the Knee Using a Bilayer Collagen Membrane with Bone Graft. A Preliminary Report. *J Bone Joint Surg Br*, 2005. **87**(3): p. 330-2.
- Bartlett, W.et al., Autologous Chondrocyte Implantation Versus Matrix-Induced Autologous Chondrocyte Implantation for Osteochondral Defects of the Knee: A Prospective, Randomised Study. *J Bone Joint Surg Br*, 2005. **87**(5): p. 640-5.
- Basad, E.et al., Matrix-Induced Autologous Chondrocyte Implantation Versus Microfracture in the Treatment of Cartilage Defects of the Knee: A 2-Year Randomised Study. *Knee Surg Sports Traumatol Arthrosc*, 2010. **18**(4): p. 519-27.
- Benya, P. D.et al., Dedifferentiated Chondrocytes Reexpress the Differentiated Collagen Phenotype When Cultured in Agarose Gels. *Cell*, 1982. **30**(1): p. 215-24.
- Bernstein, P.et al., Pellet Culture Elicits Superior Chondrogenic Redifferentiation Than Alginate-Based Systems. *Biotechnol Prog*, 2009. **25**(4): p. 1146-52.
- Bhosale, A. M.et al., Articular Cartilage: Structure, Injuries and Review of Management. *Br Med Bull*, 2008. **87**: p. 77-95.
- Biddulph, D. M.et al., Comparative Effects of Cytosine Arabinoside and a Prostaglandin E2 Antagonist, Ah6809, on Chondrogenesis in Serum-Free Cultures of Chick Limb Mesenchyme. *Exp Cell Res*, 1991. **196**(1): p. 131-3.
- Boschetti, F.et al., Tensile and Compressive Properties of Healthy and Osteoarthritic Human Articular Cartilage. *Biorheology*, 2008. **45**(3-4): p. 337-44.
- Botchwey, E. A.et al., Human Osteoblast-Like Cells in Three-Dimensional Culture with Fluid Flow. *Biorheology*, 2003. **40**(1-3): p. 299-306.
- Bouwmeester, P. S.et al., A Retrospective Analysis of Two Independent Prospective Cartilage Repair Studies: Autogenous Perichondrial Grafting Versus

- Subchondral Drilling 10 Years Post-Surgery. *J Orthop Res*, 2002. **20**(2): p. 267-73.
- Bradham, D. M.et al., In Vivo Cartilage Formation from Growth Factor Modulated Articular Chondrocytes. *Clin Orthop Relat Res*, 1998. (352): p. 239-49.
- Brehm, W.et al., Repair of Superficial Osteochondral Defects with an Autologous Scaffold-Free Cartilage Construct in a Caprine Model: Implantation Method and Short-Term Results. *Osteoarthritis Cartilage*, 2006. **14**(12): p. 1214-26.
- Breinan, H. A.et al., Autologous Chondrocyte Implantation in a Canine Model: Change in Composition of Reparative Tissue with Time. *J Orthop Res*, 2001. **19**(3): p. 482-92.
- Breinan, H. A.et al., Effect of Cultured Autologous Chondrocytes on Repair of Chondral Defects in a Canine Model. *J Bone Joint Surg Am*, 1997. **79**(10): p. 1439-51.
- Brittberg, M.et al., Treatment of Deep Cartilage Defects in the Knee with Autologous Chondrocyte Transplantation. *N Engl J Med*, 1994. **331**(14): p. 889-95.
- Bryant, S. J.et al., Hydrogel Properties Influence Ecm Production by Chondrocytes Photoencapsulated in Poly(Ethylene Glycol) Hydrogels. *J Biomed Mater Res*, 2002. **59**(1): p. 63-72.
- Bryant, S. J.et al., Controlling the Spatial Distribution of Ecm Components in Degradable Peg Hydrogels for Tissue Engineering Cartilage. *J Biomed Mater Res A*, 2003. **64**(1): p. 70-9.
- Bryant, S. J.et al., Crosslinking Density Influences the Morphology of Chondrocytes Photoencapsulated in Peg Hydrogels During the Application of Compressive Strain. *J Orthop Res*, 2004. **22**(5): p. 1143-9.
- Bryant, S. J.et al., Encapsulating Chondrocytes in Degrading Peg Hydrogels with High Modulus: Engineering Gel Structural Changes to Facilitate Cartilaginous Tissue Production. *Biotechnol Bioeng*, 2004. **86**(7): p. 747-55.
- Buckwalter, J. A.et al., .Articular Cartilage and Knee Joint Function: Basic Science and Arthroscopy. New York: Raven Press, 1990.
- Buma, P.et al., Cross-Linked Type I and Type Ii Collagenous Matrices for the Repair of Full-Thickness Articular Cartilage Defects--a Study in Rabbits. *Biomaterials*, 2003. **24**(19): p. 3255-63.

- Burdick, J. A. et al., Photoencapsulation of Osteoblasts in Injectable Rgd-Modified Peg Hydrogels for Bone Tissue Engineering. *Biomaterials*, 2002. **23**(22): p. 4315-23.
- Burdick, J. A. et al., Delivery of Osteoinductive Growth Factors from Degradable Peg Hydrogels Influences Osteoblast Differentiation and Mineralization. *J Control Release*, 2002. **83**(1): p. 53-63.
- Bursac, N. et al., Cultivation in Rotating Bioreactors Promotes Maintenance of Cardiac Myocyte Electrophysiology and Molecular Properties. *Tissue Eng*, 2003. **9**(6): p. 1243-53.
- Butnariu-Ephrat, M. et al., Resurfacing of Goat Articular Cartilage by Chondrocytes Derived from Bone Marrow. *Clin Orthop Relat Res*, 1996. (330): p. 234-43.
- Byers, B. A. et al., Transient Exposure to Transforming Growth Factor Beta 3 under Serum-Free Conditions Enhances the Biomechanical and Biochemical Maturation of Tissue-Engineered Cartilage. *Tissue Eng Part A*, 2008. **14**(11): p. 1821-34.
- Cancedda, R. et al., Chondrocyte Differentiation. *Int Rev Cytol*, 1995. **159**: p. 265-358.
- Capelhart, A. A. et al., Effects of a Putative Prostaglandin E2 Antagonist, Ah6809, on Chondrogenesis in Serum-Free Cultures of Chick Limb Mesenchyme. *J Cell Physiol*, 1991. **147**(3): p. 403-11.
- Caplan, A. I. Mesenchymal Stem Cells. *J Orthop Res*, 1991. **9**(5): p. 641-50.
- Chapekar, M. S. Tissue Engineering: Challenges and Opportunities. *J Biomed Mater Res*, 2000. **53**(6): p. 617-20.
- Cheifetz, S. et al., The Transforming Growth Factor-Beta System, a Complex Pattern of Cross-Reactive Ligands and Receptors. *Cell*, 1987. **48**(3): p. 409-15.
- Chen, F. H. et al., Mesenchymal Stem Cells in Arthritic Diseases. *Arthritis Res Ther*, 2008. **10**(5): p. 223.
- Chen, G., Ushida, Takashi, Tateishi, Tetsuya Scaffold Design for Tissue Engineering. *Macromolecular Bioscience*, 2002. **2**: p. 67-77.
- Chiang, H. et al., Repair of Porcine Articular Cartilage Defect with Autologous Chondrocyte Transplantation. *J Orthop Res*, 2005. **23**(3): p. 584-93.

- Chimal-Monroy, J.et al., Regulation of Chondrocyte Differentiation by Transforming Growth Factors Beta 1, Beta 2, Beta 3, and Beta 5. *Ann N Y Acad Sci*, 1996. **785**: p. 241-4.
- Chimal-Monroy, J.et al., Differential Effects of Transforming Growth Factors Beta 1, Beta 2, Beta 3 and Beta 5 on Chondrogenesis in Mouse Limb Bud Mesenchymal Cells. *Int J Dev Biol*, 1997. **41**(1): p. 91-102.
- Chu, C. R.et al., Articular Cartilage Repair Using Allogeneic Perichondrocyte-Seeded Biodegradable Porous Polylactic Acid (PlA): A Tissue-Engineering Study. *J Biomed Mater Res*, 1995. **29**(9): p. 1147-54.
- Chu, C. R.et al., Osteochondral Repair Using Perichondrial Cells. A 1-Year Study in Rabbits. *Clin Orthop Relat Res*, 1997. (340): p. 220-9.
- Chu, C. R.et al., Animal Models for Cartilage Regeneration and Repair. *Tissue Eng Part B Rev*, 2010. **16**(1): p. 105-15.
- Convery, F. R.et al., The Repair of Large Osteochondral Defects. An Experimental Study in Horses. *Clin Orthop Relat Res*, 1972. **82**: p. 253-62.
- Cook, S. D.et al., Repair of Articular Cartilage Defects with Osteogenic Protein-1 (Bmp-7) in Dogs. *J Bone Joint Surg Am*, 2003. **85-A Suppl 3**: p. 116-23.
- Cooper, J. A., Jr.et al., Encapsulated Chondrocyte Response in a Pulsatile Flow Bioreactor. *Acta Biomater*, 2007. **3**(1): p. 13-21.
- Cruise, G. M.et al., A Sensitivity Study of the Key Parameters in the Interfacial Photopolymerization of Poly(Ethylene Glycol) Diacrylate Upon Porcine Islets. *Biotechnol Bioeng*, 1998. **57**(6): p. 655-65.
- Czitrom, A. A.et al., Bone and Cartilage Allotransplantation. A Review of 14 Years of Research and Clinical Studies. *Clin Orthop Relat Res*, 1986. (208): p. 141-5.
- Dahir, G. A.et al., Pluripotential Mesenchymal Cells Repopulate Bone Marrow and Retain Osteogenic Properties. *Clin Orthop Relat Res*, 2000. (379 Suppl): p. S134-45.
- Darling, E. M.et al., Retaining Zonal Chondrocyte Phenotype by Means of Novel Growth Environments. *Tissue Eng*, 2005. **11**(3-4): p. 395-403.

- DeFail, A. J.et al., Controlled Release of Bioactive Tgf-Beta 1 from Microspheres Embedded within Biodegradable Hydrogels. *Biomaterials*, 2006. **27**(8): p. 1579-85.
- Dennis, J.et al., . 'Bone Marrow Mesenchymal Stem Cells'. In Sell, Stewart (ed.) Totowa: Humana Press, 2004.
- Derynck, R.et al., A New Type of Transforming Growth Factor-Beta, Tgf-Beta 3. *EMBO J*, 1988. **7**(12): p. 3737-43.
- Di Cesare, P. E.et al., Expression of Cartilage Oligomeric Matrix Protein by Human Synovium. *FEBS Lett*, 1997. **412**(1): p. 249-52.
- Diekman, B. O.et al., Chondrogenesis of Adult Stem Cells from Adipose Tissue and Bone Marrow: Induction by Growth Factors and Cartilage-Derived Matrix. *Tissue Eng Part A*, 2010. **16**(2): p. 523-33.
- Dodge, G. R.et al., Production of Cartilage Oligomeric Matrix Protein (Comp) by Cultured Human Dermal and Synovial Fibroblasts. *Osteoarthritis Cartilage*, 1998. **6**(6): p. 435-40.
- Einhorn, T. A.et al., .Orthopaedic Basic Science Foundations of Clinical Practice. American Academy of Orthopaedic Surgeons, 2007.
- Elena A. Armandola, P. 'Tissue Regeneration and Organ Repair: Science or Science Fiction?' Available from http://www.medscape.com/viewarticle/457173_print. 07/11/2003, 2003. Accessed June 27, 2007 2007.
- Elisseeff, J.et al., Transdermal Photopolymerization for Minimally Invasive Implantation. *Proc Natl Acad Sci U S A*, 1999. **96**(6): p. 3104-7.
- Elisseeff, J.et al., Transdermal Photopolymerization of Poly(Ethylene Oxide)-Based Injectable Hydrogels for Tissue-Engineered Cartilage. *Plast Reconstr Surg*, 1999. **104**(4): p. 1014-22.
- Elisseeff, J.et al., The Role of Biomaterials in Stem Cell Differentiation: Applications in the Musculoskeletal System. *Stem Cells Dev*, 2006. **15**(3): p. 295-303.
- Elisseeff, J.et al., Photoencapsulation of Chondrocytes in Poly(Ethylene Oxide)-Based Semi-Interpenetrating Networks. *J Biomed Mater Res*, 2000. **51**(2): p. 164-71.

- Elisseeff, J. et al., Controlled-Release of Igf-I and Tgf-Beta1 in a Photopolymerizing Hydrogel for Cartilage Tissue Engineering. *J Orthop Res*, 2001. **19**(6): p. 1098-104.
- Elisseeff, J. H. et al., Biological Response of Chondrocytes to Hydrogels. *Ann N Y Acad Sci*, 2002. **961**: p. 118-22.
- Erggele, C. et al., .Principles of Cartilage Repair. Sturtz Gmbh, Wurzburg Germany: Steinkopff Verlag, 2008.
- Estes, B. T. et al., Extended Passaging, but Not Aldehyde Dehydrogenase Activity, Increases the Chondrogenic Potential of Human Adipose-Derived Adult Stem Cells. *J Cell Physiol*, 2006. **209**(3): p. 987-95.
- Evans, P. J. et al., Manual Punch Versus Power Harvesting of Osteochondral Grafts. *Arthroscopy*, 2004. **20**(3): p. 306-10.
- Eyre, D. R. et al., Collagen of Fibrocartilage: A Distinctive Molecular Phenotype in Bovine Meniscus. *FEBS Lett*, 1983. **158**(2): p. 265-70.
- Fan, J. et al., Chondrogenesis of Synovium-Derived Mesenchymal Stem Cells in Photopolymerizing Hydrogel Scaffolds. *J Biomater Sci Polym Ed*, 2010.
- Feinberg, S. E. et al., Image-Based Biomimetic Approach to Reconstruction of the Temporomandibular Joint. *Cells Tissues Organs*, 2001. **169**(3): p. 309-21.
- Felson, D. T. et al., Osteoarthritis: New Insights. Part 1: The Disease and Its Risk Factors. *Ann Intern Med*, 2000. **133**(8): p. 635-46.
- Felson, D. T. et al., Osteoarthritis: New Insights. Part 2: Treatment Approaches. *Ann Intern Med*, 2000. **133**(9): p. 726-37.
- Fife, R. S. et al., Identification of Link Proteins in Canine Synovial Cell Cultures and Canine Articular Cartilage. *J Cell Biol*, 1985. **100**(4): p. 1050-5.
- Firestein, G. S. et al., .Firestein: Kelley's Textbook of Rheumatology. Philadelphia: W. B. Saunders Company, 2008.
- Fisher, J. P. et al., Thermoreversible Hydrogel Scaffolds for Articular Cartilage Engineering. *J Biomed Mater Res A*, 2004. **71**(2): p. 268-74.
- Fitzsimmons, J. S. et al., Serum-Free Media for Periosteal Chondrogenesis in Vitro. *J Orthop Res*, 2004. **22**(4): p. 716-25.

- Flik, K. R. et al., . 'Articular Cartilage'. New Jersey: Humana Press Inc., 2007.
- Freed, L. E. et al., Advanced Tools for Tissue Engineering: Scaffolds, Bioreactors, and Signaling. *Tissue Eng*, 2006. **12**(12): p. 3285-305.
- Frenz, D. A. et al., Induction of Chondrogenesis: Requirement for Synergistic Interaction of Basic Fibroblast Growth Factor and Transforming Growth Factor-Beta. *Development*, 1994. **120**(2): p. 415-24.
- Frisbie, D. D. et al., A Comparative Study of Articular Cartilage Thickness in the Stifle of Animal Species Used in Human Pre-Clinical Studies Compared to Articular Cartilage Thickness in the Human Knee. *Vet Comp Orthop Traumatol*, 2006. **19**(3): p. 142-6.
- Furukawa, T. et al., Biochemical Studies on Repair Cartilage Resurfacing Experimental Defects in the Rabbit Knee. *J Bone Joint Surg Am*, 1980. **62**(1): p. 79-89.
- Fuson RL, M Sherman, J Van Vleet, et al. The conduct of orthopaedic clinical trials. *J Bone Joint Surg Am* 1997; 79 (7):1089-98.
- Gerecht, S. et al., Hyaluronic Acid Hydrogel for Controlled Self-Renewal and Differentiation of Human Embryonic Stem Cells. *Proc Natl Acad Sci U S A*, 2007. **104**(27): p. 11298-303.
- Goessler, U. R. et al., In-Vitro Analysis of the Expression of Tgfbeta -Superfamily-Members During Chondrogenic Differentiation of Mesenchymal Stem Cells and Chondrocytes During Dedifferentiation in Cell Culture. *Cell Mol Biol Lett*, 2005. **10**(2): p. 345-62.
- Gooch, K. J. et al., Effects of Mixing Intensity on Tissue-Engineered Cartilage. *Biotechnol Bioeng*, 2001. **72**(4): p. 402-7.
- Gooding, C. R. et al., A Prospective, Randomised Study Comparing Two Techniques of Autologous Chondrocyte Implantation for Osteochondral Defects in the Knee: Periosteum Covered Versus Type I/III Collagen Covered. *Knee*, 2006. **13**(3): p. 203-10.
- Gotterbarm, T. et al., The Minipig Model for Experimental Chondral and Osteochondral Defect Repair in Tissue Engineering: Retrospective Analysis of 180 Defects. *Lab Anim*, 2008. **42**(1): p. 71-82.

- Graham, N. B. Hydrogels: Their Future, Part I. *Med Device Technol*, 1998. **9**(1): p. 18-22.
- Graham, N. B. Hydrogels: Their Future, Part II. *Med Device Technol*, 1998. **9**(3): p. 22-5.
- Griffith, M. L. et al., Freeform Fabrication of Ceramics Via Stereolithography. *J. Am. Ceram. Soc.*, 1996. **79**: p. 2601–2608.
- Grodzinsky, A. J. et al., Cartilage Tissue Remodeling in Response to Mechanical Forces. *Annu Rev Biomed Eng*, 2000. **2**: p. 691-713.
- Guilak, F. et al., Functional Tissue Engineering: The Role of Biomechanics in Articular Cartilage Repair. *Clin Orthop Relat Res*, 2001. (391 Suppl): p. S295-305.
- Guilak, F. et al., Control of Stem Cell Fate by Physical Interactions with the Extracellular Matrix. *Cell Stem Cell*, 2009. **5**(1): p. 17-26.
- Guilak, F. et al., Clonal Analysis of the Differentiation Potential of Human Adipose-Derived Adult Stem Cells. *J Cell Physiol*, 2006. **206**(1): p. 229-37.
- Gunatillake, P. A. et al., Biodegradable Synthetic Polymers for Tissue Engineering. *Eur Cell Mater*, 2003. **5**: p. 1-16; discussion 16.
- Guo, J. F. et al., Culture and Growth Characteristics of Chondrocytes Encapsulated in Alginate Beads. *Connect Tissue Res*, 1989. **19**(2-4): p. 277-97.
- Haklar, U. et al., [Mosaicplasty Technique in the Treatment of Osteochondral Lesions of the Knee]. *Acta Orthop Traumatol Turc*, 2008. **42**(5): p. 344-9.
- Haldeman, K. O. et al., The Response of Articular Cartilage to Trauma: With Special Reference to the Knee Joint. *Calif Med*, 1948. **69**(3): p. 179-82.
- Hall, B. K. *Bones and Cartilage Developmental and Evolutionary Skeletal Biology*. San Diego: Elsevier Academic Press, 2005.
- Halstenberg, S. et al., Biologically Engineered Protein-Graft-Poly(Ethylene Glycol) Hydrogels: A Cell Adhesive and Plasmin-Degradable Biosynthetic Material for Tissue Repair. *Biomacromolecules*, 2002. **3**(4): p. 710-23.
- Hamerman, D. et al., Glycosaminoglycans Produced by Human Synovial Cell Cultures. *Coll Relat Res*, 1982. **2**(4): p. 313-29.

- Han, C. W.et al., Analysis of Rabbit Articular Cartilage Repair after Chondrocyte Implantation Using Optical Coherence Tomography. *Osteoarthritis Cartilage*, 2003. **11**(2): p. 111-21.
- Han, L.-H.et al., Projection Microfabrication of Three-Dimensional Scaffolds for Tissue Engineering. *Journal of Manufacturing Science and Engineering*, 2008. **130**(021005): p. 1-4.
- Hangody, L.et al., Arthroscopic Autogenous Osteochondral Mosaicplasty for the Treatment of Femoral Condylar Articular Defects. A Preliminary Report. *Knee Surg Sports Traumatol Arthrosc*, 1997. **5**(4): p. 262-7.
- Hangody, L.et al., Autologous Osteochondral Mosaicplasty. *Surgical Technique. J Bone Joint Surg Am*, 2004. **86-A Suppl 1**: p. 65-72.
- Hangody, L.et al., Autologous Osteochondral Grafting--Technique and Long-Term Results. *Injury*, 2008. **39 Suppl 1**: p. S32-9.
- Hayamizu, T. F.et al., Effects of Localized Application of Transforming Growth Factor Beta 1 on Developing Chick Limbs. *Dev Biol*, 1991. **145**(1): p. 164-73.
- He, X.et al., Material Properties and Cytocompatibility of Injectable Mmp Degradable Poly(Lactide Ethylene Oxide Fumarate) Hydrogel as a Carrier for Marrow Stromal Cells. *Biomacromolecules*, 2007. **8**(3): p. 780-92.
- Health Resources and Services Administration, H. S. B., Division of Transplantation. '2006 Optn/Srtr Annual Report' Available from http://www.ustransplant.org/annual_reports/current/103_dh.htm. .OPTN/SRTR Data as of May 1, 2006, 2006. Accessed June 27, 2007 2007.
- Hegert, C.et al., Differentiation Plasticity of Chondrocytes Derived from Mouse Embryonic Stem Cells. *J Cell Sci*, 2002. **115**(Pt 23): p. 4617-28.
- Heine, U.et al., Role of Transforming Growth Factor-Beta in the Development of the Mouse Embryo. *J Cell Biol*, 1987. **105**(6 Pt 2): p. 2861-76.
- Hendrickson, D. A.et al., Chondrocyte-Fibrin Matrix Transplants for Resurfacing Extensive Articular Cartilage Defects. *J Orthop Res*, 1994. **12**(4): p. 485-97.
- Hidaka, C.et al., Acceleration of Cartilage Repair by Genetically Modified Chondrocytes over Expressing Bone Morphogenetic Protein-7. *J Orthop Res*, 2003. **21**(4): p. 573-83.

- Higgs, G. B. et al., . 'Cartilage Regeneration and Repair, Where Are We?' Available from http://www.orthojournalhms.org/volume1/html/cartilage_repair.html2007. Accessed June 27, 2007 2007.
- Hillel, A. T. et al., Characterization of Human Mesenchymal Stem Cell-Engineered Cartilage: Analysis of Its Ultrastructure, Cell Density and Chondrocyte Phenotype Compared to Native Adult and Fetal Cartilage. *Cells Tissues Organs*, 2009. **191**(1): p. 12-20.
- Hjelle, K. et al., Articular Cartilage Defects in 1,000 Knee Arthroscopies. *Arthroscopy*, 2002. **18**(7): p. 730-4.
- Holland, T. A. et al., Degradable Hydrogel Scaffolds for in Vivo Delivery of Single and Dual Growth Factors in Cartilage Repair. *Osteoarthritis Cartilage*, 2007. **15**(2): p. 187-97.
- Hollister, S. J. et al., Optimal Design and Fabrication of Scaffolds to Mimic Tissue Properties and Satisfy Biological Constraints. *Biomaterials*, 2002. **23**(20): p. 4095-103.
- Horas, U. et al., [Osteochondral Transplantation Versus Autogenous Chondrocyte Transplantation. A Prospective Comparative Clinical Study]. *Chirurg*, 2000. **71**(9): p. 1090-7.
- Hsiong, S. X. et al., Cyclic Arginine-Glycine-Aspartate Peptides Enhance Three-Dimensional Stem Cell Osteogenic Differentiation. *Tissue Eng Part A*, 2009. **15**(2): p. 263-72.
- Hsu, S. H. et al., Evaluation of Biodegradable Polyesters Modified by Type Ii Collagen and Arg-Gly-Asp as Tissue Engineering Scaffolding Materials for Cartilage Regeneration. *Artif Organs*, 2006. **30**(1): p. 42-55.
- Huang, J. I. et al., Chondrogenic Potential of Progenitor Cells Derived from Human Bone Marrow and Adipose Tissue: A Patient-Matched Comparison. *J Orthop Res*, 2005. **23**(6): p. 1383-9.
- Hunziker, E. B. Biologic Repair of Articular Cartilage. Defect Models in Experimental Animals and Matrix Requirements. *Clin Orthop Relat Res*, 1999. (367 Suppl): p. S135-46.
- Hunziker, E. B. et al., . 'Articular Cartilage Structure in Humans and Experimental Animals '. New York: Raven Press, 1992.

- Hwang, N. S.et al., Effects of Three-Dimensional Culture and Growth Factors on the Chondrogenic Differentiation of Murine Embryonic Stem Cells. *Stem Cells*, 2006. **24**(2): p. 284-91.
- Hwang, N. S.et al., Derivation of Chondrogenically-Committed Cells from Human Embryonic Cells for Cartilage Tissue Regeneration. *PLoS ONE*, 2008. **3**(6): p. e2498.
- Hwang, N. S.et al., Response of Zonal Chondrocytes to Extracellular Matrix-Hydrogels. *FEBS Lett*, 2007. **581**(22): p. 4172-8.
- Hwang, N. S.et al., Enhanced Chondrogenic Differentiation of Murine Embryonic Stem Cells in Hydrogels with Glucosamine. *Biomaterials*, 2006. **27**(36): p. 6015-23.
- Hwang, N. S.et al., Chondrogenic Differentiation of Human Embryonic Stem Cell-Derived Cells in Arginine-Glycine-Aspartate-Modified Hydrogels. *Tissue Eng*, 2006. **12**(9): p. 2695-706.
- Im, G. I.et al., Do Adipose Tissue-Derived Mesenchymal Stem Cells Have the Same Osteogenic and Chondrogenic Potential as Bone Marrow-Derived Cells? *Osteoarthritis Cartilage*, 2005. **13**(10): p. 845-53.
- Inoue, H.et al., Stimulation of Cartilage-Matrix Proteoglycan Synthesis by Morphologically Transformed Chondrocytes Grown in the Presence of Fibroblast Growth Factor and Transforming Growth Factor-Beta. *J Cell Physiol*, 1989. **138**(2): p. 329-37.
- Jackson, C. E.et al., A Preliminary Evaluation of a Prospective Study of Pulmonary Function Studies and Symptoms of Hypoventilation in Als/Mnd Patients. *J Neurol Sci*, 2001. **191**(1-2): p. 75-8.
- Jackson, R. W.et al., The Results of Arthroscopic Lavage and Debridement of Osteoarthritic Knees Based on the Severity of Degeneration: A 4- to 6-Year Symptomatic Follow-Up. *Arthroscopy*, 2003. **19**(1): p. 13-20.
- Jakobsen, R. B.et al., Chondrogenesis in a Hyaluronic Acid Scaffold: Comparison between Chondrocytes and Msc from Bone Marrow and Adipose Tissue. *Knee Surg Sports Traumatol Arthrosc*, 2009.
- Janjanin, S.et al., Mold-Shaped, Nanofiber Scaffold-Based Cartilage Engineering Using Human Mesenchymal Stem Cells and Bioreactor. *J Surg Res*, 2008. **149**(1): p. 47-56.

- Jeschke, B. et al., Rgd-Peptides for Tissue Engineering of Articular Cartilage. *Biomaterials*, 2002. **23**(16): p. 3455-63.
- Jeschke, B. et al., Rgd-Peptides for Tissue Engineering of Articular Cartilage. *Biomaterials*, 2002. **23**(16): p. 3455-63.
- Jiang, C. C. et al., Repair of Porcine Articular Cartilage Defect with a Biphasic Osteochondral Composite. *J Orthop Res*, 2007. **25**(10): p. 1277-90.
- Johnstone, B. et al., In Vitro Chondrogenesis of Bone Marrow-Derived Mesenchymal Progenitor Cells. *Exp Cell Res*, 1998. **238**(1): p. 265-72.
- Jones, K. L. et al., Pituitary Fibroblast Growth Factor as a Stimulator of Growth in Cultured Rabbit Articular Chondrocytes. *Endocrinology*, 1975. **97**(2): p. 359-65.
- Kavalkovich, K. W. et al., Chondrogenic Differentiation of Human Mesenchymal Stem Cells within an Alginate Layer Culture System. *In Vitro Cell Dev Biol Anim*, 2002. **38**(8): p. 457-66.
- Kavalkovich, K. W. et al., Chondrogenic Differentiation of Human Mesenchymal Stem Cells within an Alginate Layer Culture System. *In Vitro Cell Dev Biol Anim*, 2002. **38**(8): p. 457-66.
- Kawamura, S. et al., Articular Cartilage Repair. Rabbit Experiments with a Collagen Gel-Biomatrix and Chondrocytes Cultured in It. *Acta Orthop Scand*, 1998. **69**(1): p. 56-62.
- Kerin, A. J. et al., The Compressive Strength of Articular Cartilage. *Proc Inst Mech Eng [H]*, 1998. **212**(4): p. 273-80.
- Kim, B. S. et al., Development of Biocompatible Synthetic Extracellular Matrices for Tissue Engineering. *Trends Biotechnol*, 1998. **16**(5): p. 224-30.
- Kim, H. J. et al., Chondrogenic Differentiation of Adipose Tissue-Derived Mesenchymal Stem Cells: Greater Doses of Growth Factor Are Necessary. *J Orthop Res*, 2009. **27**(5): p. 612-9.
- Kim, S. et al., Synthetic Mmp-13 Degradable Ecms Based on Poly(N-Isopropylacrylamide-Co-Acrylic Acid) Semi-Interpenetrating Polymer Networks. I. Degradation and Cell Migration. *J Biomed Mater Res A*, 2005. **75**(1): p. 73-88.

- Kim, S.et al., Synthesis and Characterization of Injectable Poly(N-Isopropylacrylamide-Co-Acrylic Acid) Hydrogels with Proteolytically Degradable Cross-Links. *Biomacromolecules*, 2003. **4**(5): p. 1214-23.
- Kim, T. K.et al., Experimental Model for Cartilage Tissue Engineering to Regenerate the Zonal Organization of Articular Cartilage. *Osteoarthritis Cartilage*, 2003. **11**(9): p. 653-64.
- Klein, T. J.et al., Tissue Engineering of Articular Cartilage with Biomimetic Zones. *Tissue Eng Part B Rev*, 2009.
- Klein, T. J.et al., Strategies for Zonal Cartilage Repair Using Hydrogels. *Macromol Biosci*, 2009. **9**(11): p. 1049-58.
- Koch, T. G.et al., Stem Cell Therapy for Joint Problems Using the Horse as a Clinically Relevant Animal Model. *Expert Opin Biol Ther*, 2007. **7**(11): p. 1621-6.
- Kramer, J.et al., Embryonic Stem Cell-Derived Chondrogenic Differentiation in Vitro: Activation by Bmp-2 and Bmp-4. *Mech Dev*, 2000. **92**(2): p. 193-205.
- Kramer, J.et al., Mouse Es Cell Lines Show a Variable Degree of Chondrogenic Differentiation in Vitro. *Cell Biol Int*, 2005. **29**(2): p. 139-46.
- Kulyk, W. M.et al., Promotion of Embryonic Chick Limb Cartilage Differentiation by Transforming Growth Factor-Beta. *Dev Biol*, 1989. **135**(2): p. 424-30.
- Lahm, A.et al., Loss of Zonal Organization of Articular Cartilage after Experimental Subchondral Trauma of the Knee Joint. *Saudi Med J*, 2007. **28**(4): p. 649-52.
- Langer, F.et al., The Immunogenicity of Allograft Knee Joint Transplants. *Clin Orthop Relat Res*, 1978. (132): p. 155-62.
- Langer, R. Biomaterials in Drug Delivery and Tissue Engineering: One Laboratory's Experience. *Acc Chem Res*, 2000. **33**(2): p. 94-101.
- Lash, J. W.et al., In Vitro Studies on Chondrogenesis; the Uptake of Radioactive Sulfate During Cartilage Induction. *Dev Biol*, 1960. **2**: p. 76-89.
- Law, H. Y.et al., Rapid Antenatal Diagnosis of Beta-Thalassemia in Chinese Caused by the Common 4-Bp Deletion in Codons 41/42 Using High-Resolution Agarose Gel Electrophoresis and Heteroduplex Detection. *Biochem Med Metab Biol*, 1994. **53**(2): p. 149-51.

- Leach, B. J., Bivens, K. A. Patrick, C. W., Jr., Schmidt, C. E. Photocrosslinked Hyaluronic Acid Hydrogels: Natural, Biodegradable Tissue Engineering Scaffolds. *Biotechnol Bioeng*, 2003. **82**(5): p. 578-89.
- Leach, J. B.et al., Characterization of Protein Release from Photocrosslinkable Hyaluronic Acid-Polyethylene Glycol Hydrogel Tissue Engineering Scaffolds. *Biomaterials*, 2005. **26**(2): p. 125-35.
- Lee, H.et al., Photo-Crosslinkable, Biomimetic, and Thermo-Sensitive Pluronic Grafted Hyaluronic Acid Copolymers for Injectable Delivery of Chondrocytes. *J Biomed Mater Res A*, 2008.
- Lee, H. J.et al., Collagen Mimetic Peptide-Conjugated Photopolymerizable Peg Hydrogel. *Biomaterials*, 2006. **27**(30): p. 5268-76.
- Leonard, C. M.et al., Role of Transforming Growth Factor-Beta in Chondrogenic Pattern Formation in the Embryonic Limb: Stimulation of Mesenchymal Condensation and Fibronectin Gene Expression by Exogenous Tgf-Beta and Evidence for Endogenous Tgf-Beta-Like Activity. *Dev Biol*, 1991. **145**(1): p. 99-109.
- Levenberg, S.et al., Neurotrophin-Induced Differentiation of Human Embryonic Stem Cells on Three-Dimensional Polymeric Scaffolds. *Tissue Eng*, 2005. **11**(3-4): p. 506-12.
- Levenberg, S.et al., Differentiation of Human Embryonic Stem Cells on Three-Dimensional Polymer Scaffolds. *Proc Natl Acad Sci U S A*, 2003. **100**(22): p. 12741-6.
- Li, Q.et al., Photocrosslinkable Polysaccharides Based on Chondroitin Sulfate. *J Biomed Mater Res A*, 2004. **68**(1): p. 28-33.
- Li, W. J.et al., Cell-Nanofiber-Based Cartilage Tissue Engineering Using Improved Cell Seeding, Growth Factor, and Bioreactor Technologies. *Tissue Eng Part A*, 2008. **14**(5): p. 639-48.
- Li, W. J.et al., Multilineage Differentiation of Human Mesenchymal Stem Cells in a Three-Dimensional Nanofibrous Scaffold. *Biomaterials*, 2005. **26**(25): p. 5158-66.
- Libbin, R. M.et al., Regeneration of Growth Plate Cartilage Induced in the Neonatal Rat Hindlimb by Reamputation. *J Orthop Res*, 1989. **7**(5): p. 674-82.

- Lindenhayn, K. et al., Retention of Hyaluronic Acid in Alginate Beads: Aspects for in Vitro Cartilage Engineering. *J Biomed Mater Res*, 1999. **44**(2): p. 149-55.
- Liu, H. et al., Biomimetic Three-Dimensional Cultures Significantly Increase Hematopoietic Differentiation Efficacy of Embryonic Stem Cells. *Tissue Eng*, 2005. **11**(1-2): p. 319-30.
- Livak, K. J. et al., 'Analysis of Relative Gene Expression Data Using Real Time Quantitative Pcr and the 2⁻ΔΔct Method.' 2001.
- Lu, L. et al., Controlled Release of Transforming Growth Factor Beta1 from Biodegradable Polymer Microparticles. *J Biomed Mater Res*, 2000. **50**(3): p. 440-51.
- Lu, L. et al., Articular Cartilage Tissue Engineering. *e-biomed: The Journal of Regenerative Medicine*, 2000. **1**(7): p. 99-114.
- Lu, Y. et al., A Digital Micro-Mirror Device-Based System for the Microfabrication of Complex, Spatially Patterned Tissue Engineering Scaffolds. *J Biomed Mater Res A*, 2006. **77**(2): p. 396-405.
- Lutolf, M. P. et al., Synthetic Matrix Metalloproteinase-Sensitive Hydrogels for the Conduction of Tissue Regeneration: Engineering Cell-Invasion Characteristics. *Proc Natl Acad Sci U S A*, 2003. **100**(9): p. 5413-8.
- Lutolf, M. P. et al., Repair of Bone Defects Using Synthetic Mimetics of Collagenous Extracellular Matrices. *Nat Biotechnol*, 2003. **21**(5): p. 513-8.
- Mackay, A. M. et al., Chondrogenic Differentiation of Cultured Human Mesenchymal Stem Cells from Marrow. *Tissue Eng*, 1998. **4**(4): p. 415-28.
- Mahmoudifar, N. et al., Chondrogenic Differentiation of Human Adipose-Derived Stem Cells in Polyglycolic Acid Mesh Scaffolds under Dynamic Culture Conditions. *Biomaterials*, 2010. **31**(14): p. 3858-67.
- Majithia, V. et al., Rheumatoid Arthritis: Diagnosis and Management. *Am J Med*, 2007. **120**(11): p. 936-9.
- Mankin, H. J. et al., A Curriculum for the Ideal Orthopaedic Residency. *Academic Orthopaedic Society. Clin Orthop Relat Res*, 1997. (339): p. 270-81.

- Mann, B. K. et al., Smooth Muscle Cell Growth in Photopolymerized Hydrogels with Cell Adhesive and Proteolytically Degradable Domains: Synthetic Ecm Analogs for Tissue Engineering. *Biomaterials*, 2001. **22**(22): p. 3045-51.
- Mao, J. J. et al., Craniofacial Tissue Engineering by Stem Cells. *J Dent Res*, 2006. **85**(11): p. 966-79.
- Mapili Call, G. 'Microfabrication of Spatially-Patterned, Polymer Scaffolds for Applications in Stem Cell and Tissue Engineering', Dissertation. University of Texas at Austin, 2007.
- Mapili, G. 'Spatio-Temporally Patterned Polymer Scaffolds for the Stem Cell Differentiation of Hybrid Tissues', Preliminary Proposal. University of Texas at Austin, 2004.
- Mapili, G. et al., Laser-Layered Microfabrication of Spatially Patterned Functionalized Tissue-Engineering Scaffolds. *J Biomed Mater Res B Appl Biomater*, 2005. **75**(2): p. 414-24.
- Marcus, N. A. 'Virginia Cartilage Institute' Available from www.normanmarcusmd.com 2010. Accessed July 3, 2010 2010.
- Marlovits, S. et al., Early Postoperative Adherence of Matrix-Induced Autologous Chondrocyte Implantation for the Treatment of Full-Thickness Cartilage Defects of the Femoral Condyle. *Knee Surg Sports Traumatol Arthrosc*, 2005. **13**(6): p. 451-7.
- Marolt, D. et al., Bone and Cartilage Tissue Constructs Grown Using Human Bone Marrow Stromal Cells, Silk Scaffolds and Rotating Bioreactors. *Biomaterials*, 2006. **27**(36): p. 6138-49.
- Maroudas, A. Physical Chemistry and the Structure of Cartilage. *J Physiol*, 1972. **223**(1): p. 21P-22P.
- Marsano, A. et al., Bi-Zonal Cartilaginous Tissues Engineered in a Rotary Cell Culture System. *Biorheology*, 2006. **43**(3-4): p. 553-60.
- Martens, P. J. et al., Tailoring the Degradation of Hydrogels Formed from Multivinyl Poly(Ethylene Glycol) and Poly(Vinyl Alcohol) Macromers for Cartilage Tissue Engineering. *Biomacromolecules*, 2003. **4**(2): p. 283-92.
- Masters, K. S. et al., Crosslinked Hyaluronan Scaffolds as a Biologically Active Carrier for Valvular Interstitial Cells. *Biomaterials*, 2005. **26**(15): p. 2517-25.

- Mathison, D. J. et al., Approach to Knee Effusions. *Pediatr Emerg Care*, 2009. **25**(11): p. 773-86; quiz 787-8.
- Mauck, R. L. et al., Regulation of Cartilaginous Ecm Gene Transcription by Chondrocytes and Mscs in 3d Culture in Response to Dynamic Loading. *Biomech Model Mechanobiol*, 2007. **6**(1-2): p. 113-25.
- Mehlhorn, A. T. et al., Differential Expression Pattern of Extracellular Matrix Molecules During Chondrogenesis of Mesenchymal Stem Cells from Bone Marrow and Adipose Tissue. *Tissue Eng*, 2006. **12**(10): p. 2853-62.
- Meinel, L. et al., Engineering Cartilage-Like Tissue Using Human Mesenchymal Stem Cells and Silk Protein Scaffolds. *Biotechnol Bioeng*, 2004. **88**(3): p. 379-91.
- Mello, M. A. et al., High Density Micromass Cultures of Embryonic Limb Bud Mesenchymal Cells: An in Vitro Model of Endochondral Skeletal Development. *In Vitro Cell Dev Biol Anim*, 1999. **35**(5): p. 262-9.
- Mengshol, J. A. et al., Interleukin-1 Induction of Collagenase 3 (Matrix Metalloproteinase 13) Gene Expression in Chondrocytes Requires P38, C-Jun N-Terminal Kinase, and Nuclear Factor Kappab: Differential Regulation of Collagenase 1 and Collagenase 3. *Arthritis Rheum*, 2000. **43**(4): p. 801-11.
- Meyer, U. et al., .Bone and Cartilage Engineering. Berlin Heidelberg: Springer Verlag, 2006.
- Moioli, E. K. et al., Sustained Release of Tgfbeta3 from Plga Microspheres and Its Effect on Early Osteogenic Differentiation of Human Mesenchymal Stem Cells. *Tissue Eng*, 2006. **12**(3): p. 537-46.
- Moses, H. L. et al., Transforming Growth Factor Production by Chemically Transformed Cells. *Cancer Res*, 1981. **41**(7): p. 2842-8.
- Mow, V. C. et al., Fluid Transport and Mechanical Properties of Articular Cartilage: A Review. *J Biomech*, 1984. **17**(5): p. 377-94.
- Muggli, D. S. et al., Crosslinked Polyanhydrides for Use in Orthopedic Applications: Degradation Behavior and Mechanics. *J Biomed Mater Res*, 1999. **46**(2): p. 271-8.

- Murdoch, A. D. et al., Chondrogenic Differentiation of Human Bone Marrow Stem Cells in Transwell Cultures: Generation of Scaffold-Free Cartilage. *Stem Cells*, 2007. **25**(11): p. 2786-96.
- Murray, R. C. et al., Subchondral Bone Thickness, Hardness and Remodelling Are Influenced by Short-Term Exercise in a Site-Specific Manner. *J Orthop Res*, 2001. **19**(6): p. 1035-42.
- Nasseri, B. A. et al., Tissue Engineering: An Evolving 21st-Century Science to Provide Biologic Replacement for Reconstruction and Transplantation. *Surgery*, 2001. **130**(5): p. 781-4.
- Nettles, D. L., Elder, Steven H. and Gibert, Jerome A. Potential Use of Chitosan as a Cell Scaffold Material for Cartilage Tissue Engineering. *TISSUE ENGINEERING*, 2002. **8**(6): p. 1009-1016.
- Nettles, D. L. et al., Photocrosslinkable Hyaluronan as a Scaffold for Articular Cartilage Repair. *Ann Biomed Eng*, 2004. **32**(3): p. 391-7.
- Newman, E. et al., The Potential of Sheep for the Study of Osteopenia: Current Status and Comparison with Other Animal Models. *Bone*, 1995. **16**(4 Suppl): p. 277S-284S.
- Ng, K. W. et al., Zonal Chondrocytes Seeded in a Layered Agarose Hydrogel Create Engineered Cartilage with Depth-Dependent Cellular and Mechanical Inhomogeneity. *Tissue Eng Part A*, 2009. **15**(9): p. 2315-24.
- Niederauer, G. G. et al., Evaluation of Multiphase Implants for Repair of Focal Osteochondral Defects in Goats. *Biomaterials*, 2000. **21**(24): p. 2561-74.
- Nixon, A. J. et al., Arthroscopic Reattachment of Osteochondritis Dissecans Lesions Using Resorbable Polydioxanone Pins. *Equine Vet J*, 2004. **36**(5): p. 376-83.
- Noth, U. et al., In Vitro Engineered Cartilage Constructs Produced by Press-Coating Biodegradable Polymer with Human Mesenchymal Stem Cells. *Tissue Eng*, 2002. **8**(1): p. 131-44.
- Novick, N. 'Cartilage Regeneration - an Overview'. 6/4/2003, 2007. Accessed June 27, 2007.
- Nuttelman, C. R. et al., In Vitro Osteogenic Differentiation of Human Mesenchymal Stem Cells Photoencapsulated in Peg Hydrogels. *J Biomed Mater Res A*, 2004. **68**(4): p. 773-82.

- O'Driscoll, S. W. Preclinical Cartilage Repair: Current Status and Future Perspectives. *Clin Orthop Relat Res*, 2001. (391 Suppl): p. S397-401.
- 'Osteoarthritis: National Clinical Guideline for Care and Management in Adults'. ed. Conditions, The National Collaborating Centre for Chronic London: Royal College of Physicians, 2008.
- Oyajobi, B. O. et al., Expression of Type X Collagen and Matrix Calcification in Three-Dimensional Cultures of Immortalized Temperature-Sensitive Chondrocytes Derived from Adult Human Articular Cartilage. *J Bone Miner Res*, 1998. **13**(3): p. 432-42.
- Pacifici, M. et al., Cell Hypertrophy and Type X Collagen Synthesis in Cultured Articular Chondrocytes. *Exp Cell Res*, 1991. **192**(1): p. 266-70.
- Pacifici, M. et al., Retinoic Acid Treatment Induces Type X Collagen Gene Expression in Cultured Chick Chondrocytes. *Exp Cell Res*, 1991. **195**(1): p. 38-46.
- Pacifici, M. et al., Development of Articular Cartilage: What Do We Know About It and How May It Occur? *Connect Tissue Res*, 2000. **41**(3): p. 175-84.
- Pan, Y. et al., Hand-Held Arthroscopic Optical Coherence Tomography for in Vivo High-Resolution Imaging of Articular Cartilage. *J Biomed Opt*, 2003. **8**(4): p. 648-54.
- Park, H. et al., Delivery of Tgf-Beta1 and Chondrocytes Via Injectable, Biodegradable Hydrogels for Cartilage Tissue Engineering Applications. *Biomaterials*, 2005. **26**(34): p. 7095-103.
- Park, J. W. et al., Effects of a Cell Adhesion Molecule Coating on the Blasted Surface of Titanium Implants on Bone Healing in the Rabbit Femur. *Int J Oral Maxillofac Implants*, 2007. **22**(4): p. 533-41.
- Park, Y. et al., Bovine Primary Chondrocyte Culture in Synthetic Matrix Metalloproteinase-Sensitive Poly(Ethylene Glycol)-Based Hydrogels as a Scaffold for Cartilage Repair. *Tissue Eng*, 2004. **10**(3-4): p. 515-22.
- Patel, R. V. et al., Microstructural and Elastic Properties of the Extracellular Matrices of the Superficial Zone of Neonatal Articular Cartilage by Atomic Force Microscopy. *Front Biosci*, 2003. **8**: p. a18-25.

- Pei, M.et al., Engineering of Functional Cartilage Tissue Using Stem Cells from Synovial Lining: A Preliminary Study. *Clin Orthop Relat Res*, 2008. **466**(8): p. 1880-9.
- Pei, M.et al., Synovium-Derived Stem Cell-Based Chondrogenesis. *Differentiation*, 2008. **76**(10): p. 1044-56.
- Pei, M.et al., Bioreactors Mediate the Effectiveness of Tissue Engineering Scaffolds. *FASEB J*, 2002. **16**(12): p. 1691-4.
- Pek, Y. S.et al., Degradation of a Collagen-Chondroitin-6-Sulfate Matrix by Collagenase and by Chondroitinase. *Biomaterials*, 2004. **25**(3): p. 473-82.
- Pelton, R. W.et al., In Situ Hybridization Analysis of Tgf Beta 3 Rna Expression During Mouse Development: Comparative Studies with Tgf Beta 1 and Beta 2. *Development*, 1990. **110**(2): p. 609-20.
- Peppas, N. A.et al., Hydrogels in Pharmaceutical Formulations. *Eur J Pharm Biopharm*, 2000. **50**(1): p. 27-46.
- Peppas, N. A.et al., Physicochemical Foundations and Structural Design of Hydrogels in Medicine and Biology. *Annu Rev Biomed Eng*, 2000. **2**: p. 9-29.
- Petersen, J. P.et al., Present and Future Therapies of Articular Cartilage Defects. *European Journal of Trauma*, 2003. p. 10.
- Phil Campbell, S. R. S. C. G. F. 'Bone Tissue Engineering Initiative ' Available from <http://www.cs.cmu.edu/~tissue/2007>. Accessed June 27, 2007 2007.
- Poole, A. R.et al., Composition and Structure of Articular Cartilage: A Template for Tissue Repair. *Clin Orthop Relat Res*, 2001. (391 Suppl): p. S26-33.
- Poolsup, N.et al., Glucosamine Long-Term Treatment and the Progression of Knee Osteoarthritis: Systematic Review of Randomized Controlled Trials. *Ann Pharmacother*, 2005. **39**(6): p. 1080-7.
- Potter, H. G.et al., Magnetic Resonance Imaging of Articular Cartilage: Trauma, Degeneration, and Repair. *Am J Sports Med*, 2006. **34**(4): p. 661-77.
- Prestwich, G. D.et al., Controlled Chemical Modification of Hyaluronic Acid: Synthesis, Applications, and Biodegradation of Hydrazide Derivatives. *J Control Release*, 1998. **53**(1-3): p. 93-103.

- Puetzer, J. L. et al., Comparative Review of Growth Factors for Induction of Three-Dimensional in Vitro Chondrogenesis in Human Mesenchymal Stem Cells Isolated from Bone Marrow and Adipose Tissue. *Tissue Eng Part B Rev*, 2010.
- Radisic, M. et al., High-Density Seeding of Myocyte Cells for Cardiac Tissue Engineering. *Biotechnol Bioeng*, 2003. **82**(4): p. 403-14.
- Rahman, M. S. et al., Enhancement of Chondrogenic Differentiation of Human Articular Chondrocytes by Biodegradable Polymers. *Tissue Eng*, 2001. **7**(6): p. 781-90.
- Rapp, A. et al., Evaluation of Chondroitin Sulfate Bioactivity in Hippocampal Neurons and the Astrocyte Cell Line U373: Influence of Position of Sulfate Groups and Charge Density. *Basic Clin Pharmacol Toxicol*, 2005. **96**(1): p. 37-43.
- Rasanen, T. et al., Regional Variations of Indentation Stiffness and Thickness of Normal Rabbit Knee Articular Cartilage. *J Biomed Mater Res*, 1996. **31**(4): p. 519-24.
- Reboul, P. et al., The New Collagenase, Collagenase-3, Is Expressed and Synthesized by Human Chondrocytes but Not by Synoviocytes. A Role in Osteoarthritis. *J Clin Invest*, 1996. **97**(9): p. 2011-9.
- Recklies, A. D. et al., Regulation of Cartilage Oligomeric Matrix Protein Synthesis in Human Synovial Cells and Articular Chondrocytes. *Arthritis Rheum*, 1998. **41**(6): p. 997-1006.
- Redman, S. N. et al., The Cellular Responses of Articular Cartilage to Sharp and Blunt Trauma. *Osteoarthritis Cartilage*, 2004. **12**(2): p. 106-16.
- Redman, S. N. et al., Current Strategies for Articular Cartilage Repair. *Eur Cell Mater*, 2005. **9**: p. 23-32; discussion 23-32.
- Roberts, A. B. et al., New Class of Transforming Growth Factors Potentiated by Epidermal Growth Factor: Isolation from Non-Neoplastic Tissues. *Proc Natl Acad Sci U S A*, 1981. **78**(9): p. 5339-43.
- Robinson, D. et al., Characteristics of Cartilage Biopsies Used for Autologous Chondrocytes Transplantation. *Cell Transplant*, 2001. **10**(2): p. 203-8.
- Robinson, D. et al., Regenerating Hyaline Cartilage in Articular Defects of Old Chickens Using Implants of Embryonal Chick Chondrocytes Embedded in a New Natural Delivery Substance. *Calcif Tissue Int*, 1990. **46**(4): p. 246-53.
- Rosner, B. *Fundamentals of Biostatistics*. Belmont: Thomson Higher Education, 2006.

- Rucklidge, G. J. et al., Collagen Type X: A Component of the Surface of Normal Human, Pig, and Rat Articular Cartilage. *Biochem Biophys Res Commun*, 1996. **224**(2): p. 297-302.
- Salinas, C. N. et al., The Enhancement of Chondrogenic Differentiation of Human Mesenchymal Stem Cells by Enzymatically Regulated Rgd Functionalities. *Biomaterials*, 2008. **29**(15): p. 2370-7.
- Salinas, C. N. et al., Chondrogenic Differentiation Potential of Human Mesenchymal Stem Cells Photoencapsulated within Poly(Ethylene Glycol)-Arginine-Glycine-Aspartic Acid-Serine Thiol-Methacrylate Mixed-Mode Networks. *Tissue Eng*, 2007. **13**(5): p. 1025-34.
- Sawhney, A. S. et al., Interfacial Photopolymerization of Poly(Ethylene Glycol)-Based Hydrogels Upon Alginate-Poly(L-Lysine) Microcapsules for Enhanced Biocompatibility. *Biomaterials*, 1993. **14**(13): p. 1008-16.
- Sawhney, A. S. et al., Optimization of Photopolymerized Bioerodible Hydrogel Properties for Adhesion Prevention. *J Biomed Mater Res*, 1994. **28**(7): p. 831-8.
- Schinagl, R. M. et al., Depth-Dependent Confined Compression Modulus of Full-Thickness Bovine Articular Cartilage. *J Orthop Res*, 1997. **15**(4): p. 499-506.
- Schuurman, W. et al., Zonal Chondrocyte Subpopulations Reacquire Zone-Specific Characteristics During in Vitro Redifferentiation. *Am J Sports Med*, 2009. **37 Suppl 1**: p. 97S-104S.
- Schwartz, E. R. et al., Effect of Ascorbic Acid on Arylsulfatase a and B Activities in Human Chondrocyte Cultures. *Connect Tissue Res*, 1976. **4**(4): p. 211-8.
- Sebra, R. P. et al., Controlled Polymerization Chemistry to Graft Architectures That Influence Cell-Material Interactions. *Acta Biomater*, 2007. **3**(2): p. 151-61.
- Segura, T. et al., Crosslinked Hyaluronic Acid Hydrogels: A Strategy to Functionalize and Pattern. *Biomaterials*, 2005. **26**(4): p. 359-71.
- Seliktar, D. et al., Mmp-2 Sensitive, Vegf-Bearing Bioactive Hydrogels for Promotion of Vascular Healing. *J Biomed Mater Res A*, 2004. **68**(4): p. 704-16.
- Shapiro, F. et al., Cell Origin and Differentiation in the Repair of Full-Thickness Defects of Articular Cartilage. *J Bone Joint Surg Am*, 1993. **75**(4): p. 532-53.

- Sharma, B.et al., Designing Zonal Organization into Tissue-Engineered Cartilage. *Tissue Eng*, 2007. **13**(2): p. 405-14.
- Shepherd, D. E.et al., Thickness of Human Articular Cartilage in Joints of the Lower Limb. *Ann Rheum Dis*, 1999. **58**(1): p. 27-34.
- Shortkroff, S.et al., Healing of Chondral and Osteochondral Defects in a Canine Model: The Role of Cultured Chondrocytes in Regeneration of Articular Cartilage. *Biomaterials*, 1996. **17**(2): p. 147-54.
- Silverman, R. P.et al., Injectable Tissue-Engineered Cartilage Using a Fibrin Glue Polymer. *Plast Reconstr Surg*, 1999. **103**(7): p. 1809-18.
- Smedslund, G.et al., Effectiveness and Safety of Dietary Interventions for Rheumatoid Arthritis: A Systematic Review of Randomized Controlled Trials. *J Am Diet Assoc*, 2010. **110**(5): p. 727-35.
- Solchaga, L. A.et al., Cartilage Regeneration Using Principles of Tissue Engineering. *Clin Orthop Relat Res*, 2001. (391 Suppl): p. S161-70.
- Soloman, D. J.et al., . 'Marrow Stimulation and Microfracture for the Repair of Articular Cartilage Lesions'. New Jersey: Humana Press Inc., 2007.
- Song, L.et al., Mesenchymal Stem Cell-Based Cartilage Tissue Engineering: Cells, Scaffold and Biology. *Cytherapy*, 2004. **6**(6): p. 596-601.
- Stewart, M. C.et al., Phenotypic Stability of Articular Chondrocytes in Vitro: The Effects of Culture Models, Bone Morphogenetic Protein 2, and Serum Supplementation. *J Bone Miner Res*, 2000. **15**(1): p. 166-74.
- Strauss, E. J.et al., Biochemical and Biomechanical Properties of Lesion and Adjacent Articular Cartilage after Chondral Defect Repair in an Equine Model. *Am J Sports Med*, 2005. **33**(11): p. 1647-53.
- Suh, J. K.et al., Application of Chitosan-Based Polysaccharide Biomaterials in Cartilage Tissue Engineering: A Review. *Biomaterials*, 2000. **21**(24): p. 2589-98.
- Swindle, M. M.et al., Swine as Models in Experimental Surgery. *J Invest Surg*, 1988. **1**(1): p. 65-79.
- Tallheden, T.et al., Gene Expression During Redifferentiation of Human Articular Chondrocytes. *Osteoarthritis Cartilage*, 2004. **12**(7): p. 525-35.

- Tare, R. S. et al., Tissue Engineering Strategies for Cartilage Generation--Micromass and Three Dimensional Cultures Using Human Chondrocytes and a Continuous Cell Line. *Biochem Biophys Res Commun*, 2005. **333**(2): p. 609-21.
- Temenoff, J. S. et al., Review: Tissue Engineering for Regeneration of Articular Cartilage. *Biomaterials*, 2000. **21**(5): p. 431-40.
- Thirion, S. et al., Culture and Phenotyping of Chondrocytes in Primary Culture. *Methods Mol Med*, 2004. **100**: p. 1-14.
- Thomas, B. et al., Differentiation Regulates Interleukin-1beta-Induced Cyclo-Oxygenase-2 in Human Articular Chondrocytes: Role of P38 Mitogen-Activated Protein Kinase. *Biochem J*, 2002. **362**(Pt 2): p. 367-73.
- Tomford, W. W. et al., Fresh and Frozen Articular Cartilage Allografts. *Orthopedics*, 1992. **15**(10): p. 1183-8.
- Toumadje, A. et al., Pluripotent Differentiation in Vitro of Murine Es-D3 Embryonic Stem Cells. *In Vitro Cell Dev Biol Anim*, 2003. **39**(10): p. 449-53.
- Trattnig, S. et al., Matrix-Based Autologous Chondrocyte Implantation for Cartilage Repair: Noninvasive Monitoring by High-Resolution Magnetic Resonance Imaging. *Magn Reson Imaging*, 2005. **23**(7): p. 779-87.
- Tuli, R. et al., Current State of Cartilage Tissue Engineering. *Arthritis Res Ther*, 2003. **5**(5): p. 235-8.
- van Susante, J. L. C. et al., Linkage of Chondroitin-Sulfate to Type I Collagen Scaffolds Stimulates the Bioactivity of Seeded Chondrocytes in Vitro. *Biomaterials*, 2001. **22**(17): p. 2359-69.
- Varghese, S. et al., Chondroitin Sulfate Based Niches for Chondrogenic Differentiation of Mesenchymal Stem Cells. *Matrix Biol*, 2008. **27**(1): p. 12-21.
- Varghese, S. et al., Chondrogenic Differentiation of Human Embryonic Germ Cell Derived Cells in Hydrogels. *Conf Proc IEEE Eng Med Biol Soc*, 2006. **1**: p. 2643-6.
- Vasara, A. I. et al., Immature Porcine Knee Cartilage Lesions Show Good Healing with or without Autologous Chondrocyte Transplantation. *Osteoarthritis Cartilage*, 2006. **14**(10): p. 1066-74.

- Vozzi, G.et al., Fabrication of Plga Scaffolds Using Soft Lithography and Microsyringe Deposition. *Biomaterials*, 2003. **24**(14): p. 2533-40.
- Vunjak-Novakovic, G.et al., Dynamic Cell Seeding of Polymer Scaffolds for Cartilage Tissue Engineering. *Biotechnol Prog*, 1998. **14**(2): p. 193-202.
- Vunjak-Novakovic, G.et al., Bioreactor Studies of Native and Tissue Engineered Cartilage. *Biorheology*, 2002. **39**(1-2): p. 259-68.
- Wakitani, S.et al., Mesenchymal Cell-Based Repair of Large, Full-Thickness Defects of Articular Cartilage. *J Bone Joint Surg Am*, 1994. **76**(4): p. 579-92.
- Wei, X.et al., Maturation-Dependent Repair of Untreated Osteochondral Defects in the Rabbit Knee Joint. *J Biomed Mater Res*, 1997. **34**(1): p. 63-72.
- West, J. L.et al., Polymeric Biomaterials with Degradation Sites for Proteases Involved in Cell Migration. *Macromolecules*, 1999. **32**(1): p. 241-244.
- Williams, C. G.et al., In Vitro Chondrogenesis of Bone Marrow-Derived Mesenchymal Stem Cells in a Photopolymerizing Hydrogel. *Tissue Eng*, 2003. **9**(4): p. 679-88.
- Williams, R. J.et al., . 'Articular Cartilage Resurfacing Using Sythetic Resorbable Scaffolds'. New Jersey: Humana Press Inc., 2007.
- Williams, R. J.et al., .Cartilage Repair Strategies. New Jersey: Humana Press Inc., 2007.
- Winter, A.et al., Cartilage-Like Gene Expression in Differentiated Human Stem Cell Spheroids: A Comparison of Bone Marrow-Derived and Adipose Tissue-Derived Stromal Cells. *Arthritis Rheum*, 2003. **48**(2): p. 418-29.
- Wood, D.et al., . 'Matrix-Induced Autologous Chondrocyte Implantation'. New Jersey: Humana Press Inc., 2007.
- Woodfield, T. B.et al., Polymer Scaffolds Fabricated with Pore-Size Gradients as a Model for Studying the Zonal Organization within Tissue-Engineered Cartilage Constructs. *Tissue Eng*, 2005. **11**(9-10): p. 1297-311.
- Xue, C.et al., Characterisation of Fibroblast-Like Cells in Pannus Lesions of Patients with Rheumatoid Arthritis Sharing Properties of Fibroblasts and Chondrocytes. *Ann Rheum Dis*, 1997. **56**(4): p. 262-7.
- Yoo, H. S.et al., Hyaluronic Acid Modified Biodegradable Scaffolds for Cartilage Tissue Engineering. *Biomaterials*, 2005. **26**(14): p. 1925-33.

- Yoo, J. U. et al., The Chondrogenic Potential of Human Bone-Marrow-Derived Mesenchymal Progenitor Cells. *J Bone Joint Surg Am*, 1998. **80**(12): p. 1745-57.
- Zein, I. et al., Fused Deposition Modeling of Novel Scaffold Architectures for Tissue Engineering Applications. *Biomaterials*, 2002. **23**(4): p. 1169-85.
- Zelle, S. et al., Arthroscopic Techniques for the Fixation of a Three-Dimensional Scaffold for Autologous Chondrocyte Transplantation: Structural Properties in an in Vitro Model. *Arthroscopy*, 2007. **23**(10): p. 1073-8.
- Zhang, L. et al., Chondrogenic Differentiation of Human Mesenchymal Stem Cells: A Comparison between Micromass and Pellet Culture Systems. *Biotechnol Lett*, 2010.
- Zuk, P. A. et al., Multilineage Cells from Human Adipose Tissue: Implications for Cell-Based Therapies. *Tissue Eng*, 2001. **7**(2): p. 211-28.

Vita

Lonnissa Hong Nguyen was born in Baria, Vietnam on September 19, 1980, daughter of Cuong Van Nguyen and Lan Ngoc Nguyen. She has two sisters, one brother, and a pug named Lilo. After graduating in 1999 from California High School in San Ramon, she pursued her undergraduate studies at the University of California in Los Angeles where she received her dual Bachelor of Science Degree in Cybernetics and Applied Mathematics. After obtaining her bachelor's degree, Lonnissa worked in the Physics department at UCLA as a Project Coordinator. She then became Product Development Manager at Applied DNA Sciences, Inc. in Los Angeles.

In August 2005, Lonnissa moved to Austin and began her doctoral studies in the Department of Biomedical Engineering at the University of Texas. She received her Master of Science degree in December 2007 and continued her efforts in studying the influence of biomaterial composition in the chondrogenic differentiation of MSCs. Lonnissa presented her work at several leading biomedical conferences and will publish two first author papers in peer reviewed journals. In February of 2010, Lonnissa was the recipient of the "Innovative Research Award" given by the Graduate and Industry Networking conference. Lonnissa also received the "Student Travel Award Recognition," given by the Society of Biomaterials in Seattle, Washington for the outstanding quality of her abstract. Lonnissa is engaged to Adrien Ponticorvo and plans to have a small wedding in the Bahamas next year.

Permanent address (or email): 150 Terrazzo Circle, San Ramon, California 94583

This dissertation was typed by Lonnissa Hong Nguyen.